HIGH-RESOLUTION STRATIGRAPHIC ARCHITECTURE AND SEDIMENTOLOGICAL HETEROGENEITY WITHIN THE MIOCENE DAM FORMATION, EASTERN PROVINCE, EASTERN SAUDI ARABIA

BY

Syed Haroon Ali

A Thesis Presented to the

DEANSHIP OF GRADUATE STUDIES

KING FAHD UNIVERSITY OF PETROLEUM & MINERALS

DHAHRAN, SAUDI ARABIA

In Partial Fulfillment of the
Requirements for the Degree of

MASTER OF SCIENCE

In

GEOLOGY

May, 2015

KING FAHD UNIVERSITY OF PETROLEUM & MINERALS

DHAHRAN- 31261, SAUDI ARABIA

DEANSHIP OF GRADUATE STUDIES

This thesis, written by **SYED HAROON ALI** under the direction of his thesis advisor and approved by his thesis committee, has been presented and accepted by the Dean of Graduate Studies, in partial fulfillment of the requirements for the degree of **MASTER OF SCIENCE IN GEOLOGY**.

Dr. Osman Abdullatif
(Advisor)

Dr. Abdulaziz Al-Shaibani
Department Chairman

Dr. Khalid Al-Ramadan
(Co-Advisor)

Dr. Salam A. Zummo
Dean of Graduate Studies

Dr. Gabor Korvin
(Member)

20/8/15
Date

عمادة الدراسات العليا
DEANSHIP OF GRADUATE STUDIES

Dr. Fawwaz AlKhaldi
(Member)

Dr. Lamidi O. Babalola
(Member)

This work is dedicated to deceased parents Mr. Syed Akhtar

Ali Shah (father) and Syeda

Khurshid Begum (mother).

Acknowledgment

In the name of Allah, the Most Gracious, the Most Merciful, who provided me the opportunity, patience and ability to complete this research.

I would like to extend my sincere thanks and appreciations to Dr. Osman Abdullatif who served as my major advisor and his invaluable assistance to the accomplishment of this research. The assistance and guidance received from him during the field, laboratory and final results are certainly valued. I would also like to thank the other members of my thesis committee, Dr. Khalid Al-Ramadan, Dr. Gabor Korvin, Dr. Fawwaz Al-Khaldi and Dr. Lamidi Olabode Babalola. Special thanks are due to Dr. Hassan Eltom for his help during the initial phase of the fieldwork and for organizing refresher course on carbonate sedimentology for the research group members.

King Fahd University of Petroleum and Minerals is thanked for providing scholarship to pursue my graduate studies and supporting this research. In addition, I would like to acknowledge Dr. Abdulaziz Al-Shaibani for his continuous guidance during my stay at KFUPM. All the faculty members, course instructors and staff of Earth Science Department are thanked for their assistance. I want to thank Saudi Aramco for the Miocene Research Program and for support and encouragement. Dr. Aus Tawil is also appreciated for his invaluable contribution for this project. I would also like to express my sincere gratitude to Dr. Abdullah Sultan, CPM, KFUPM for his support and guidance in the course of carrying out this research.

I thank my friends, Ammar, Jarrah, Moaz, Saad, Naveed, Imran, Kamal, Mobeen, Waseem, Ayyaz, Waleed, Hammad, Asif, Amjad, Harris, Haseeb and Arslan. I wish them success and all the best in all their endeavors.

My sincere admiration is devoted to my Father and Mother; they were so interested in my career progress and studies. May Allah be pleased with their souls and grant them in eternal peace (amen). The moral support and back-up support received from my wife in the course of my studies at KFUPM are deeply appreciated. My sister and brother in-law are also appreciated and thanked for incessant supplications for me. Thank you all for your kind support.

Contents

Acknowledgment v
List of Figures x
List of Tables xiii
Thesis Abstract xiv
Chapter 1 1
INTRODUCTION 1
1.1 Introduction 1
1.2 Location of study Area 2
1.3. Problem Statement 3
1.4. Objective 3
1.5. Background 4
1.5.1 Literature Review 4
Chapter 2 16
Geologic Setting 16
2.1 Introduction 16
2.2 Tectonic features 16
2.3 Paleogeography 21
Chapter 3 24
Methodology 24
3.1. Introduction 24
3.2. Research Plan 25
3.2.1. Methodology 25
3.2.2. Field Investigation 26
3.2.2.1. Lithostratigraphic Sections 26
3.2.2.2. Sampling 26
3.2.2.3. Palaeocurrent analysis 27
3.2.2.4. Geometry 28
3.2.2.5. Polished Slabs 28
3.2.3. Laboratory Studies 28
3.2.3.1. Petrographic analysis 29
CHAPTER 4 30
RESULTS 30

LITHOFACIES ANALYSIS 30
4.1. Introduction 30
4.1.1. Coated Skeletal Grainstone (Csg) 32
4.1.2. Coated bioclastic grainstone (Cbg) 34
4.1.3. Peloidal Burrowed Wackestone (Pbw) 37
4.1.4. Bioclastic peloidal grain-dominated packstone (Bpp) 40
4.1.5. Ooid grainstone (Og) 42
4.1.6. Micritised oolitic peloidal grainstone (Mpg) 45
4.1.7. Sandy peloidal skeletal grainstone (Spg) 48
4.1.8. Dolomitic Skeletal Wackestone (Dsw) 50
4.1.9. Foraminiferal peloidal grainstone (Fpg) 52
4.1.10. Sandy Peloidal grainstone-packstone (Spgp) 55
4.1.11. Peloidal Packstone (Pp) 58
4.1.12. Sandy peloidal packstone (Marl) (Spep) 61
4.1.13. Fine to medium Quartz Sandstone (Qfs) 64
4.1.14. Miliolid Peloidal Packstone-Wackestone (Mpw) 67
4.1.15. Calcareous Fine Sandstone (Cfs) 69
4.1.16. Paleosols (Ps) 71
4.1.17. Mud cracked siltstone and mudstone facies (Msm) 73
CHAPTER 5 75
RESULTS 75
SEQUENCE STRATIGRAPHY 75
5.1. Introduction 75
5.2. Cycle Definition and Correlation 76
5.3. Composite Sequences 77
5.4. Sequence Boundaries 78
5.5. Composite Sequence-1 80
5.5.1. Composite Sequence (CS-1 TST) DM-1 80
5.5.2. Composite Sequence (CS-1 HST) DM-1 81
5.6. Composite Sequence (CS-2) DM-2 81
5.6.1. Composite Sequence (CS-2; HFS-1 TST) DM-2 82
5.6.2. Composite Sequence (CS-2; HFS-1 HST) DM-2: 83
5.6.3. Composite Sequence (CS-2; HFS-2 TST) DM-3: 83

5.6.4. Composite Sequence (CS-2; HFS-2 HST) DM-3 85
5.7. Composite Sequence (CS-3) DM-4 85
5.7.1. Composite Sequence (CS-3; TST) DM-4 85
5.7.2. Composite Sequence (CS-3; HST) DM-4 85
5.8. Composite Sequence (CS-4) DM-5: 90
5.8.1. Composite Sequence (CS-4 TST) DM-5: 90
5.8.2. Composite Sequence (CS-4 HST) DM-5: 90
5.9. Facies maps 91
5.9.1. Composite Sequence 1 HST 91
5.9.2. Composite Sequence 2 TST 91
5.9.3. Composite Sequence 3 TST 92
5.9.4. Composite Sequence 4 TST 92
5.9.5. Composite Sequence 4 HST 92
CHAPTER 6 94
DISCUSSION 94
6.1. Discussion 94
6.1.2. Conceptual Depositional Environment: 98
6.1.3. Lithofacies Geometry 107
6.1.3.1. Carbonate Geobodies 107
6.1.3.2. Carbonate Geobodies Types 107
6.1.3.3. Sheet Geobodies 107
6.1.3.4. Lens Geobodies 107
6.1.3.3. Channel Geobodies 109
6.1.4. Seismites 114
6.2. Facies Mosaic 116
6.2.1. Facies Outcrop-10 116
6.2.2. Facies Outcrop-6 121
6.2.3. Facies Outcrop-7 125
6.2.4. Facies Outcrop-26 129
6.2.5.Facies Outcrop-25 133
6.3. Lateral Facies Changes 137
6.4. Palaeocurrent Direction 139
6.5. Geochemical Data 141

Conclusion 145
References 146
Vitae 163

List of Figures

	Page Number
Figure-1.1 Location of the studied area, a) The Satellite map of Arabian Plate, showing location of study area in Eastern Province, b) Geological map showing distribution of Dam Formation and locations of available sections in Eastern Province, Saudi Arabia, C) The location of outcrops used in this study Outcrops 7, 6, 10, 25 and 26.	6
Figure-1.2. General Stratigraphy of the area from Eocene to Pliocene. (Modified from Powers et al. 1966)	7
Figure-1.3 Schematic lithostratigraphic column of Dam Formation at Jabel Midra Al Janubi and Jebel Umm Er Rus (Weijermars, 1999).	8
Figure-1.4This section represents ten lithostratigraphic sections in Miocene Dam Formation North to South as shown in Figure-1 (After Tayyib, 2007)	10
Figure-1.5 Dam Formation at the type section after Steineke and Koch (1935)	13
Figure-1.6 Outcrop 5 characterized by AlKhaldi, 2009	15
Figure-2.1 Structural and Tectonic map of Arabian Plate	18
Figure 2.2: Stratigraphic column showing geological time, stratigraphy, tectonic mega sequence development (Zeigler, 2001)	20
Figure-2.3. The Middle Miocene Transgression	22
Figure-2.4 Paleofacies of Miocene Hadrukh, Dam and Hofuf Formations	23
Figure-3.1 Methodology to be followed in the study	25
Figure 4.1 Representative sedimentological logs from the studied outcrop	31
Figure 4.2 Coated skeletal grainstone facies	33
Figure 4.3 Coated bioclastic grainstone facies,	35
Figure 4.4Peloidal burrowed wackestone facies	38
Figure 4.5 Bioclastic peloids packstone facies	41

Figure 4.6 Ooid grainstone facies 43
Figure 4.7. Micritised ooid peloidal grainstone facies 46
Figure 4.8 Skeletal sandy packstone facies 49
Figure 4.9 Dolomitic skeletal wackestone facies 51
Figure 4.10 Formaniferal grainstone to packstone facies 53
Figure 4.11 Sandy peloidal grainstone-packstone facies 56
Figure 4.12 Peloidal packstone facies 59
Figure 4.13 Sandy peloidal packstone facies 62
Figure-4.14.Quartz sandstone facies 65
Figure-4.15. Miliolid peloidal packstone wackestone facies 68
Figure-4.16. Calcareous fine sandstone facies 70
Figure-4.17. Paleosols facies 72
Figure-4.18. Mud cracked siltstone to mudstone facies 74
Figure-5.1 Diagram of sequences, key surfaces and system tracts. 75
Figure 5.2. Diagram of Eustatic cycle order, sequence stratigraphic unit 77
Figure-5.3. General composite sequence of Dam 78
Figure-5.4. The High Resolution stratigraphic model 79
Figure-5.5. Sequence boundary between CS-2 quartz sandstone facies overlying CS-1 paleosols, black line represent sequence boundary. 81
Figure-5.6. CS-1 DM-1 skeletal mudstone to foraminiferal skeletal packstone 82
Figure-5.7. The top of CS-1 DM-1 composed oolitic grainstone facies 83
Figure-5.8. CS-2 DM-2 composed of skeletal packstone to oolitic grainstone 84
Figure-5.9. CS-2 DM-2 composed of bioturbated sandstone 84
Figure-5.10. CS-2, DM-3 & 4 composed of skeletal packstone to oolitic grainstone 86
Figure-5.11. Middle of CS-2, DM-3 mainly composed of bioturbated skeletal mudstone 86
Figure-5.12. Top of CS-2 DM-3 mainly composed of mudcracked shale 87

Figure-5.13. Top of CS-2 and CS-3 DM-1 underlying DM-3 87
Figure-5.14. Base of CS-2 and CS-3; DM-3 & DM-4, the incised bioturbated channelized sandstone marks the base of DM-2 88
Figure-5.15. The basal most unit of CS-3 DM-3. DM-3 is represented by interbedded sandstone and shale and the shale is highly mudcracked. 88
Figure-5.16. The CS-3 cross bedded sandstone facies interbedded with mudcracked shale facies of DM-4. 89
Figure-5.17. CS-3 and CS-4, skeletal packstone of DM-5 overlying mudcracked shale facies of DM-4. 89
Figure-5.18. The CS-3, CS-4 and DM-5. 90
Figure-5.19 Facies maps 93
Figure 6.1. Photomicrograph of *Borelis melo melo* in Dsw facies 100
Figure-6.2. Depositional model 106
Figure-6.3. Sheet Geobodies 110
Figure-6.4. Lens Geobodies 111
Figure-6.5. Channel Geobodies 113
Figure 6.6. Field photograph showing characteristic feature of seismites 114
Figure-6.7. Facies mosaic of outcrop 10 118
Figure. 6.8. Facies Mosaic outcrop -6 122
Figure-6.9. Facies mosaic of outcrop 7 126
Figure-6.10. Facies Mosaic outcrop-26 130
Figure-6.11. Facies Mosaic outcrop -25 134
Figure-6.12. Palaeocurrent indicators 140
Figure-6.13. Ternary diagram using Quartz, Clay and Calcite 142

Page Number

List of Tables

Table-6.1. Summary of Facies, environment of deposition, dimensions and geometry of geobodies. 108

Thesis Abstract

Name of Student: Syed Haroon Ali

Title of study: High-resolution stratigraphic architecture and sedimentological heterogeneity within the Miocene Dam Formation, Eastern Province, Eastern Saudi Arabia

Major Field: Geology

Date of Degree: May, 2015

The Cenozoic to Mesozoic carbonate-siliciclastic succession are important reservoirs in the Arabian Plate. Outcrops have more advantages than subsurface data. The industry commonly uses limited and large spaced subsurface datasets (e.g. cores and well logs) to characterize reservoirs. The Dam Formation outcrops in the Al-Lidam Area, Eastern Province of Saudi Arabia were studied in order to understand its stratigraphic architectures and facies heterogeneity. The study involved high resolution photographs, establishing facies, facies association, architecture, lateral variations and mapping lithofacies on the outcrop face. The lithofacies defined from 1-D sequence and 2-D correlation are 1) estuarine quartzose channelized calcareous sandstone with bioturbated calcareous mudstone intercalations represents estuarine environment, 2) skeletal grainstone sheets and mounds representing skeletal banks setting 3) red mudstone beds suggesting subaerial exposure and paleosols, 4) oolitic grainstone, stromatolites heads, peloidal facies and microbial laminites deposited in an intertidal environment. Several interbeddings of mud cracked shales and sandstones indicate a terrigenous source. This is in agreement with the regional paleogeography and implies that the sediments in this area are more proximal than from those to the southwest. Although these mixed carbonate-siliciclastic facies were deposited in different sub environments and paleogeographic areas, a high resolution stratigraphic model of the Dam Formation was made. Four sequences (CS1, CS2, CS3 and CS4) were defined on the basis of cyclicity and stacking patterns, the sequences CS2 was further subdivided in two High Frequency Sequences, (HFS1 and HFS2). The north eastern sections of the Dam Formation in Lidam area shows an increase in percentage of siliciclastic sediments in

the updip sections while carbonates dominate in downdip towards the southwestern sections. Rising sea-level pushed the siliciclastic sediments further northeast and deposited mixed siliciclastic sediments in southwest. This study shows that in the absence of subsurface data, we can measure and analyze the sedimentological heterogeneity from outcrops on macro, meso and micro scale. Mixed carbonate-siliciclastic sediments were deposited as a result of rising sea level under arid and hypersaline conditions. The study recommends the analyses of strontium, oxygen and carbon isotopes for understanding of depositional environments and climate.

ملخص الرسالة

الاسم الكامل: سيد هارون على

عنوان الرسالة :التحليل الطبقي المعماري الدقيق والسحنى لمكون دام (الميوسين)، المنطقة الشرقية، المملكة العربية السعودية

التخصص: الجيولوجيا

تأريخ الدرجة العلمية: مايو 2015

يعنى هذا البحث بدراسة مكون دام الميوسينى بمنطقة اللدام في المنطقة الشرقية في المملكة العربية السعودية. يهتم البحث بدراسة السحنات الرسوبية والطبقية المعمارية لمكون دام في خمسة منكشفات صخرية في منطقة الدراسة. تعتبر رسوبيات الحقب الأوسط والحديث الجيريةوالفتاتية المختلطة مهمة لاحتوائها على مكامن بترولية عديده في الجزيرة العربية. هدفت الدراسة الى تحديد نوع وتغيير وتوزيع السحناتالرأسيوالأفقي والمعمارية الطبقيةعلى امتداد مقاطع المنكشفات الصخرية.
يشير التحليل السحنى الى وجود عدة س حنات رسوبية في مكون الدام وهي سحنة الحجر الرمليالجيري القنوى المتطبق مع سحنة الحجر الطينيالجيري، سحنة الحجر الجيريالحبيبيالهيكلي، سحنة الطبقات الطينية الحمراء، سحنة الاستروماتولايت وسحنة الاولايت. كشف التحليل السحنى الرأسي الى وجود أربعة تتابعات طبقية مركبة. وتنقسم التتابعات الطبقية المركبة بناء على نمط وتكرار السحنات الى عدة تتابعات طبقية دقيقة. كما تشير الدراسة أيضا الى أن نسبة الرواسب السحنية الفتاتية تزداد في اتجاه أعلى الميلان في اتجاه الشمال الشرقي(اتجاه اليابسة) بينما تزداد نسبة السحنات الجيرية في اتجاه أسفل الميلان في اتجاه الحوض. توفر هذه الدراسة تطبيق عملي في غياب معلومات تحت سطحية لتحديد الخصائص الرسوبية على عدة مستويات كبيرة، ومتوسطة وصغيرة. وهذه المعلومات تساعد تحديد التغييرات الجانبية والرأسية للسحنات. توصى هذه الدراسة بتحليل نظائر الاسترونشيوم والاوكسجين والكربون وذلك لفهم البيئات الترسيبيةوالمناخ.

Chapter 1

INTRODUCTION

1.1 Introduction

Dam Formation of Early to Middle Miocene age is a mixed carbonate siliciclastic unit defined by most workers. Carbonate rocks are of great economic importance because they host over 50% of the world's hydrocarbon reserves (Flugel, 2004). Though carbonate rocks are mineralogically simple, they are highly variable and heterogeneous in terms of their facies stacking pattern, facies architecture, facies geometry, diagenesis and reservoir qualities. The study of carbonate rocks involves an understanding of water depth, paleotemperature, ocean chemistry, detrital components, biocomponents and their depositional environments. All these factors make the study of carbonate sedimentology challenging. Normally, in the industry limited, low resolution and widely spaced subsurface well data are used to characterize carbonate reservoirs. Outcrop analog studies helps to bridge the gap and the limitations of the well data Meyar et al. (1996).

Owing to the interest of oil companies on the vast hydrocarbon resources in carbonate reservoirs in Saudi Arabia, carbonate rocks in the Kingdom have been extensively studied and still attracting desired attention.

Outcrop analog studies help us to understand the subsurface reservoirs in terms of their stratigraphy and sedimentological characteristics. The outcrops represent subseismic scale for observation in both lateral and vertical directions which lead us to understand their subsurface

equivalents in terms of their reservoir heterogeneity. The geometries of depositional bodies cannot be assessed with seismic or core data due to limitations in resolution, scale and well spacing. This was achieved by integrating traditional and new digital techniques in the field aided with laboratory studies to understand (Abdullatif et al., 2012; Yassin et al., 2012). The best way to characterize reservoir rock is to understand the interplay between carbonate sedimentology, high resolution sequences, diagenesis and pore geometry (Hughes, 2004a; 2004b; 1996; 2005; 2008; 2009; Hughes et al., 2008a; 2008b). The main idea of diagenesis lies in the generation of fluids which destroy the porosity and determination of properties of flow units.

The results obtained through this study are based upon sedimentological parameters, facies high resolution mosaic, facies distribution maps. This would allow us to model and map the spatial distribution of facies in Dam Formation on a regional scale. The reservoir analogue model will help us to understand facies types, facies distribution, facies association and offer improved perceptive of reservoir heterogeneity and stratigraphical architecture for mixed carbonate-siliciclastic reservoirs in the subsurface. The present study subdivides the Dam Formation in to facies and sequences. It also helps to define the depositional environment within a high resolution framework. The Dam formation is divided in to four sequences (S), and the S-2 is further subdivided into High Frequency Cycles HFS-1 and HFS-2. This study has been conducted along a North-South Transect in Al-Lidam Area, Eastern Province. The present study focuses on detailed sedimentology and stratigraphy with established detailed of high resolution sequence stratigraphy of Dam Formation for five outcrops in the Al-Lidam area and, attempt correlation tool within Lidam area.

1.2 Location of study Area

The Dam Formation which is the focus of this proposed research is named after its type locality, the Jabal Al-Lidam. The type locality which is geographically positioned between 26°21’42”N and 49° 27’42”E, lies within the Lidam Escarpment, along the Dammam-Riyadh highway (Figure-1.1). This area which is about 70km from Dhahran is easily accessible and contains very well exposed Middle Miocene Dam Formation outcrops. In Al-Hofuf, the upper contact relationship of the Dam is positioned at occurrence of quartz pebble bed overlying

limestone beds. The lower contact is marked by the appearance of fossiliferous marl containing echinoids species of *Echinocyamus* over sandstone of the Hadrukh Formation (Figure-1.2). The lower beds are exposed near the Al-Lidam area while the upper part is exposed near Al-Umayghir (26°17' 15"N: 49° 30'24"E).The mixed carbonate-siliciclastic Miocene Dam Formation was deposited in a closed embayment (Zeigler, 2001). The dominant lithologies of Dam Formation are limestone, sandstone, and mudstone. The upper part contains fossiliferous sandy-silty limestone with minor amount of marl. The lower part of the formation contains white fossiliferous calcareous marl with minor amount of sand and clay (Figure-1.3), foraminifera, indeterminate corals, vertebrate fragments, crab claws and ostracodes(Weijermars, 1999) and the Dam Formation was assigned to a Middle Miocene age and correlated to the Lower Fars Formation of Iraq (Henson, 1950).

1.3. Problem Statement

The stratigraphic description of Dam Formation was established various researchers including Steineke and Koch (1935), Thralls and Hasson (1956), Steineke et al. (1958),Tleel (1972, 1973), Irtem (1986), Powers (et al. 1966; 1968), Weijermars (1999), Zeigler (2001), Hughes(2004) and Hughes et al., (2013), Al-Enezi (2006), Tayyib (2007), Al-Khaldi (2009) and Al-Khaldi el al. (2010) and was followed by Abdullatif et al. (2012), and Yassin et al. (2012). However, these earlier studies did not clearly indicate the role of lithofacies and their heterogeneity from north (escarpment) to south (distal) in terms of high resolution stratigraphy and correlation of facies from one outcrop to another. Then construction of lithofacies on such a framework based on correlated sequence will enable us to define lithofacies geometries.

This will not only help in local scale of understanding but will also give the picture of the formation in terms of the heterogeneity and architecture of its carbonate reservoir successions.

1.4. Objective

The main objective of the proposed study is to:

- To determine the facies architecture and heterogeneity (microscale (thin section), mesoscale to macro-scales (outcrop) of, and to attempt correlation of the sequences in the Dam Formation outcrops in the AL-Lidam along a NS- transect.

- To characterize Miocene Dam Formation in terms of sedimentology, attempt and 2D-Correlation (2-dimension).
- To identify carbonate geobodies and architecture for understanding depositional environment.

Achieving these setup research goals and objective will lead to better understand the subsurface reservoir equivalents of the Dam outcrops in terms of their facies heterogeneity and architecture.

1.5. Background

1.5.1 Literature Review

The Miocene succession in the Eastern Saudi Arabia has not been previously studied in much detail because it was less interest to the oil companies than the Pre-Eocene petroliferous formations. Along with Hadrukh and Hofuf Formations, the name Dam Formation was first introduced by Steineke and Koch (1935).in. Thralls and Hasson (1956) used the name "Dam Formation" in their publication on geology and oil resources of Eastern Province, Saudi Arabia. Steineke et al. (1958) gave a detailed lithological description of Dam Formation at its type locality, the Jabal Al-Lidam. Powers et al. (1966) and Powers (1968) reported numerous fossils for Middle Miocene age and formally published the name Dam Formation (Figure-1.5).

Tleel (1972, 1973) described a Dam Formation section at Jabal Midra Al-Janubi Where he found out that the formation contains several facies including a coral algal reef which grades laterally into a mollusc-rich facies containing pellets, foraminiferal, echinoidal and stromatolitic limestones were identified along the flanks of dome. The author found out that the basal contact of the Dam Formation is unconformable and indicates a period of erosion, and there are two periods of growth of the dome. The first event was before the deposition of Dam Formation around the Dammam Dome, and second after its deposition to present elevation.

Irtem (1986) reported different forms of stromatolites in the AL-Lidam area, and inferred that the stromatolites which are interbedded with thinly bedded oolitic grainstones were formed in the same environment as oolites. He described three upward deepening sequences showing shallow subtidal to lower intertidal environment of deposition in the study locality. Whybrow et al. (1987) studied the geology and vertebrate paleontology of Miocene.

Weijermars (1999) studied the lithostratigarphy of Dam Formation in the Dammam Peninsula at Jabal Midra Al-Janubi, Jebel Midra Ash Shamali and Jabal Umm Er Rus. According to this author, the minimum thickness of Dam Formation at Jebel Midra Ash Shamali is 75m. The basal part the formation composed of 0.5-1.5 m thick multi colored conglomerates eroded from the Khobar limestone. At Midra Al-Janubi, the basal unit is composed of 1.8m yellow grey sandy limestone (microcrystalline) unconformably overlying Midra Shale. The basal sand beds in both localities are overlain by pink to purple 1m thick stromatolitic limestone At Midra Al-Janubi. The stromatolites beds are overlain by thick (31m) sequence of calcarenite, clastic carbonates, calcarenite with microcrystalline matrix, algal limestones, fecal pellets in micritic matrix and sandy limestone. Clastic carbonates are cross bedded.

The upper most part of the succession is composed of15m cliff forming massive limestone; this unit contains 6m calcarenite (containing pebbles and boulders of cryptocrystalline limestone) at its base. At Jabal Umm Er Rus, the Dam Formation unconformably overlies the Rus Formation. It is about 16m thick bioherm reef facies, blue-green algal growth, mollusks, it contains Peneroplis farensis has been reported from Dam Formation (Henson, 1950) from Umm Er Rus and based on this index fossil it has been correlated to Lower Fars Formation (Miocene) of Iraq. Echinoids and Neogene Foraminifera (wide range) have been reported from the Dam Formation (Tleel, 1973).

Zeigler (2001) published map of paleofacies of the Dam Formation and indicated transitional to marine environment of deposition. Hughes(2004) and Hughes et al., (2013) studied the Dam Formation(75m) outcrops in the Jabal al Midra Janubi and found that its base is composed of sandy limestone, followed by stromatolites beds, microcrystalline limestone and karst filled limestone with cobbles and pebbles.

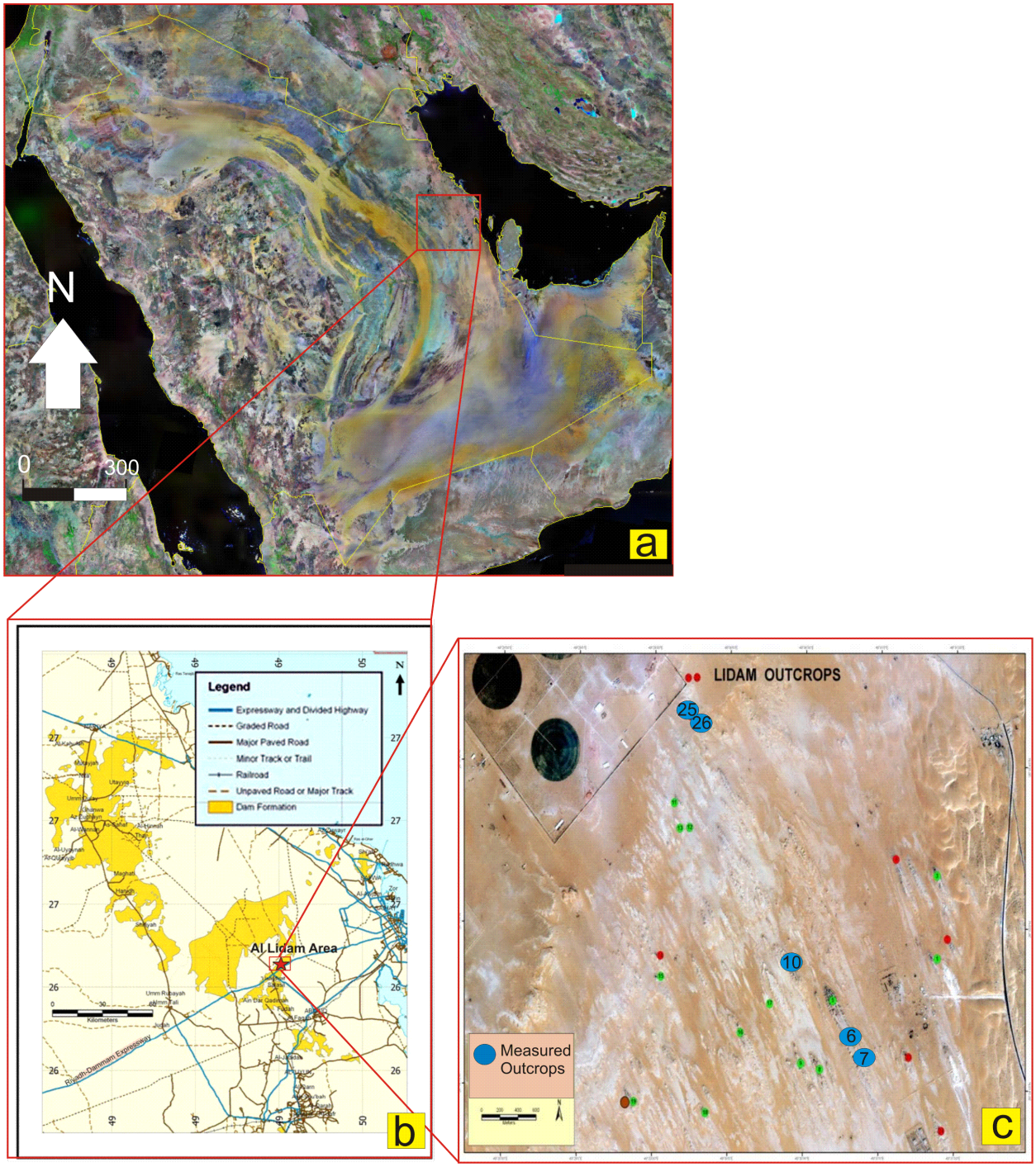

Figure-1.1 Location of the studied area, a) The Satellite map of Arabian Plate, showing location of study area in Eastern Province, b) Geological map showing distribution of Dam Formation and locations of available sections in Eastern Province, Saudi Arabia (After, Tayyib, 2007) C) The location of outcrops used in this study Outcrops 7, 6, 10, 25 and 26.

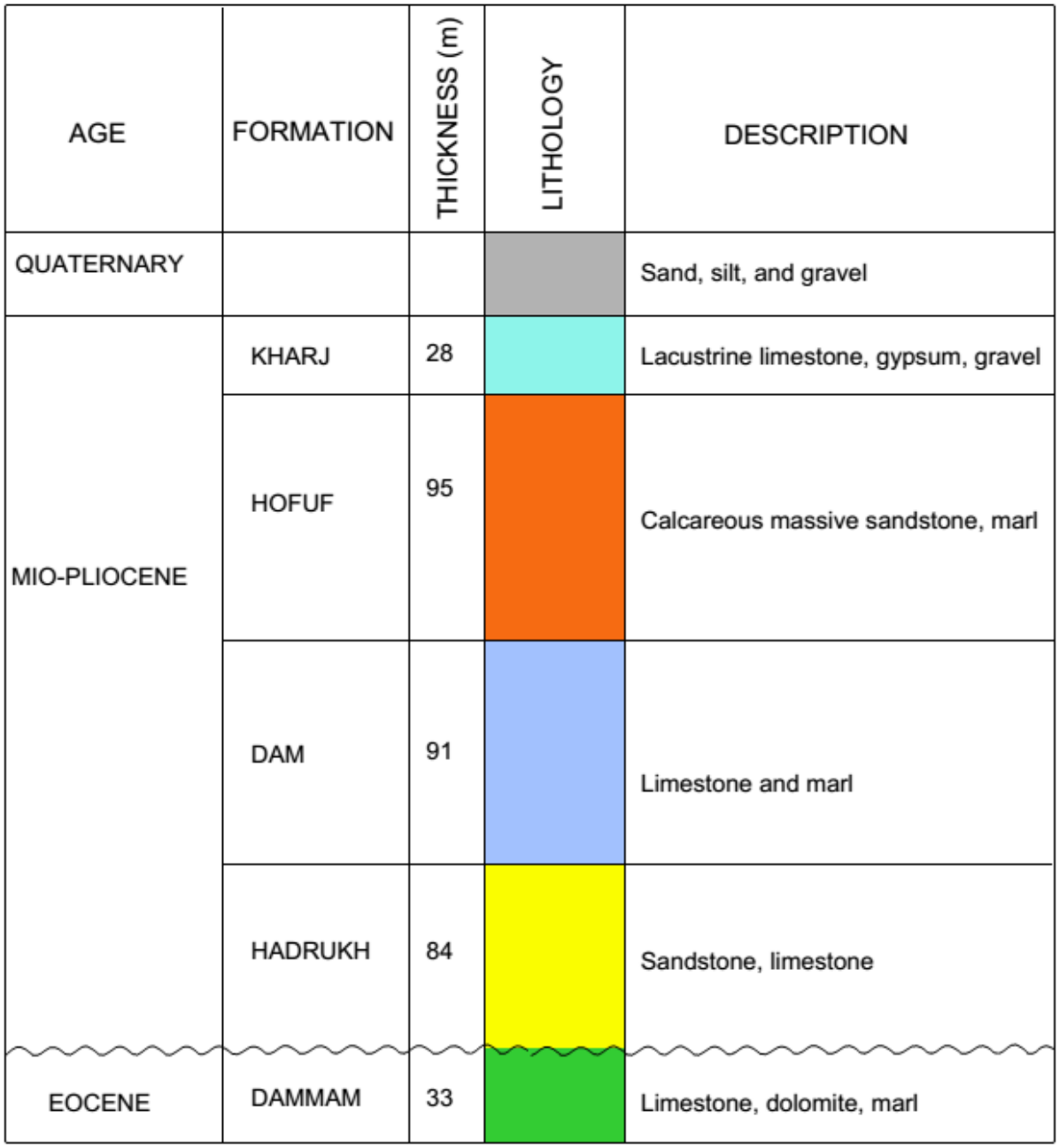

Figure 1.2 General Stratigraphy of Ghawar area, Eastern Province, from Eocene to Pliocene. (Modified from Powers et al. 1966).

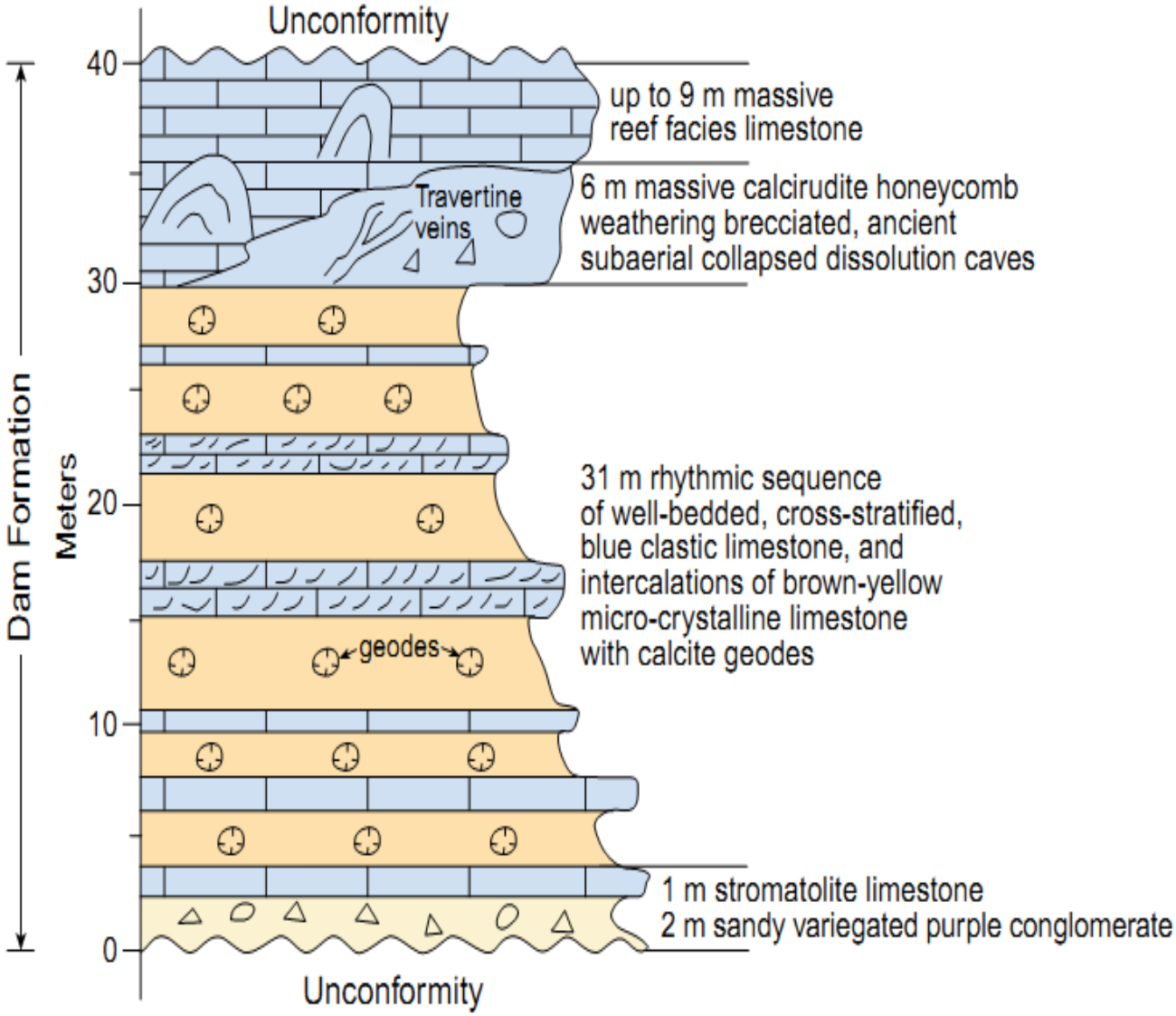

Figure-1.3 Schematic lithostratigraphic column of the Dam Formation at Jabal Midra Al Janubi and Jebel Umm Er Rus (Weijermars, 1999).

The authors also indicated that the presence of corals in Dam formation suggests the presence of a coral reef in Dam Formation at this locality. Al-Enezi (2006) compared the foraminiferal assemblages in recent sediments of the Arabian Gulf and compare with those of the Dam outcrop at Jabal Midra Al-Janubi. On the basis of these foraminiferal assemblages, he defined small scale shallowing cycles in the form of grainstone, packstone and wackestone. Tayyib (2007) studied the effect of depositional setting on the Portland cement quality of the Dam Formation at twelve locations in Eastern Province. He suggested more circulation in warm water lagoon in north and northwestern parts are best for cement, hypersaline tidal pond setting in the middle which is good for cement and high silica content and dolomitization in southern sections due to muddy lagoons and tidal channels which is considered poor quality for cement.

From their study of the controls on sequence stratigraphy of the Dam Formation, Al-Khaldi (2009) (Figure-1.6)and Al-Khaldi el al. (2010), found out that the mixed carbonate-siliciclastic sediments of the formation are characterized by three composite sequences. These are, CS1(composite sequence 1) consist of four meter scale cycles while CS2 and CS3 are composed each of two high frequency (HFS1, HFS2, HFS3 and HFS4) cycles.TST flooding on Type-1 SB (Sequence Boundary) formed HFS2 and HFS3. HFS 2 and HFS4 were results of TST flooding on Type 2 SB (Figure-1.6).

The presence of eolianites facies on Lidam Escarpment and scattered gypsum crystals in Red mudstone beds shows arid climate and in sea-level, the stromatolites show shallow subtidal environment and the monospecific shell beds show hypersaline conditions. Abdullatif et al. (2012) studied facies of the Dam and Hofuf Formations to predict reservoir quality and heterogeneity and find out that the facies distribution and variation are controlled by both dynamic and static depositional controls. Yassin et al. (2012) studied Dam and Hofuf Formation in terms of micro and mesoscopic lithofacies heterogeneity and their effects on reservoir heterogeneity and architecture. These authors found out that the porosity and permeability patterns are highly variable, and indicate that the both depositional and diagenetic controls are present.

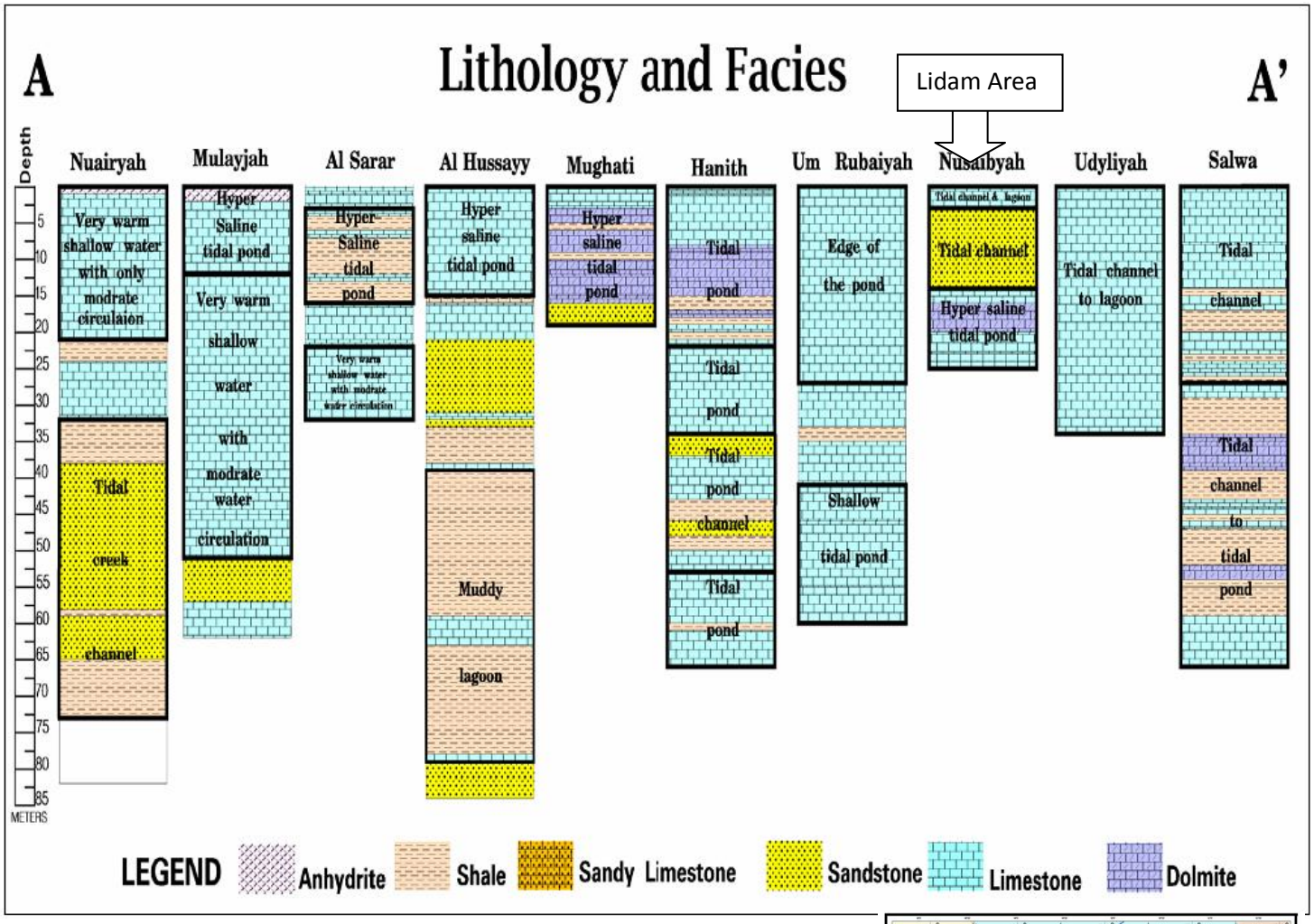

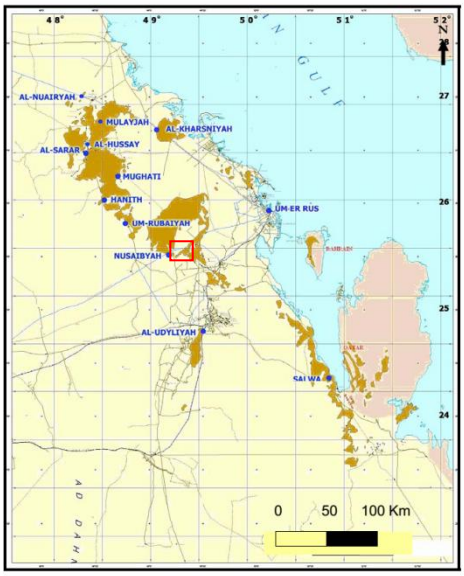

Figure-1.4This section represents ten lithostratigraphic sections in Miocene Dam Formation North to South as shown in Inset Map (After Tayyib, 2007)

Al-Khaldi et al., (2014) studied the Miocene sequence of Lidam area to examine the effects of glacio-eustasy during moderate Antarctic glaciations, in the back buldge basin distal from Zagros Fold and Thrust Belt. They suggested that the updip sections of Dam Formation are dominated by siliciclastic grading downdip into carbonates under semi-arid conditions and locally hypersaline conditions and that the subsidence rates were slower than in the proximal foredeeps in Iran. These conditions resulted in the formation of paleosols near sequence boundaries in the Hadrukh Formation and Dam Formation.

The Dam Formation is present in the other parts of the Middle East (United Arab Emirates, Iran, Qatar, and Iraq. Peebles (1999) used stable isotope to study the Miocene in United Arab Emirates. The stable isotope study failed to provide dates for the Shuwaihat Formation and Baynunah Formation due to diagenetic alterations of the sediments.

The Dam Formation in Qatar has been investigated in much more details than in Saudi Arabia (Cavelier (1970); Abu-Zied et al., (1983); Hewaidy (1991); Khalifa et al., (1993); Al-Saad et al., (2002)). Cavelier (1970) subdivided the Dam Formation in Qatar into a lower unit and an upper unit. Abu-Zied et al. (1983) studied the claystone intervals in Miocene argillaceous rocks to refine the work of Cavelier's. They subdivided Dam Formation into A and B Members. Hewaidy (1991) used the foraminiferal contents in the Dam succession at Jabal Al-Nakhash and Al Kharrara to assign the formation established Burdigalian-Helvetian age (Early-Mid Miocene). In their study of the Dam Formation B Member at Jabal Al-Nakhash, Khalifa and Mahmoud (1993) identified three different types of algal stromatolites and suggested protected tidal flat as their depositional environments. Al-Saad and Ibrahim (2002) studied the Dam Formation, in Qatar and subdivided it into two members, the basal Al-Kharrara Member (limestone, marl and claystone facies) and overlying Al-Nakhash Member (carbonate, evaporite and algal stomatolite facies). They inferred inner neritic zone for Al-Kharrara Member to tidal flat for Al-Nakhash Member.

Dill et al. (2005) integrated the sedimentary facies, geochemical and mineralogical compositions of the Dam Formation succession to recognize facies associations and subdivided the formation into five members (the lower, the middle, the upper Salwa, the Al Nakhsh and the Abu Samrah Members). They also concluded that the dissolution of Eocene rocks at depth

controls the differentiation of Dam Formation lithofacies. Shawkat (1979) studied the Lower Fars Formation, an equivalent of the Dam Formation in northern Iraq in terms of its petrography and sedimentology. He identified subtidal, intertidal to supratidal environments for its deposition. Al-Banna et al. (2005) studied the microfacies and depositional cycles of the Miocene Formations in the NW Iraq .Two major cycles interpreted as products offshore-barrier, barrier, subtidal, patch reef and intertidal environments were identified from the study. Al-Banna (2008) also studied the Miocene sequence in Iraq to decipher the debatability of the Oligocene-Miocene Boundary. On the basis of planktonic foraminifera's distribution patterns, he identified four biostratigraphic zones. Al-Ameri et al. (2011) studied the hydrocarbon potentials of the Jeribe Formation (Miocene) in NE Iraq and found out that the formation is mostly dolomitic limestone with porosity within the range 10-24% and a 30mD mean permeability. Investigated through the study of the biostratigraphy, chronostratigraphy and sequence stratigraphy of Oligocene-Miocene carbonates of the Kirkuk Group, Southern Kurdistan, Iraq, Ala (2012) identified five biozones, twenty two microfacies, and nine depositional sequences which were deposited in inner ramp to outer ramp. Kharajiany et al., (2014) established the stratigraphic boundaries and described the depositional system tracts in the Oligocene-Miocene rocks of the Mamlaha anticline in Kurdistan region of Iraq. In his study of the microfacies and high resolution stratigraphy of the Oligocene-Miocene sequence in Kurdistan Region, Iraq, Al-Qayim et al. (2014) identified complete cyclicity in microfacies comprising of three cycles in the succession. Moghaddam et al. (2006) found four upward shallowing cycles in Asmari Formation in Iran and interpreted that the facies were deposited in a wide range of environments including shelf lagoon, tidal flat, carbonate shoal and slope. Ranjbaran et al. (2007) also described seven major lithofacies and three subfacies deposited on carbonate ramp from the Asmari Formation (equivalent of Dam Formation) in southwestern region of Iran. Ehrenberg et al. (2007) used strontium stable isotopes to study the stratigraphy of the Asmari Formation in Southwestern Iran. These authors described eight depositional cycles which are characterized a generally a shallowing upward sequence and a decrease in accommodation space. Mossadegh et al. (2009) studied distribution of the grain types and microfacies from outcrops of the Asmari Formation in Central Zagros, Iran and noted that significant changes in salinity conditions during deposition of the sequence has direct relationship with the facies in study area.

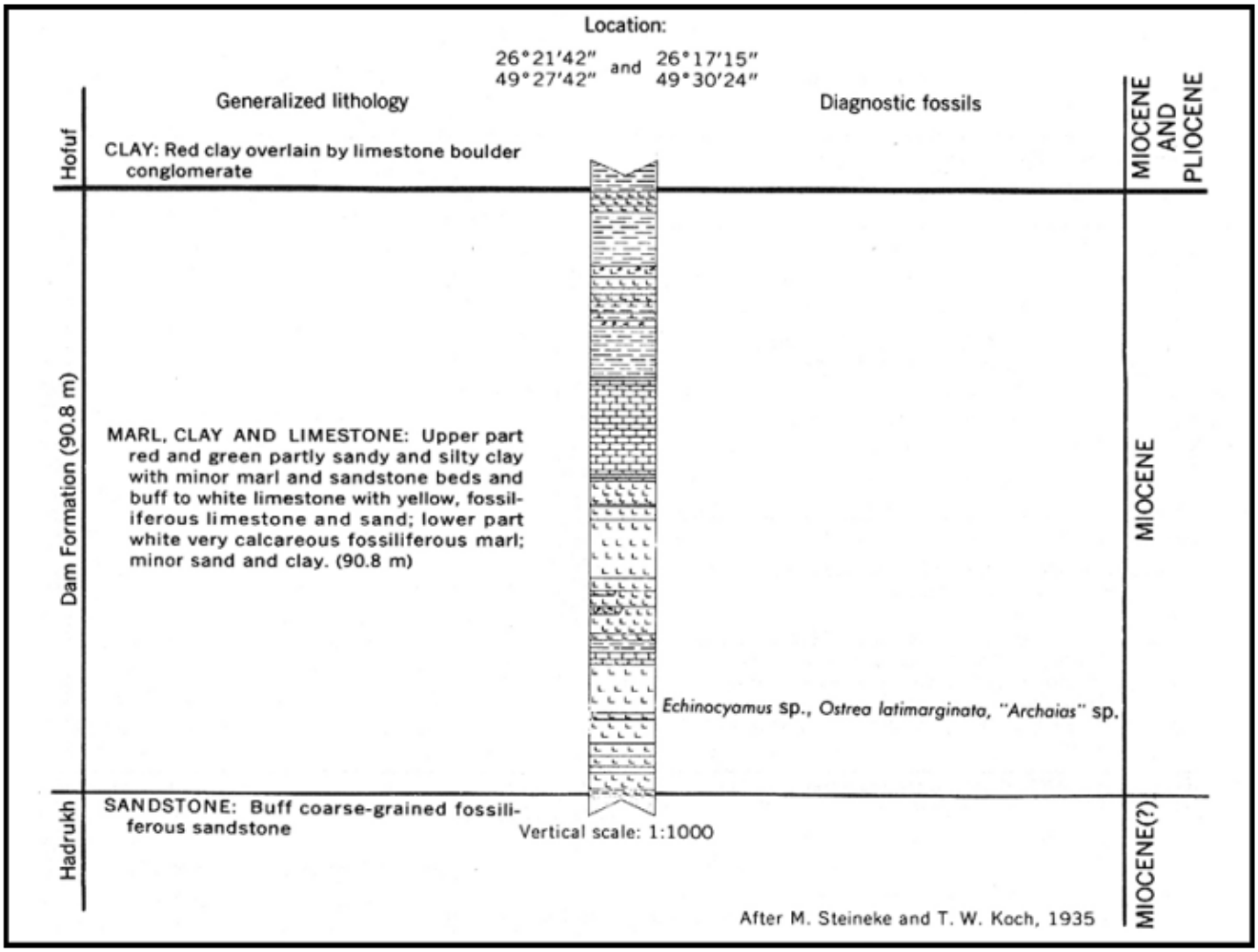

Figure-1.5 Dam Formation at the type section after Steineke and Koch (1935)

Al-Aasm et al. (2009) used petrographic and stable isotope analyses of carbonate successions from the Gascharan Oil field and surrounding areas to study the diagenetic changes in the Asmari Formation in southwestern region of Iran. They identified four types of dolomites and found several episodic growths of fracturing, calcite cementation and dolomitization. Reichenbacher et al. (2011) carried out an extensive work on the Tabriz Basin NW Iran to understand Late Miocene stratigraphy, paleoecology and palaeogeography of the depositional basin. These authors found out that the basin was connected to Caspian Sea via an ancient river. Heidari et al. (2013) constructed a diagenetic model of Lower to Middle Miocene Guri Member of Mishan Formation (equivalent of Dam Formation) in the SE part of Zagros Basin in Iran, and divided the diagenetic processes into four stages, namely marine, meteoric, burial and uplift.

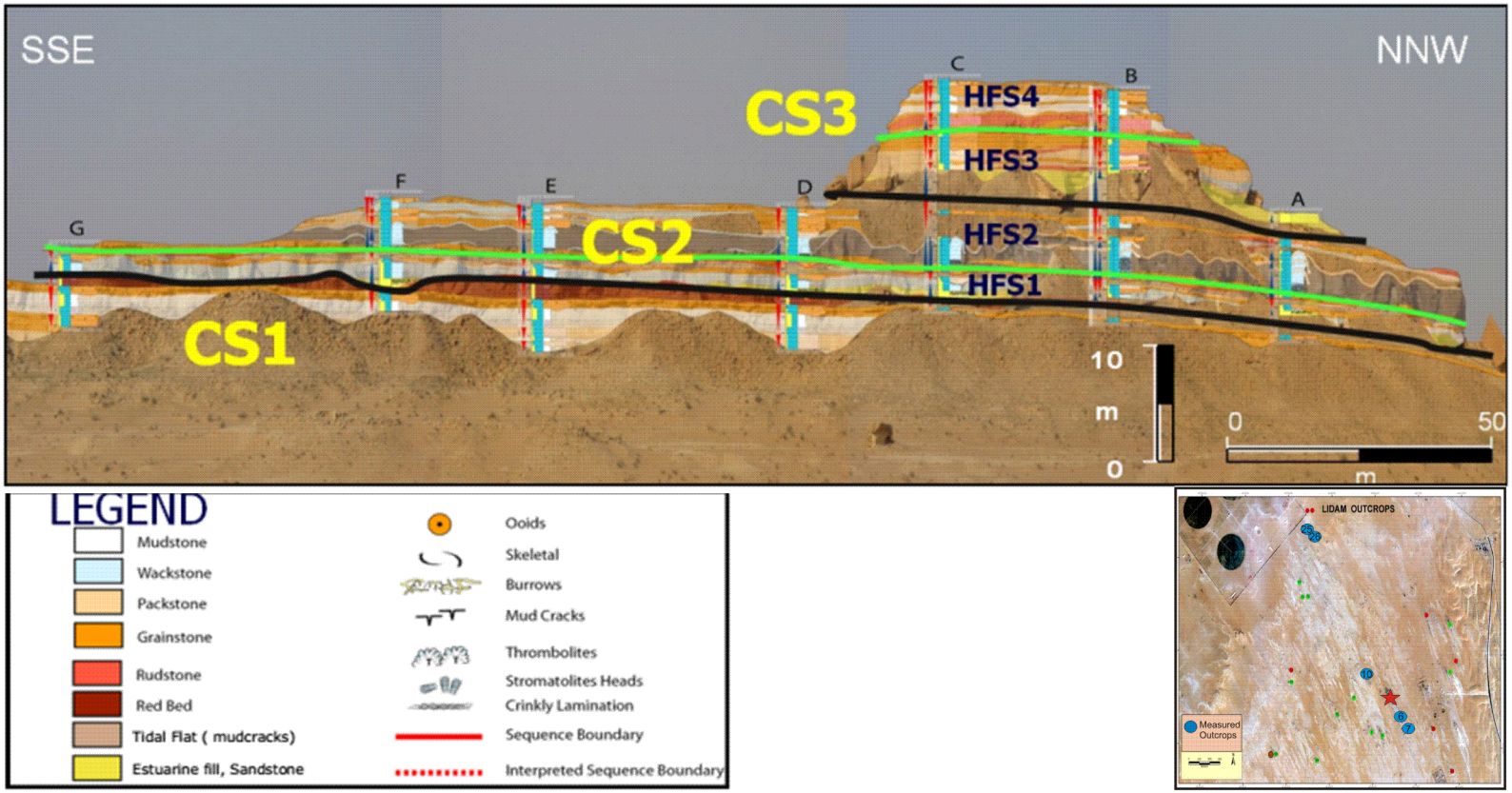

Figure-1.6Outcrop 5 characterized by AlKhaldi, 2009. Located between outcrops 6 and 10. Three composite sequences separated by black lines. The three Composite Sequences are CS1, CS2, and CS3. CS1 consists of 4 cycles. CS2 consists of 2 High Frequency Sequences (HFS1 and HFS2). CS3 consists of 2 High Frequency Sequences (HFS3 and HFS4) (AlKhaldi, 2009).

Chapter 2

Geologic Setting

2.1 Introduction

The major occurrence of Dam Formation is in the eastern and northeastern parts of the Arabian Peninsula. The Arabian Plate is composed of Arabian shield basement in west and Arabian platform in east. The Arabian shield is comprised of igneous and metamorphic rocks. The last main tectonic occurrence recorded on Arabian Plate was Pan-African Orogeny. The shallow marine sedimentary basins are divided in to two groups, a) the broad homocline and basins in Northeast, b) the Arabian Gulf and Zagros Region in east (Powers et al., 1967). Pre-tertiary sedimentary rocks were deposited when the Arabian and African Plates were joined together and the Arabian Gulf was a continental margin along the Tethys Sea. The remainder of the Tethys was closed at the end of tertiary, while the Arabian Plate collided with the Eurasian Plate. The Arabian Plate was separated from the African Plate and started moving towards the landmass of Eurasian Plate in the Middle Miocene. The Gulf of Aden and Red Sea were opened as a result of separation between Arabian and African landmasses. The Arabian Plate moving northward is bounded by in Red Sea and Gulf of Aden by oceanic ridges, Gulf of Aden in southeast, Dead Sea fault in northeast, Owen Fracture zone in southwest and by the Zagros mountains in northwest(Figure-2.1).

2.2 Tectonic features

The north eastern edge of Arabia is typified by sedimentation, accommodation space, subsidence and folding since the Early Miocene. Some researchers such as Dunnington et al.,

(1958) suggested that these events started before the Eocene in Arabian Gulf-Zagros Basin (Figure-2.1). The folding and subsidence are restricted to a strip 300 km west of Zagros basin. The major sedimentary rocks are anhydrites, limestones, marine shales, sandstones and rock salt. Since the late Miocene, the Zagros has been the zone of intense folding, especially the Pliocene. A large number of folds were developed during these periods. The wavelengths of these folds are 5 to 30 km and their amplitudes may go beyond 5km. Since the folding was occurring at the same time as sedimentation, so the thicknesses of late tertiary sediments vary greatly. As an example, the structural difference is greater than 9 km within a distance of 20km in the anticline-syncline in Kuh-e-Khami, SW Iran (Hull et al., 1970). Some researchers have suggested calculating the magnitude of subsidence from the thicknesses of sediments in synclines (Figure-2.1). Folding distribution is controlled by the thrusting present in the earth crust. Bird (1978), used FMS (focal mechanism solutions) to demonstrated that the thrusting of about 400km wide and 40 km thick is present throughout the crust. The data from the thrusting and folding proposed parallel compression normal towards the Zagros in ENE direction.

In the Miocene, the Arabian Plate separated from the African Plate and stared moving towards the Eurasian Plate, leading to the development of Zagros Foredeep and Foreland. A strong compressional force moved the Arabian Plate towards the Eurasian landmass and away from the African Plate. This was the time of Burdigalian phase of Alpine Orogeny (Zeigler, 2001; Figure-2.2).This led to the initiation of the Gulf of Aden, and onset of the Red Sea rift which began to separate Arabia from Africa. The complex strike slip faulting in the vicinity of Dead Sea led to the uplift of the Syrian Arc. The effect of collision of Arabia resulted in the inversion in the Palymrides and the Sinjar uplift. Transgression events were recorded in Euphrates Graben during this period. In the eastern part of Arabia, the thrusting of Sanandaj-Sirjan zone into the Arabian Plate is an evidence of collision of the Arabian and Eurasian Plates.

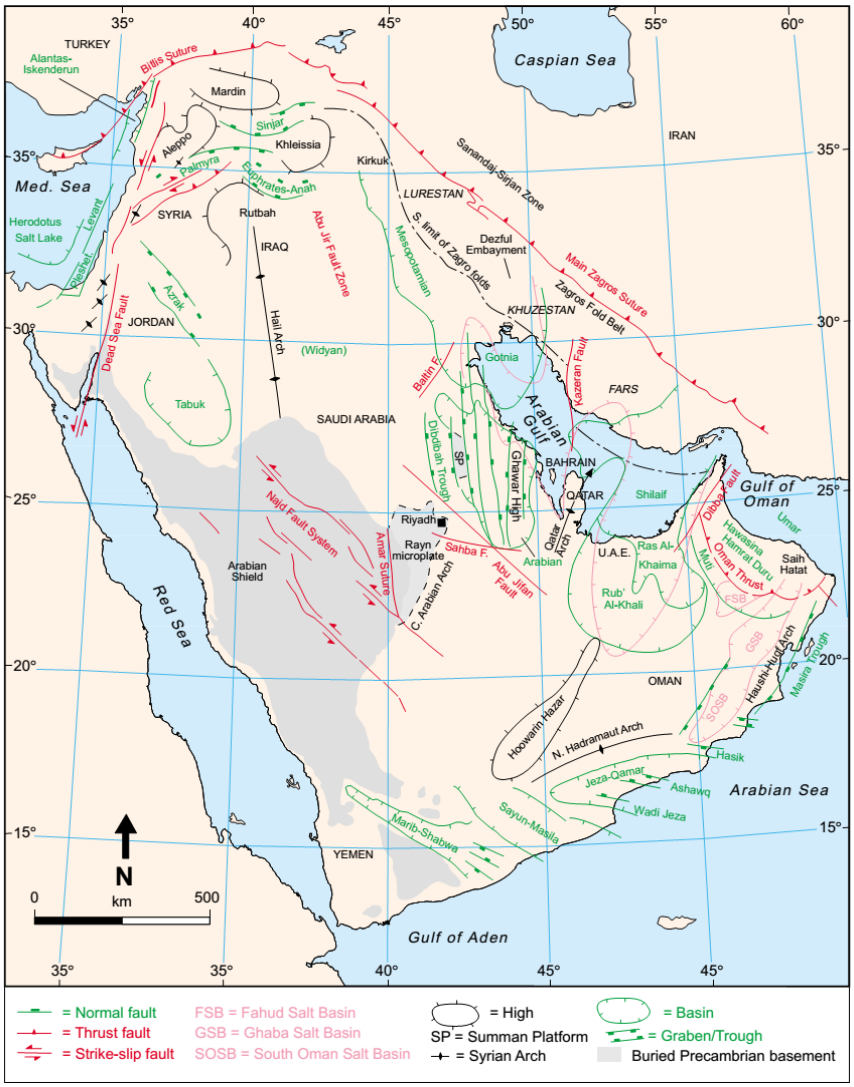

Figure-2.1 Structural and Tectonic map of Arabian Plate representing inclination of faults, volcanic lineaments, folds, basement, paleaostress and epicenter of earthquake events (Zeigler, 2001).

In the process, there was a large supply of continental deltaic clastic sediments and shales (shallow marine) which accumulated in the quickly subsiding Zagros Basin (Al-Sharhan et al., 1995). In the Dezful Embayment of the Zagros Basin, post-Asmari (Miocene-Recent) sediments reached a thickness of over 5000m (Al-Sharhan et al., 1995).There was an active margin in the eastern part of the Arabian Plate during the Miocene. Volcanic activity took place at the same time in Western Arabia. This event is associated to Red Sea rifting. Historical eruptions in the areas of Madina show that volcanism is still in progress. The lava fields (180,000sq.km) named Harrats which extend from Yemen to Turkey are one of the largest basaltic provinces in the world (Al-Sharhan et al., 1995).

The sedimentation continued in the Zagros Basin during the Miocene (Al-Sharhan et al., 1995; Figure-2.4). This time period witnessed the deposition of the Hadrukh, the Dam and the Hofuf Formations in Saudi Arabia while the Fars, the Agfa Jeri and the Gachsaran Formations deposited in Iran. The continental deposits of the Hadrukh Formation were deposited along with the accumulation of marine sediments of the Dam Formation in the Arabian Arch. In the Miocene the deposits of this area were the Hadrukh (calcareous sandstones, sandy limestones with chert), the Dam (Marl, limestone, coquina and chalk) and the Hofuf (marly and sandy limestone, gravel and calcareous sandstone(Figure-2.3). The gravels in the Hofuf Formation were as a result of rapid erosion in Arabian shield areas. Provenance studies have shown that the igneous, metamorphic and sedimentary rocks were sources of the Hofuf Formation sediments.

Thin sediments cover near the Arabian Shield area are thin but and become thicken eastwards and may exceed 8 kilometers near the Arabian Gulf(Al-Sharhan et al., 1995). The alteration in facies reflects changes in accommodation space as result of continued subsidence from Mesozoic to Cenozoic.

Paleofacies map published in Zeigler (2001) show downwarping in east continues up to the present. This is evidenced by the thickening of Cenozoic sediments. As a result of the development of the Zagros Mountains, there was a continuous downwarping in the NE-edge of the Arabian Peninsula. This downwarping resulted in the development of subsidence and accommodation space.

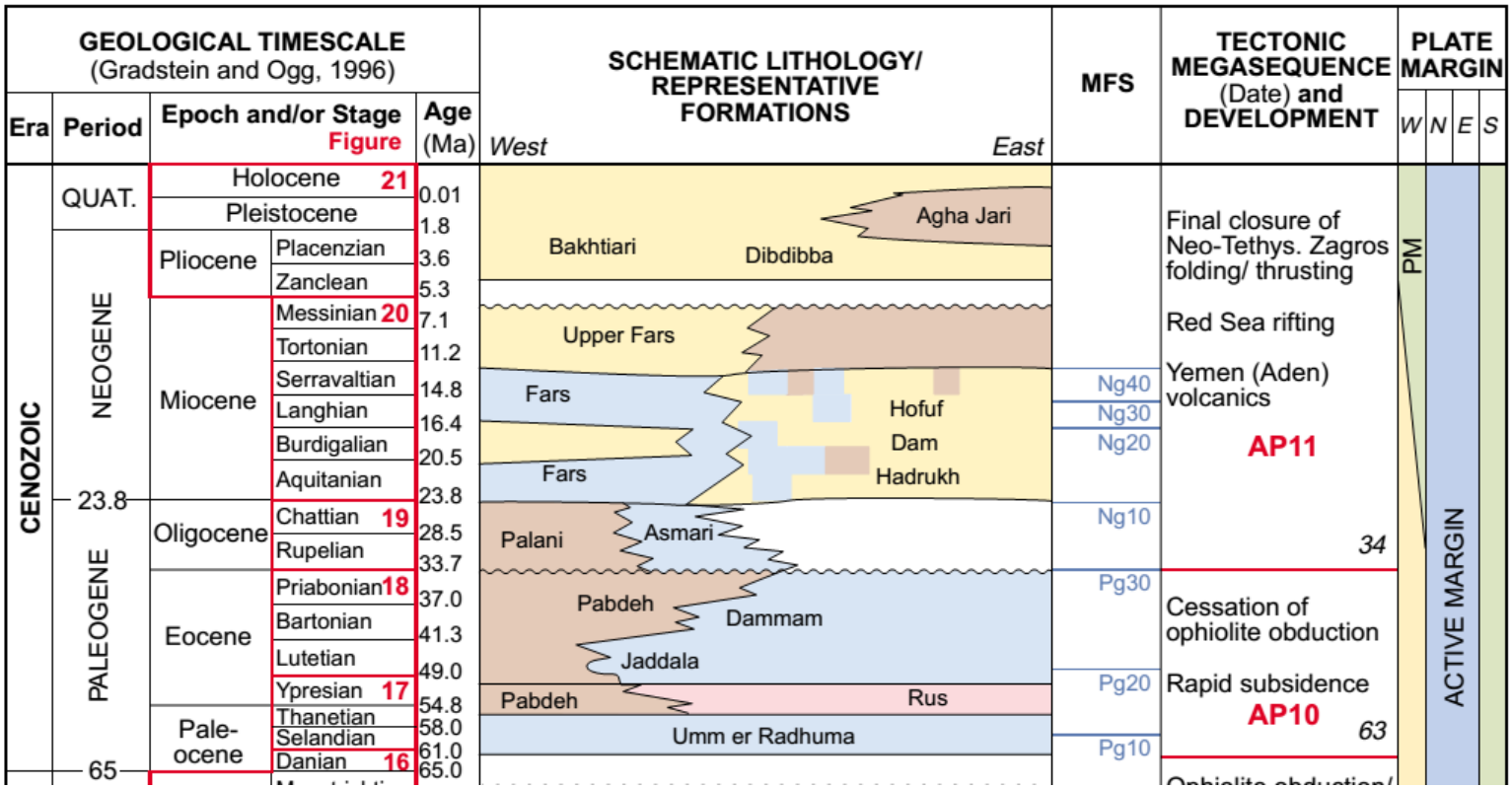

Figure 2.2: Stratigraphic column showing geological time, stratigraphy, tectonic mega sequence development and Arabian Plate margin from Late Permian to Holocene (Zeigler, 2001). The figure also shows that the eastern margin of the Arabian Plate was an active margin in the Middle Miocene time.

The tectonics as well as the paleogeography controlled the deposition of the Dam Formation. The anti-clockwise movement of the Arabian Plate allowed the deposition of the Miocene succession from east to west (Zeigler, 2001). The increase in thickness of the Mesozoic to Cenozoic strata towards north and northeast shows continuous subsidence in these areas (Weijermars R., 1999; Zeigler, 2001). Facies changes were also controlled by the sea level rise in response to tectonic movements in the Al-Lidam Area and as a result, the facies in southeast are more carbonate rich and basinward. On the other hand, the facies in the northwest are more siliciclastic and landward.

2.3 Paleogeography

As a result of collision between African and Arabian Plate with the Eurasian Plate, the seaway between the Indian Ocean and Mediterranean Sea was closed during Middle Miocene. Land bridge allowed a discrete passage connecting the continents. Middle Miocene, was the time when the Paratethys, seaways (Rogl, 1999; Figure-2.3).Between Indian Ocean, the Mediterranean closed and opened occasionally. During Late Miocene, the Paratethys was strongly reduced and led the development of endemic development of fauna. The Arabian and African plate anticlockwise rotation resulted in an impact with the Anatolian Plate. The seaway between the Indian Ocean and Mediterranean was cut off from each other. The Hercynian Lineaments (N-Trending) of Central Arabian Arch extend far north in to the Zargos Foredeep (Rogl, 1999).

Paleofacies around the Arabian Arch, of Hadrukh Formation (continental) to Dam Formation (continental-marine) sediments were deposited. Hofuf Formation in the interior of age equivalent lacustrine sediments were deposited(Figure-2.4). Sandy limestone and calcareous to silty sandstone with chert concretions, Dam Formation consists of marls, shales, chalk, limestone and coquinas, the Hofuf consists of calcareous sandstone and gravels. The presence of fresh water conditions is represented by gastropods (Powers, 1966). At the time of Hofuf Formation the rapid erosion and uplift in the western parts of the Arabia resulted in the abundance of gravels. The clasts in the Hofuf Formation range from igneous, metamorphic and sedimentary rocks from the Jabal Tuwaiq Escarpment.

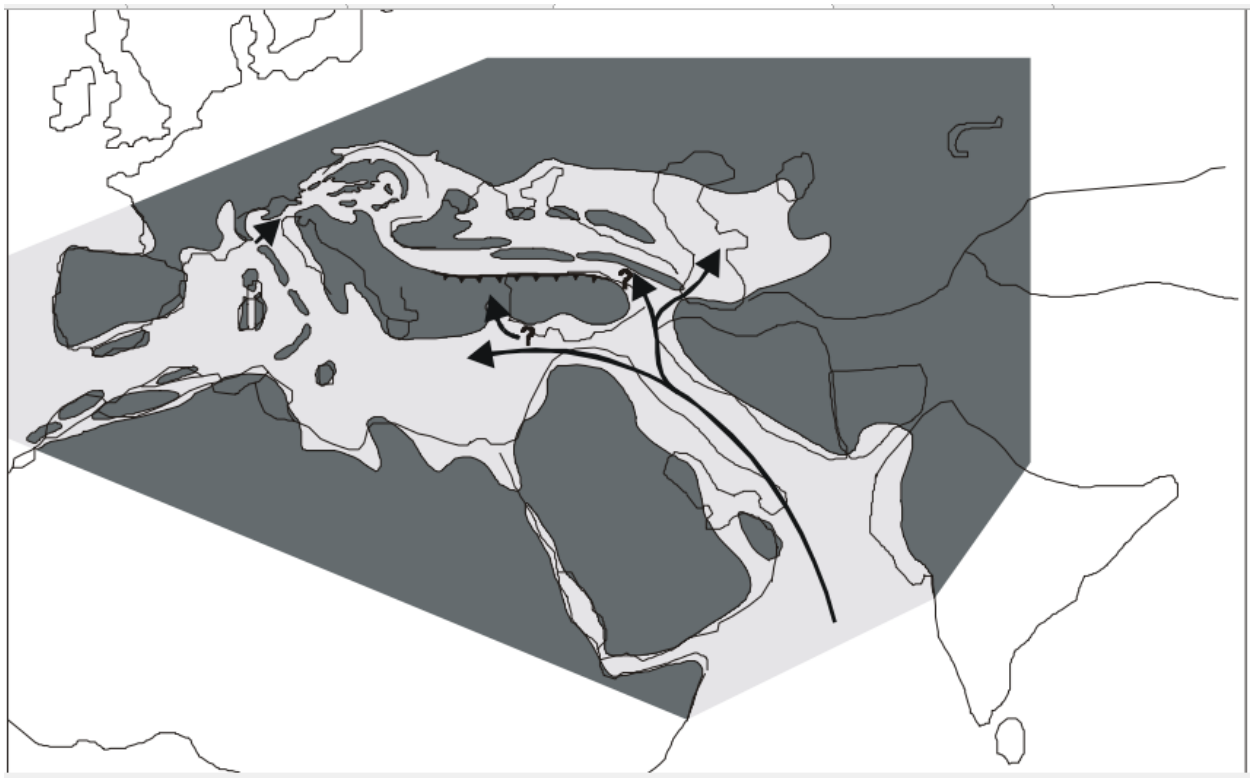

Figure-2.3. The Middle Miocene Transgression flooded the entire Mediterranean and Paratethys, the seaway from Indian Ocean opened once again (Rogl, 1999).

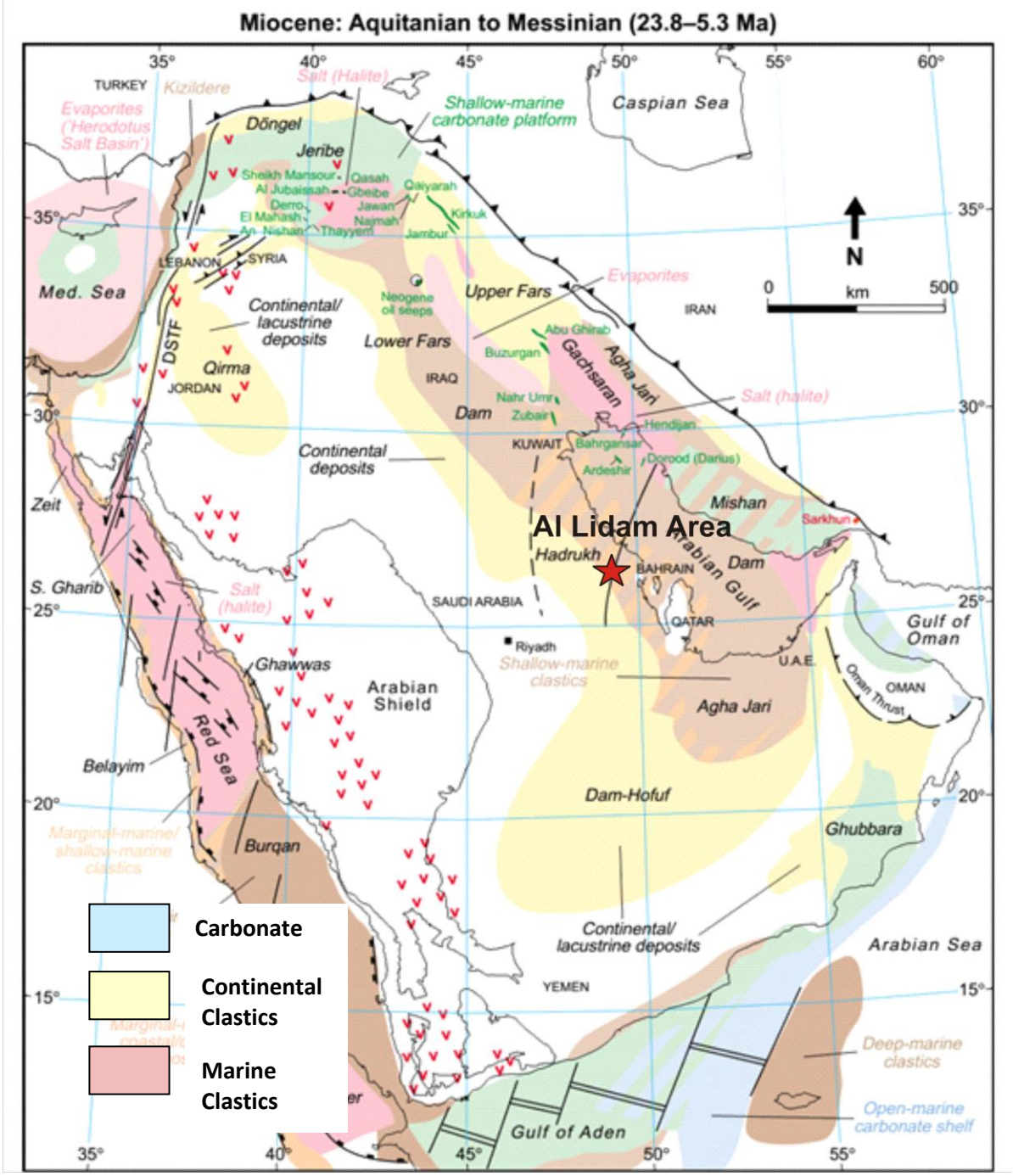

Figure-2.4 Paleofacies of the Miocene Hadrukh, Dam and Hofuf Formations and their regional equivalents, sediment accumulation mainly in Zagros Foredeep and Foreland. Note marine and continental facies of Dam Formation (Zeigler, 2001).At this time, the Arabian Plate was separated from the African Plate and was pushed towards the Eurasian Plate.

Chapter 3

Methodology

3.1. Introduction

The methodology used in this involved both field and laboratory investigations, includes High resolution mosaics were acquired and used to illustrate the distribution of rock facies. The facies on the outcrop face were mapped. The outcomes using this methodology were detailed outcrop mosaic, detailed sedimentological sections, facies mosaic based on closely spaced vertical sections to make them high resolution, and petrographic analysis to second the field observation.

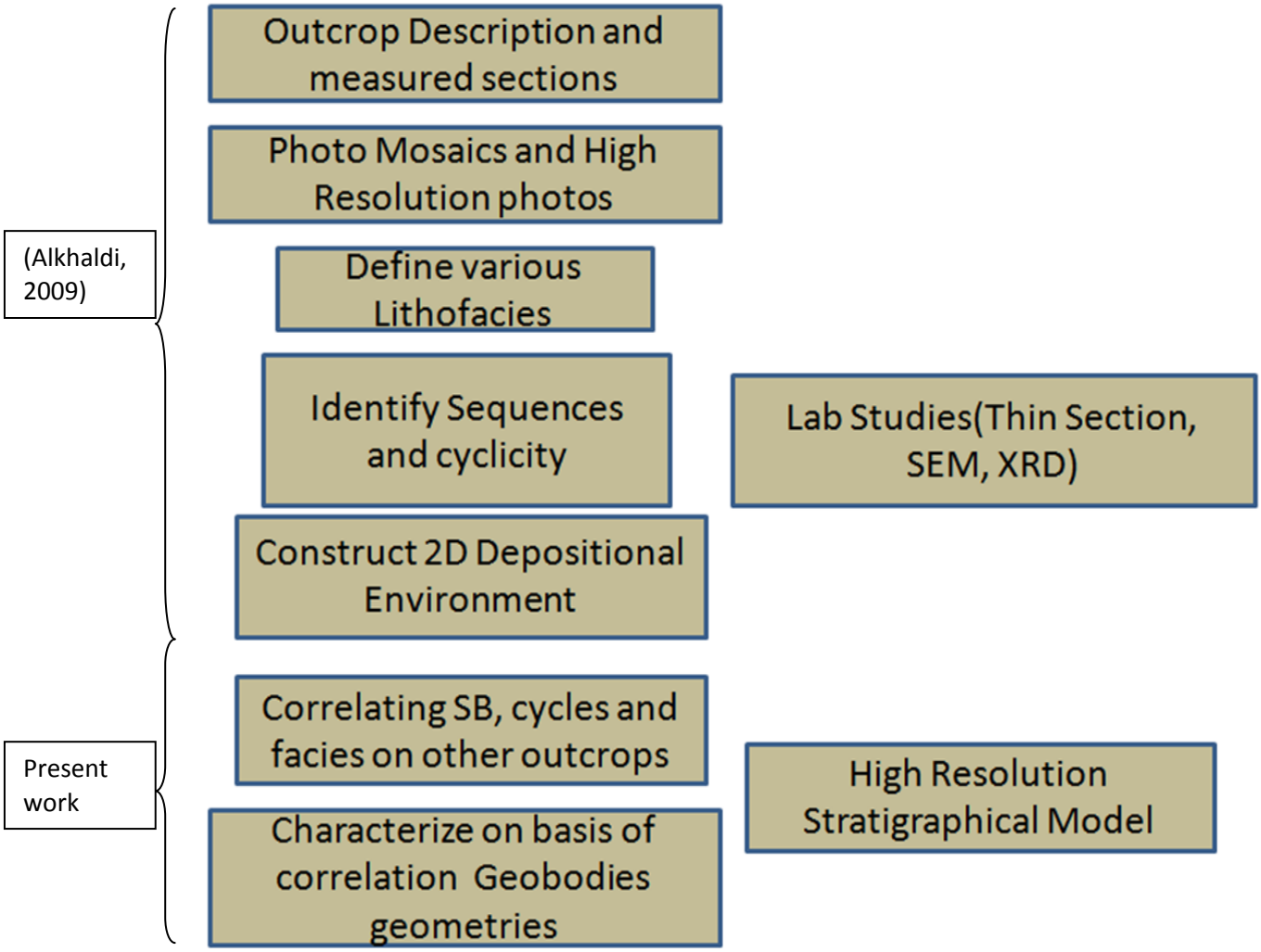

Figure-3.1.Methodology followed in the study is represented here.Field and lab are both integral part of this study. The same methodology was used by AlKhaldi (2009)

3.2. Research Plan

3.2.1. Methodology

The research plan involved seven steps, the first step was to describing the outcrop faces and measure sections, photo mosaic and high resolution photos, define different lithofacies based on grain types using Dunham classification, identify sequence and cyclicity, added with lab studies on thin sections, SEM and XRD, construction of 2D depositional environment, correlating sequence boundary, cycles and facies on outcrops, development of high resolution stratigraphic models and constructing carbonate geobodies. The other steps include finding

cyclicity archived in the outcrops, and constructing construct stacking patterns based on the cyclicity (Figure 3.1).

3.2.2. Field Investigation

The field mapping process included both vertically and laterally to completely describe the detail lithostratigraphic mosaic and to select locations of vertical stratigraphic sections (Figure-3.1). Photomosaic and high resolution photographs were taken in the initial stage of the field work. The high resolution photos were used to describe and map the stratigraphic units and document important sedimentary textures and structures in the beds.

The sedimentary parameters that were documented in the field include color, grain size, bed thickness, bed numbers, mineralogy, grain type and size variation and, texture. The beds geometry of sand bodies, their vertical and lateral dimensions was documented. Bed contacts and surfaces were identified and described. The sedimentary structures (e.g. cross bedding, bioturbations surfaces, fractures est.) archived in the beds were noted and palaeocurrent measurements were carried out on cross bedding laminae. Photographs of important features were taken during this stratigraphic section description.

3.2.2.1. Lithostratigraphic Sections

The lithostratigraphic sections are an important part of the stratigraphic and sedimentological analyses. These section lines were selected at the outcrops. One to three sections taken close to each other were logged in outcrops. In the lithostratigraphic logs are described in terms on mineralogy, texture and sedimentary structures along with the facies thickness. On the basis of the high resolution interpretation of photos were used for the construction of photo mosaic and the locations are selected. These photos are described at their respective locations with the help of a legend to distinguish them from other rock facies in the outcrop. Facies association and facies relationship both vertical and lateral, sequences (high resolution sequences), sequence boundaries, stacking patterns and stacking boundaries.

3.2.2.2. Sampling

Each sample location were marked on high resolution photos and detailed sedimentological logs. These representative facies were traced laterally and when there was a

change in sedimentological parameters, a sample was taken and marked. Two or three samples were taken in thick beds depending upon their thicknesses and variability. The samples were taken from every representative facies. The samples were described to determine their fabric following the Dunham classification scheme.

3.2.2.3. Palaeocurrent analysis

Palaeocurrent data provide useful information on paleogeography, paleoslope and current direction and as such, they for interpreting source of sediments in a sedimentary facies Palaeocurrent is important attribute of a lithofacies and complete description. Palaeocurrent measurements were carried out on the cross bedded, channelized sandstone and the high energy limestone facies in the studied outcrops.

3.2.2.3.1. Sedimentological Analysis

The detailed outcrop sedimentology and thin section studies led to the identification of the different lithofacies were in the investigated outcrops. The parameters used in the lithofacies identification include the grain type, Dunham texture, fossils and sedimentary structures. These facies are grouped into facies associations based on their depositional environments(Figure- 3.1; Köhrer et al., 2011).

3.2.2.3.2. Sequence Stratigraphy:

The 1-D sequence stratigraphy involved the determination of cyclicity and stacking patterns (Figure- 3.1). Parasequence and parasequence sets, and high frequency sequences (HFS) were identified. In turn this high frequency sequence. The composite sequence and high frequency sequences in this work is equivalent to S-1 is DM-1, S-2 HFS-1 is DM-2, S-2 HFS-2 is DM-3, S-3 HFS-3 is DM-4 and S-3 HFS-4 is DM-5.

3.2.2.3.3. Correlations:

The thickness variations between the different sections, lateral facies changes, cyclicity, sequence boundaries, number of cycles, differential subsidence and complex correlation geometries are basic criteria used for correlation. Thus the simple looking mixed carbonate-clastic were characterized in terms of high resolution stratigraphy.

3.2.2.4. Geometry

Carbonate Geobodies:

Measuring dimensions, shapes and orientations of geobodies provides with quantitative data for characterizing heterogeneity. Characterization of carbonate geobodies is important as they reflect the controlling factors on carbonate depositional environment (Jung, 2012).These depo-elements are basically facies associations and architectural elements. As an example depo-shape (mound shaped) is made up of core and flanks as elements. Depo-facies are in turn, the units of depo-elements, and are classified on the basis of grain types, sedimentary structures, Dunham texture and porosity.

3.2.2.5. Polished Slabs

The samples collected during the field work were slabbed and polished for further analyses. These polished slabs were studied using binocular stereoscopic microscope to identify the mineralogy and textures. Polished slabs provide valuable information in terms of sedimentary structures and texture. The slabs were photographed using special stage having a scale. The slabs were mounted on china clay to make it exposed to maximum light. In the process of taking the photographs, the camera resolution was set for each sample. Once all the slab photographs were collected, they were uploaded into the Corel Draw 13 for digital description.

3.2.3. Laboratory Studies

The laboratory studies were conducted to support the field observations. The thin sections were described in terms of grain type, fossil type, grain size, porosity type and percentages and effective porosity type.

3.2.3.1. Petrographic analysis

The rock samples were used to prepare thin sections for petrographic analyses. The thin sections were studied using petrographic microscope to identify their mineralogical content, grain size, and other textural attributes.

Scanning electron microscopy (SEM), X-Ray Diffraction (XRD) and X-Ray Florescence (XRF) studies were also carried out on selected representative samples from each lithofacies to determine their mineralogical compositions. Apart from using SEM for mineralogical determination, it was also used to identify grain types and dissolution.

CHAPTER 4

RESULTS

LITHOFACIES ANALYSIS

4.1. Introduction

The lithofacies in Dam formation are first divided on to carbonate and siliciclastic. The grain supported lithofacies are subsequently classified on the basis of the grain type in to skeletal and non-skeletal components. The mud-supported lithofacies classified either as mudstone or microbial (stromatolitic facies). Based on these criteria seventeen lithofacies, were identified in five outcrops along NW-SE transect across the Al-Lidam Area. The division of lithofacies is based on texture, sedimentary structures, thin section petrography fossil contents and other characteristic features. The identified lithofacies are presented in (Figures 4.1):

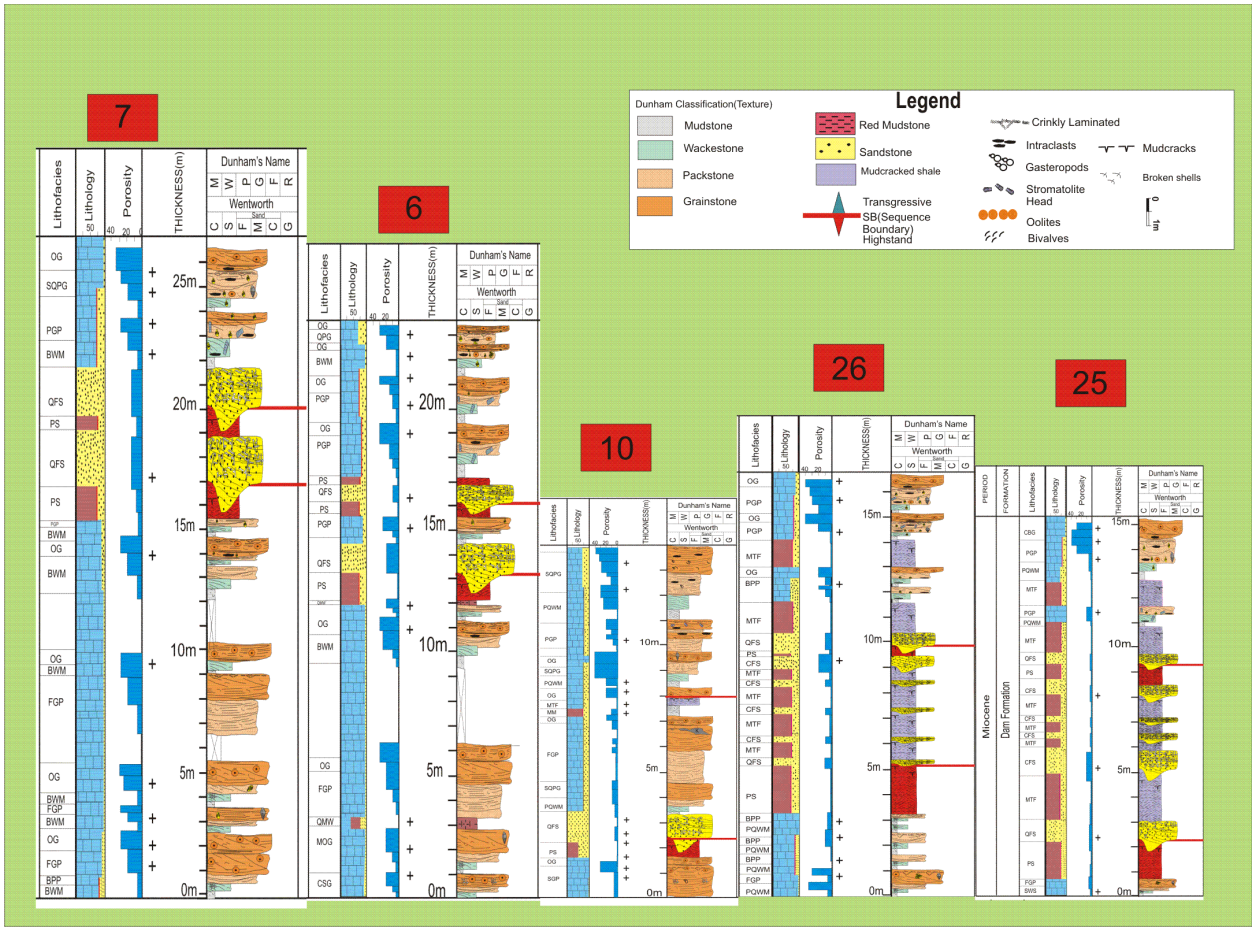

Figure-4.1. Representative sedimentological logs from the studied outcrop sections illustrating vertical facies relationships, vertical scale in meters.

4.1.1. Coated Skeletal Grainstone (Csg)

The basal lithofacies encountered in the Outcrops-6 and 7, is the coated skeletal grainstone facies. The base of this lithofacies is not exposed. This facies is present in outcrop 6, but thins in outcrop 7 is characterized by abundant skeletal fragments. The base of this lithofacies is not exposed at the outcrops. It is also present in outcrop 26 where skeletal fragments became very abundant and the mud content decreases. This is found below the oolitic foram-grainstone, intraclastic skeletal facies and intraclastic oolitic skeletal grainstone facies.

This tan to cream lithofacies which is about 1.9 to 2m thick consists of coated grains, skeletal (mostly bivalves fragments, peloids) and ooids grains. The grain size ranges from medium to coarse with some pebble size, subangular to rounded, and poor to moderately sorted (Figure 4.2). Bioturbations and cross bedding are the dominant sedimentary structures in the facies (Figure 4.2). The skeletal grains were dominantly dissolved to form moldic porosity. The range of porosity in this facies varies from 25% to 30% (Figure 4.2b). The XRD analysis shows that the facies is composed of dominantly carbonate with minor amount of quartz (5%) suggesting the dominance of carbonate accumulation.

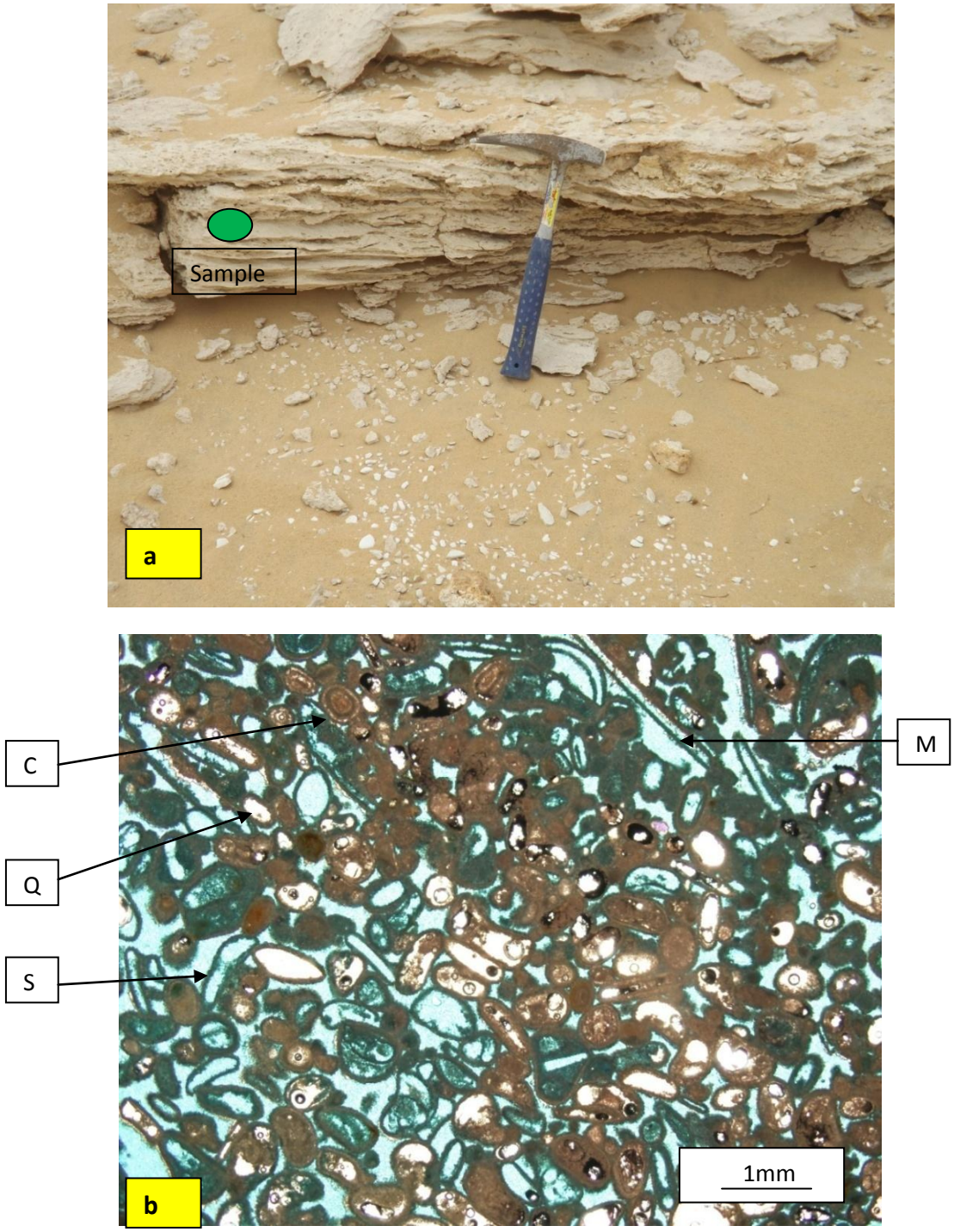

Figure 4.2 a) Field photograph showing coated grains skeletal grainstone facies, cross bedding, Outcrop 6 photograph of the Dam Formation, in Al-Lidam Area, b) Photomicrograph of a sample from the facies, showing skeletal fragments; Note large size of the skeletal fragments having micritised envelopes. Micritised grains, medium sand to pebble size. The average porosity in the section is around 15-20%. C=coated grains, S=skeletal, M=moldic, Q=quartz

4.1.2. Coated bioclastic grainstone (Cbg)

The coated bioclastic grainstone facies (Cbg) which is, characterized by rich in bioclastic fragments overlies the Csg facies. Cbg facies is prominently present in Outcrop 10 and thins out in Outcrop 7. It is encountered in outcrop 25 skeletal fragments became very abundant. This facies is found below the skeletal wackestone and quartzose mudstone facies.

This tan to cream lithofacies which is about 1.0 to 1.2m thick consists of bioclasts (bivalves and gastropods), and coated grains. Bioclasts are the dominant grain types in the lithofacies. The grain are from medium to coarse with scattered pebble size, subangular to rounded, and poor to moderately sorted (Figure 4.2a). Some bioclasts are completely micritised and have no internal structure. Crinkled lamination is the dominant sedimentary structures in the facies (Figure 4.2). The grains were dominantly dissolved to form moldic porosity. Bivalves are the dominant grain type ranges from very coarse to granule size. This facies is differentiated on the presence of crinkly lamination as compared to cross bedding in Csg, and presence of coarse peloids, fine grained coated grains, and absence of quartz grains.

The porosity this facies ranges from 25 to 30% (Figure 4.2b). Facies is composed of 100% carbonate minerals. The SEM images of CBG facies, show dissolved bioclasts (Figure 4.2c). EDS analysis shows abundance of Ca, Mg and Si indicate presence of clays (Figure 4.2d).

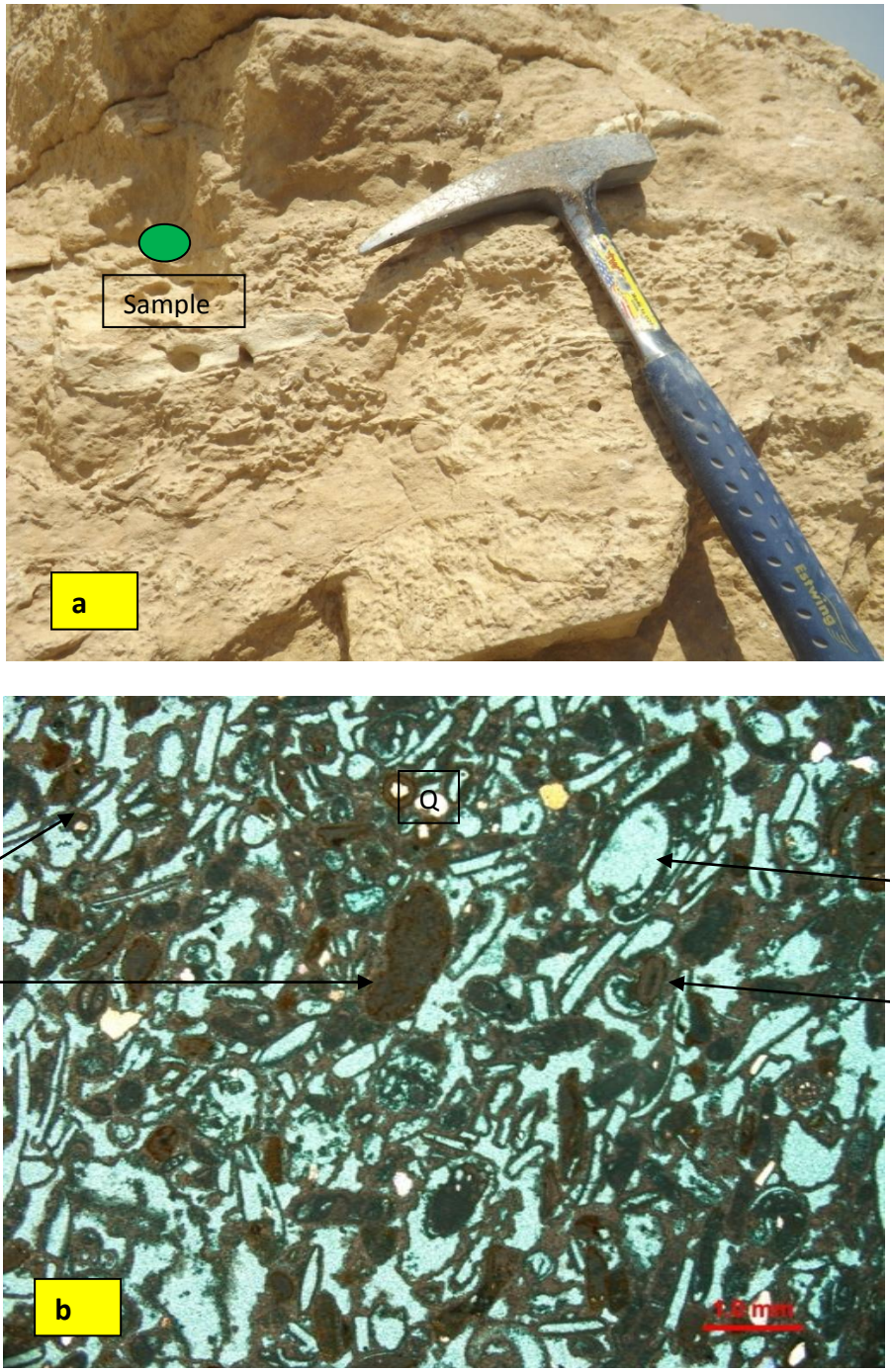

Figure 4.3 a) Coated bioclastic grainstone facies, Outcrop 25 photograph of the Dam Formation, in Al-Lidam Area, b) Photomicrograph of a sample from the facies, showing bioclastic fragments; Note large size of the bioclasts fragments having micritised envelopes. Micritised grains, Medium sand to very coarse size. Moldic porosity with whole grain dissolved. The average porosity in the section is around 15-20%. C=coated grains, S=skeletal, M=moldic, P=peloids.

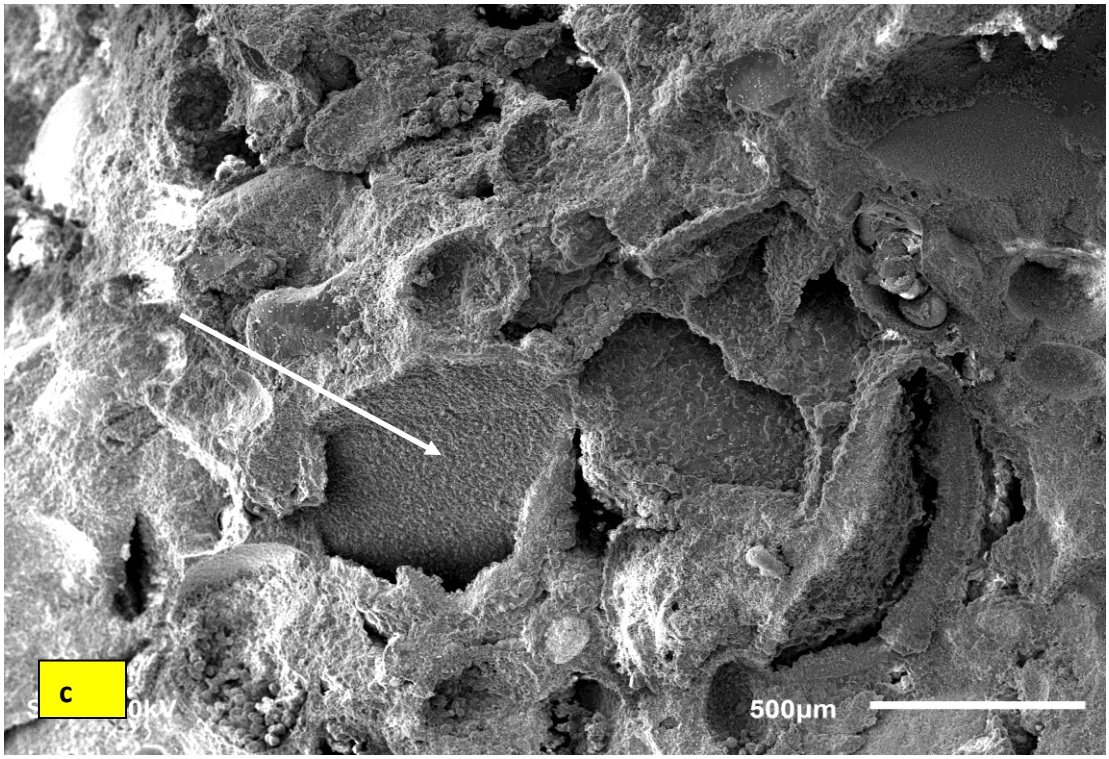

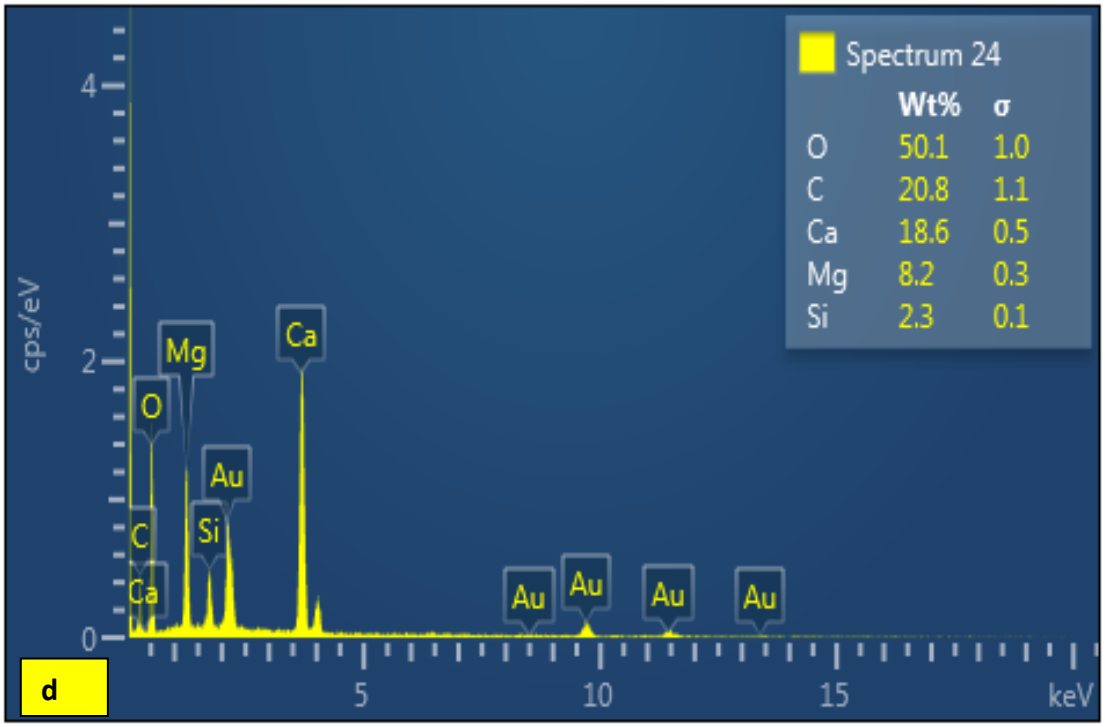

Figure 4.3c) SEM image of coated bioclastic grainstone facies, showing dissolved bioclasts, d) EDS analysis shows abundance of Ca and Mg.

4.1.3. Peloidal Burrowed Wackestone (Pbw)

Facies which overlies foraminiferal bioclastic grainstone-packstone facies is present in two cycles in outcrop-26 and it overlies the micritized ooid grainstone in outcrop7. It is also present at the base of a cliff forming interval in outcrop 10 the thickness of this facies ranges from 0.5 to 1.5m. This facies is associated by Laterally Linked Hemispherical (LLH) stromatolites which overlies tidal flats sand/mud, and graded upward to digitate stromatolites. The LLH stromatolites which are present in medium to thick beds, around 10-20cm diameter, 4 cm thick, it is overlain by branching digitates that are of 1.5cm diameter and 10cm high. The matrix between the successive heads is composed of peloids, intraclasts grains (Figure-4.4). The stromatolites are found to be nucleating around the intraclasts and scoured surfaces.

The fine grain few bioclasts and quartz particles are important constituents of this facies. The porosity ranges in this facies ranges from less than 5-7% (Figure 4.4b).XRD analysis shows that the facies is composed of more than 86% carbonate and 14% quartz and accessory minerals. A part of the thin section shows evidence of burrowing containing grainstone fabric derived from a pre-existing bed(Figure 4.4b). SEM image shows dissolved skeletal fragment at 100 microns, note the dissolved bioclast and white colour quartz grains (Figure 4.9c). The EDS high Ca, Mg and Si and shows clay palygorskite in this facies (Figure 4.9d).

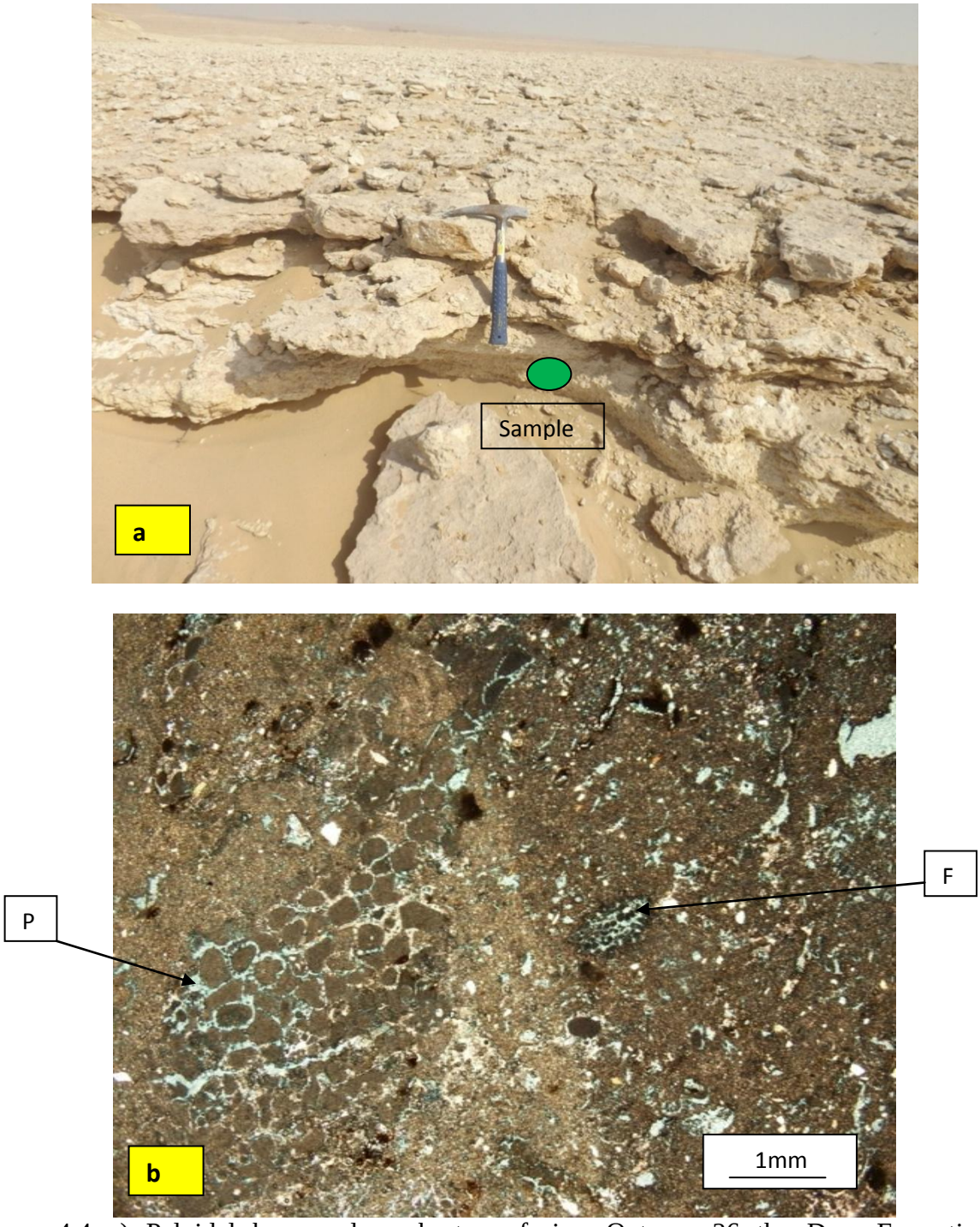

Figure 4.4 a) Peloidal burrowed wackestone facies, Outcrop 26 the Dam Formation, b) Photomicrograph of a sample from the facies, showing burrows filled by grain dominated fabric; Note fine size of the peloids fragments and scattered shell fragments having micritised grains, Medium sand to very coarse size, Mainly moldic, intragranular and burrowed porosity. The average porosity in the section is around 5-10%.P=Peloids, F=Forams.

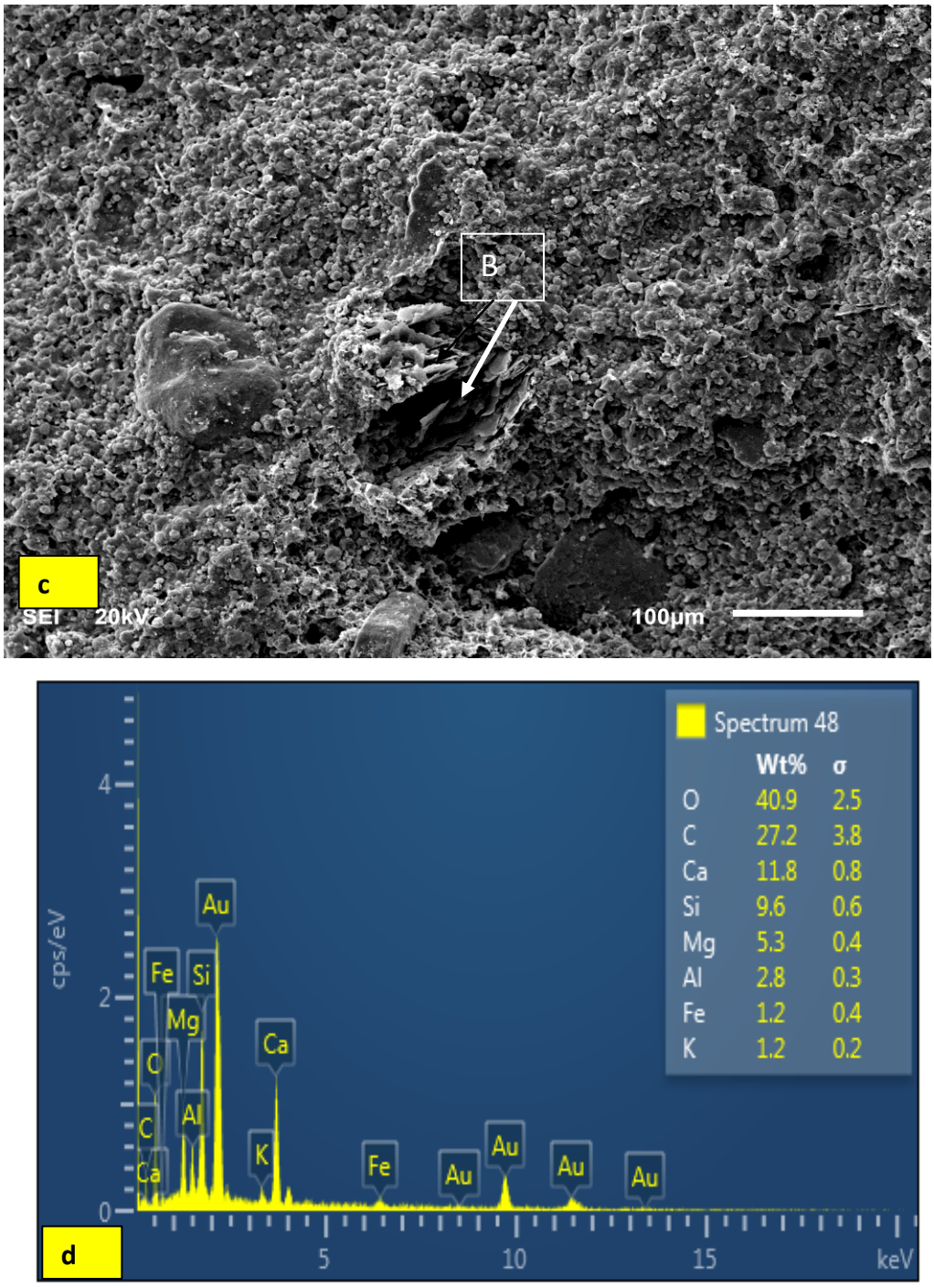

Figure 4.4c) SEM image of peloidal burrowed wackestone facies, showing dissolved fine bioclasts in carbonate mud, the dominant are grains here, d) EDS analysis shows abundance of Ca, Si and Mg. B=bioclasts

4.1.4. Bioclastic peloidal grain-dominated packstone (Bpp)

This lithofacies underlies the marl facies in Outcrops 25 and overlies the coated bioclastic grainstone facies in Outcrop 10(Figure 4.5a). The beds of this facies are highly lithified and have sharp contact with the underlying marl facies. The beds laterally change in thickness and their geometry is controlled by the overlying facies. Facies varies in thickness from about 0.5-1.2m and consists of light pink to tan colored, fine to medium grained and moderately to poorly sorted grains. The main grain types present are molluscs, others skeletal grains, intraclasts and coated grains. The skeletal grains are in micritised envelopes.

The grain size ranges from medium sand to few pebble size grains are also present. The porosity in this facies ranges from 2 to 5% (Figure 4.5b). Facies which is composed of 95% carbonate and 5% quartz, and show dominance of carbonate accumulation.

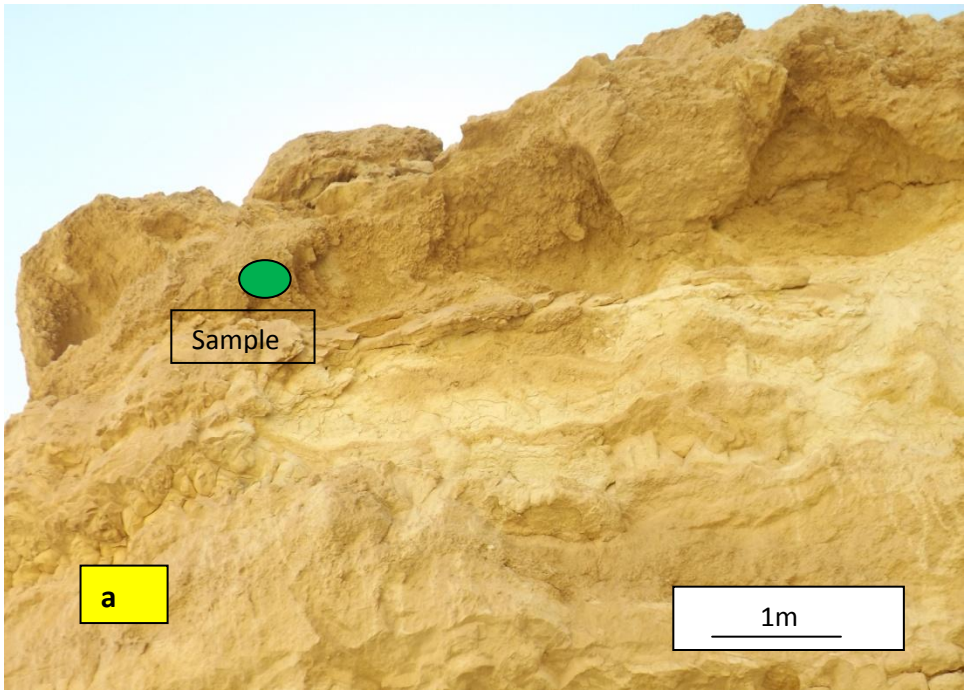

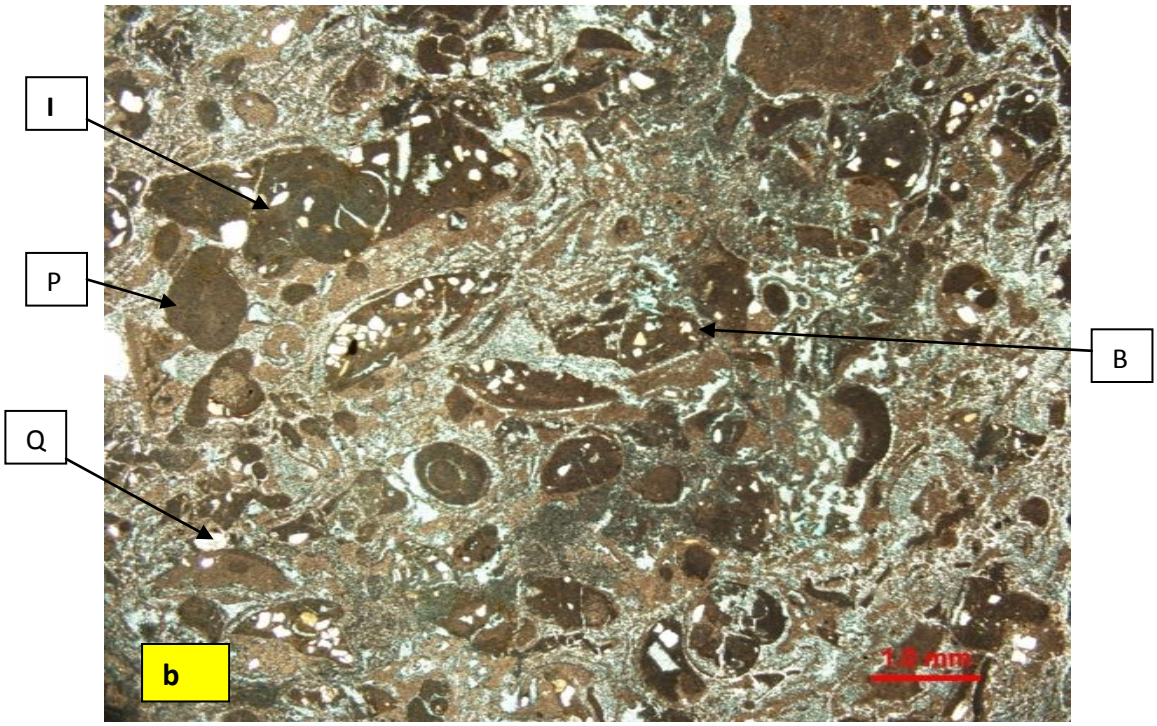

Figure 4.5 a) Bioclastic peloids packstone facies in Outcrop 26 of the Dam Formation, b) Thin section of a samples from the facies, showing peloids; Note different size of the bioclasts fragments having micritised grains, very coarse size bioclasts, coarse peloids and some intraclasts and is highly cemented. I=intraclasts, Q=quartz, B=bioclasts, P=peloids.

4.1.5. Ooid grainstone (Og)

This 0.2-1m thick, creamy white to tan, medium grained facies is dominantly composed of ooids (Figure 4.6a). The ooids are well rounded and well sorted. This facies is characterized by very low angle cross-bedding. The facies occurs above the skeletal quartzose packstone grainstone facies and coated bioclastic grainstone facies in Outcrops 6 and 7. It overlies the miliolid mudstone facies in Outcrop 26 and the formaniferal grainstone facies in Outcrop 10. It marks the top of cycles and has a sheet-like geometry. It is correlatable across Outcrops 6, 7 and 10. In the top cycles, the beds are dominated by intraclasts (of coated grains) and skeletal particles along with ooids, hence marking a slight transition in environment to skeletal banks and shifting of facies with sea level changes.

In addition to low angle cross-bedding, crinkled lamination and mudcracks are present in parts of the lithofacies intervals. Molds of molluscs and forams are present in this facies. The skeletal grains also show grading in bedding. Some of the ooid grains are leached molds. The porosity in this facies ranges from 15 to 20% (Figure 4.6b). This facies is composed of more than 95% carbonate and accessory minerals. Most of the pores are intergranular and moldic porosity. The ooids and skeletal grains are covered by micritised envelopes. Grains are freely packed and dominant cement type is meniscus and it bounds rounded pores.

SEM images shows ooid grains at 500 microns and enlarged ooid grain (Figure 4.6d, e) at 50microns. It also shows micritic mud coating see the grains coating on the ooid, this coating is of micrite mud (Figure 4.6d, e). The EDS analysis shows moderate Mg and Ca concentrations suggesting the possibility of dolomitization of this facies (Figure 4.6f).

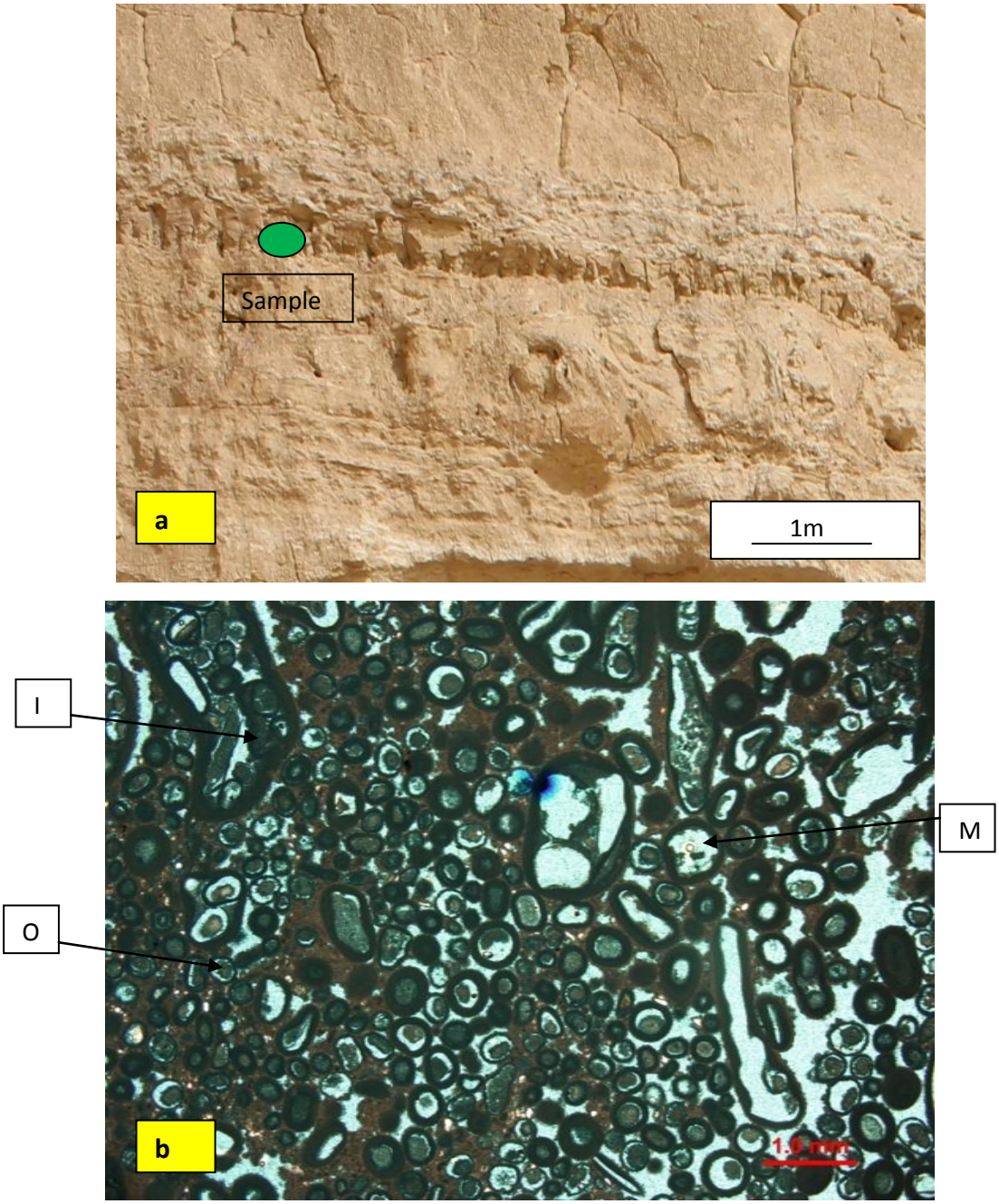

Figure 4.6a) Ooid grainstone facies in Outcrop 6 of the Dam Formation, showing crinkly lamination, b) Thin section of a samples from the facies, showing ooids; Note medium to coarse size of the ooids, some skeletal fragments with having micritised envelopes, very coarse size, coarse peloids and some intraclasts, moldic porosity. The average porosity in the section is around 15-20%. O=ooids, I= Intraclasts, M=moldic.

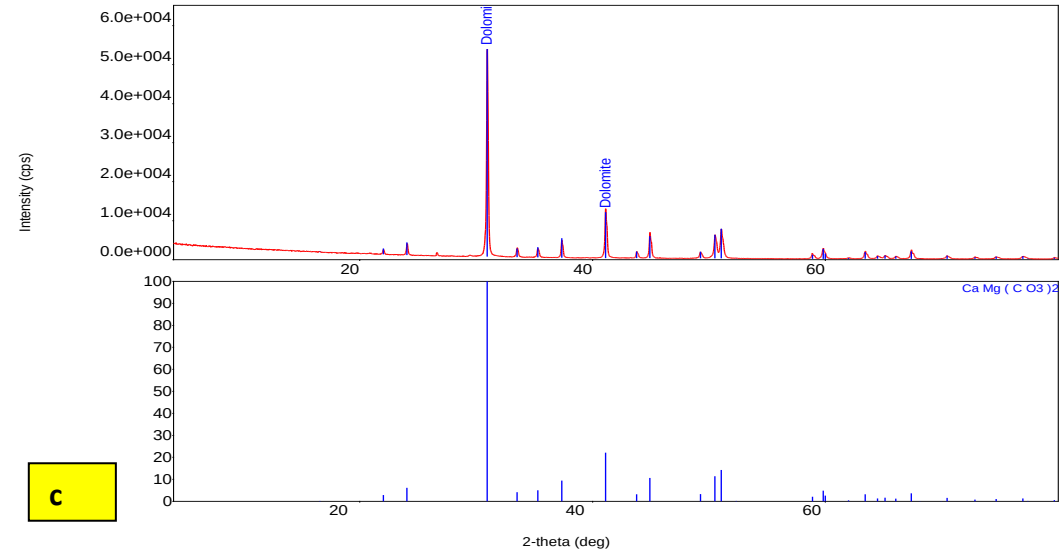

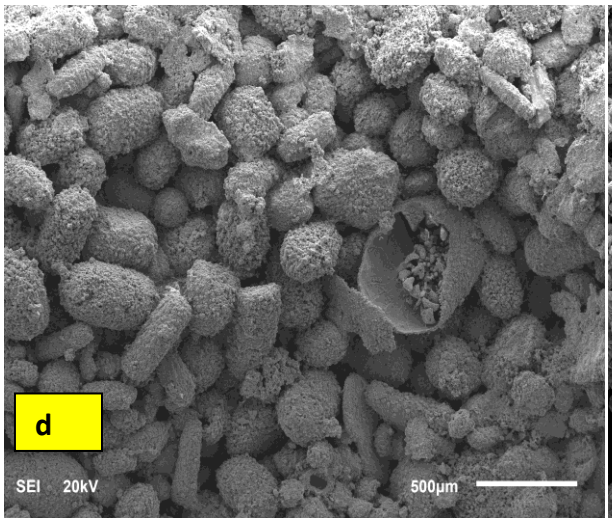

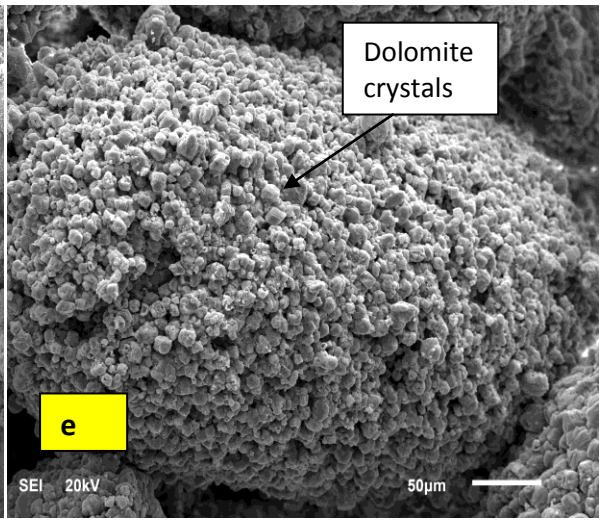

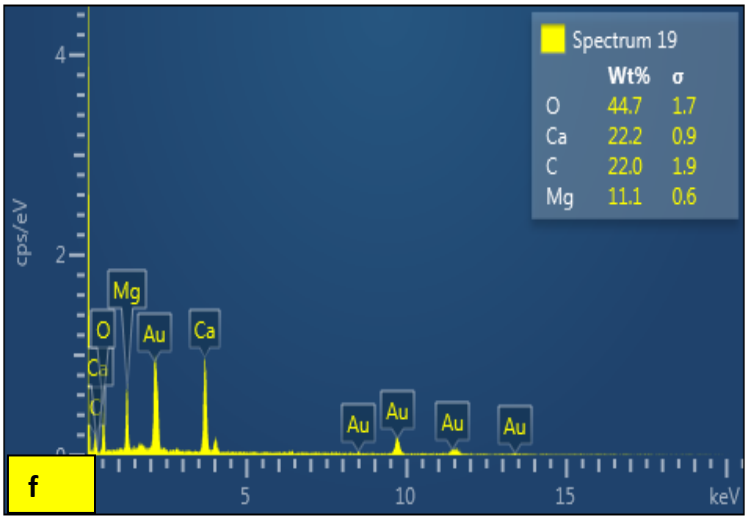

Figure 4.6c) XRD analysis representing dominance of carbonate minerals, d)SEM images of ooids, having some broken shells, f) enlarged image of ooid having micritic crust on it, d) EDS analysis shows abundance of Ca and Mg.

4.1.6. Micritised oolitic peloidal grainstone (Mpg)

This well sorted, light brown to tan colored, facies is massively bedded at its base and is characterized by well-preserved cross-bedding near the top. The thickness of this facies ranges from 0.5-2m with individual bed thickness of about 20cm. Carbonate grains are dominated by well sorted ooid grains or fine to medium grained size. Crinkled lamination and mudcracks are present as sedimentary structures capping the cycles. Some of the molluscs and forams show moldic porosity (Figure 4.7b).

This facies is the most frequent facies in all the studied outcrops. It occurs above the skeletal wackestone to packstone facies (Figure 4.7a). In outcrop 6, it is bounded on top by the oolitic grainstone facies and by the foraminiferal skeletal grainstone facies at the base. In outcrop 26, it is bounded on base and top by coated skeletal grainstone facies which shows cyclicity in facies. This bed laterally pinches out and grades in to other facies like the contorted with cross bedded wackestone facies. Mineralogically the XRD analysis shows the dominance of carbonate minerals (Figure 4.7c) and the EDS analysis shows abundance of Ca, Mg and Si (Figure 4.7e).

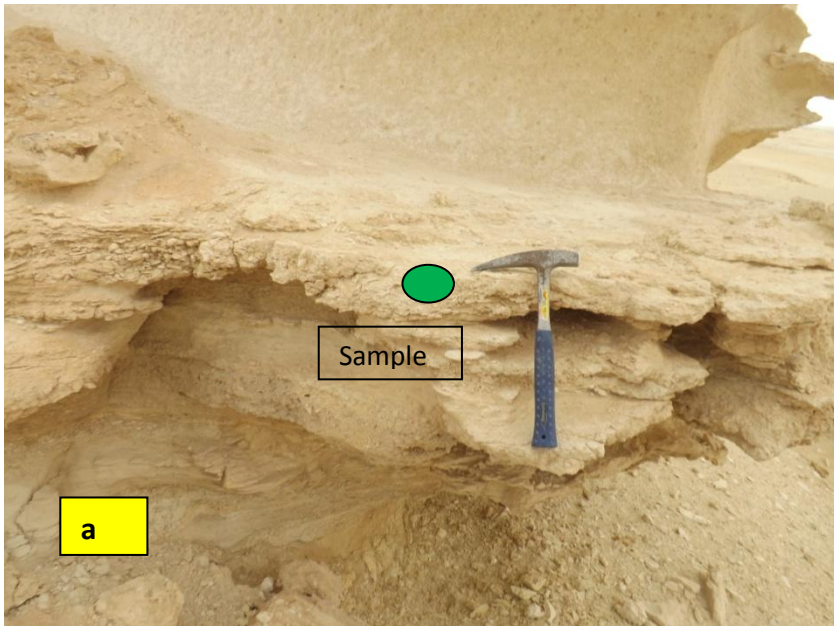

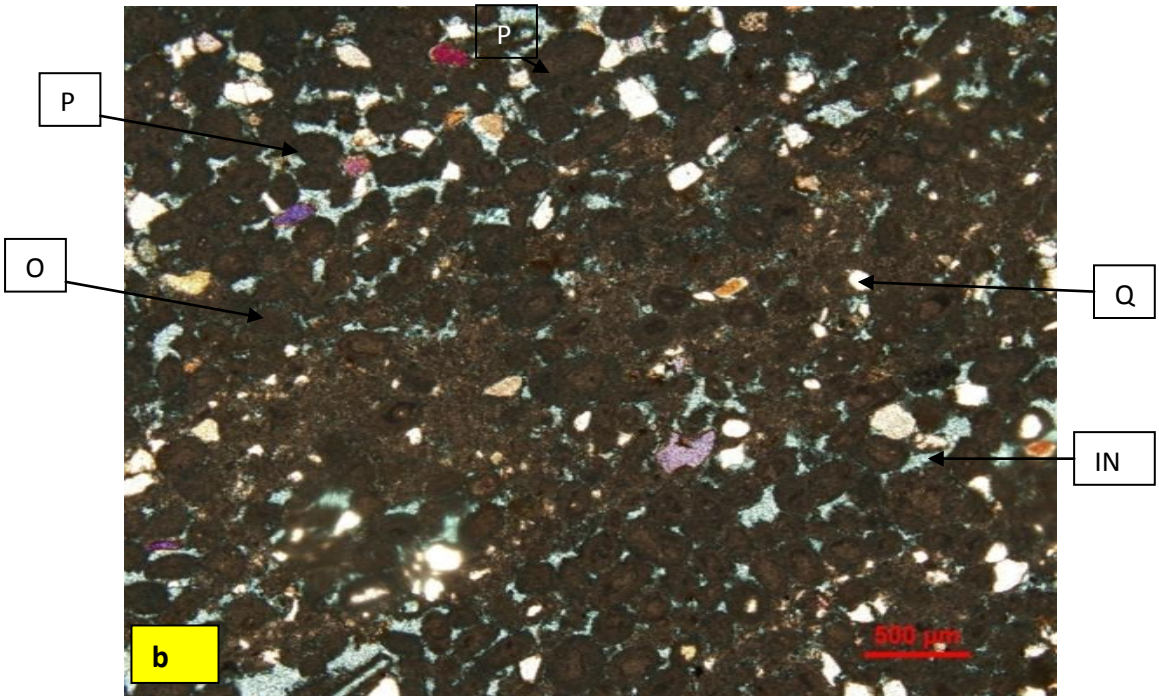

Figure 4.7a) Micritised oolitic peloidal grainstone facies in Outcrop 6 of the Dam Formation, showing crinkled lamination, b) Thin section of a sample from the facies, showing Micritised ooids(O); Note the medium size of the ooids, peloids (P) and some skeletal fragments having micritised envelopes, intergranular porosity(IN), Quartz=Q. The average porosity in the section is around 5-10%.

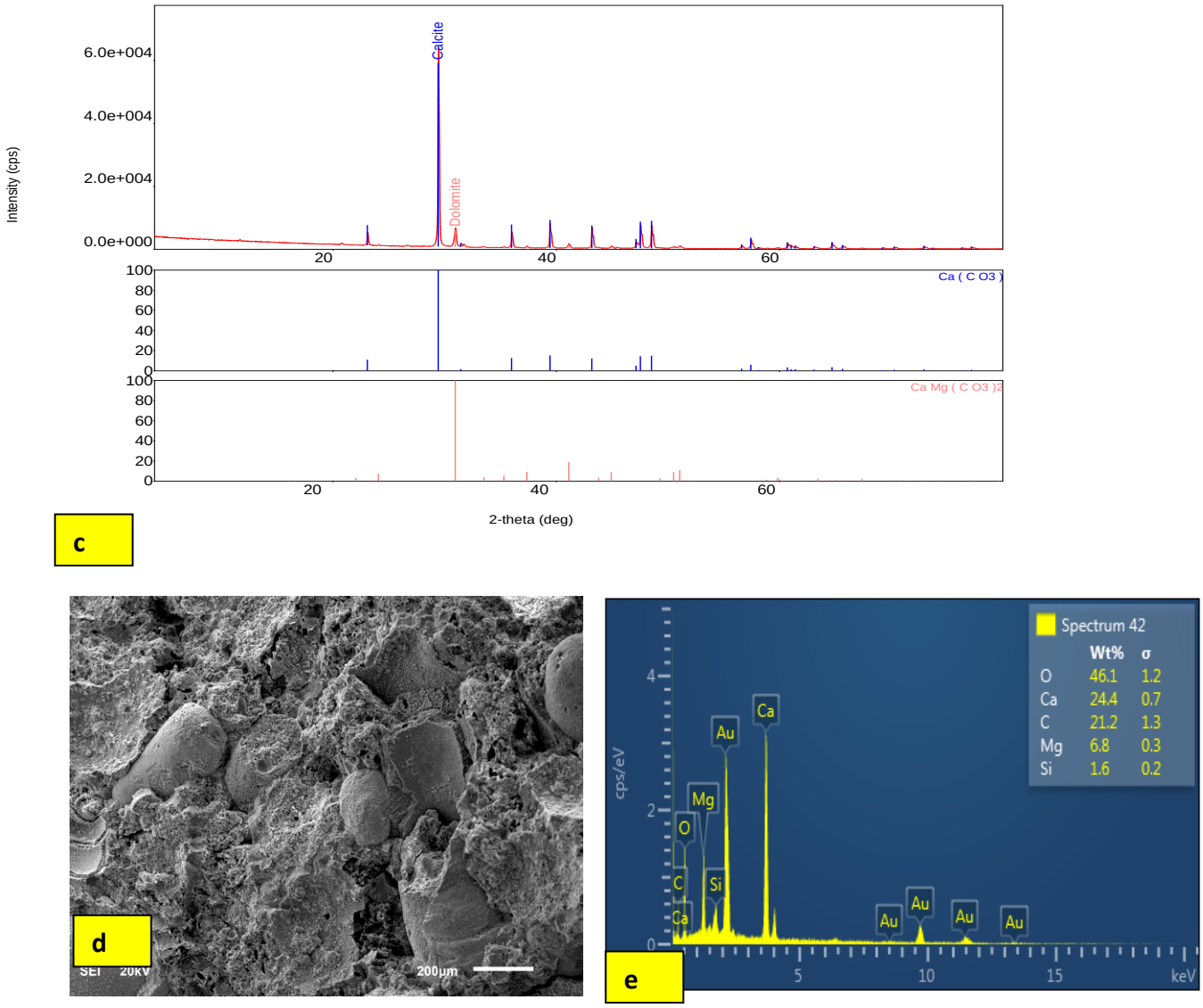

Figure 4.7c) XRD analysis representing dominance of carbonate minerals, d) SEM images of micritised ooids, having some broken shells, e) EDS analysis shows abundance of Ca, Mg and Si.

4.1.7. Sandy peloidal skeletal grainstone (Spg)

This facies is about 1m thick.It consists of light pink to tan colored, fine to medium grained sediments. The main grain types present are molluscs, quartz, skeletal grains and coated grains. Some intraclasts also present in its beds in Outcrop 26.This lithofacies underlies the peloids grainstone facies in Outcrops 6. The beds of this facies are highly lithified and have sharp contact with the overlying facies. The beds laterally change in thickness and their geometry is controlled by the overlying facies. The skeletal grains in the facies are dissolved to form moldic and shelter porosity types. The size of bivalves, the dominant grain type, ranges from medium sand size to pebble size. The porosity in facies ranges from 10 to 15% (Figure 4.8b). The facies is composed of 70% carbonate and 30% quartz (Figure 4.8b). The skeletal fragments are in micritised envelopes.

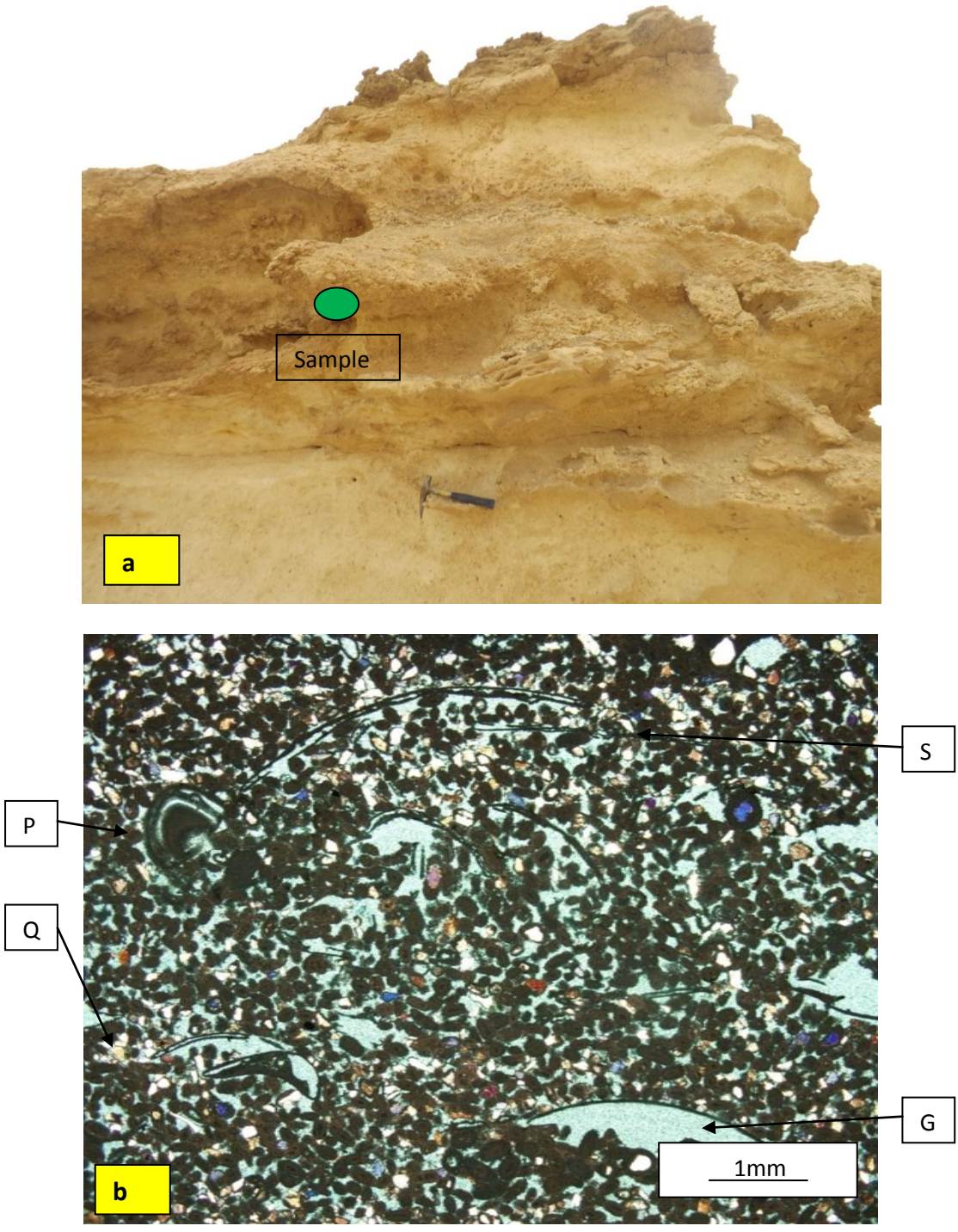

Figure 4.8a) Sandy peloidal skeletal grainstone facies in outcrop 6 of the Dam Formation, showing crinkly lamination, b) Thin section of a sample from the facies showing skeletal(S) and quartz particles(Q); Note medium grain size of the peloids(P), quartz, some skeletal fragments with having geopetal structure(G), and micritic envelopes on skeletal grains. The average porosity in the section is around 10-15%.

4.1.8. Dolomitic Skeletal Wackestone (Dsw)

This facies in the outcrop occurs as light to dark brown to buff colour beds. The bed thickness ranges from 0.5-1m (Figure 4.9b). This facies is present in both Outcrops 25 and 26 and the basal contact is not exposed. It is separated from the overlying sandstone facies by paleosols in outcrop 25. The main constituents of the facies are carbonate mud, rare skeletal and quartz (Figure-4.9c). The fine sand to very coarse sand and rare fine silt sized quartz particles are important constituents of this facies. The sediments are poorly to moderately sorted. The porosity in this facies ranges from less than 15-20% (Figure 4.9c). XRD analysis shows that the, facies is composed of more than >95% carbonate and less than 5% quartz and accessory minerals. The thin section image and the SEM and EDS show the presence of dolomitization and diagenesis.

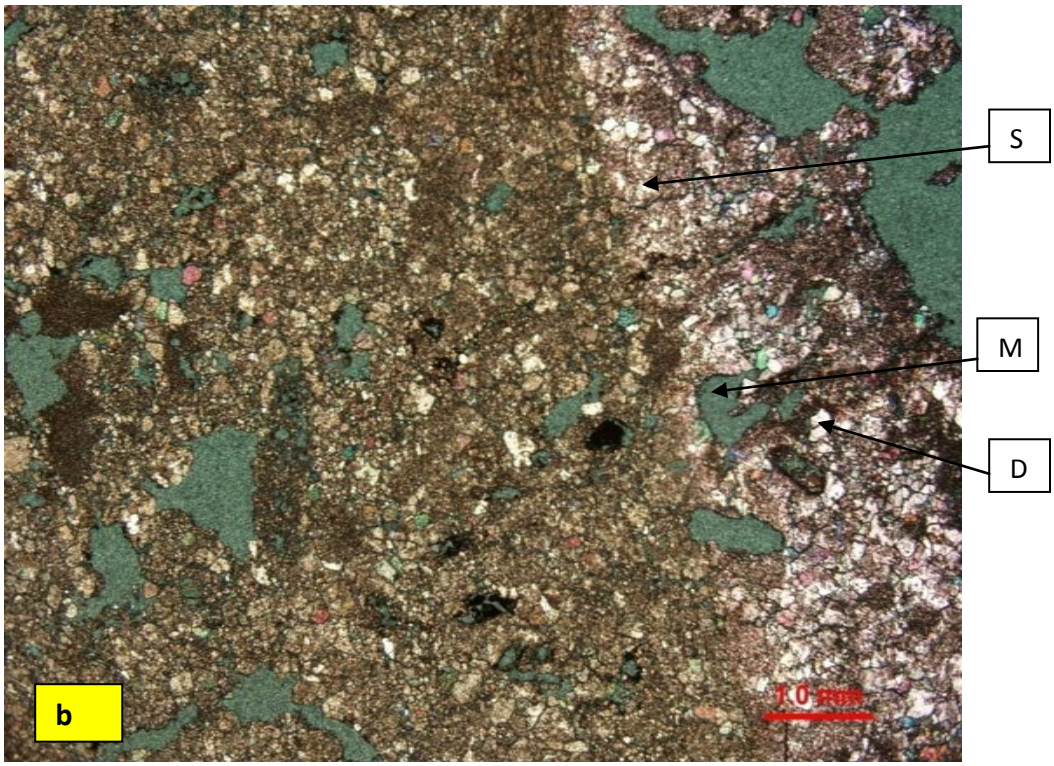

Figure 4.9 b) Dolomitic skeletal wackestonefacies Outcrop 25 of the Dam Formation, c) Thin section of samples from the facies showing skeletal and quartz particles; mouldic porosity. The average porosity in the section is around 5-10%. D=dolomite, S=skeletal, M=moldic.

4.1.9. Foraminiferal peloidal grainstone (Fpg)

Foraminfera peloidal grainstone facies occurs in outcrops as tan to creamy coloured. The bed ranges in thickness from 1-1.7 m (Figure 4.10a). This facies occurs above the coated skeletal grainstone facies, in outcrops 6, 7 10 and 25. It underlies the marl facies. It is crinkly laminated in some localities like in Outcrops-7 and 10, and shows its presence near the top contact with peloidal quartzose wackestone mudstone facies. In Outcrop 7 and 26 the skeletal are replaced by bioclasts and also result in increase in borings by organisms. In outcrop 6 the facies is dominated by skeletal fragments. The facies laterally is massive while here it is characterized by low angle cross-bedding. The dominant grain types are skeletal fragments of foraminferas, peloids and quartz. The grain size is dominantly coarse grained with some scattered pebble size. The particles are angular to subangular. SEM image shows foraminfera surrounded by micrite (Figure 4.10c). EDS analysis shows the absence of Si and hence the presence of Mg and Ca shows that facies contains dolomite which is minor (Figure 4.10d). The fine sand to pebble sized skeletal grains and fine silt sized quartz particles are important constituents of this facies. The porosity ranges in this facies from less than 15-20% (Figure 4.10c). XRD analysis shows that the, facies is composed of more than 86% carbonate and accessory minerals (Figure 4.9b).

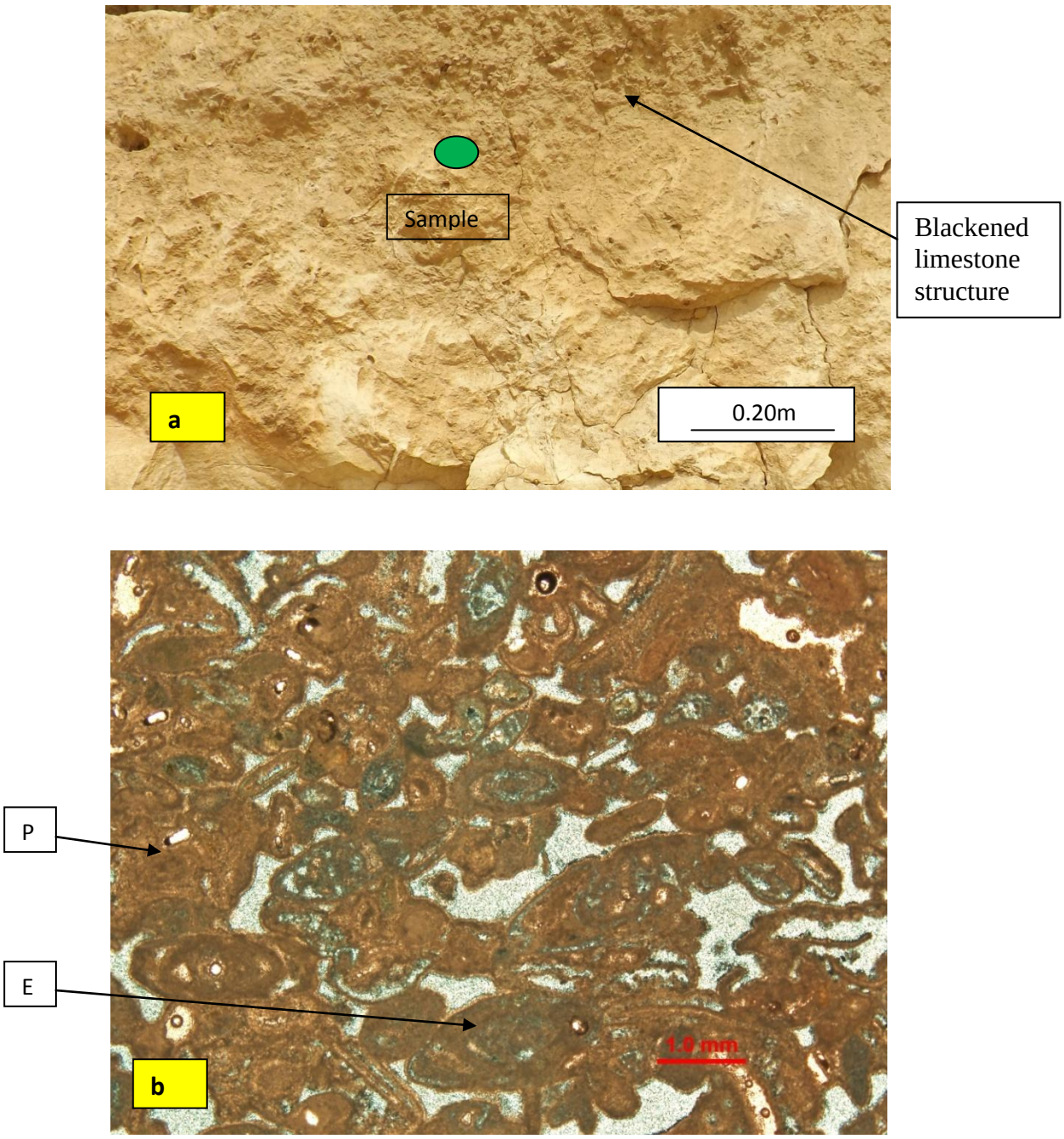

Figure 4.10a) Formaniferalgrainstone to packstone facies Outcrop 6 the Dam Formation, b) Thin section of a samples from the facies showingE=*Elphidium sp.*,Foraminifera and skeletal particles; Note medium to coarse size of the forams and skeletal fragments with, and intergranular and moldic porosity. The average porosity in the section is around 10-15%. P=peloids.

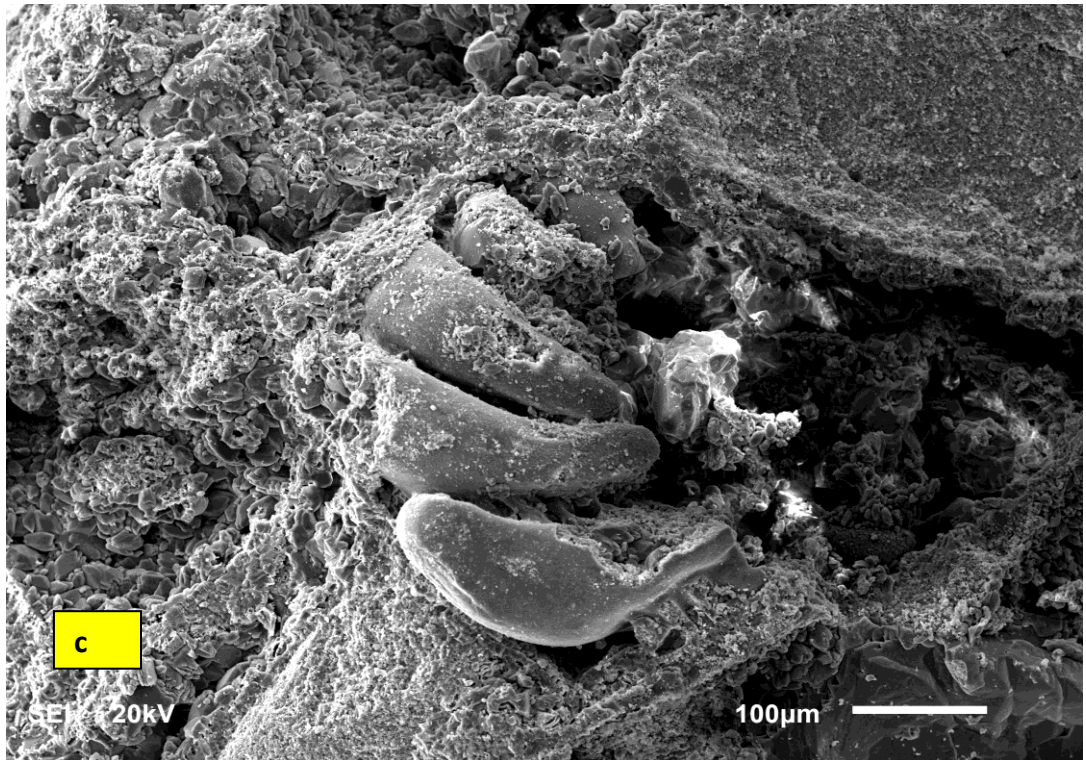

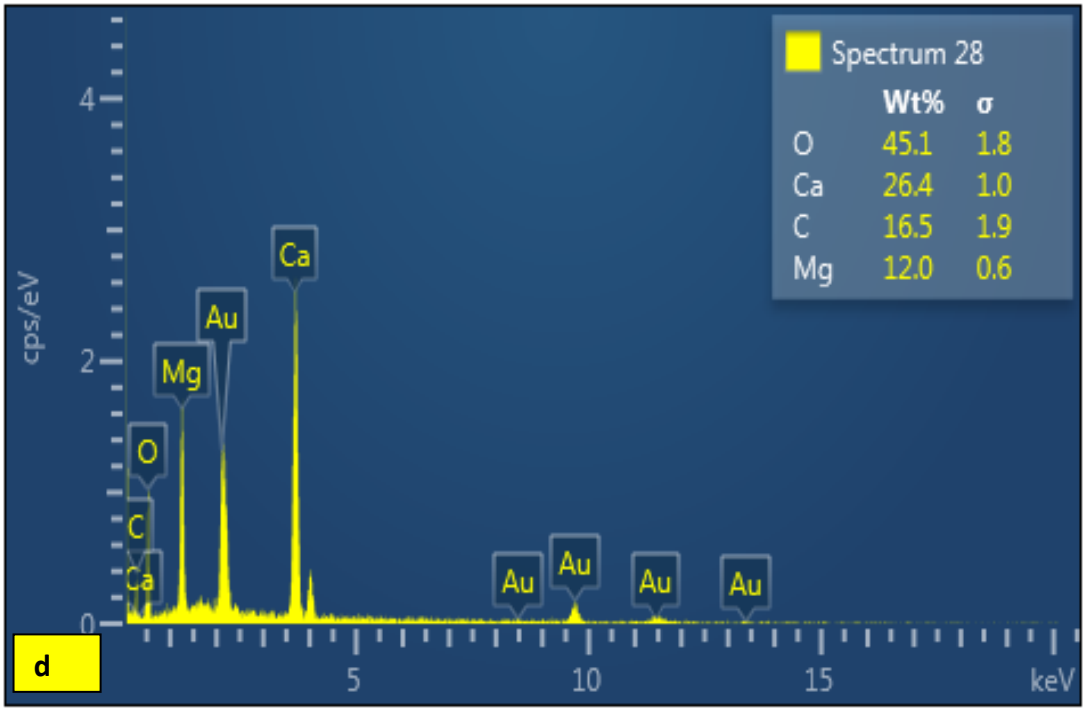

Figure 4.10c) SEM images of foraminfera in carbonate mud, d) EDS analysis of foraminfera (c) shows abundance of Ca and Mg.

4.1.10. Sandy Peloidal grainstone-packstone (Spgp)

This facies which is present in outcrop 6, 7, 10 and 25, marks the topmost facies of the cycles. It can be traced along the stratigraphic transect. The tan to dark brown coloured facies, this facies is overlies the peloidal quartzose wackestone mudstone facies (Figure 4.11a). In petrography this facies is composed of peloids, skeletal debris and quartz, with interparticle and intraparticle porosity. Grainsize for quartz and peloids dominate in Outcrop-6 and in overlying marl facies. It contains substantial amount of fine to medium grain quartz and it is marked by algal laminae and sharp grain boundary exists between quartz particles. The peloids are tightly packed, and show some deformation (Figure 4.10c). The facies ranges in thickness from 1-1.6m. Massive nature is characteristics of this facies, but on close examination crinkly lamination is observed. The grain size ranges from fine to medium size. The particles are moderately to poorly sorted. The quartz particles are angular to subangular. The porosity ranges in this facies from less than 5-10% (Figure 4.11b). XRD analysis shows that the, this facies is composed of more than >60% carbonate and 40% quartz and accessory minerals. SEM image shows dissolved oncoids surrounded by mud (Figure 4.11c).

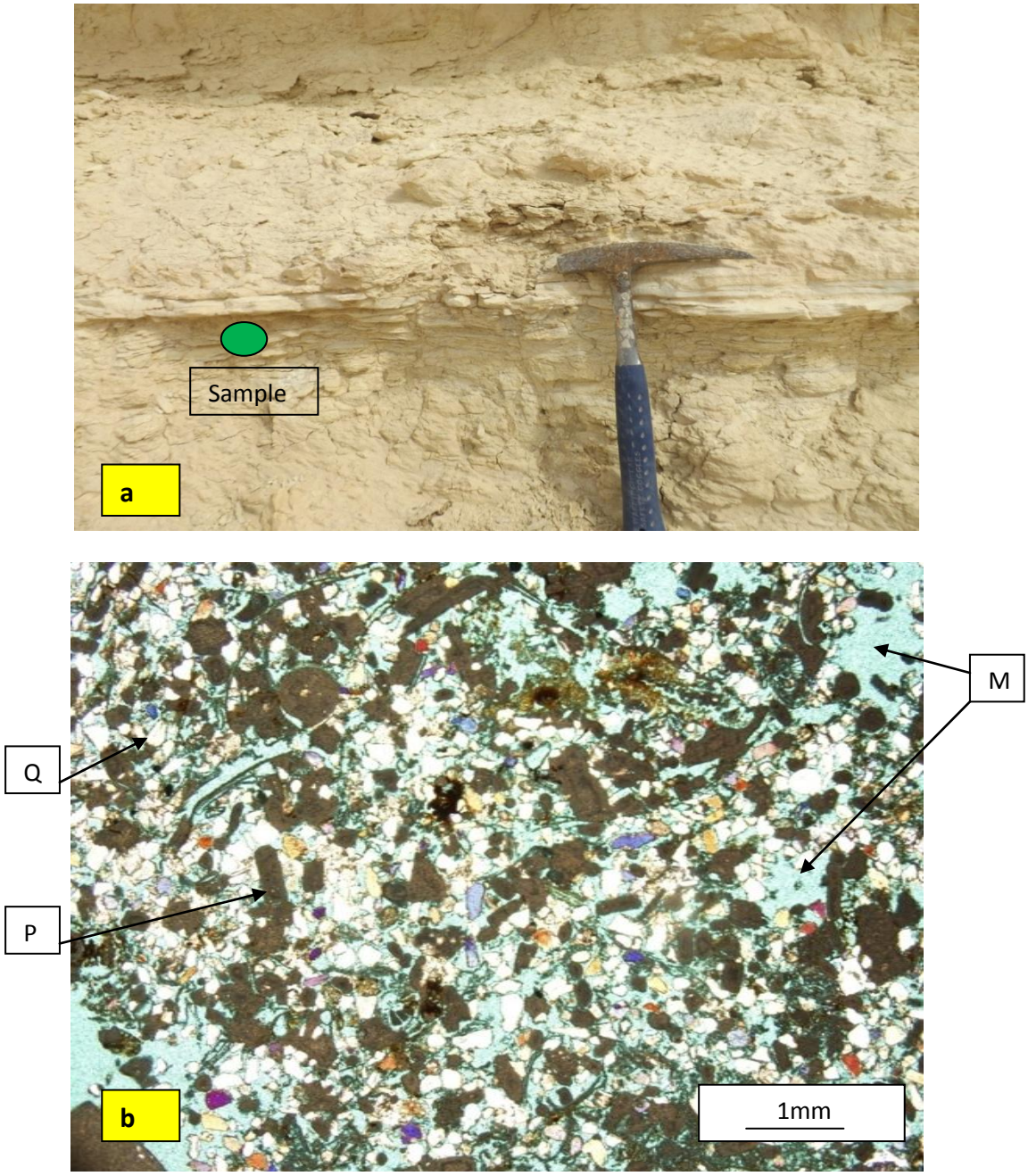

Figure 4.11a) Sandy peloidal grainstone-packstone facies, outcrop 26 photograph of the Dam Formation, b) Thin section of a sample from medium grained peloids(P) and quartz(Q) ; Note medium size, intergranular and moldic porosity(M). The average porosity in thin section is around 15-30%.

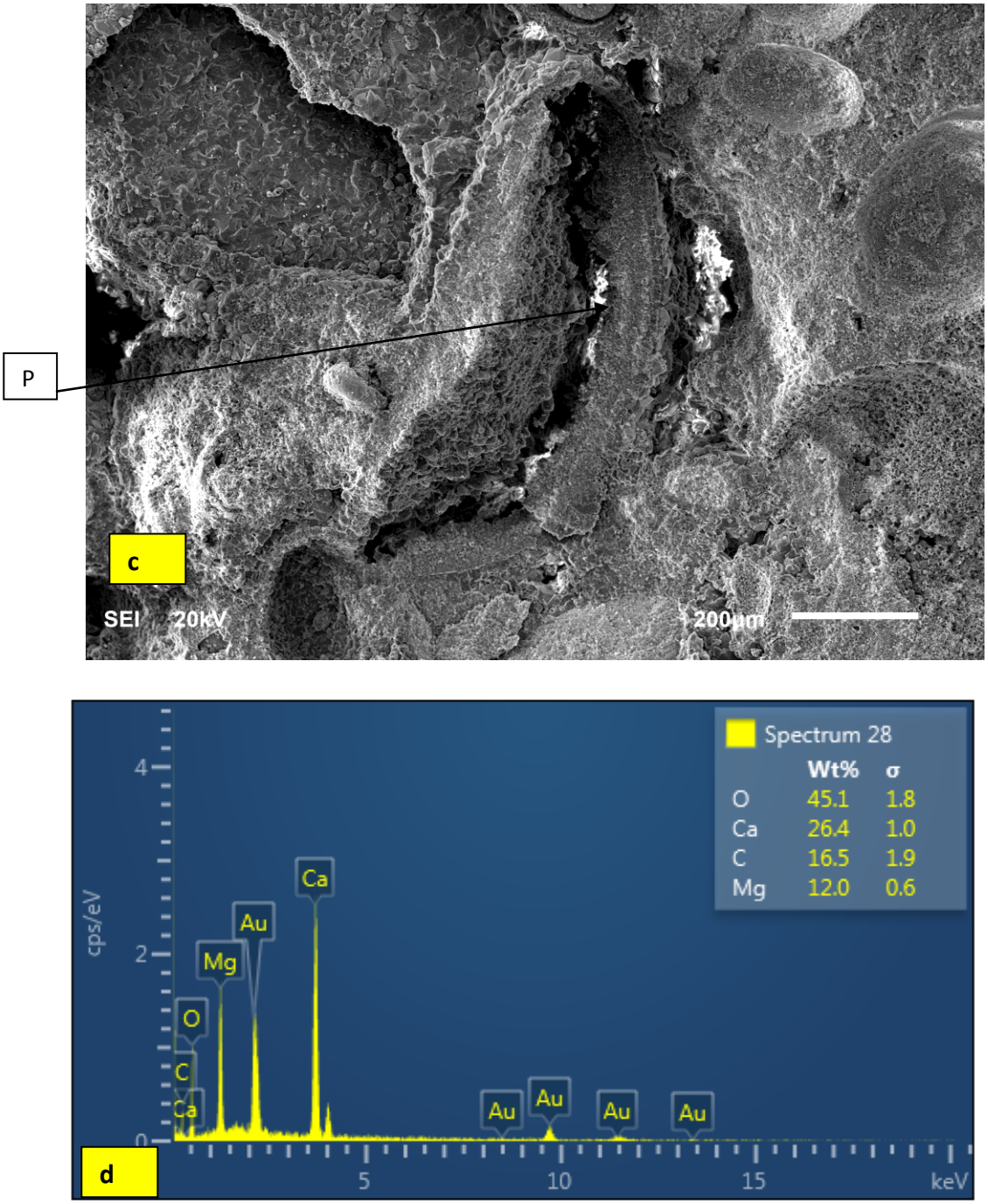

Figure 4.11.c) SEM images of peloids (P) in carbonate mud, d) EDS analysis of (c) shows abundance of Ca and Mg.

4.1.11. Peloidal Packstone (Pp)

Peloidal packstone in the outcrop occurs as tan to light grey color beds (Figure 4.12a). Facies occurs below the peloids grainstone facies, in outcrop 7. The bed thickness ranges from 10 to 20cm and the facies thickness ranges from 0.5 to 1.5 m. This facies shows contorted bedding or seismites in Outcrop 10 see section 6.1.4 for details. This facies is also characterized by the presence of intraclasts in the cycles near top of outcrop 10.

The grains constituents of the lithofacies include are peloids, quartz and mud (Figure 4.12b). The grain size ranges from fine to medium suggesting moderately sorting. The grains are rounded to subrounded and show high sphericity (Figure 4.12d).

During the deposition of facies, carbonate sediments production was diluted by the influx abundant clastic sediments into the depositional basin (Flugel, 2004). The deposition took place under dry and warm conditions (Figure 6.2). The skeletal grains, in the facies were preserved as molds and show moldic porosity. The porosity ranges in this facies from 5% (Figure 4.11b). XRD analysis shows that the, facies is composed of more than 86% carbonate and 14% quartz and accessory minerals. Most of the pores shown are occluded by micrite.

SEM images shows shell fragment at 100 microns, the fine grain material seen around is micrite. The EDS analysis of the fine grain material show medium values of Mg and Ca, suggests the possibility of dolomitization of this facies (Figure 4.12d).

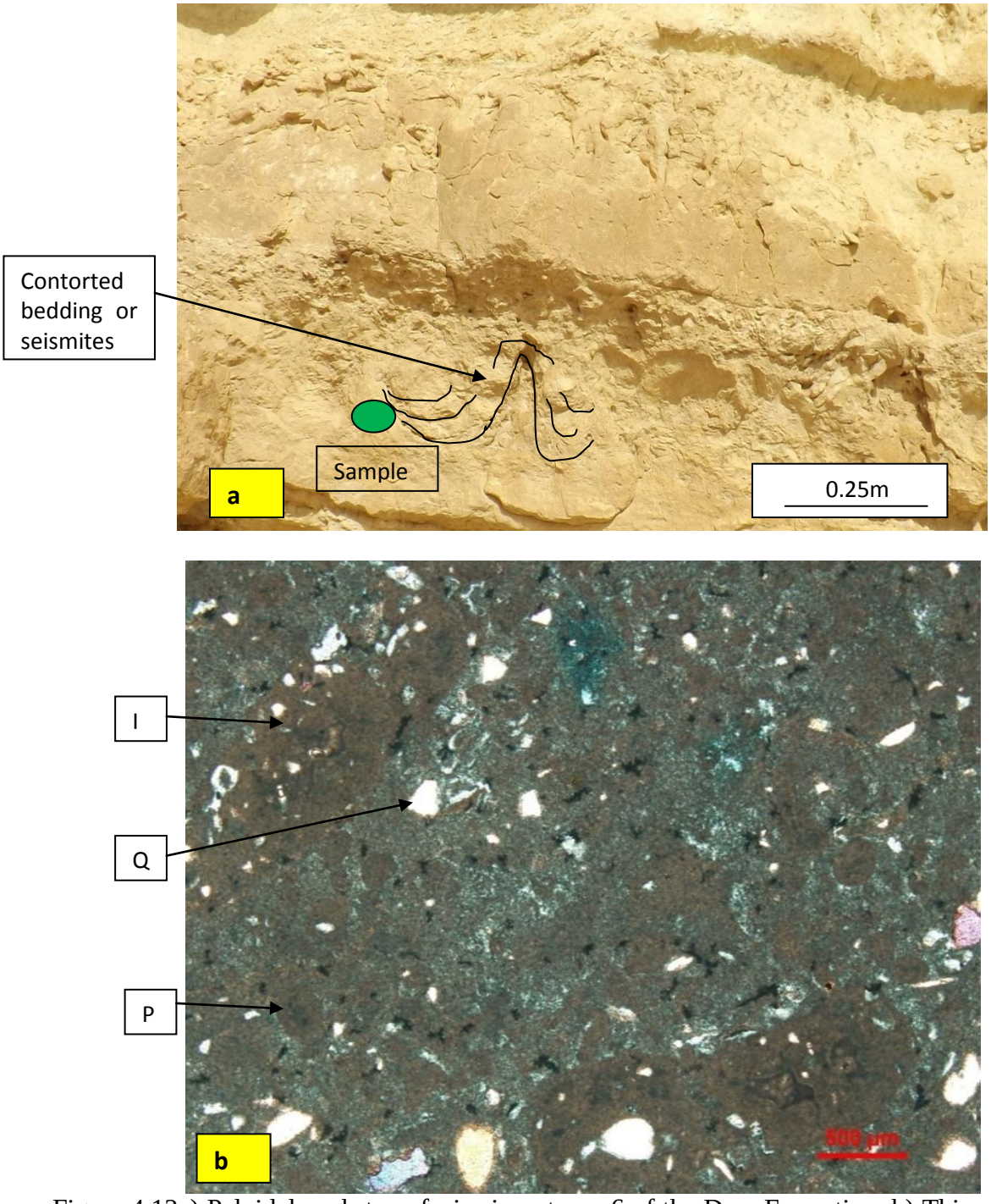

Figure 4.12a) Peloidal packstone facies in outcrop 6 of the Dam Formation, b) Thin section of a sample from the facies showing medium grained peloids(P) and quartz(Q); Note absence of skeletal and only dominance of mud, but some section have more than 10% grains, peloidal grains are visible in the picture along with quartz. The grain size ranges from medium sand to granule. The average porosity in the section is around 5%. I=Intraclasts.

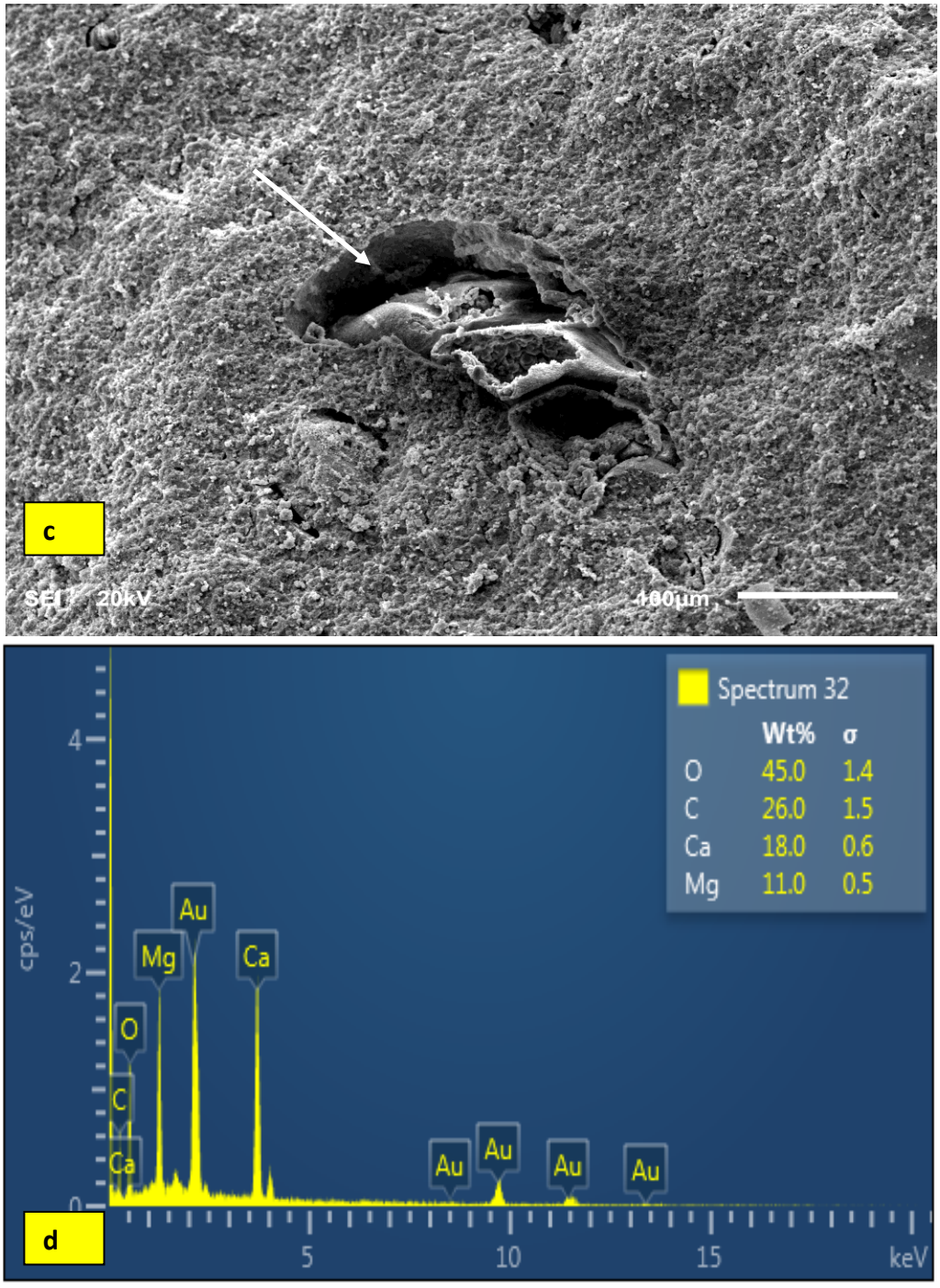

Figure 4.12.c) SEM images of broken Bioclast (B) in carbonate mud, d) EDS analysis of (c) shows abundance of Ca and Mg.

4.1.12. Sandy peloidal packstone (Marl) (Spep)

This facies is composed of alternating light green to dark brown marl beds, mud and silt size particle layers. The mudcracks are filled by silt size material. In addition to mud cracks, rootlets are also observed in this facies in the Marl Beds (Figure 4.13a). The bed thickness in this facies ranges from 0.5 to 3 meters. This facies overlies the foraminiferal grainstone to packstone facies in outcrop 10 and tidal flat estuarine sandstone in Outcrops-26 and 25, and is underlain by skeletal wackestone packstone facies in Outcrops 10 and 26.

The sediments are moderately sorted fine grain peloids grains. Fine silt sized quartz particles are also present of this facies. The porosity in this facies from is less than 5% (Figure 4.13b). XRD analysis shows that the, facies is composed of more than >75% carbonate and 25% quartz (Figure 4.13c). SEM image shows dissolved skeletal fragment surrounded by mud (Figure 4.13d).

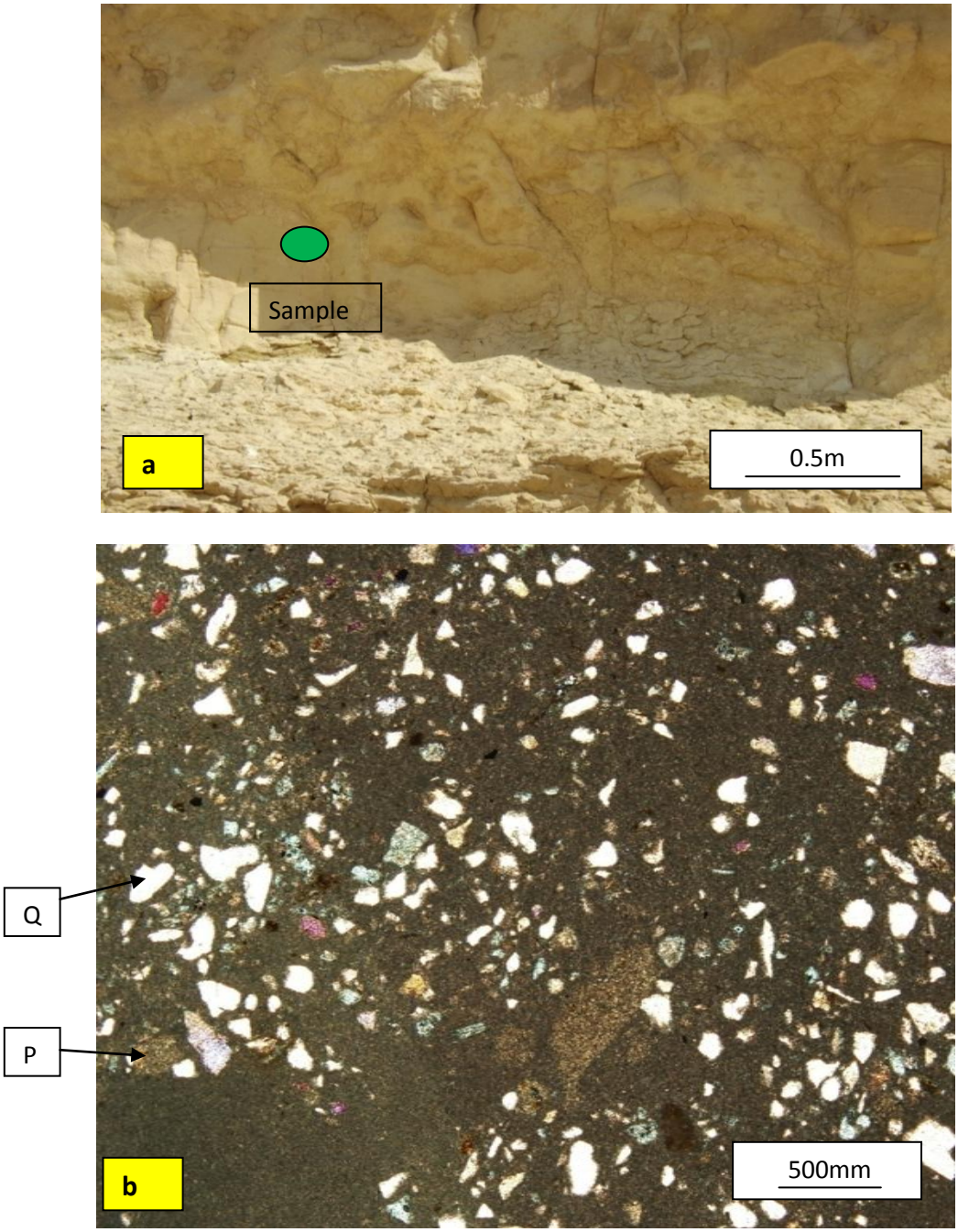

Figure 4.13a) Sandy peloidal packstone (Marl) facies Outcrop25 of the Dam Formation, b) Thin section of samples from the facies fine to medium grained peloids (P) and quartz (Q).

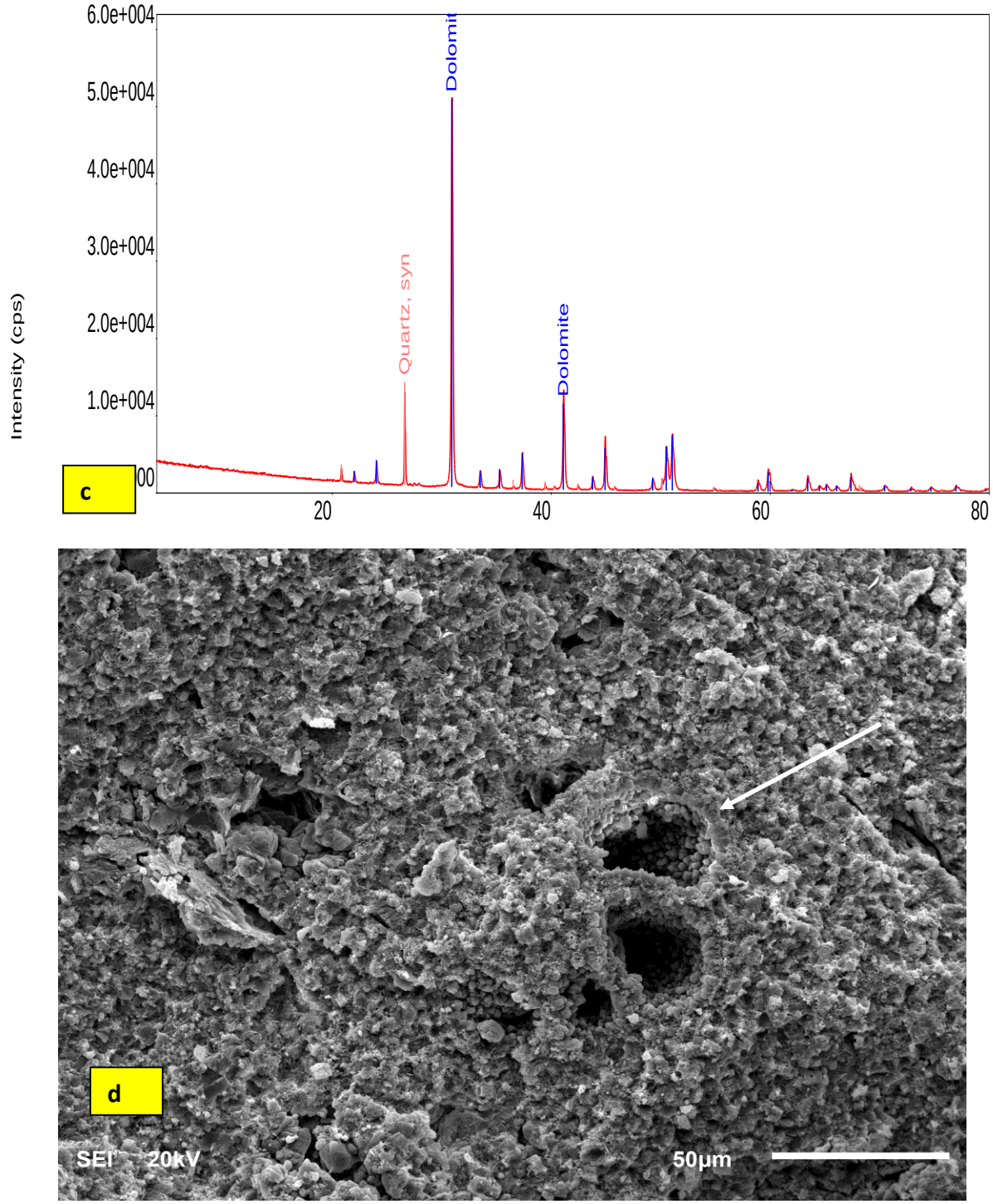

Figure 4.13.c) XRD shows the presence of quartz and dolomite minerals, d) SEM images of dissolved skeletal grain in carbonate mud.

4.1.13. Fine to medium Quartz Sandstone (Qfs)

This sand and mud interbedded facies, with sand dominating over mud beds in different proportions. The thickness of sand beds ranges from 0.5-2m, tan to light green coloured bioturbated, very fine to medium grained and moderately to poorly sorted sandstone (Figure-4.14a). It is composed of quartz, orthoclase and clay particles. The sand particles are angular to subangular. The proportion of mud and sand becomes dominant as we move from south to north where it is almost mixed sand/mud couplet. Thickness is variable, and sand content decreases upwards. Bioturbations is rare in this facies in north, while the upper sand bed overlying mud is enriched in glossifungites ichnofacies, diameters of these trace markers, in this facies ranges from 0.25m to 0.3m.

The interbeddings between sand and mud termed as inclined heterolithic stratifications, which is observed in outcrop 25 and 26 in this facies. This sandstone overlies the red mudstone or paleosols and a sharp contact is observed. This sandstone bed has channelized geometry and cuts all the facies previously deposited. This is observed in outcrop 6 where the channel marks the second stage of sandstone incision in the succession just above the first unconformity.

Abundant trace fossils are present in the middle of this sandstone and are spread all over the borders of this facies. These trace fossils are very distinctive feature of the facies. The abundance and density of trace fossil increases from base to top. The trace fossils include ophiomorpha or glossifungites (Figure-4.13f). The prominent sedimentary structure is cross bedding (Figure 4.14c &e).

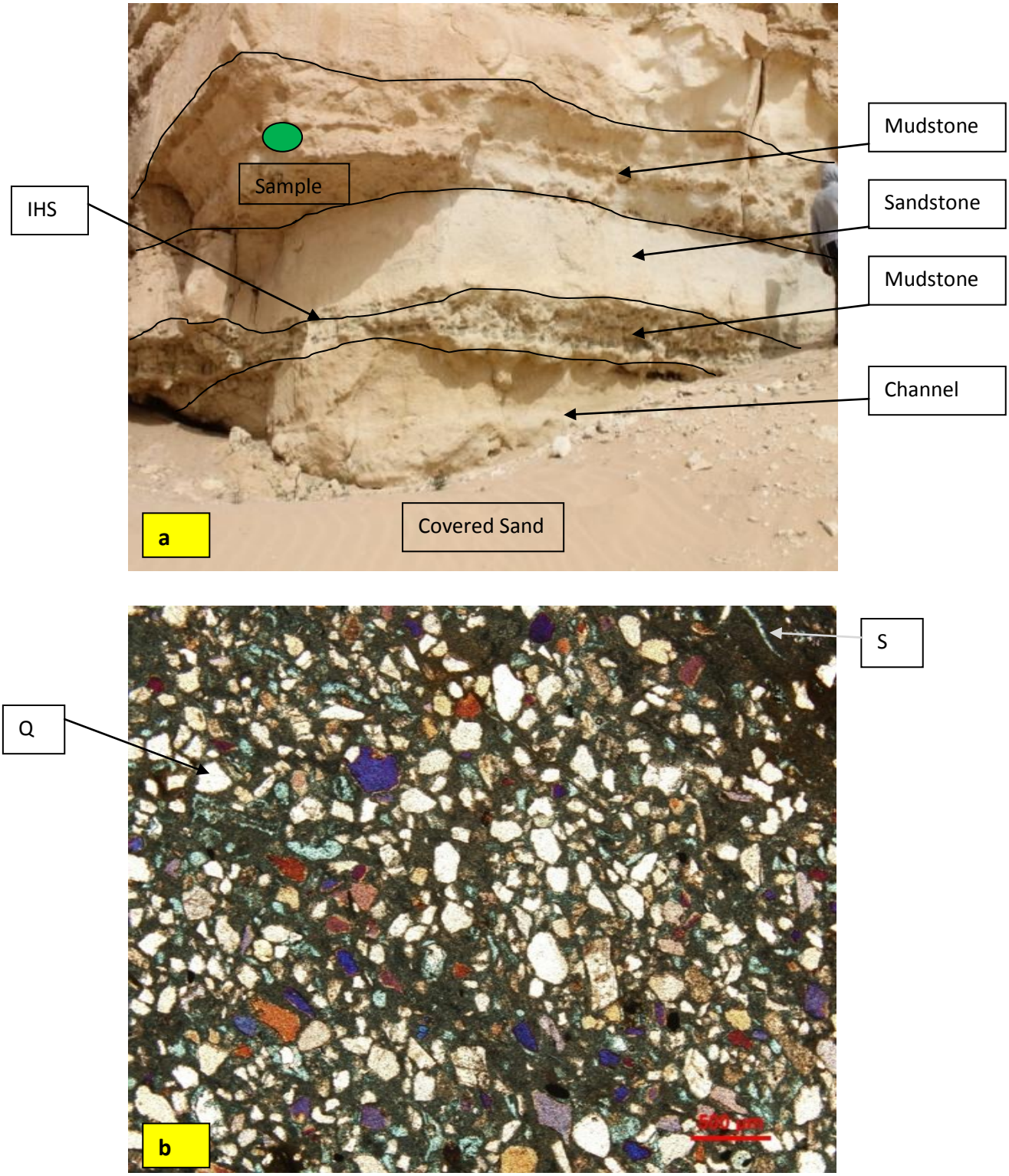

Figure 4.14a) Quartz sandstone faciesOutcrop10 of the Dam Formation, b) Thin section of samples a from the facies showing fine to medium grained quartz; Note: absence of skeletal. Q=quartz, S=skeletal, IHS= Inclined heterolithic stratifications

.

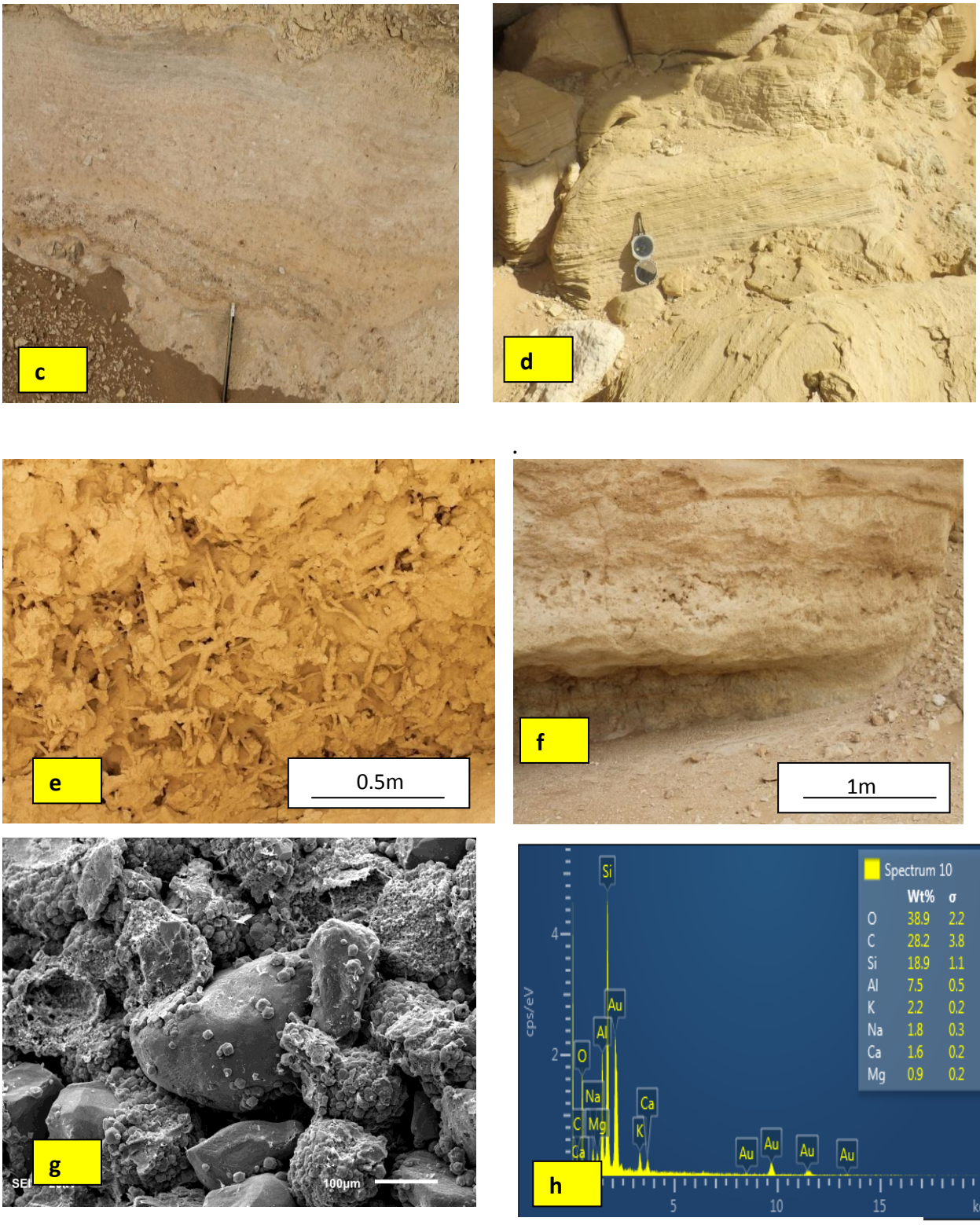

Figure 4.14.c) Channel lag and fining upward d) cross bedding, e) glossifungites ichnofacies,f) channels cutting paleosols below g) SEM images of quartz grain, clay is also present, f) EDS abundance of Si

4.1.14. Miliolid Peloidal Packstone-Wackestone (Mpw)

This facies is composed of alternating laminated white to cream beds of packstone, alternating mud and silt size particle layers, mud cracked. The mudcracks are filled by silt size material. In addition to lamination, mud cracks, rootlets are also observed in this facies (Figure 4.15a). The bed thickness in this facies ranges from 0.5 to 3 meters. This facies overlies the ooid grainstone facies in outcrop 10 and estuarine sandstone in Outcrop-26 and 25, and is underlain by Peloidal quartzose wackestone mudstone facies in outcrop 10 and 26.

The fine grain to pebble sized skeletal grains and fine silt sized quartz particles are important constituents of this facies. The porosity in this facies is less than 5% (Figure 4.15b). XRD analysis shows that the, Mpw facies is composed of more than >95% carbonate and 5% accessory minerals. SEM image shows dissolved miliolid surrounded by mud (Figure 4.15c).

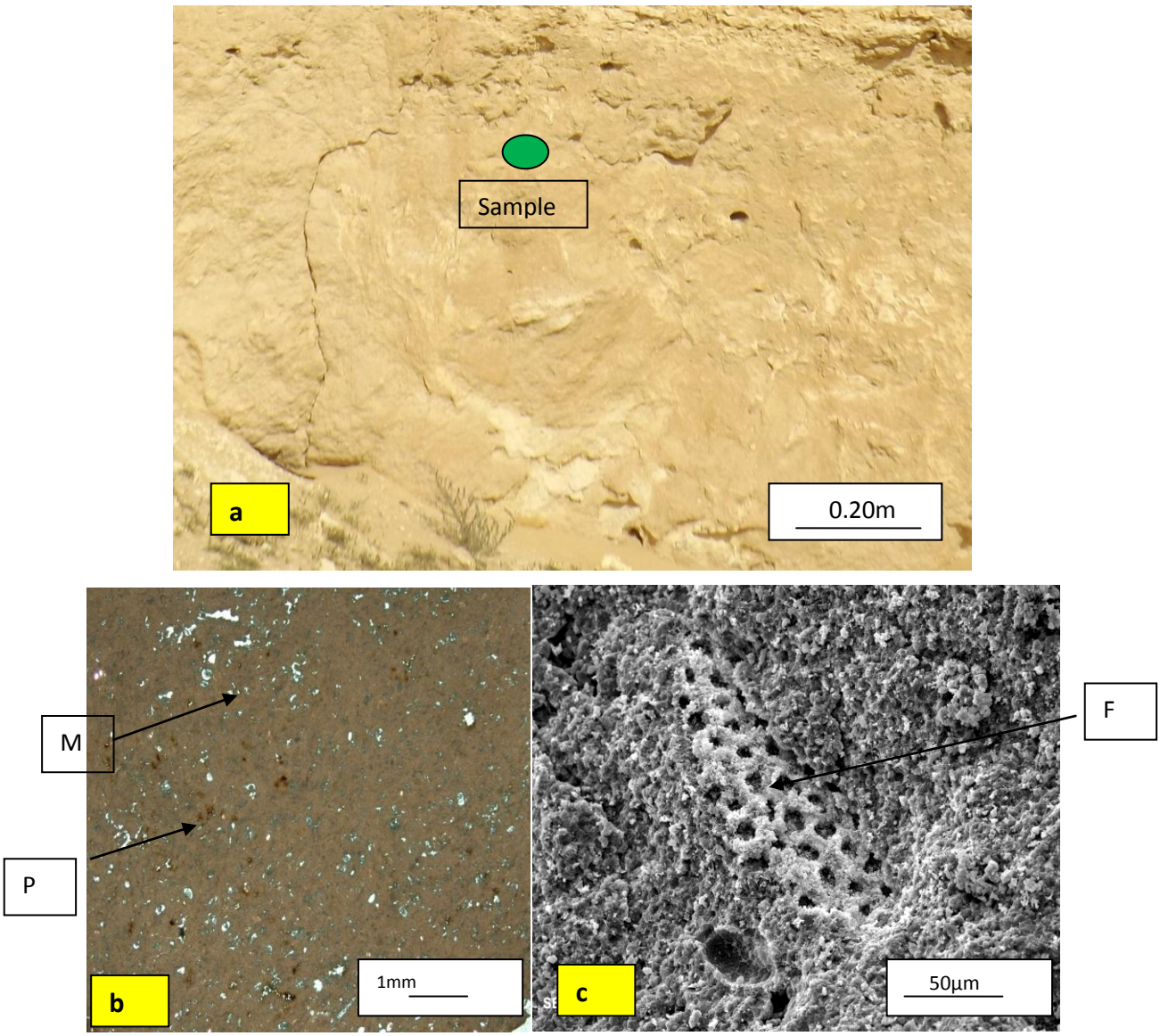

Figure 4.15a) Miliolid peloidal packstone wackestone Outcrop10 of the Dam Formation, b) Thin section of a sample from the facies showing mud and fine grains of miliolid, c) SEM image of (b),Note absence of skeletal grains. M=miliolid, peloids=P, Foram=F.

4.1.15. Calcareous Fine Sandstone (Cfs)

The calcareous sandstone facies occurs as dominant facies in Outcrops 25 and 26. The sand beds in calcareous sandstone facies dominate over mud beds in unequal proportions. The thickness of sand beds ranges from 0.2-1.2m, light grey, bioturbated, very fine to medium grained and moderate to poorly sorted sandstone. It is composed of angular to subangular quartz, orthoclase feldspar and clay particles. The rock is cemented by carbonate cements. The proportion of mud and sand become equal as we move from south to north where it is almost mixed sand/mud couplets. The thickness is variable, and sand content decreases upwards. Bioturbations is rare in this facies in north. The upper sand bed overlying mud marks the absence of ichnofacies.

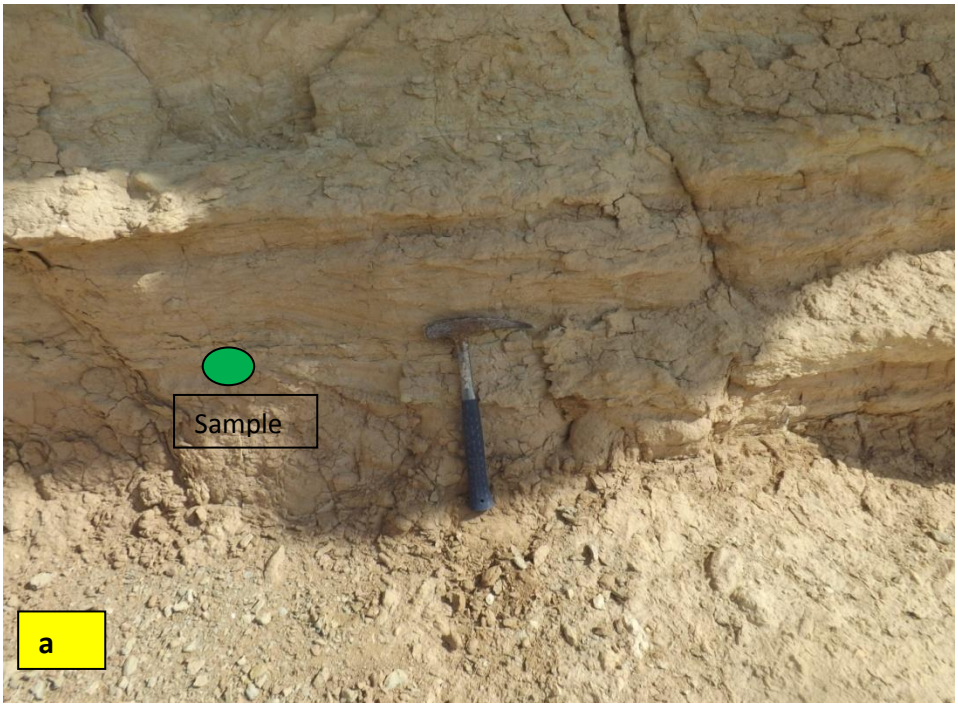

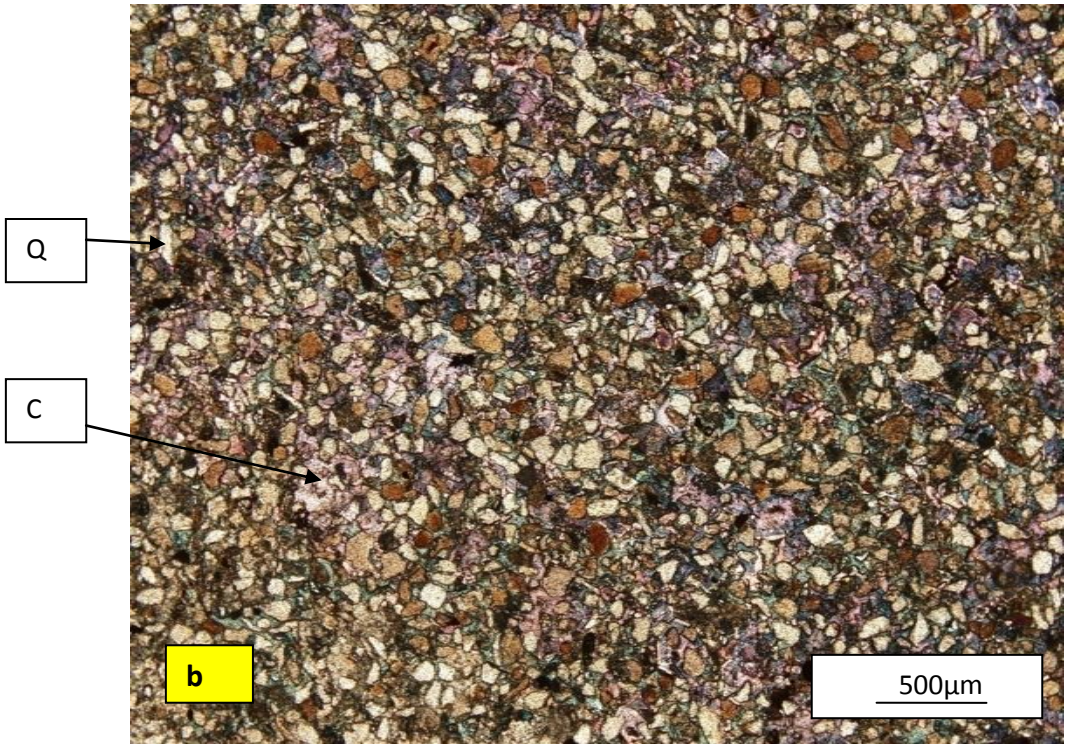

Figure 4.16a) Calcareous fine sandstone facies in Outcrop10 of the Dam Formation. Note cross-bedding, b) Thin section of a sample from the facies showing fine to medium sand, cemented by calcite cement.Q=quartz, calcite=C.

4.1.16. Paleosols (Ps)

This facies is composed of alternating red to dark brown mudstone and thin sand thin lenses. It is structureless and mud cracked, and has not any distinct bedding character. The thickness of this facies ranges from 0.75 to 2 meter (Figure 4.17a). This facies which is very important and present below the channelized sandstone facies which marks the period of non-deposition, marking sequence boundary above it and it also cuts the strata to start a new cycle of deposition. This facies, is present in sheet geometry, is traceable across most of the outcrops. This facies serves as a good datum for correlating the sections. The dominant sedimentary structures are in this facies are mudcracks and bioturbations. This mudstone is considered to be a part of paleosols based on the presence of rootlets, structure similar to recent soil horizon and their structure (Figure 6.2). Paleosols are very useful in documenting the biota, climate, time and vegetation. These paleosols marked by exposure and was used previously by various authors e.g. Al-Khaldi (2009) to identify unconformities within Dam Formation.

The fine sand to silt size quartz particles and clays are important constituents of this facies. XRD analysis shows that, this facies is composed of more than 50% clays and 50% quartz and accessory minerals.

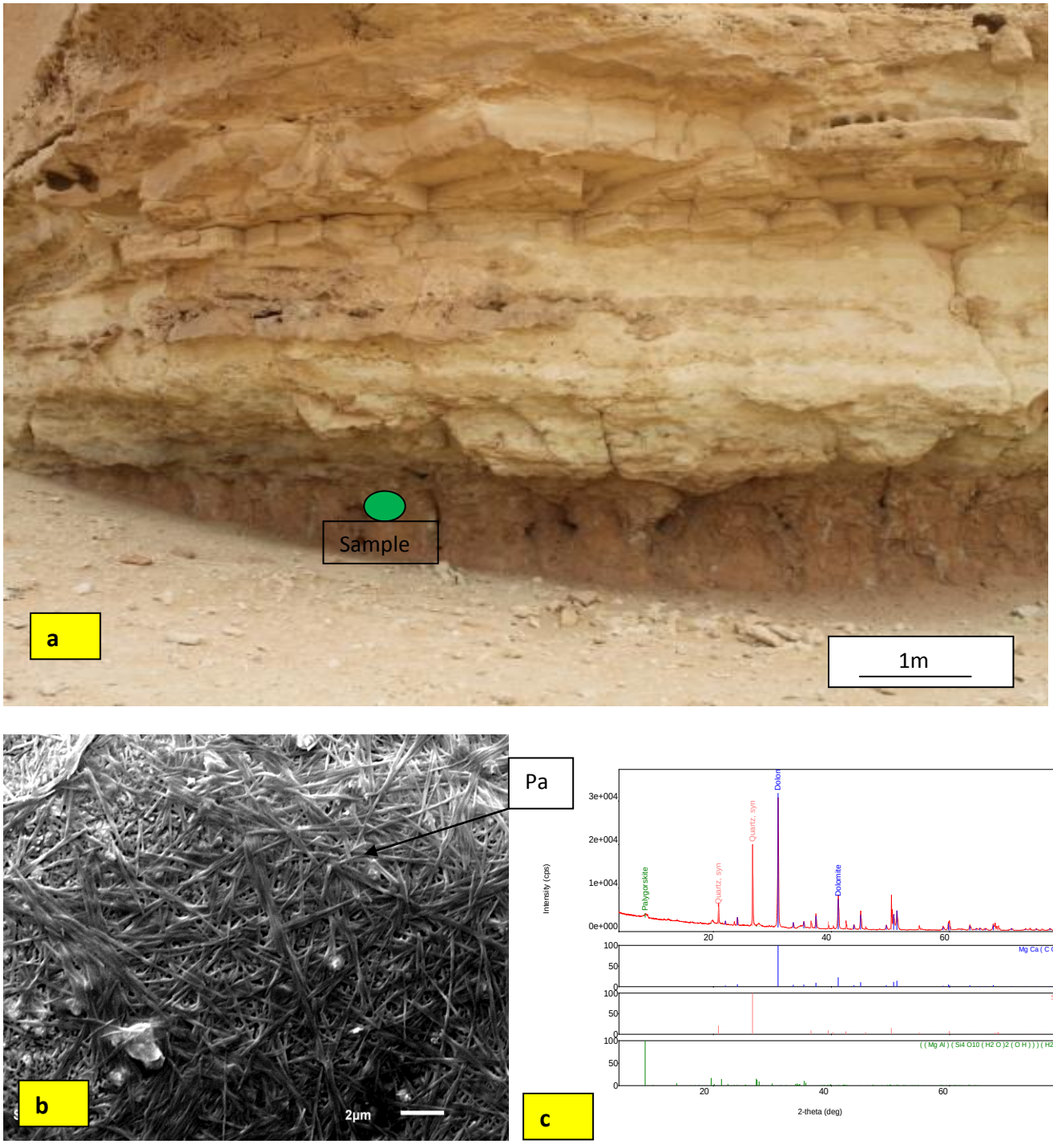

Figure 4.17a) Paleosols facies, outcrop10 photograph of the Dam Formation, note structureless, b) SEM image of palygorskite clay mineral dominate constitute clay in the facies, c) XRD analysis confirm the presence of palygorskite and quartz minerals. Pa=palygorskite.

4.1.17. Mud cracked siltstone and mudstone facies (Msm)

This facies is composed of alternating light green to dark brown siltstone and mudstone beds (Figure 4.18a, b). This facies overlies the foraminiferal grainstone-packstone facies in Outcrop 10 and tidal flat estuarine calcareous sandstone in Outcrops-26 and 25. It is underlain by the peloidal sandy wackestone mudstone facies in Outcrops 10 and 26.The bed thickness in this facies ranges from 0.5 to 3 meters. This facies overlies the foram grain-packstone facies in outcrop 10 and tidal flat estuarine calcareous sandstone in outcrop-26 and 25, and is underlain by peloidal quartzose wackestone mudstone facies in outcrop 10 and 26.

This facies grain size ranges from clay to silt size. The porosity ranges in this facies from less than 15-20% (Figure 4.18c). XRD analysis shows that the, facies is composed of more than >95% clay particles, and 5% quartz and accessory minerals.

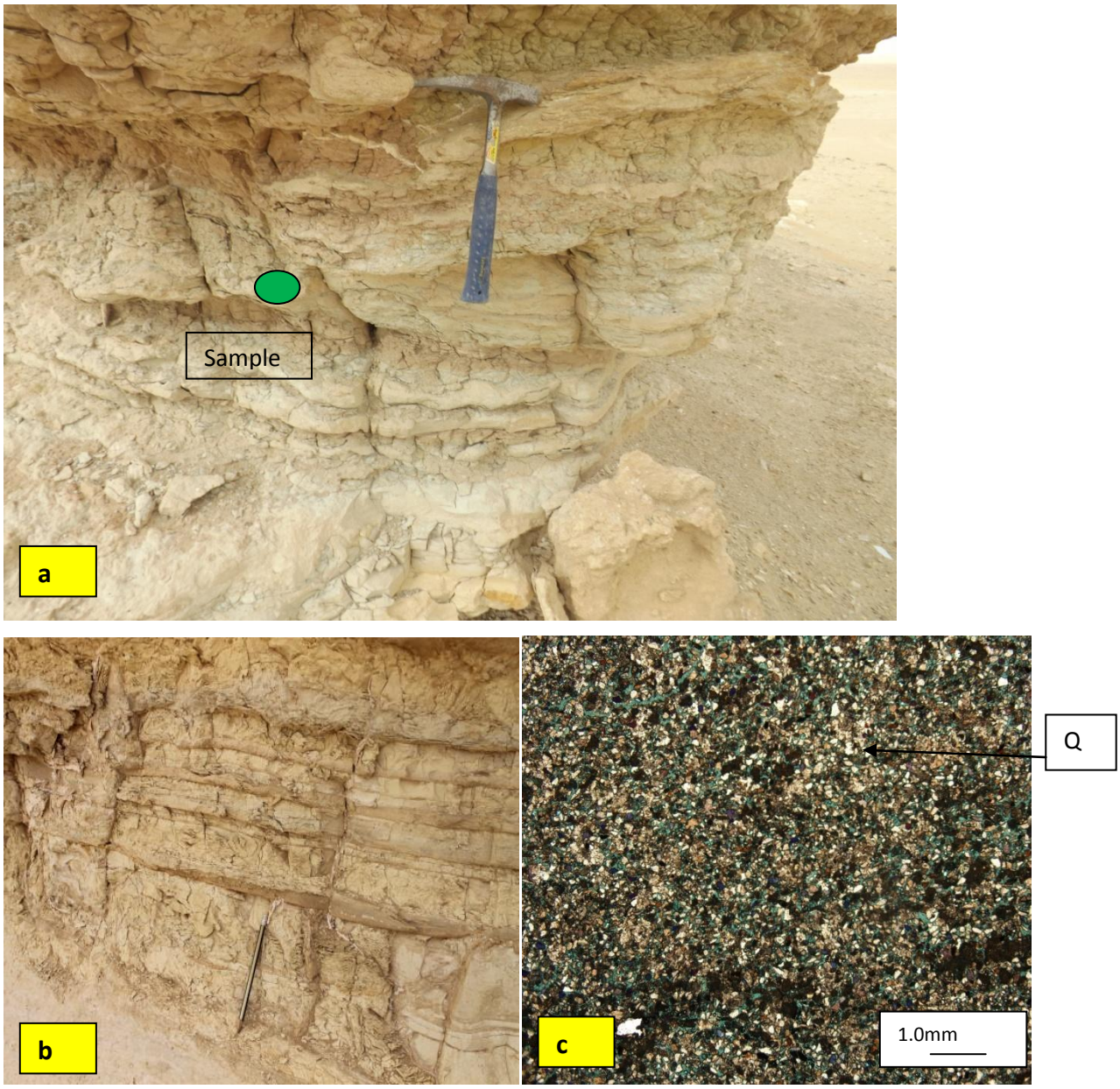

Figure 4.18a) Mud cracked siltstone to mudstone facies, outcrop25 photograph of the Dam Formation, note structureless, b) Mudcracks filled with silt size material, c) thin section of silt lenses in the facies note the presence of clastic mud and quartz. Q=quartz.

CHAPTER 5

RESULTS

SEQUENCE STRATIGRAPHY

5.1. Introduction

The basic unit sequence is defined as a conformable succession of strata that are genetically related and bounded by sequence boundaries, otherwise their correlative conformities (Van Wagoner et al., 1988; 1990). The time gap missing represents time of non-deposition or surfaces of erosion is presented by sequence boundaries (Figure-5.1).

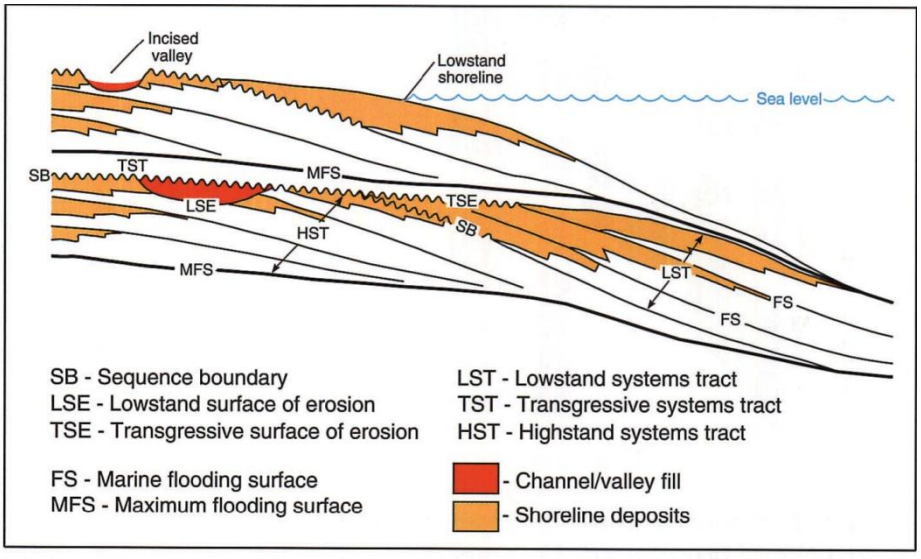

Figure-5.1 Diagram of sequences, key surfaces and system tracts (Van Wagoner et al., 1988).

Sea-level changes are the major control on deposition. Tectonic subsidence and eustatic sea-level changes in turn control the relative/local sea-level changes. There are particular system tracts that develop during the specific periods of sea-level changes, Low-stand System Tract (LST), Transgressive System Tract(TST)and Highstand System Tract(HST). The sequences are produced during periods of changes in sea-level and the covering unconformities are produced during the time of fall in relative sea level. The sedimentary facies of falling sea level and Lowstand times in these cycles is generally represented by soil development which marks the hiatus.

In our study we used markers within the Dam Formation to identify the low level and high level, relative sea level changes to confirm our interpretation. Paleosols and channelized sandstone are important and provide data as they are sensitive to sea-level changes. Stratigraphic sequences of mixed carbonate-siliciclastic facies, the sequence development is often described as mutual sedimentation expressed by the alteration of platform carbonates during transgressive and highstand times and basinal low stand accumulation of siliciclastic material. These sequence stratigraphic successions are well studied and modeled from wide shelves of large scale carbonate systems interacting with major sources of siliciclastic influx (Lopez-Blanco., 2000; Tucker, 2003; Wilson, 2005; Campbell, 2005). On a smaller scale, high frequency cycles are a characteristic feature of these carbonate ramps (Pomar, 1991; D'Argenio et al., 2005). These cycles are shallowing upward parasequences, bounded by marine flooding surfaces (mfs).

5.2. Cycle Definition and Correlation

Vail et al., (1977) and Haq et al., (1988) used the time to subdivide the sequence and cycles from first to sixth order. Parasequence is an equivalent of cyclothem, used to describe the Mesozoic shallow water peritidal carbonate cycles of Apennines by D'Argenio et al.(1999) and the simple carbonate sequence cycles of Upper Miocene of Mallorca(Pomar, 1991). The relative tectonic-eustatic/eustatic cycle orders and their sequence stratigraphic units, their duration is described in the table below.

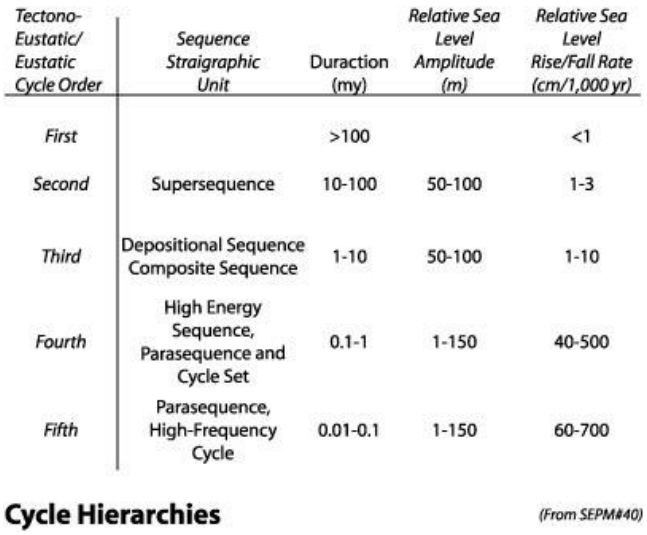

Figure 5.2. Diagram of Eustatic cycle order, sequence stratigraphic unit and their duration (Van Wagoner et al., 1988).

Facies relationships expressed in the lithofacies section of the Dam offer important insights and help in recognizing and defining cycles in the formation's outcrops in the Al-Lidam Area. It is significant to note that the styles of cyclicity are in agreement with and similar to styles documented by AlKhaldi (2009) and AlKhaldi et al., (2010; 2014).

5.3. Composite Sequences

Composite sequences (CSs) are defined as sets of genetically related sequences which are arranged in distinctive progradational, aggradational and retrogradational patterns. These higher order sequence stacks into highstand, transgressive and highstand tracts (Figure-5.3; Keran et al., 2002).

There are four sequences present in Dam Formation along the NS transect. The cycles are identified on the basis of shallowing upward of the facies. Then the individual cycles within the sequence boundaries are counted. The correlation is made on the cycle sets and then by matching this trend with the sections in the correlative outcrops. The first sequence boundary between CS-1 and CS-2 was identified and used as a datum that can be traced across the three outcrops in south. The real challenge was to correlate Outcrop 10 and rest of them to Outcrops 25 and 26

located approximately 2.3km apart. This is achieved by using the same correlation technique and matching the trends within the CS-2 in Outcrops 10 and 26.

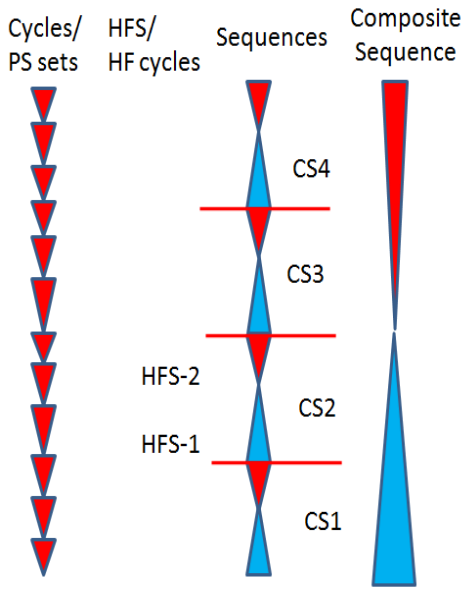

Figure-5.3. General composite sequence of Dam is divided into 24 cycles and four CS, each of them is marked by sequence boundary (the presence of channelized sandstone over the paleosols).The sequence-2 is further subdivided in to HFS-1 and HFS-2 based on the presence of two HST and 2 TST, within one sequence.

The most important part of this correlation is that we were able to find a definite pattern in facies within individual parasequences. The CSs start with TST, and erosive sandstone overlying paleosols, and then capped by oolitic grainstone facies. The presence of wackestone to mudstone facies marks the MFS. The MFS marks here the boundary between TST and HST. These are topped by oolitic grainstone which marks the top of the cycle. The evidences used for making these observations are the changes in sea level, wave base and stromatolites.

5.4. Sequence Boundaries

Sequence boundaries are based on (sandstone overlying paleosols).It is only last sequence boundary is identified on paleosols directly underlying packstone facies (absence of quartzose sandstone facies). The absence of sandstone facies above the paleosols could an indicator that

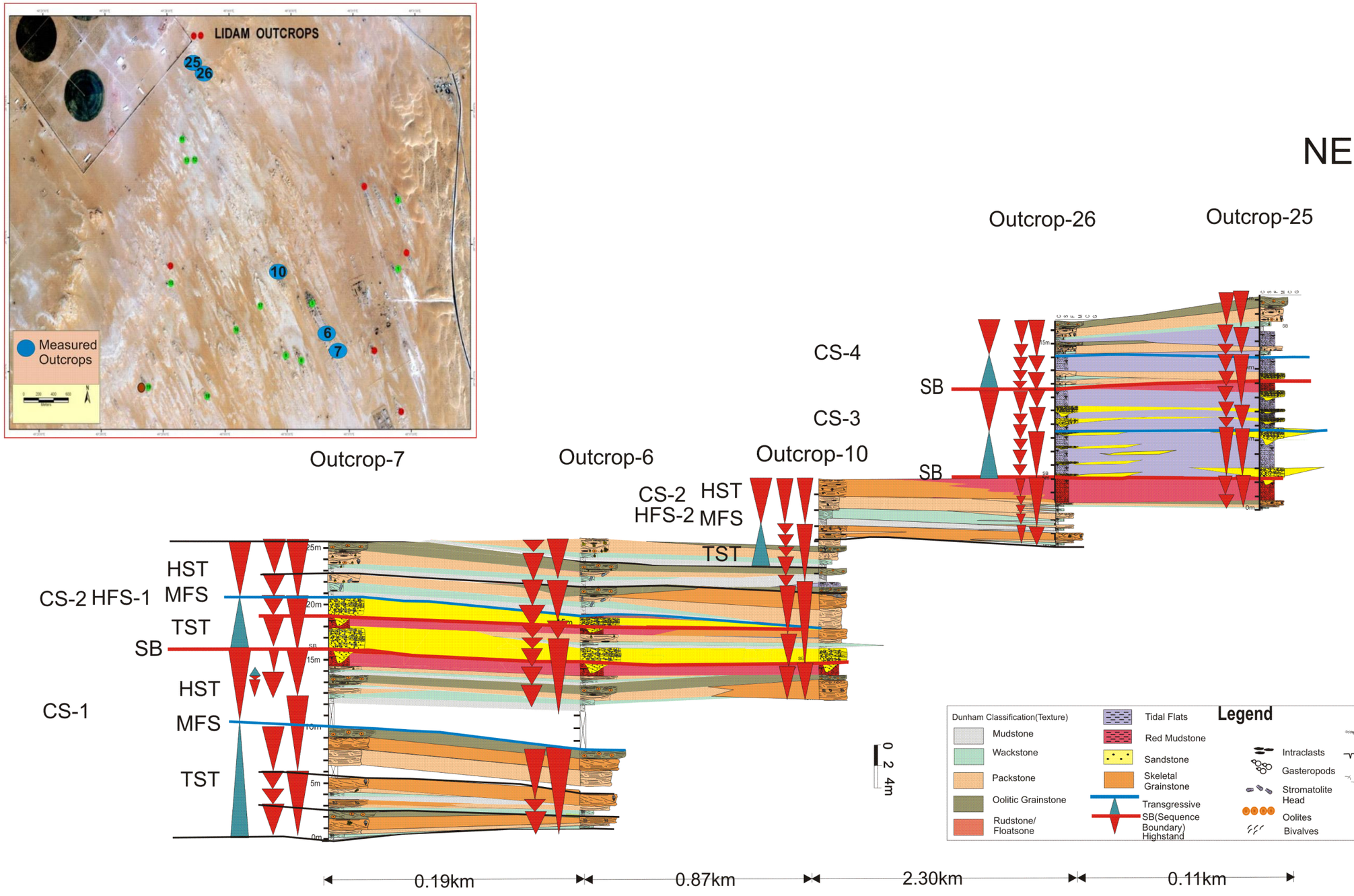

Figure-5.4. Thehigh resolution stratigraphic model, correlation of cycles in all outcrops. Important observations related to the correlation model is the start of a sequence by channelized erosive sandstone deposited over paleosols and then continuing the TST, the presence of mudstone and wackstone marks the presence of MFS and after that the HST starts and these are topped by oolitic grainstone bodies.

the deposition time gapwas small and the break in carbonate deposition took place soon after the unconformity. This observation is also supported by the decrease in the thickness of paleosols Outcrops 25 and 26.

5.5. Composite Sequence-1

This sequence which is composed of 6 cycles is about 13-15.5m. The lower boundary of the sequence is not exposed. The lowest unit exposed in the NS-transect is represented by the bioturbated wackestone to mudstone facies. The upper boundary is defined by erosive contact with CS-2, which is filled by estuarine sandstone of CS-2 on Paleosols of CS-1(Figure-5.4). These paleosols in turn overlie the skeletal packstone facies. The carbonate dominated ramp composite sequence includes grainstones, packstones and wackestones rich in ooids and skeletal fragments (bivalves and gastropods). The maximum vertical thickness of this sequence is 10 meters, and the carbonate facies are topped in the landwards direction. Distally, the facies are dominated by wackestone to mudstone facies. The coarse grainstone and packstone within the association show internal structures such as cross bedding. These sedimentary suggest deposition above the wave base and probably represent intertidal to skeletal banks setting influenced by tides and waves. Oolitic grainstone comprising of ooids, peloids and rare skeletal grains constitute important part of this composite sequence. They occur as sheets thin to medium bedded with a lateral extent of about 1km. These oolitic sheets have crinkly lamination and have close association with stromatolitic laminae as suggested by Irtem (1987). These sheets develop on top of lens geobodies of the skeletal grainstones of low topographic relief and may represent an oolitic carpet. The size of this sheet varies from 0.5 to 1 meter in thickness. The ooids represent to a depth controlled and represents intertidal conditions. Therefore, that the oolitic grainstone were likely developed above wave base. A wackestone to mudstone bed occur locally in this sequence and some skeletal fragments are also observed in these beds. The presence of paleosols and channelized on its top marks the sequence boundary.

5.5.1. Composite Sequence (CS-1 TST) DM-1

The transgressive facies of CS-1 consists of beds of skeletal pack-grainstone beds represents marine transgression, overlain by oolitic grainstone facies (Figure-5.4). This CS that is comprised of four cycles is about 10m in thickness. It is capped by three beds of oolitic

grainstone, show very rapid transgression. This is interpreted that the top of this unit was deposited as a result of shallowing in this composite sequence. The base of this CS is composed of massive burrowed wackestone. Near the top of this CS the crinkly laminated packstone/grainstone is present. This is capped by sandstone beds which mark the base of MFS. This separates the CS-1 TST from CS-1 HST (Figure-5.5.).

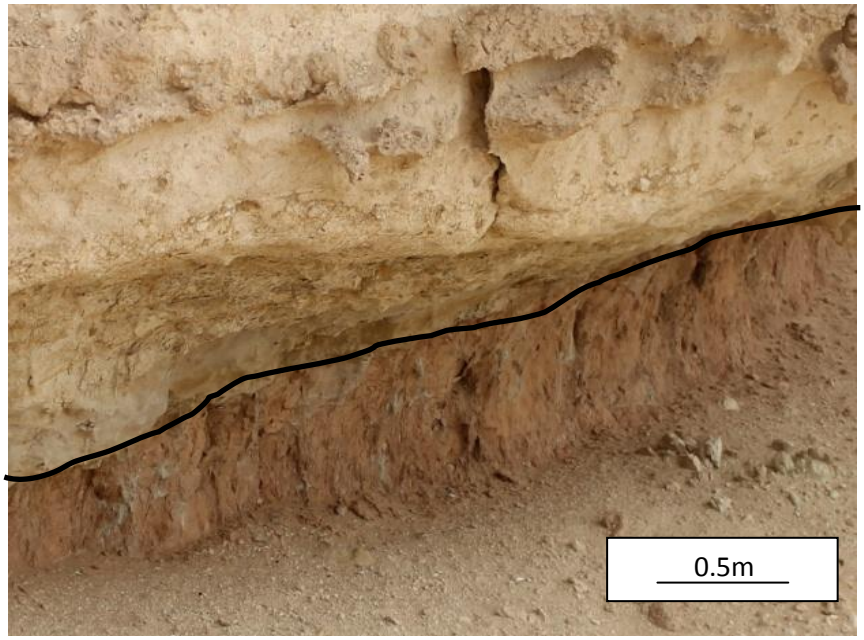

Figure-5.5. Sequence boundary between CS-2 quartz sandstone facies overlying CS-1 paleosols, black line represents sequence boundary.

5.5.2. Composite Sequence (CS-1 HST) DM-1

The HST part of CS-1 is composed of 2 cycles. This part of composite sequence starts with wackestone to mudstone and is capped by one oolitic grainstone bed. This CS-1 HST is about5.5m in thickness. The middle of this CS is composed of massive burrowed wackestone/mudstone. Paleosols is capped by channelized sandstone beds which mark the base of incision on the Sequence Boundary (SB-1). This separates the CS-1 from CS-2(Figure-5.5).

5.6. Composite Sequence (CS-2) DM-2

CS-2 one of the most extensive composite sequences observed in almost all the outcrops in the study area is the 9-15m thick, this CS-2. The CS-2 is the thickest sequence in the studied outcrop sections.

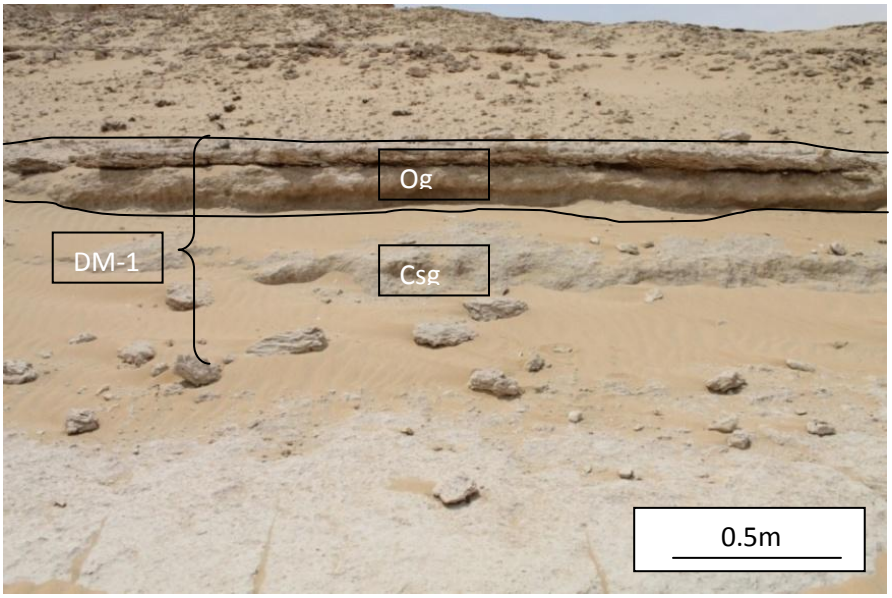

Figure-5.6.CS-1DM-1 composed of coated skeletal grainstone. The top of DM-1 is marked by the presence of oolitic grainstone facies.

The base of this CS-2 is marked by an erosive and incised bed associated with asequence boundary. However, two episodes of erosion were observed in Outcrops-6 and 7. Two high frequency sequences, they are part of HFS-1 and HFS-2, flooding surface separate formed this CS. However, overall trend in transgression is evident by the increase in the accommodation space from HFS-1 to HFS-2(Figure-5.7, 5.8).

5.6.1. Composite Sequence (CS-2; HFS-1 TST) DM-2

The total thickness of HFS-1 is 9m. The HFS-1 TST portion of it is 4.5m thick. The HFS-1 marks the incision in Dam Ramp as a result of fall in sea-level.HFS-1 is composed of bioturbated sandstone with mudstone intercalations. These sandstone beds are intensively borrowed top. The intensity of borrowing increases upward. The deposits are mainly of karst as a result of marine transgression (Figure-5.8). The top is marked by the presence of mudstone to wackestone of the HFS-1 TST.

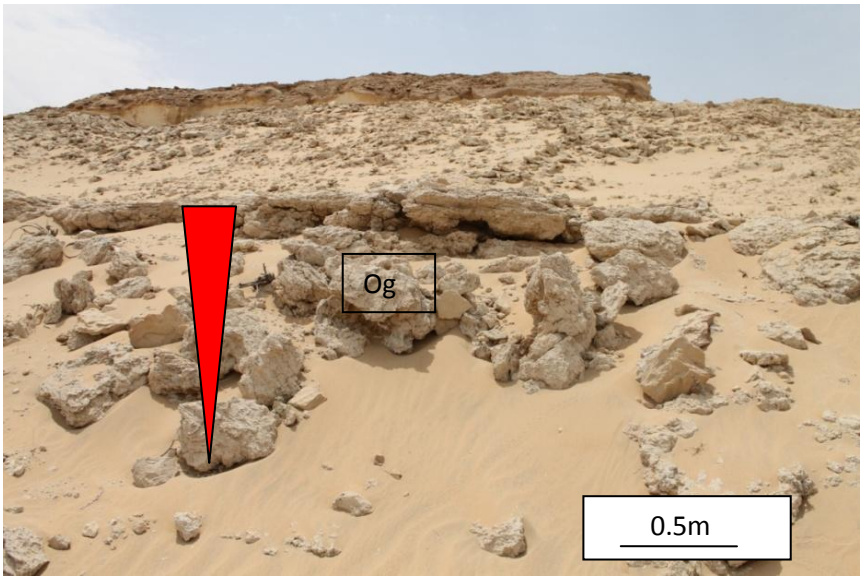

Figure-5.7.Top of CS-1DM-1 composed oolitic grainstone facies.

5.6.2. Composite Sequence (CS-2; HFS-1 HST) DM-2:

This part of HFS-1 is composed of a 4.5m peloidal grainstone facies, and thick oolitic grainstone facies on top. This sequence is composed of crinkly laminated foraminiferal grainstone to sandy skeletal wackstone/packstone and ooid grainstone facies. This shows decreased in accommodation at top of the HFS-1 (Figure-5.8.).

5.6.3. Composite Sequence (CS-2; HFS-2 TST) DM-3:

The 6.7m thick of HFS-2 is composed of 4 cycles. It underlies the CS-3 and its top is marked by paleosols. The boundary between HFS-1 and HFS-2 is not clear. There were not any paleosols found within the sequence, and the contact is placed using retrogradational stacking patterns of cycles present in CS-2. HFS-2 TST thickness is around 4m. The base of this sequence is placed on wackestone to mudstone facies. This HFS-2 TST is also bioturbated. It is mostly composed of clay and silt. The bioturbations marks the presence of distal facies on top of the HFS-1.

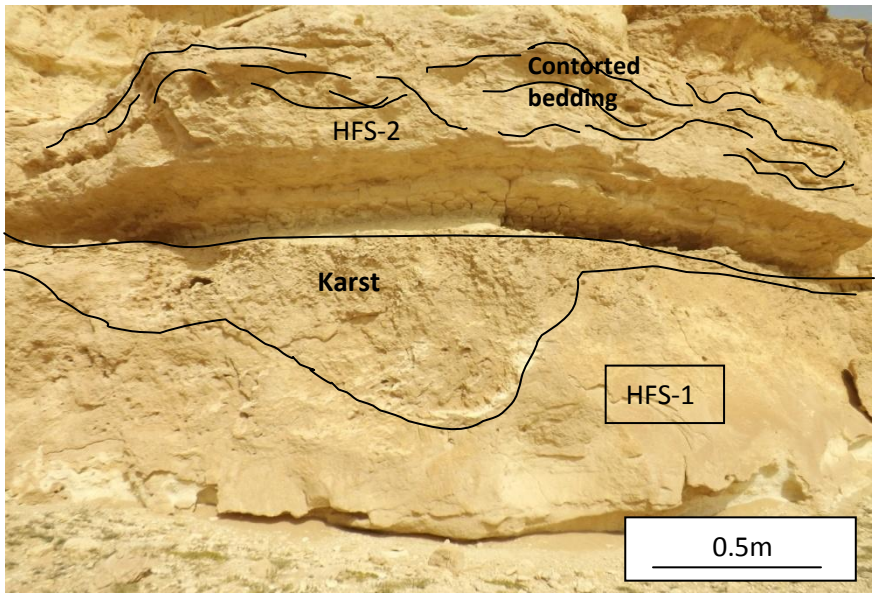

Figure-5.8.CS-2 DM-2 composed of formaniferal packstone to oolitic grainstone. This sequence shows the presence of karstification on top, which might represents a sequence boundary (?).

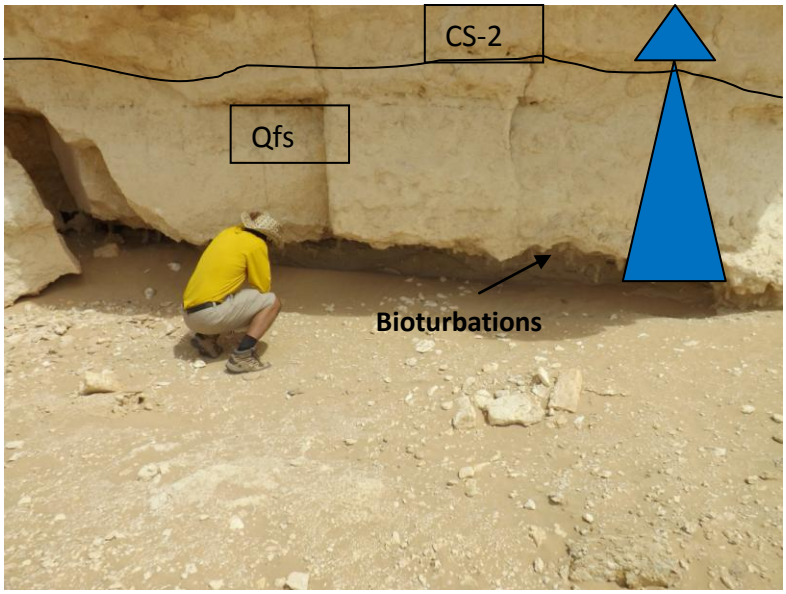

Figure-5.9.CS-2 DM-2 composed of bioturbated sandstone (Qfs) which is marked by glossifungites and intercalations of mudstone. This sequence base is marked by incision and marks sequence boundary between shale of DM-1.

The next stages of this HFS-2 TST are marked by skeletal ooidal packstone. The next facies in this HFS-2 TST is the peloidal bioclastic grainstone facies. This facies is marked by contorted bedding which marks the presence of seismic activity (Figure-5.9). The sequence is capped by skeletal grainstone facies.

5.6.4. Composite Sequence (CS-2; HFS-2 HST) DM-3

A ~3m HFS-2 HST is composed of one cycle. The HFS-2 HST is made up of skeletal ooidal grainstone that shallows upwards to packstone facies. This represents very shallower marine water conditions at the time of deposition. The facies marks the top of CS-2 and similarly the top of HFS-2. The top of HFS-2 is marked by paleosols, that are structureless and mark exposure which corresponds to the second major sequence boundary separates the CS-2 and CS-3(Figure-5.9.).

5.7. Composite Sequence (CS-3) DM-4

The CS-3 with a thickness ranging from3-7m is composed of 6 cycles. The major difference between this sequence and the other sequences is that both it and CS-4, are dominated by tidal flat and are more proximal than CS-1 and CS-2. This sequence is bounded by sequence boundary defined by bioturbated sandstone overlying paleosols of CS-2 (Figure-5.9).

5.7.1. Composite Sequence (CS-3; TST) DM-4

This HFS-3 HST is about3.4m of the CS3. This unit comprised chiefly of siliciclastic facies. This part of the CS-3 is dominated by clastic sediments. The system tract is composed of 3 cycles. The sandstone beds decrease in thickness upward, marking an overall transgressive. The varicolored siltstones and mudstones (different from paleosols) are present here. These siltstones and mudstones are marked by bedding fissility, mudcracks and rootlets. These features are evidence of exposure at this level of CS-3 (Figure-5.11; 12; 13).

5.7.2. Composite Sequence (CS-3; HST) DM-4

This 3.6-4m CS-3 HST is composed of 3 cycles. This CS-3 HST is comprised of shale and sandstone facies. It is distinguished based on continuous sandstone lenses from Outcrop-25 and 26.

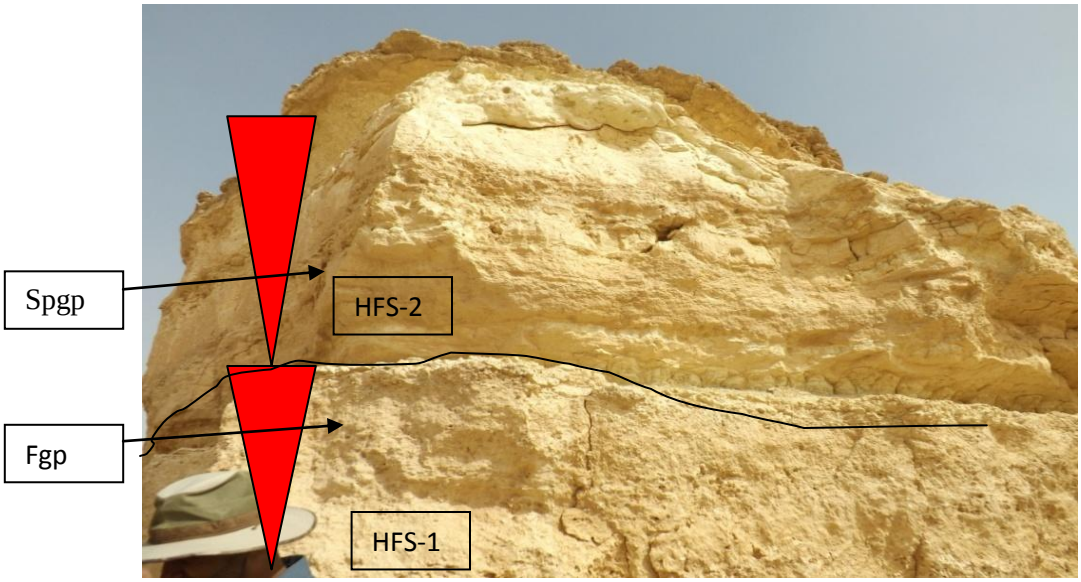

Figure-5.10.CS-2, DM-3 & 4 composed of foraminfera grainstone packstone (Fgp) and peloidal bioclastic grainstone. Then the DM-5 starts with skeletal mudstone to foraminiferal grainstone facies.

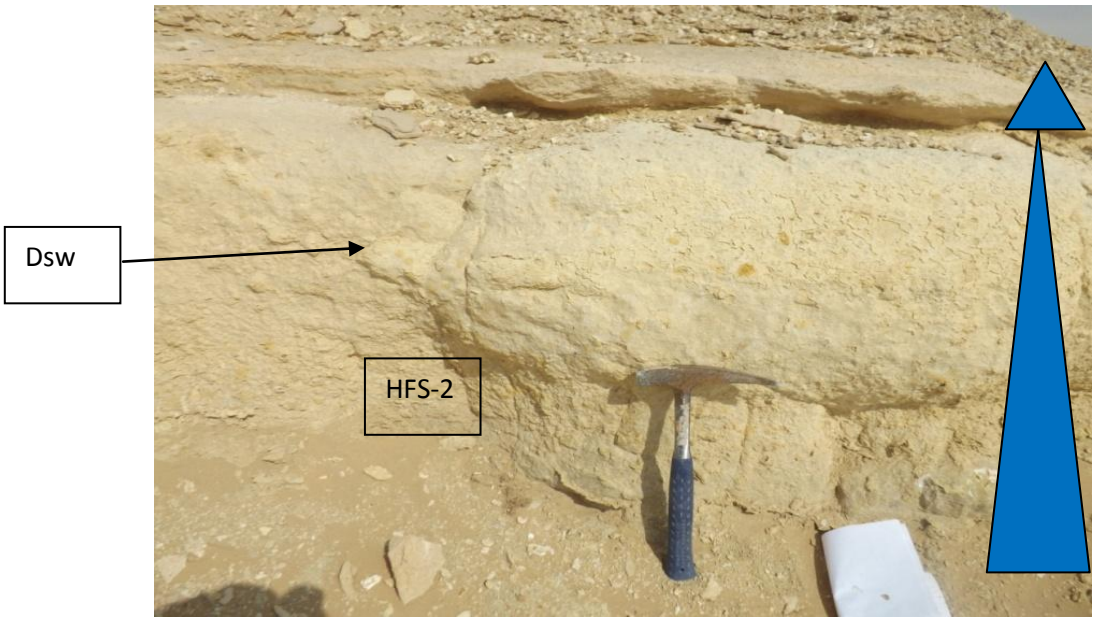

Figure-5.11.Middle ofCS-2**,** DM-3 mainly composed of dolomitized skeletal wackestone and is overlain by mudcracked shale lithofacies.

Figure-5.12.Top of CS-2 HFS-2 (DM-3) mainly composed of siltstone and mudstone (Msm), some sand lenses (arrow) and thin beds are present in this unit.

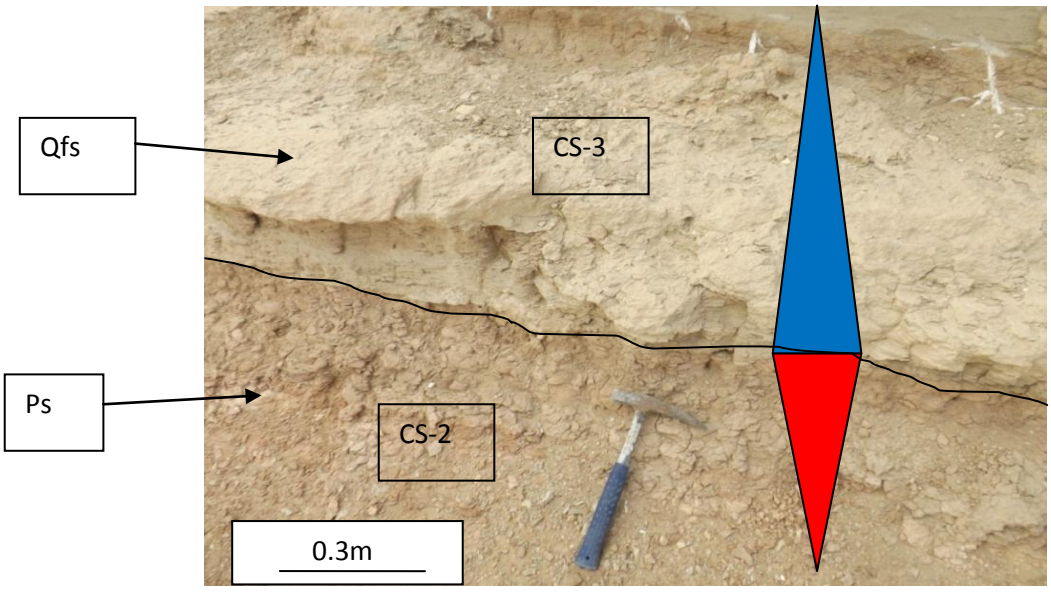

Figure-5.13.Top of CS-2 and CS-3DM-1 underlying DM-3, DM-4 is mainly composed of paleosols(PS), some sand lenses and thin beds are present in this unit. The incised bioturbated channelized sandstone (Qfs) marks the base of DM-2,black line represent sequence boundary.

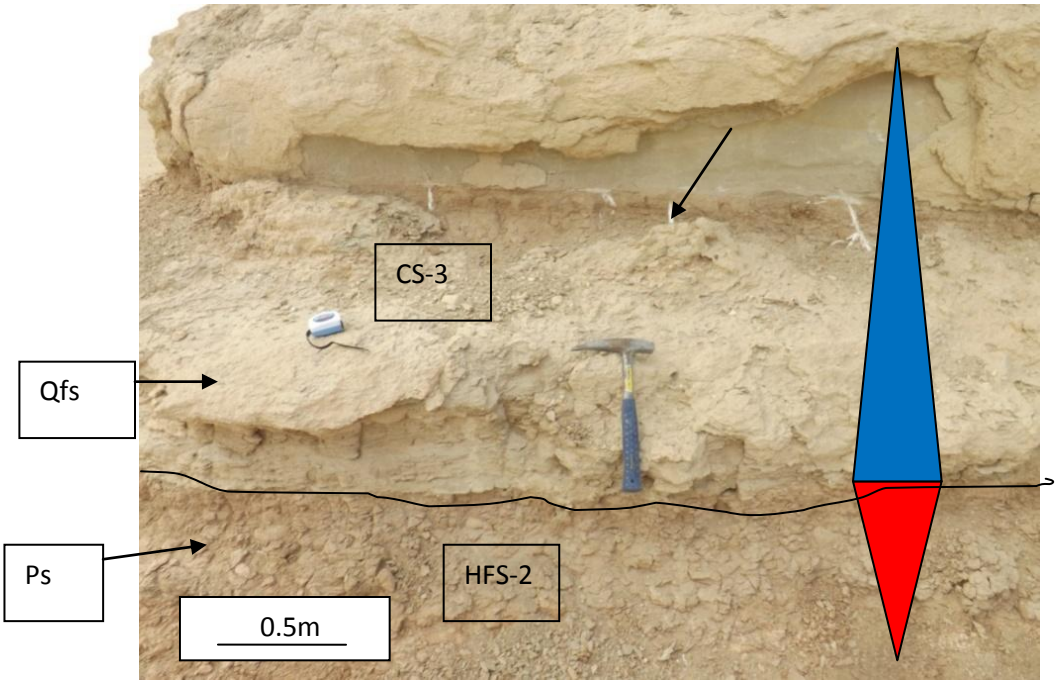

Figure-5.14.Base of CS-3;DM-3 & DM-4, the incised bioturbated channelized sandstone marks the base of DM-2. This sequence is mainly sandstone and shale interbeddings. The rootlets show exposure at the time of its deposition black line represents sequence boundary.

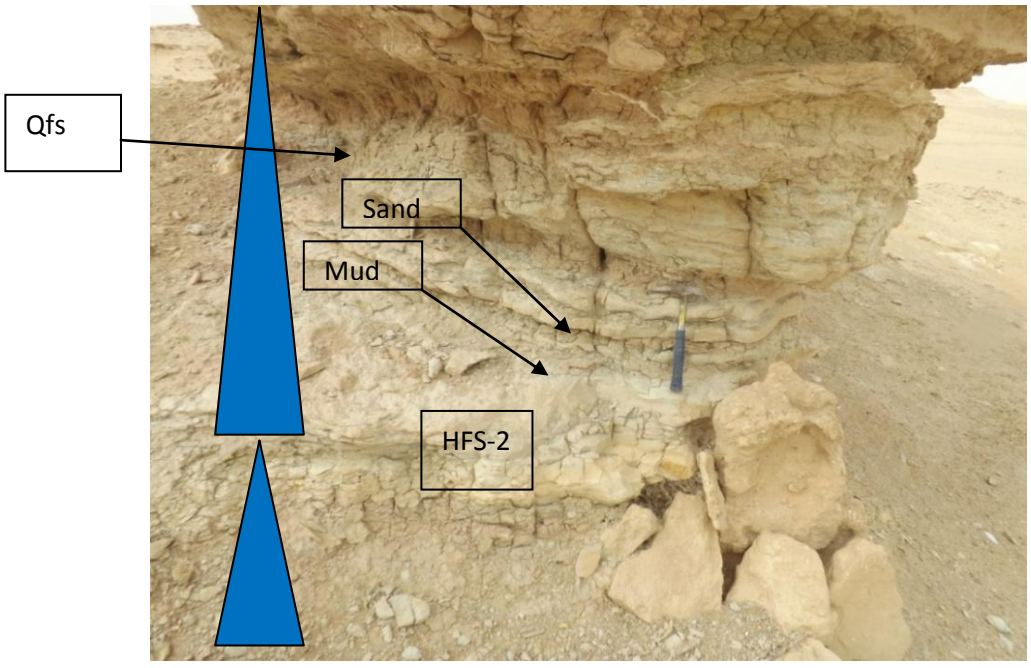

Figure-5.15. The basal most unit of CS-3DM-3. DM-3 is represented by interbedded sandstone and shale and the shale is highly mudcracked.

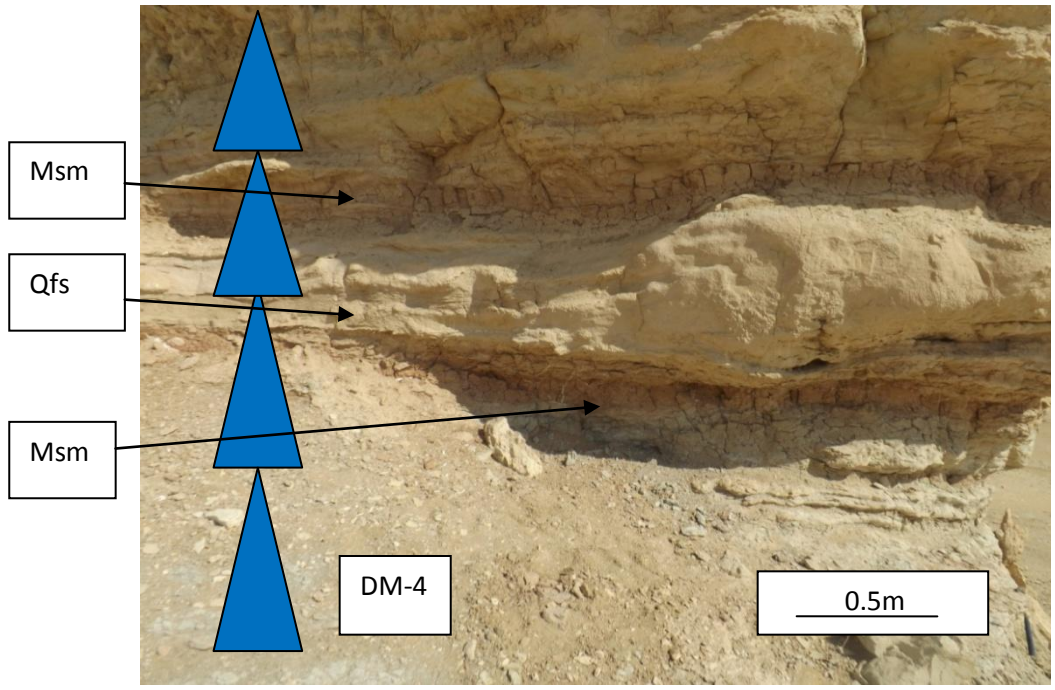

Figure-5.16.The CS-3cross bedded quartz fine sandstone (Qfs) facies interbedded with mudcracked siltstone and mudstone facies (Msm) of DM-4.

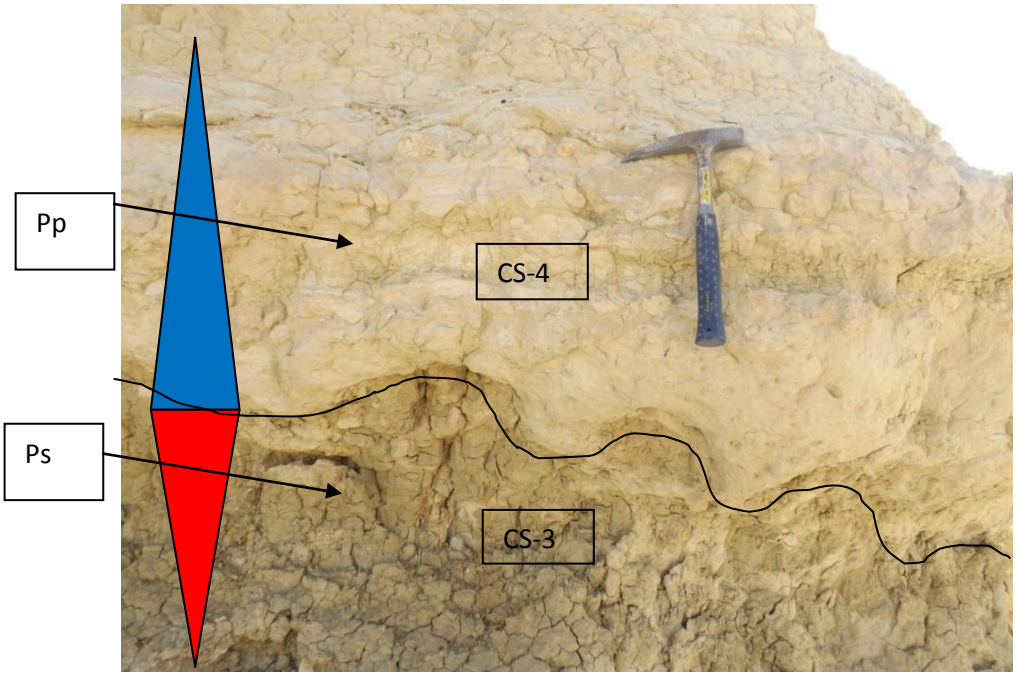

Figure-5.17CS-3 and CS-4,peloidal packstone (Pp) of DM-5 overlying Paleasols (Ps) of DM-4, black line represent sequence boundary.

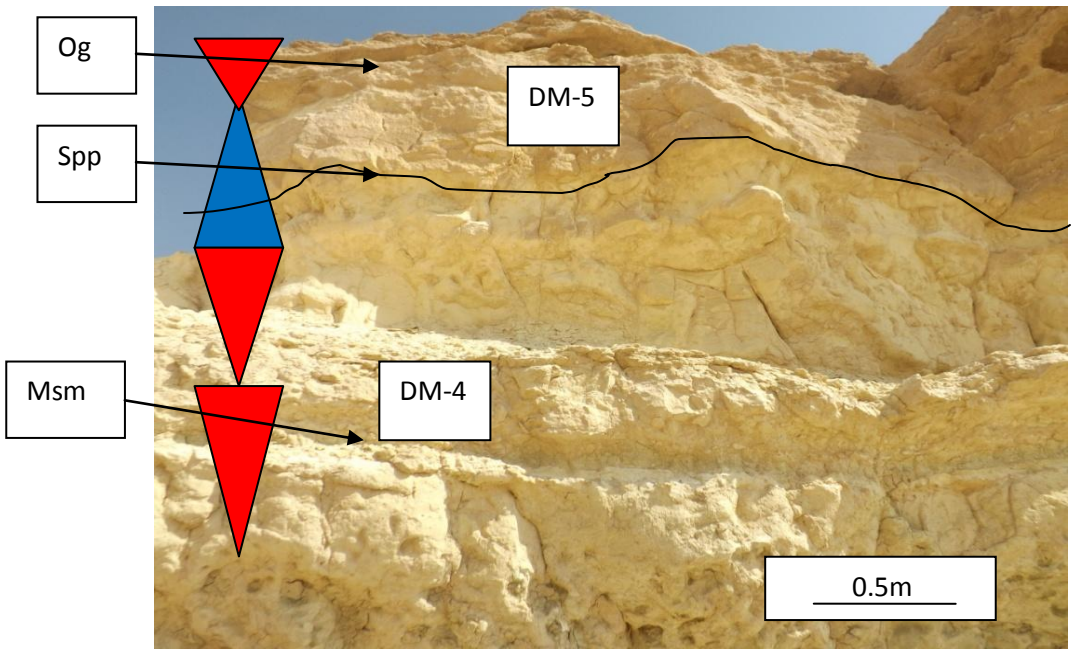

Figure-5.18The CS-3 and CS-4crinkly laminated peloidal grainstone/packstone to oolitic grainstone which marks the top of the sequence DM-5.

This sequence is aggradational and topped by paleosols. The paleosols here are around 1m and are less thick than previous sequence boundary between CS-2 (Figure-5.14).

5.8. Composite Sequence (CS-4) DM-5:

5.8.1. Composite Sequence (CS-4 TST) DM-5:

The CS-4 composed of 5 cycles, is about 6-6.5 m thick. The CS-4 TST is around 3m in thickness. This CS-4 TST is composed chiefly of peloidal grainstone packstone facies and is made up of 3 cycles. That marks the presence of mudcracked shale facies inter tidal to sub tidal. The sequence peloidal packstone contains stromatolites heads, broken. The sequence is topped by shale beds. The overall facies trend in this composite sequence is transgressive. The occurrence of packstone on paleosols marks the base of HST (Figure-5.17; 18).

5.8.2. Composite Sequence (CS-4 HST) DM-5:

This CS-4 TST, is about3-4m in thickness, is composed of 2 cycles. This system tract is dominantly comprised of skeletal packstone facies. This facies marks the presence of inter-tidal

to sub tidal conditions similar to CS-2 HFS-1 HST. There are two oolitic grainstone beds in this sequence. This grainstone facies marks the top of the Dam Sequence and CS-4(Figure-5.17; 18).

5.9. Facies maps

Facies maps exhibit the main depositional intervals which were produced to understand the matching time slice during basin development. Facies maps show the spatial distribution of facies, facies types and facies association within different composite sequences, are here compiled for selected system tracts certain time intervals. The basic technique used for making these maps is by placing the outcrop locations on the map and bounding the area with a line to show the facies lateral relationship. Then the vertical relationship of the facies in individual composite sequence is noted and then using Walther's law, the conceptual depositional pattern was created(Figure-5.19a). The maps we made to show the facies in map view as observed in different outcrops. The maps are made by keeping in view the shallowest facies is mudcracked facies while the skeletal mudstone and wackstone are the most basinward. Palaeocurrent data, lithofacies, cycles and stacking patterns are used. On the basis of these principles the different CS are shown in terms of maps.

5.9.1. Composite Sequence 1 HST

The facies map for this interval shows the oolitic grainstone in sheet geometry overlying skeletal banks. As this map represents HST, no sandstone was found here. The lack of the sandstone facies within this HST interval was likely due to the transgressive nature of estuarine sandstone (Figure-5.19b).

5.9.2. Composite Sequence 2 TST

The line separating the sandstone (yellow) body from all the other facies represents a sequence boundary. The sandstone incised all most all the underlying facies. Oolitic grainstone is not well developed within the system tracts, oolitic grainstone mostly represents still-stands in HST (Figure-5.19c).The paleosols underlying the sandstone facies can is also present within the faces map interval. And there distribution is largely controlled by sandstone incision.

5.9.3. Composite Sequence 3 TST

A facies map of interval starting from second sequence boundary up to the Maximum Flooding surfaces is presented here. The sandstone overlies paleosols and cuts all the underlying facies. Note the presence of skeletal grainstone bodies. The absence of the oolitic grainstone from this sequence could be due to the inhibition of the growth of oolitic sheets by the prevailing depositional energy at time the interval was deposited(Figure-5.19d).

5.9.4. Composite Sequence 4 TST

This CS shows the area covered by tidal flat deposits and mudcracked shale lithofacies. Oolitic grainstone bodies and skeletal grainstone were not deposited within this CS. It shows the dominance of tidal flat environment in the setting. The tidal flats deposits are dominant in the north (Outcrops-25 & 26) (Figure-5.19e). Note the absence of oolitic grainstone shows its likelihood to occur during highstand. While the dominance of tidal flat and presence of mud cracks and rootlets represents transgressive nature of this facies map.

5.9.5. Composite Sequence 4 HST

The dominance of oolitic grainstone and overlying thick skeletal packstone facies in CS 4 HST, suggest that the conditions that led to deposition of older CS were repeated during its deposition. The facies map shows the dominance of oolitic grainstone in sheet geometry overlying skeletal grainstone in lens geometry formed in skeletal banks. An important observation to be made here is that, absence of sandstone facies in this facies map. The absence of sandstone is indicator of the fact that sandstone is found only in transgressive section (Figure-5.19f).

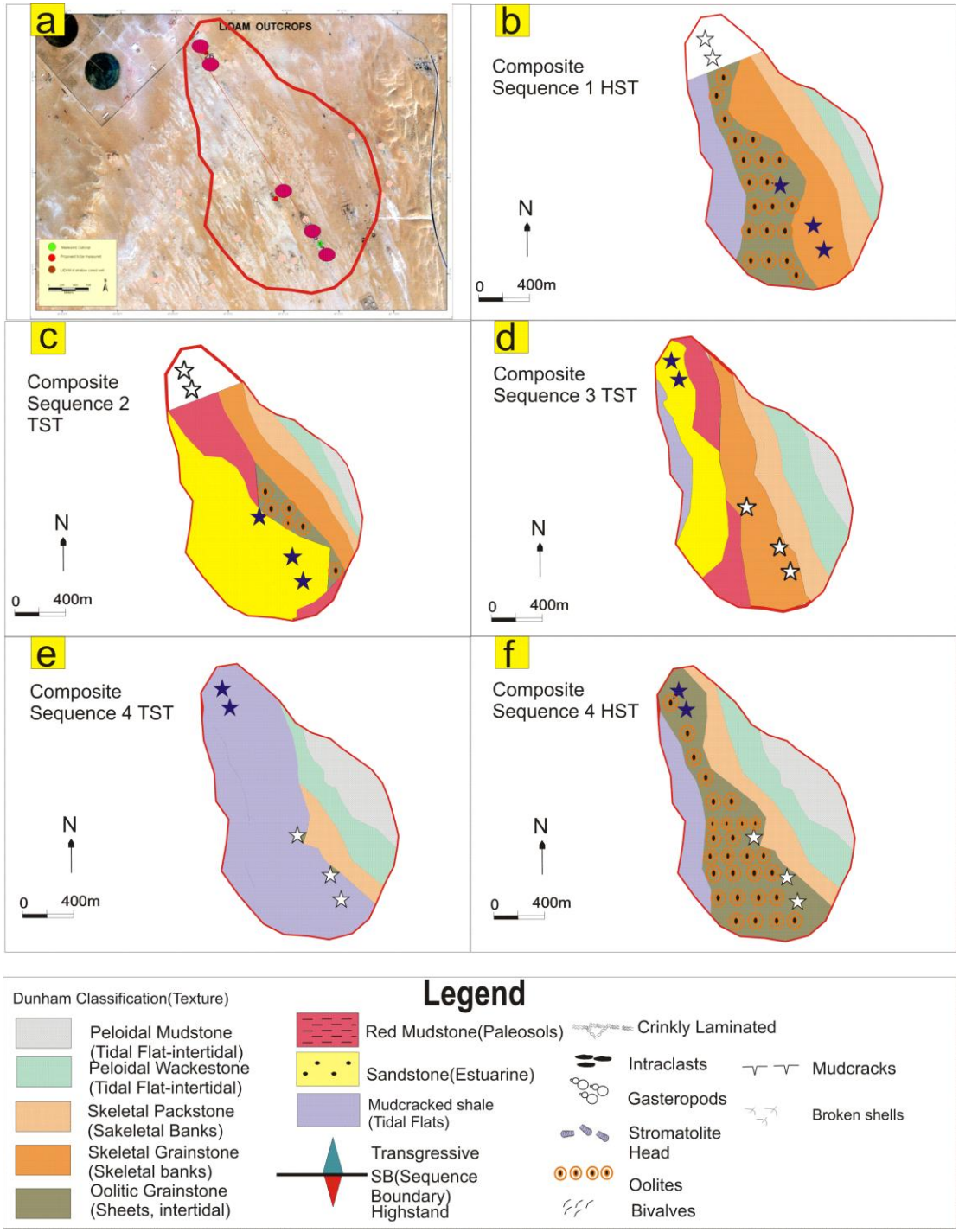

Figure-5.19 Facies maps are made to show the facies in map view as observed in different outcrops.The maps are constructed by keeping in view the shallowest facies is mudcracked tidal flat facies while the skeletal mudstone and wackstone are the most distal facies. Blank stars denote inferred information and not based on actual data while the filled ones indicate interpretation based on actual data.

CHAPTER 6

DISCUSSION

6.1. Discussion

The integration of field studies, petrography and geochemical data provides new geological insight into the cyclicity and stacking patterns and depositional environments of the Dam Formation in Al-Lidam Area. This study may help improve our understanding mixed carbonate-siliciclastic systems, especially Dam Formation. The seventeen lithofacies identified in this study suggest more detailed documentation on, their vertical relationship and presence of skeletal banks and estuarine as additional subenvironments in the different outcrops. The ooids found to be in sheets associated with stromatolites. They do not form shoals and are concentrated within the algal laminas. The modern analogue exists in the Hamelin Pool of Western Australia.

There are unconformities within the Dam Formation succession. It comprises of one composite sequence, where the lower part was deposited in inner neritic zone and the upper part was deposited in tidal flat environment. The Dam Formation exposed in Al-Lidam area is more characteristic mixed carbonate and siliciclastic succession. In Qatar it is dominated by carbonate and evaporites(Al-Saad et al., 2002). On the basis of the present study, the succession in Qatar, seem to be more distal and subjected to carbonate deposition. The Al-Lidam area is relatively proximal as evident by the presence of mixed carbonate-siliciclastic facies in the studied outcrops. The lithofacies here present more variety, cyclicity and stacking patterns. The outcrops

in north are dominated by tidal flat deposits are even more proximal than those in the more distal ones in the south, dominated by skeletal packstone interbeds.

The occurrence of evaporites in Qatar indicates more arid condition leading to the existence of sabkha environment is also indicated by the presence of gypsum and celestite in the Dam succession. However, the evaporites minerals do exist in the tidal flat facies of the Dam in the study are not much dominant. The presence of stromatolites, red mudstone, mud cracks and rootlets indicate the existence of arid climatic conditions during the time of deposition of the succession. According to Al-Saad (2002) the Dam was deposited in very shallow tidal flat setting under warm climatic conditions. The lithofacies identified in our study area, however, suggest more variety of depositional environments ranging from supratidal, tidal flats, intertidal, skeletal banks to distal. This shows the Dam Formation was deposited under a range of water depths, and also about variety of sub-environments and their interrelationship in terms of vertical stacking and cyclicity.

The carbonate geobodies are important in this aspect as they aid in the identifying the depositional elements and environment of deposition(Köhrer et al., 2011). The skeletal banks are present as lenses which help in the interpretation of carbonate skeletal banks. The ooids occurred as sheets along with stromatolites instead of created the oolitic shoals and creating any barrier. Instead the small skeletal banks were creating barrier and led to the deposition of wackestone and mudstone facies in the intertidal zone shoreward from them. The ooid sheet shifting pattern is observed from successive composite sequences towards the shore(Irtem, 1987). A similar pattern observed for skeletal bank lenses shows the changing sea-level and its control on the individual sequence and facies.

On the basis of these facies, the Dam is described to have been deposited in a restricted environment. This interpretation was based on the dominance of gypsum and evaporite minerals. But the occurrences of shelly packstone and stromatolitic limestone indicate skeletal banks and intertidal conditions respectively (Tleel, 1973). The diagenetic history includes dolomitization and meteoric leaching (Tleel, 1973). These finding are in agreement with our work, as extensive leaching has been observed in some of the facies where entire bivalves and ooids were completely dissolved. The outcrop-25 indicates crystalline dolomite in crystalline limestone

facies. This facies is only restricted to outcrops in north which probably indicate proximity to the inland waters which were responsible for this transformation.

The depositional environment ranges from terrestrial to open marine setting (Weijermars, 1999). Several of the facies identified in this study are available in above listed facies. This setting is very similar to our study area, except the report of channelized sandstone facies which marks the unconformity in our study area. Deposition in case of Jeribe Formation (Iraq) seems continuous with small breaks as indicated by paleosols, and the locations were located on same ramp with subtle topographic variations (Al-Ameri et al., 2011).

Moghaddam et al. (2006) found four upward shallowing cycles in Asmari Formation in Iran and ten lithofacies. The upper Asmari is an equivalent of the Dam its lithofacies included by Planktonic forman-bearing mud-wackestone(outer slope to basin), bioclastic-rich planktonic foram bearing wacke-packstone(outer slope), Planktonic foram-bioclastic rich nummulitid wacke-packstone (slope), nummulitid bearing bioclastic-coral wackestone to packstone(upper slope), bioclastic grainstone(shoal, platform margin), foram-coral-bioclastic pack-grainstone(platform margin towards lagoon), bioclastic rich miliolid-borelisid wackestone to packstone(shelf lagoon), miliolid-intraclast-bioclast packstone to grainstone(restricted lagoon), mudstone containing shell fragments(restricted lagoon), and stromatolites bearing boundstone(low intertidal to supratidal). According to the authors the whole succession was deposited on a ramp. The basin and slope of the environment was separated from the lagoon by a shelf margin. Sequence stratigraphically the Asmari Formation is divided in to four episodes of shallowing and deepening upward(Moghaddam et al., 2006). Numerous facies identified in this study are similar to Asmari, but their work seems to be more aligned to foraminfera and biostratigraphy. The sequence boundaries between composite sequences were identified using stromatolitic boundstone. However, there is no report of rootlet bearing paleosols, mudrocks and channelized sandstone in the work, which makes us make interpret that the Asmari Formation was more distal as compared to its equivalent Dam. Also as indicated by the above listed sedimentary features, the environment of the Asmari Formation was less arid than that of the Dam.

These observations are in agreement with AlKhaldi et al., (2014) work which examined the effects of glacio-eustasy during moderate Antarctic glaciations. They suggested that the updip sections of the Dam Formation are dominated by siliciclastic sediments grading downdip into carbonates under semi-arid and locally hypersaline conditions and that the subsidence rates were slower than in the proximal foredeeps in Iran. These conditions resulted in the formation of paleosols near the sequence boundaries in the Hadrukh and Dam Formations. These subsidence rates were even reflected at scale of composite sequence as the sequence boundaries are marked by channelized sandstone overlying paleosols.

Several of the sedimentary features found in their study are recorded in of the facies, identified in this study. The development of stromatolites is seen in outcrop 6 and 7. The important addition to this study is that these stromatolites are not present as extensive sheet. The reason could be due to the influx of clastic sediments which inhibited the growth of stromatolites on whole the Lidam area. However, there are two episodes noted for stromatolites growth in the area. The first one is observed in Composite Sequence-2 between Outcrops 6, 7 and 10. The second event is in Composite sequence-4. The lithofacies identified in this study suggest more details, as five outcrops are correlated on the basis of facies described and show more distal facies in SE while more proximal facies in NW.

The 2D-Correlation is very helpful in deciphering the Composite sequences present in the study area. First, the sequences are broken down along sequence boundaries and then the numbers of cycles used for correlation, helps in the identification of the composite sequence and their lateral continuity. On this basis, four composite sequences were identified. The identification based on the stacking patterns and three sequence boundaries. The basis for putting this sequence follows facies lateral and vertical relationship, geometry, number of cycles and sequence boundaries. These sequences are more extensive, the sequence starts with wackestone/mudstone facies and is capped by oolitic grainstone facies. The channelized erosive sandstone deposited over paleosols and then continued to the TST. The presence of mudstone and wackestone marks the presence of MFS and after that the HST starts and these are topped by oolitic grainstone bodies. Our criteria for making these observations include variation in sea-level, wave base, presence or absence of stromatolites, and ooids.

6.1.2. Conceptual Depositional Environment:

The seventeen identified in the study are the facies skeletal coated skeletal grainstone (Csg), coated bioclastic grainstone (Cbg), peloidal bioclastic wackestone (Pbw), bioclastic peloids packstone (Bpp), ooid grainstone (Og), micritised ooid peloidal grainstone (Mpg), Sandy peloidal skeletal grainstone (Spg), dolomitized skeletal wackestone (Dsw), formaniferal peloidal grainstone (Fpg), Sandy peloidal grainstone-packstone (Spgp), peloidal packstone (Pp), Sandy peloidal packstone(Spep), quartzose fine-medium sandstone (Qfs), miliolid peloidal packstone to wackestone (Mpw), calcareous fine sandstone (Cfs), paleosols (Ps) and mud cracked siltstone mudstone facies (Msm).

The grain contents and sedimentary structures of Coated Skeletal Grainstone (Csg) facies indicate it was deposited by high energy and agitation within skeletal banks which occur within a shoreface environment(Figure 6.2). These conditions are often met where a change in energy conditions of the basin coincides with the tidal or wave action (Scholle, 1983). The increase in skeletal fragments from south to north suggests the presence of main skeletal bodies in the north at the time of deposition (Flugel, 2004; Figure-6.2). Modern examples probably include skeletal banks in the south Florida platform area (Bears, 1962).

The grain content and sedimentary structures of Coated bioclastic grainstone (Cbg) facies indicate it was deposited in high energy, within skeletal banks which occur within occur within a shoreface environment. The occurrence of grainstone texture indicates that there was no protection at the time of deposition due to the absence of carbonate mud (Figure-6.2).

Peloidal Burrowed Wackestone (Pbw) facies is, interpreted to be deposited in more distal environments is than that of the coated skeletal grainstones and ooid grainstones, in low energy environment probably in a shallow subtidal. This interpretation is also supported by the matrix that is formed by peloids, and its stratigraphic position above the tidal flats facies (Flugel, 2004). Possible Modern day analogue is peloidal grainstone at the Hamelin pool, in Shark Bay (Hoffman, 1976).

Bioclastic peloidal grain-dominated packstone (Bpp) Facies is interpreted to have been deposited by fluctuations of fair wave weather base. The presence of quartz particles and broken shells indicates high energy waves while the packstone fabric was likely produced by relatively

moderate to high energy at the wave base (Figure 6.2; Flügel, 2004). Facies is interpreted as a transitional between carbonate banks and tidal flat (Figure6.2). Facies occur in upward shallowing cycles. The presence of intraclasts (skeletal and quartz bearing) in facies indicates erosion of some preexisting sheet and its proximity to the source area, as no such clasts are found in distal outcrops.

The Ooid grainstone (Og) facies marks the development in oolitic shoals is very typical of the Dam Formation. The environment of deposition of the facies is interpreted as intertidal (Figure 6.2;Scholle, 1983).The oolitic sheets along with some foraminfera and skeletal were once a part of large sheets blanketing the region. This facies marks the top of the cycle that started with the deposition of micritised mud. The skeletal grains are characterized by clean appearance which was likely formed in agitated water under high energy conditions such as an intertidal environment and nearshore where waves and currents have strong effect (Flugel, 2004). On the basis of sedimentological observations the environment of deposition is sub tidal to intertidal (Scholle, 1983).Possible Modern day analogue is the Joulters ooid sand shoals in the Great Bahamas Bank that occurs as sheets controlled by winds(Harris, 1984).

This Micritised oolitic peloidal grainstone (Mpg) facies provides the platform for skeletal and oolitic skeletal facies to form (Figure 6.2). The environment of deposition of this facies is interpreted as intertidal to carbonate banks (Scholle, 1983). Micritised ooid grainstone are formed in subtidal to environments where the stromatolites were growing (Irtem, 1987).The amount of quartz in this lithofacies would suggest that it was deposited in more distal environment (landward) than the pure oolitic grainstone where there is little or no quartz. The closely to land allowed for influx of clastic detritus. The repeating patterns of lithofacies suggest that the sedimentation was cyclic (Grammer et al., 2005). The ooids are micritised, medium grain ooids occurred at base and fine grain ooids at top. The possible modern day environment with similar depositional setting to this facies is found in the Shark bay (Flugel, 2004). The presence of cross-bedding suggests prevalence of high energy at varying depths.

In Sandy peloidal skeletal grainstone (Spg) the quartz particles and broken shells indicate high energy waves while the grainstone was likely produced by relatively high energy at fair weather base(Flugel, 2004). The depositional environment for this facies is transitional between carbonate banks and tidal flat. This facies occur in upward shallowing cycles. This interpretation

is also strengthened by the presence of intraclasts in this facies that indicates erosion of some preexisting sheet and its proximity to the source area, as no such clasts are to be found in distal outcrops. Possible modern analogue is peloidal skeletal grainstone of south Florida Banks (Bears, 1962).

In the Dolomitic Skeletal Wackestone (Dsw) crystals seem to be resultant of recrystalization of carbonate mud during diagenesis. The dull appearance of samples from the facies also favors this interpretation. The rock is composed almost of crystals and fine mud and it means deposition in a low energy substrate (Figure-6.2). Deposition is similar to clastic mudstone. The mud starts aragonite needles of 5 to 10 microns in length and formed by calcareous algae (Flugel, 2004). Modern example for carbonate mud deposition exists in the internal part of the Florida Bay Lagoon (Bears, 1962). The occurrence of *Borelis melo melo* (Figure-6.1) places in Lower part of Dam Formation exposed at Outcrop-25 shows that it is equivalent to the Al-Nakash Member of Dam in Qatar (Al-Saad el al, 2002).

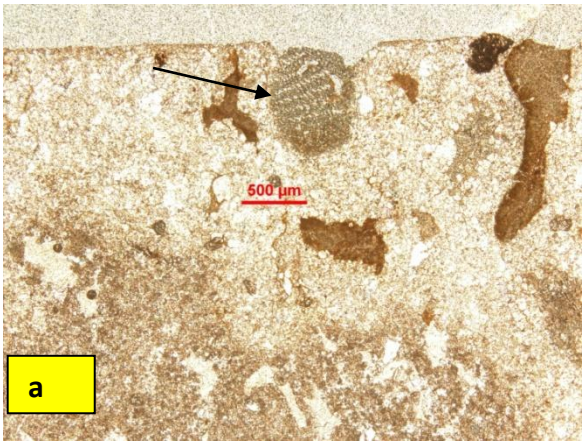

Figure 6.1. Photomicrograph of *Borelis melo melo* in Dsw (Dolomitic skeletal wackestone) facies.

The sedimentary structures and grain size of Foraminiferal peloidal grainstone (Fpg) facies indicates high energy, below the fair weather wave base. This facies is thought to be deposited in skeletal banks. This interpretation is strengthened by the absence of carbonate mud and grain dominated nature of this facies (Figure-6.2; Scholle, 1983).Karstification is important feature for identifying break in deposition. The karstified grainstone and it is overlain by tidal flat shales, show the presence of early diagenetic process and subaerial exposure, by occurrence

of crystal silts and prismatic cements (Flugel, 2004). The outcrop section is dominated by blackened limestone structure for example and alveolar textures (Figure 4.10a) are also found in this facies (Nakazawa et al., 2004). The alveolar texture is formed by penetration of rootlets in sediments, which cause micritization of adjacent channels (Curran, 1995). The overlying tidal flat deposit is 1 meter thick and is a clastic unit.

Sandy Peloidal packstone (Spep) represents as laminated and is interpreted as intertidal to subtidal environment (Figure-6.2). The presence of some intraclasts indicates storm reworking. On the basis of presence of shells and grain supported fabric this facies is interpreted to be deposited in subtidal to intertidal (Flugel, 2004; Scholle, 1983).On the basis of sedimentary structures(contorted bedding and bioturbations), the environment of deposition of Peloidal packstone (Pp) interpreted as tidal flat (Scholle, 1983).The grain size and sedimentary structure of this facies indicates low to medium depositional energy below the fair weather wave base, this facies is thought be deposited in tidal flats. Modern day example possibly includes South Florida, where mud is accumulated by physical layered sedimentation of packstone and creates mounds (Bears, 1962).

The sedimentary structures in sandy peloidal packstone (Marl) (Spep)show wave or current that alternate with slack water. The texture and sedimentary structure indicates deposition was under the supratidal conditions (Figure 6.2;Flugel, 2004).

During this time, the carbonate sediments were diluted due influx and the abundance of clastic sediments. The presence of mudcracks suggests that the deposition took place under dry and warm conditions (Scholle, 1983). Modern analogue of tidal flat environment is Trucial coast of Abu Dhabi (Al-Sharhan et al., 2002).The glossifungites reflects medium energy and semi-consolidated substrate at the time of Fine to medium Quartz Sandstone (Qfs) facies deposition. This trace fossil indicates firm ground, in tidal flat to estuarine zones. The intraclasts at base result of flooding at the base. (Figure 6.2).

The fine to medium grained quartz particles, orthoclase and clays are important constituents of Qfs facies. The porosity ranges in this facies from less than 3% (Figure 4.14b). XRD analysis shows that the, this facies is composed of more than 95% quartz and accessory minerals. Grains are closely packed and dominant cement type is quartz overgrowth (Figure 4.14b). The grain size ranges from fine to medium sand size. The particles are poorly sorted.

SEM image show quartz grains at 100 microns, note the quartz grains are also coated by clay minerals probably palygorskite which favors our interpretation of removing preexisting sediments and redepositing them again(Figure 4.14g). The EDS yellow curve represent high Si is due to abundance of quartz (Figure-4.14f). The facies is cross-bedded in places and massive in some other part. The cross beds may have been well preserved where the facies shows little or no bioturbations in the northern outcrops. The massive nature of the beds suggests rapid deposition. While the presence of mudstone suggests deposits as when the sandstone was restricted to an off shore transition zone. The deposition might have taken place under unidirectional currents. The presence of glossifungites shows semi consolidated substrate. Based on the lithology and sedimentary structure the sandstone is estuarine in nature (Bressan et al., 2009).

These inclined heterolithic stratifications(IHS) are indicator of estuarine point bars and are built as a result of vertical and lateral accretion in subtidal environment. The modern day analogue is Modern Estuarine channel in Willapa Bay, Washington (Schoengut, 2011). The variation in thickness of this IHS sets is regarded to change due to fluctuation of tidal currents, the increase in sand unit as compared to mud unit thickness in south is indicator of high energy and sedimentation rates, and this is indicator of subtidal conditions. The increase in mud content and increase in bioturbations indicates low energy and slow sedimentation rates. The other interpretation could be upper portion of the facies is exposed.

The texture and sedimentary structure in Miliolid Peloidal Packstone-Wackestone (Mpw) facies indicates deposition in tidal flat (Flugel, 2004; Figure 6.2). During this time the carbonate sediments were abundant and absence of clastic sediments. The deposition took place under dry and warm conditions as is witnessed by the presence of mudcracks (Scholle, 1983). Modern analogue of this facies is in tidal flat environment is Trucial coast of Abu Dhabi (Al-Sharhan et al., 2002).

This Calcareous Fine Sandstone (Cfs) is calcareous in nature and is devoid of any trace fossils. The prominent sedimentary structure in this facies is cross bedding (Figure 4.14a). The overall geometry of the facies is channel shaped and it appears to be a valley fill (Figure 4.14b). The thick bedded nature of the facies suggests the possibility of a rapid deposition (Figure 6.2). The presence of mudstone interbeds within the thick sandstone bodylenses suggests intermittent

episodes of low energy. Based on the lithology and sedimentary structure the sandstone is estuarine to tidal flat deposited (Bressan et al., 2009).

During the time of Paleosols (PS) deposition the carbonate sediments were absent and were characterized by the abundance of clastic sediments. The deposition took place under dry and warm conditions as is witnessed by the presence of mudcracks. These paleosols are weathered overbank deposits and consist of rootlets that show topsoil. The paleosols facies in the cycle boundaries above are similar but are more like weathered in to sandstone channels above in the stratigraphic section. These show oxidation and depletion of iron, which include rootlets and haloes. The iron depletion indicates high water table and poor drainage in the area (Prochnow, 2005).On the basis of sedimentary structures like mud cracks and bioturbations show exposure at the time (Scholle, 1983).

The fibers seen in the SEM image (Figure 4.17b), are palygorskite covered almost all small grains as envelopes in a very similar way as the micrite covers most carbonate grains. Its occurrence shows fluctuation between dry land and lacustrine lake, as is seen in the Neogene paleolakes of Kalahari basin, South Africa (Botha et al., 1992). The XRD analysis also shows presence of Palygorskite along with peaks of quartz (Figure 4.17c).

The presence of mud-cracks and evaporite minerals (gypsum and anhydrite) in the form of nodules, in this Mud cracked siltstone and mudstone facies (Msm) facies shows features characteristic of arid tidal flat environment (Figure-6.2). The sedimentary structures in siltstone beds show setting of wave or current action that alternate with slack water.

In depositional model, these facies are placed according to the level of deposition energy. The lowermost facies represents high deposition energy while the uppermost represents low deposition energy (Figure-6.2). Despite the dissolution of the skeletal and oolitic grains in the Dam Formation in Al-Lidam Area, the depositional fabrics are well preserved and permit detailed facies analysis. The main environments identified on the basis of sedimentary structures, grain types, vertical relationship and cyclicity are supratidal, tidal flats, intertidal, skeletal banks and distal basin. The coated skeletal grainstone facies (Csg) and coated bioclastic grainstone (Cbg), skeletal bank to proximal basin. Ooid grainstone (Og) and micritised ooid peloidal grainstone (Mpg) indicates intertidal to skeletal bank, sandy peloidal skeletal grainstone

facies(Spg) represents skeletal banks to intertidal setting. Peloids packstone (Pp) corresponds to intertidal, to proximal basin. Paleosols facies (Ps) signifies supratidal and subaerial exposure. Bioturbated quartz sandstone with mudstone facies(Qfs) and calcareous sandstone (Cfs) were deposited in tidal flat and estuarine, Peloidal burrowed wackestone (Pbw) and bioclastic peloidal packstone indicates intertidal to skeletal banks while the foraminiferal grain-packstone facies(Fgp) supratidal to tidal flat, miliolid peloidal packstone wackestone (Mpw), Marl and mud crack marl represent tidal flat environment (Msm) indicate tidal flat. The peloidal grainstone facies (Pgp) represents skeletal bank to proximal basin and skeletal wackestone shows intertidal to tidal flat setting (Schlager, 2005). The shallowest facies is paleosols that passes laterally in to tidal flat mudcracked and bioturbated facies. The ooids and peloidal facies are the next facies that represents intertidal environment, skeletal are next to come along with carbonate banks. The skeletal oolitic occurs adjacent to the environment of tidal flat grades into carbonate banks (Carozzi, 1989; Walker et a., 1992).

Mostly proximal facies are commonly of muddy texture and reddish colour. These are marked by subaerial exposures such as karstification, paleosols, mudcracks and rootlets and are recognized as supratidal deposits. The blackened karstified foram grainstone-packstone was partly deposited tidal flat setting close to the shoreface(Franseen et al., 1996; Walker et a., 1992). The bioturbated sandstone containing mud interbeds and rich in ichnofacies of glossifungites, was deposited in estuarine to tidal flat setting. It is important to note that the facies of low energy setting are of muddy texture and are commonly bioturbated. Tidal flat facies is composed of shales and fine grain clastic sediments, mudcracked and abundant rootlets, white to light grey colour, were deposited in tidal flat environment, with small exposure episodes represented by mud cracks. Skeletal wackestone facies with the most of its texture altered due to dolomitization was deposited in sheltered environment of tidal flat. It was likely a skeletal mudstone to wackestone was dolomitized to form crystalline dolomitic limestone, as few skeletal moulds could be seen under the thin section. As we move from proximal to distal setting with more energy, facies become more grain dominated. Ooid grainstone and micritised ooid grainstone with sharp bases and cross bedding are interpreted as moderate energy intertidal to skeletal banks

environment. This depositional environment contains stromatolitic heads and digitates with peloids. The sandy peloidal packstone was also deposited near the intertidal setting (Figure-6.2).

The stromatolites as described by Irtem (1987) occur as thin sheets of ooids. Distally, we are near the skeletal banks environment, here the deposition energy is moderate to high. The sandy skeletal grain-packstone facies was deposited here. The presence of quartz indicates influx of clastic sediments carried by winds in to the environment. This interpretation is made on the small size of quartz grains and their uniform size. The distal facies are light to dark brown in colour and bioturbated, are comprised of few skeletal particles passed from skeletal banks to proximal basin setting. This coated skeletal grainstone, while more offshore the peloidal quartzose wackestone mudstone was deposited.

The cyclic alterations of muddy proximal and grainy distal facies are well exposed in outcrops, weathering outlines. Muddy interval, that is more prone to weathering conditions (Schlager, 2005). These beds form recessive units in the outcrops. In contrary, the grainy units are more weathering resistant and form persistent cliffs. Following the (Figure-1.6)AlKhaldi (2009) for work on an outcrop (Outcrop-5) in the Lidam area, the grainy dominated cross-bedded intertidal oolitic grainstone represents the top of the cycle, and marks the base of a new cycle. Rooted and mudcracked tidal flats marks the fall in sea-level. The paleosols and channelized sandstone facies are important for high resolution stratigraphic interpretation and used to delineate sequence boundaries in Dam Formation.

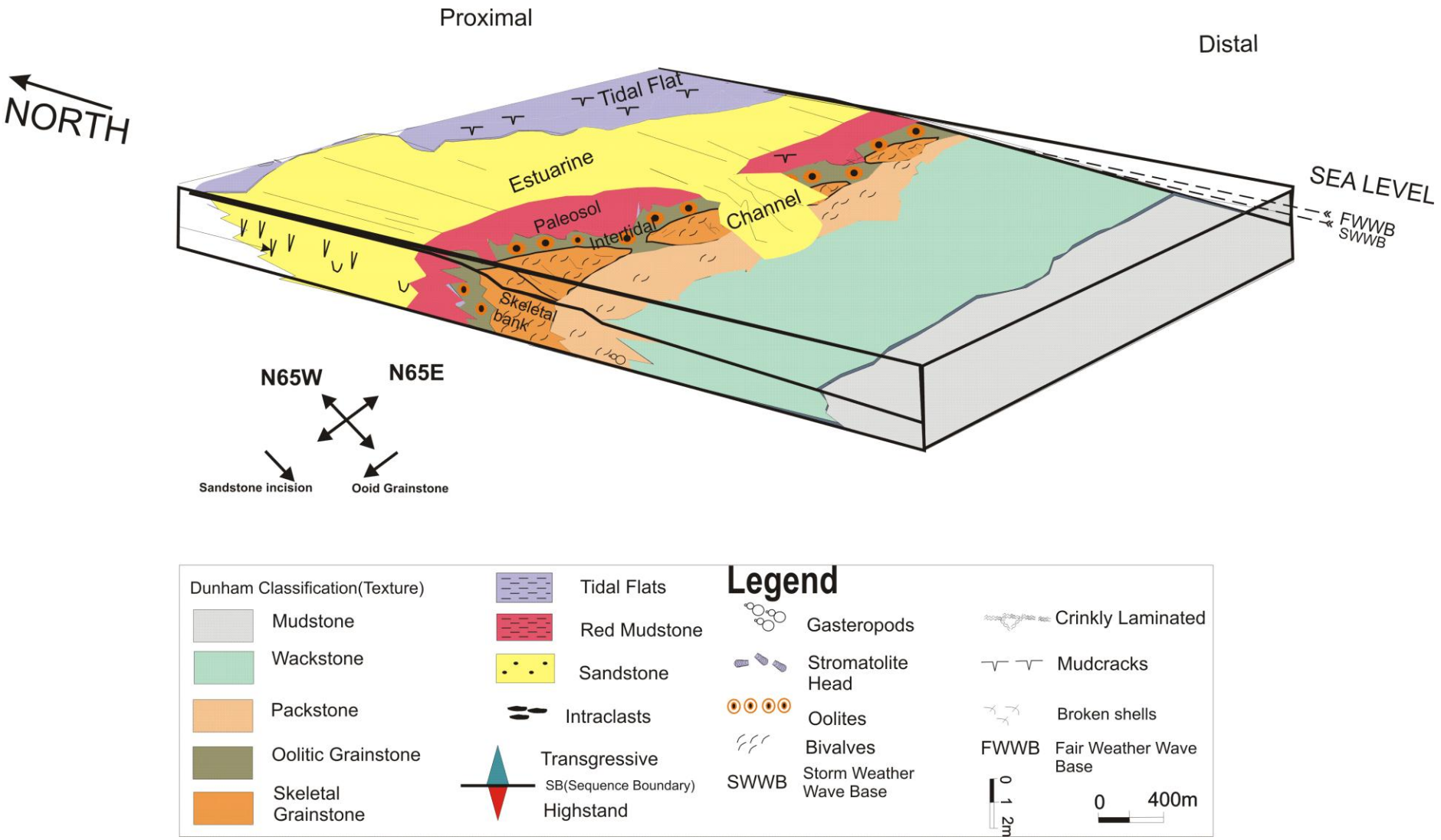

Figure.6.2. Depositional model for the mixed carbonate-siliciclastic Miocene Dam Formation, Al-Lidam Area, Eastern Province, Saudi Arabia. The outcrops in the south are rich in carbonate while the outcrops in north are dominantly characterized by siliciclastic sediments. Bioturbated sandstone channels bypassed the proximal inner ramp and transported the material on distal inner ramp. This bioturbated sandstone marks the sequence boundaries and is very useful for correlation across the NS-Transect.

6.1.3. Lithofacies Geometry

6.1.3.1. Carbonate Geobodies

Measuring dimensions, shapes and orientations of geobodies provides us with quantitative data for characterizing the facies heterogeneity. Characterization of carbonate geobodies is important as they reflect the controlling factors on carbonate depositional environments (Table-4.1.; Jung, 2012).

6.1.3.2. Carbonate Geobodies Types

Carbonate geobodies are identified based on data that were obtained from facies mosaics, high resolution model and modern day carbonate environments. Based on these criteria, three carbonate geobodies were identified. These are sheets, lens and channel bodies.

6.1.3.3. Sheet Geobodies

This type of geometry is presented by the tidal flats, wackestone to mudstone and ooid grainstone along with stromatolites. As a result of terrigenous influx into the basin, the stromatolites were not able to grow over the whole area (Figure-6.3). The ooids did not forming carbonate shoals. They ooids are present with stromatolites as suggested by Irtem (1987). The siltstone and mudstone lithofacies (tidal flats) are the dominant facies outcrops 25 and 26 located in the proximal part of the studied transect. These tidal flats occur as sheets that in the northern part and they serve as important ingredient of CS-4 and CS-5. The bioturbated wackestone and mudstone facies show marine setting and are distally located with respect to the Al-Lidam Area towards the Arabian Gulf. These are important as they mark the marine transgression and are also to place the MFS and used to separate HST and TST. The sheet geometry is easily recognizable it is 3.5 kilometer long, 10 meters wide and the height is normally about 3 meters.

6.1.3.4. Lens Geobodies

This type of geometry is presented by skeletal grainstone. The lens shaped skeletal banks are build up of bivalves, gastropods and skeletal fragments (Figure-6.4). These are home to tides and waves action, and form a relatively shallow sheltered environment. The facies with lens geometry are good in terms of porosity as they have large clasts that have been completely dissolved and provide good reservoir target. The lens skeletal geobodies are shifting towards the

Facies	Ooid grainstone	Sandy peloidal skeletal grainstone	Quartzose fine sandstone	Micritized ooid peloidal grainstone	Dolomitized skeletal wackestone	Sandy peloids grainstone packstone
Depositional Environment	Intertidal	Skeletal banks	Estuarine	Intertidal	Tidal Flat	Intertidal
Sedimentary Structures	Low angle cross bedding	Crinkled lamination	Bioturabati-ons , Low angle cross-bedding	Cross-Bedding	Lamination	Contorted bedding
Dimension	X=3.5km Y=10m Z=3m	X=1km Y=15m Z=1.5m	X=1km Y=15m Z=2m	X=3.5km Y=10m Z=3m	X=3.5km Y=10m Z=3m	X=3.5km Y=10m Z=3m
Shape	Sheet	Lenses	Channel	Sheet	Sheet	Sheet
						

Table-6.1. Summary of Facies, environment of deposition, dimensions and geometry of geobodies(X=Length, Y=Width, Z=Height).

shore as the Dam Formation passes from older to younger sequences. So the skeletal banks geometry is very much prone to sea level change and thus they provide important observation for changing sea level. This observation could only be met when we recognize the geometry from mesoscale to macroscopic heterogeneity. The skeletal banks which are present in almost all outcrops, these are dominant in the relatively distal facies. They are present in abundance in Outcrops-7, 6, 10. These provide important horizon for correlation chart. The lens shape geobodies are 1km long. The height reaches up to 1.5m. The skeletal banks lens geobodies mark the top of cycles in absence of oolitic sheets as can be seen in CS-1 and CS-2. It is not present in

CS-3 and CS-4, as these are dominated by tidal flats. The idea of knowing the geometry is important for reservoir modelers to model skeletal banks and make interpretations on this data.

6.1.3.3. Channel Geobodies

This type of geometry is presented by channelized sandstone facies (Figure-6.5).Though, some quartz sand occurs in sandy limestone, only the pure sandstone form channelized geobodies. These geobodies are present all over the area, can be easily recognized on facies mosaic of high resolution stratigraphic model some peloids are found in the zone where the channelized sandstone starts, which marks erosion of older existing facies before deposition of the sandstone. However, few broken shells dissolved in moulds are also present.

The sandstone geobodies are variable in porosity. The base channel lag is rich in clasts and is good in porosity (10-15%), but as the channels type which is characterized by fining upward trend shows, a decrease in porosity upwards(3-5%). The sections in north, however, show good porosity values.

The sandstone facies needs to be mapped in more detail to decipher its chances as a target for reservoir, as the sandstone in outcrop is very friable and shows good porosity. There are two channel geobodies present in Outcrops-6, 7 and are pinched out in 10. This probably the depositional condition in which the distal areas in the environment were under more sea level changes. However, the presence of packstone body in two channels in Outcrop-6 that indicates a short episode of carbonate deposition. This geometry is present from mesoscale to macroscopic scale and provides the significance of heterogeneity on different scales. The channelized sandstone is which is normally stacked on top of paleosols serves as a sequence boundary. There are sandstone bodies that are present in channelized geobodies form but do not represent sequence boundary. These forms are part of tidal flat sequence as seen in CS-3 and CS-4. These geobodies which are about km in length, 15 meters in wide and 2m in height. The sandstone geobodies are more dominant in distal Outcrops-6 and 7. This shows their estuarine nature. The thickness of these bodies in CS-2 is larger than the thickness in preceding sequences. There are stacked channels in proximal areas relative to sea-level change and are proximally located with respect to the Arabian Gulf.

SW

Geometry	X (Length)	Y (Width)	Z (Height)
Sheet	3.5km	10m	3m

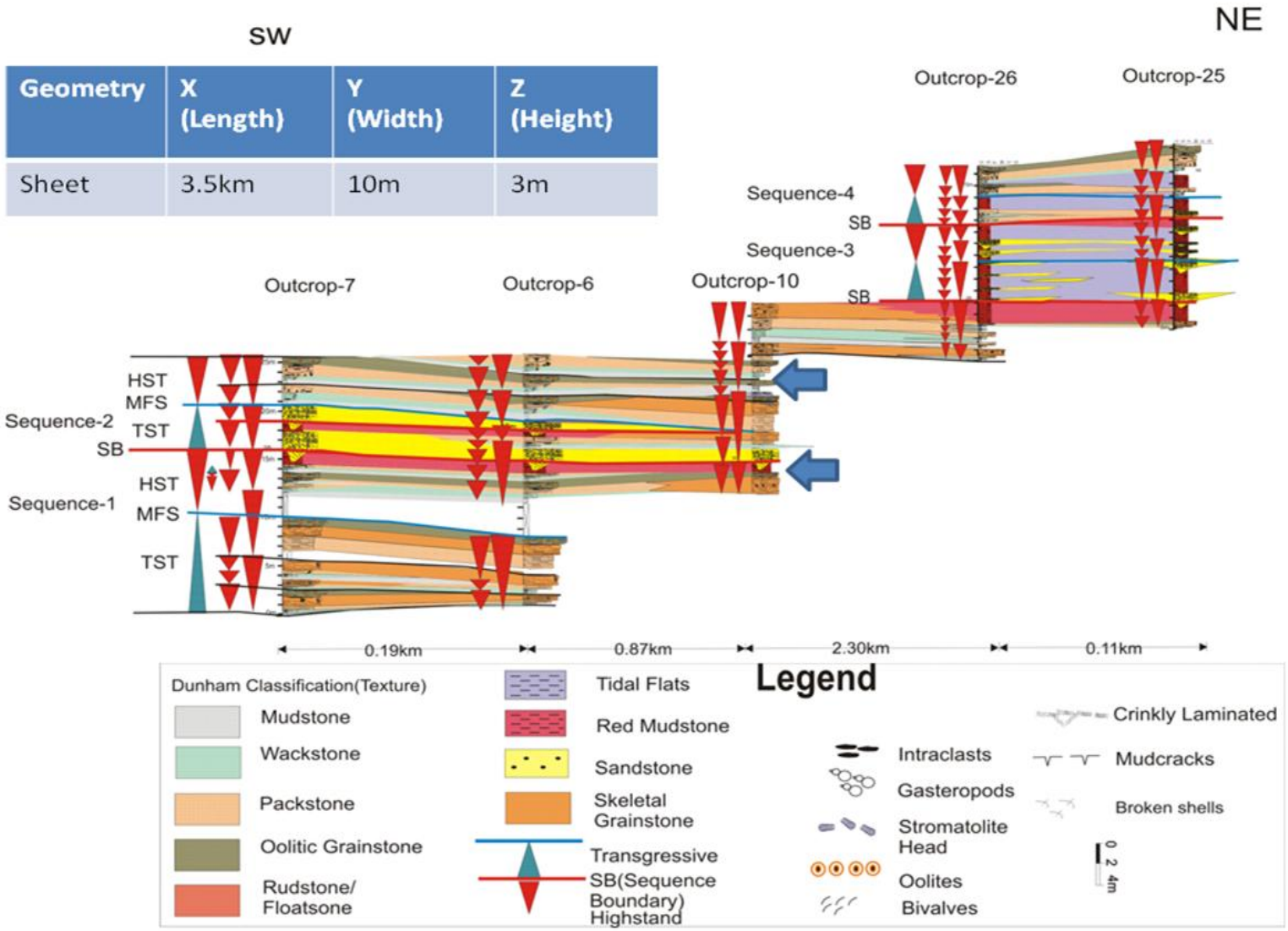

Figure-6.3. Sheet Geobodies, as seen in Facies mosaic, dimensions, 2D-Correlation chart and their shapes. It is represented by bioturbated wackestone to mudstone, ooid grainstone with stromatolites and tidal flats.

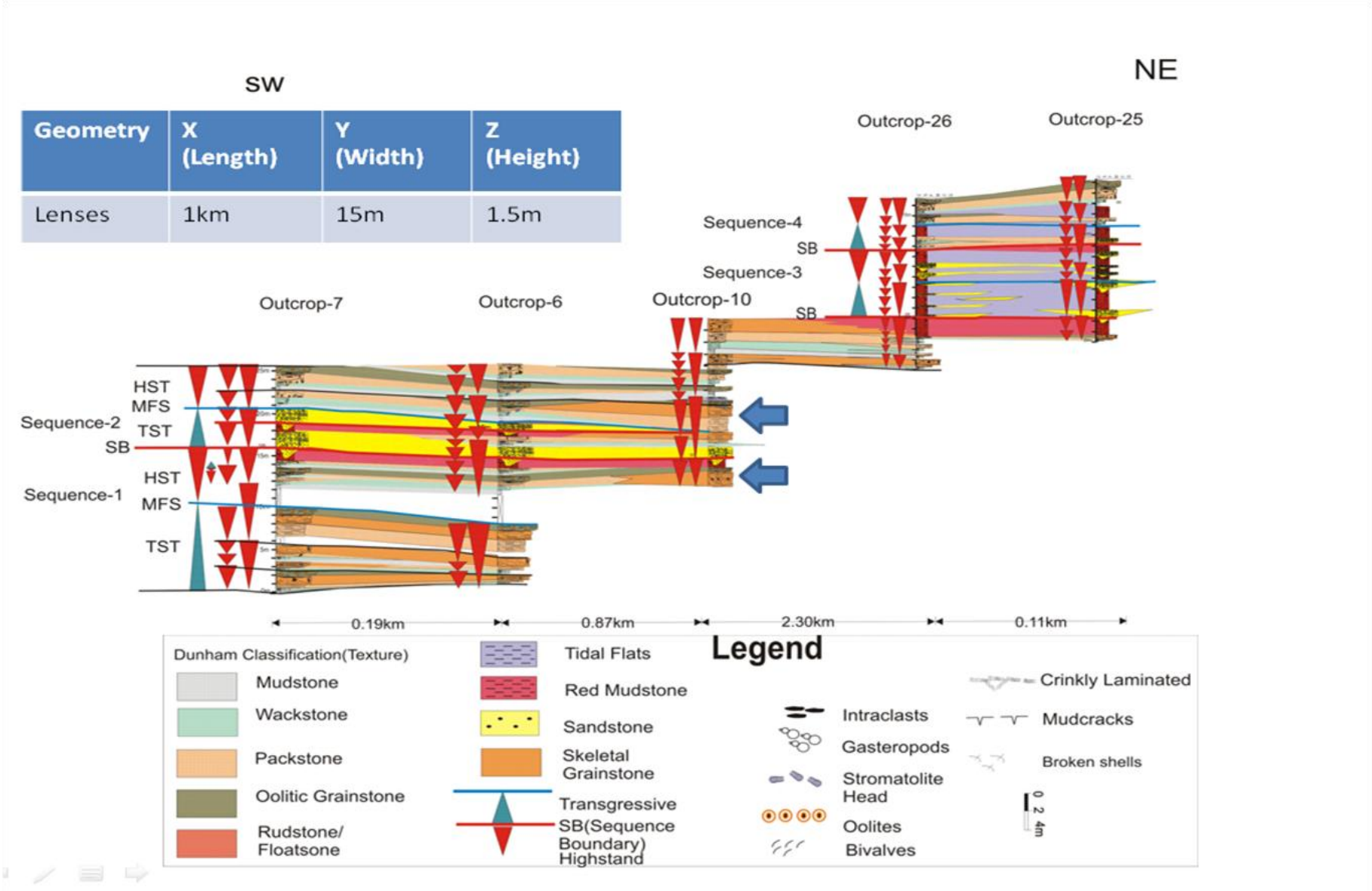

Figure-6.4.Lens Geobodies, as seen in Facies mosaic, dimensions 2D-Correlation chart and their shapes. It is represented by skeletal grainstone facies.

The data collected here is an example of the usefulness of outcrop observations for reservoir engineers. The quantitative data on outcrop is important for deterministic as well as stochastic reservoir facies models. The data can be used for reservoir modelling. However, the collection of such data is very time consuming and hard in the field. We can also use satellite images as well as the facies mosaic to collect the data for facies geometries and spatial distribution. The classification used here was adopted from Jung et al., (2012).

For example, a mound can amalgamate to form mound ridges which will then fall in bar shape category. However, the classification used here can be modified, when we have more and more case studies and understand their interrelationship. New shapes can be added and some overlap can be removed.

This type of work invites people related to reservoir engineering and geostatistics to come and work together with geoscientists. However, more it can be more useful if we use reservoir analogue software to map high resolution images and provide more precise estimate of depo-shapes and interpretation. For further studies, porosity and permeability data can also be added to prepare the dynamic reservoir facies model. The spatial distribution of depo-shapes is related to sequence stratigraphy and locally acting forces. The individual geobodies are affected by local controls. These controls involve accommodation space and sediment supply.

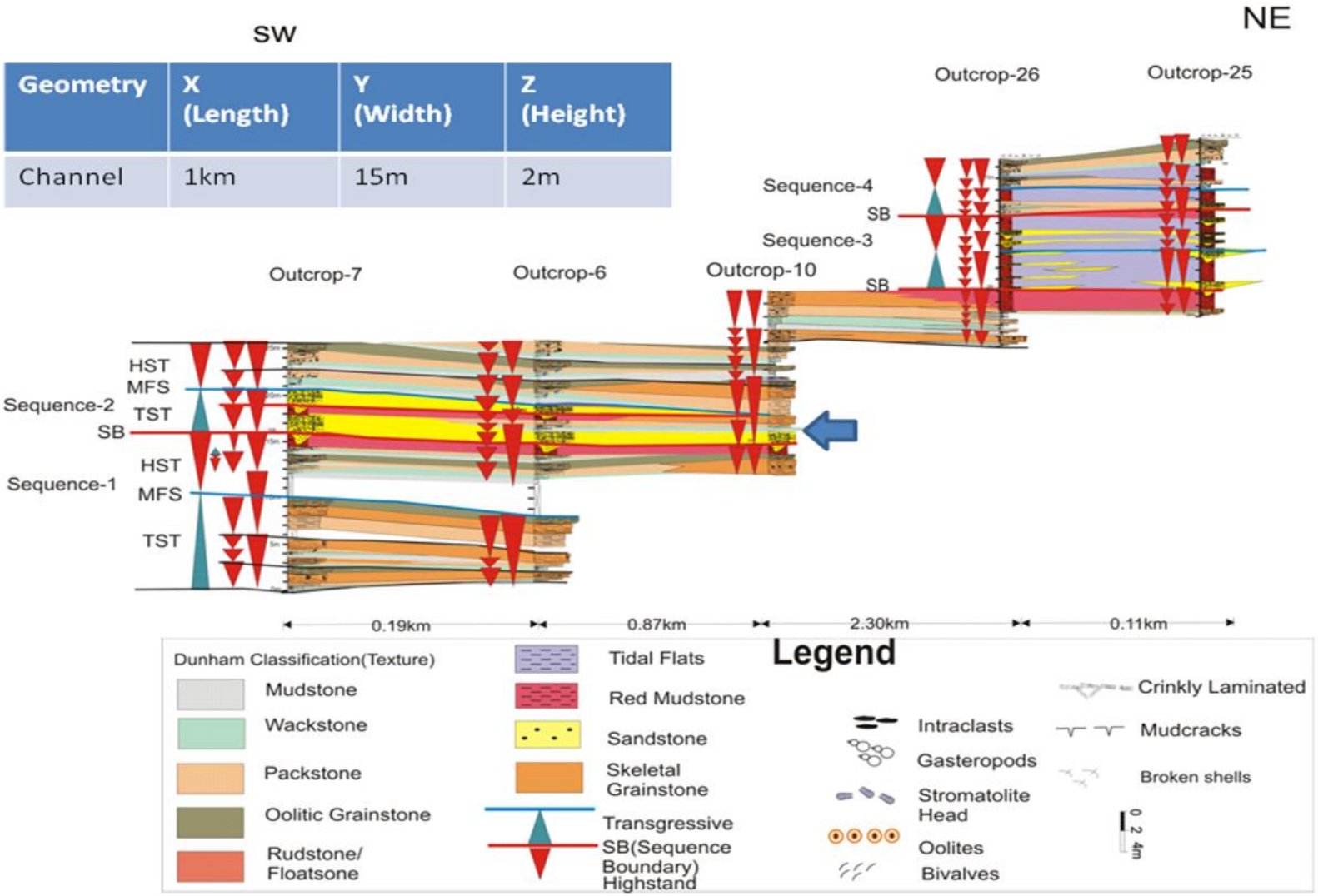

Figure-6.5.Channel Geobodies, as seen in Facies mosaic, dimensions 2D-Correlation chart and their shapes. Represented by Bioturbated channelized sandstone and tidal flats.

6.1.4. Seismites

Seismites are sedimentary structures and beds deformed as a result of seismic trembling. This term was introduced by a Seilacher in 1969 to describe the earthquake deformed beds. The seismites are very useful to understand paleoseismiticity in the area. If we can sort out the age and spatial distribution of these features the seismic hazard and recurrence interval can be evaluated. The type and distribution of seismites depends upon the hydrodynamic, sedimentologic, diagenetic characteristics of the deposits subjected to seismic shocks (Monttenat et al., 2007). It occurs in peloidal packstone (Pp) facies in Outcrops-10 and 7.

Peloidal packstone in the outcrop occurs as tan to light grey color beds (Figure 4.12a). Facies occurs below the peloids grainstone facies, in outcrop 7. The bed thickness ranges from 10 to 20cm and the facies thickness range from 0.5 to 1.5 m. This facies shows contorted bedding or seismites in Outcrop-10.

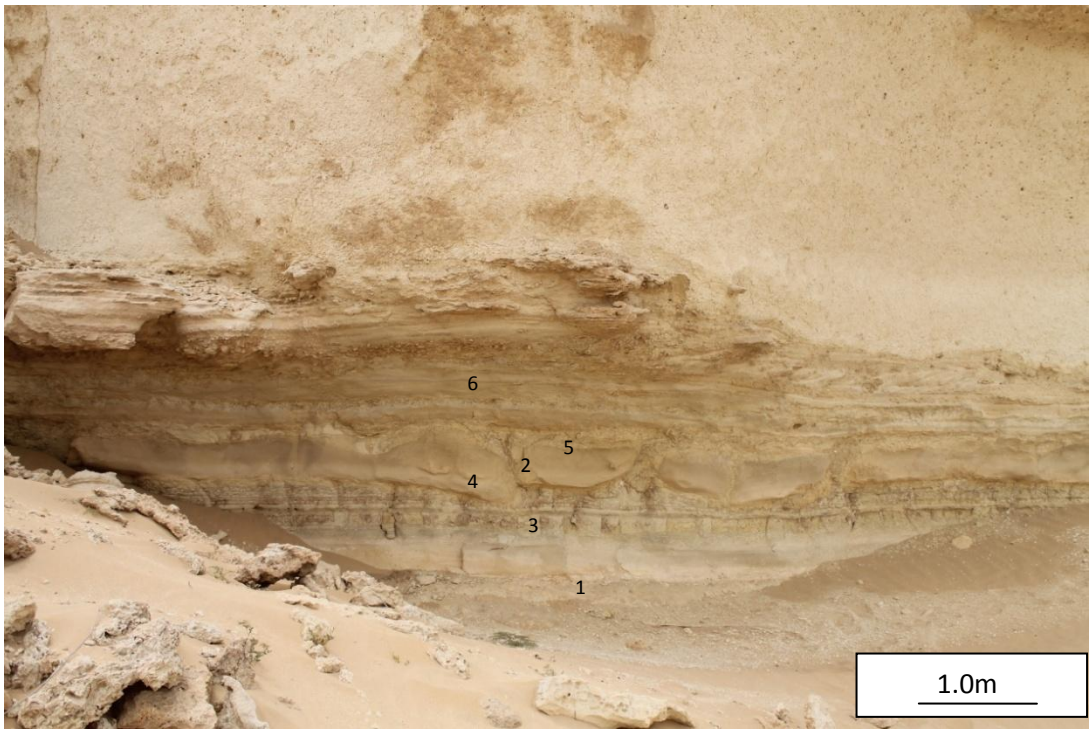

Figure 6.6. Field photograph showing characteristic feature of seismites, 1. Undeformed basal beds, 2. Upturning of beds (sandy), 3. Fragments of disturbed beds swept by flow of liquefied sediments. 4. Preservation of the depositional structures of deformed bed, 5. superficial flow of ejected sediments. 6. Undeformed beds at top sealing the deformation.

This facies is also characterized by the presence of intraclasts in the cycles near top of outcrop 10.The mechanism that produced sweeping of mud dominated facies and grain dominated facies set out as fissures of the soil. In form of sand volcanoes, a detailed is discussed in Fig.6.6. There are several volcanoes that seem to connect to single source fissure. They dominantly develop in wet plains and occasionally in tidal flats environment. In cross-sectional view the sand volcanoes show extrusive structures, the centrifugal movement of limbs. If the disturbed beds are restored to its original position, which resulted from stretching of soft sedimentary bed, before it was broken and was displaced and formed a sand volcano. It seems that the soft sediments were subjected to ductile deformation before they broke off. The limbs were overturned and were not subjected to flattening and compaction. The core of the volcano shows fluidized structure due to extrusion of fluidized sediment (Mugnier et al., 2011). The disturbed bed is sealed from top as seen in Fig6.6 (6). The deformed sedimentary sequence of Dam including seismites is about 1.5 m thick and includes episodes of seismites, and each event shows different type of deformation, depending upon the compaction and lithification of Dam sediments.

6.2. Facies Mosaic

Facies Mosaic for each outcrop was constructed (AlKhaldi, 2009) following the general procedure listed below. The mosaic was developed using Coral Draw-13 software.

- Segmented photos of each outcrop were acquired and merged to develop photomosaic.
- High resolution close-up photos of each outcrop were obtained. Rocks separated from talus on the slope.
- Ensured that the image taken are not tilted and provided necessary overlap
- A master log of each outcrop was constructed to document the major rock types.
- High resolution description interpretation of the images was carried out in the field.
- The sedimentary structures like cross bedding, lamination, fossil content and fractures were document on the photographs.
- Sequence boundaries, were marked based on bed contacts of high resolution images.
- Carbonates were described based on Dunham Classification for limestone and siliciclastic rocks based on QFL classification.
- The parasequence of the cycles were based on shallowing upward trend in facies.
- Measured sections were selected so they cover most of the facies and evenly distributed on the outcrop.

6.2.1. Facies Outcrop-10

There are ten lithofacies identified in the Dam Formation in outcrop-10. The dominant lithofacies are the foraminiferal grainstone to packstone facies, paleosols, channelized sandstone, peloidal grainstone, oolitic grainstone and mud cracked siltstone and mudstone. The succession starts with foram grainstone packstone which is characterized by shallowing upward trend to oolitic grainstone facies. The shallowing upward trend continued until the ramp was exposed to weathering. The estuarine conditions started with the deposition of bioturbated quartz fine sandstone facies over the paleosols (Figure-6.7a, b, c). The deposition of the estuarine sandstone was followed by a major transgression which led to the deposition of peloidal grainstone facies. The grainstone which is characterized by a sequence is shallowing upward trend was topped by crinkly laminated skeletal grainstone to packstone facies.

The karstification feature below the oolitic grainstone facies marks a slight emergence and exposure of the ramp. The oolitic grainstone facies shows small episode of deepening upward(Figure-6.7a). The environment becomes shallower when the miliolid peloidal packstone wackestone facies were deposited. The facies on the top are the commenced the beginning of another cycle with a mudstone at base and an oolitic grainstone on top. The same cycle repeats itself and the contorted structure in the skeletal grainstone to packstone facies marks the presence of tidal flat environment in the sequence. The top of cycle is again marked by the presence of oolitic grainstone with foraminfera assemblage. The next cycle starts with the skeletal packstone and the introduction of carbonate banks and topped by grainstone having stromatolitic heads and intraclasts. The cycle commenced with the tidal flat environment. The topmost cycle represents the same as the previous but here amount of intraclasts. The porosity of the topmost facies oolitic grainstone ranges from 20 to 30%. The shallower condition, the porosity is enhanced by the dissolution of ooids and skeletal fragments. The mudstone beds are barriers as they show low porosity values (<1%).

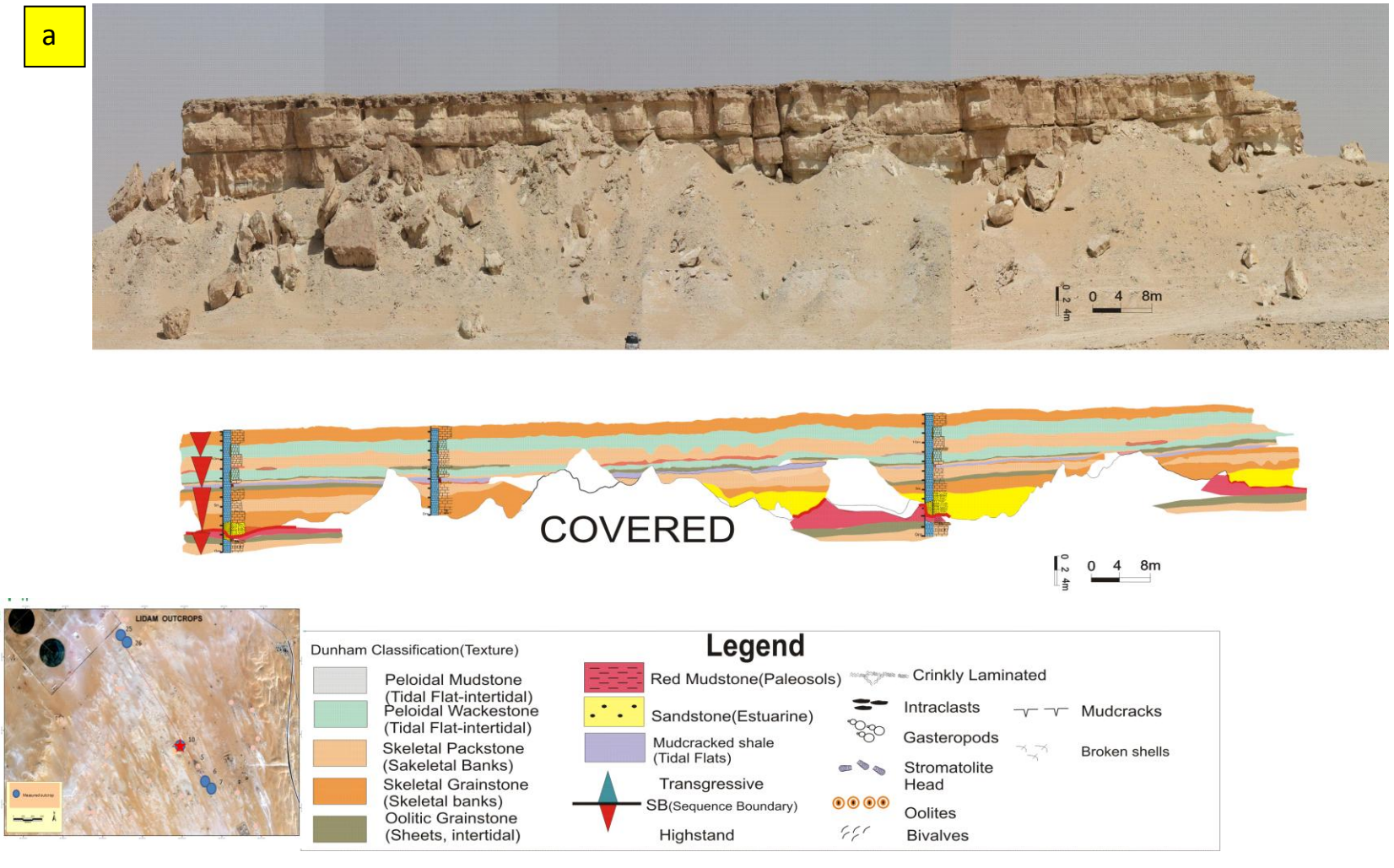

Figure-6.7.a) Facies mosaic of outcrop 10 starts with skeletal grainstone and are abruptly overlain by paleosols and then by channelized and erosive contact of sandstone that marks the sequence boundary. The carbonate succession is thicker here while sand bodies are thick on southern side, which also depicts the architecture and geometry of carbonate geobodies present in Dam.

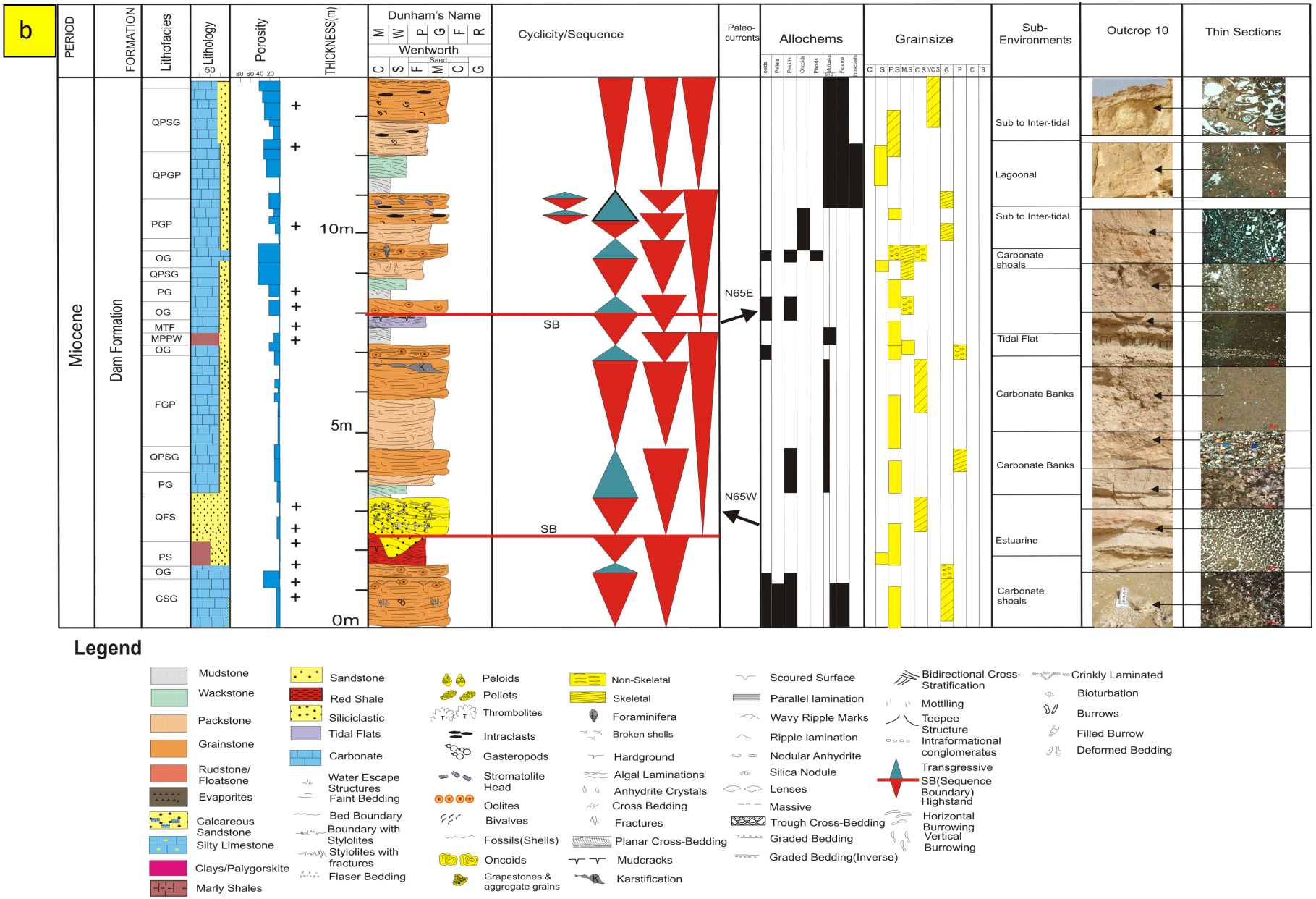

Figure-6.7.b) Composite log of outcrop-10and please note that it is dominated by oolitic grainstone (Intertidal-subtidal), capped by paleosols and quartz sandstone (estuarine), middle dominated by foraminiferal grainstone, peloidal grainstone packstone facies on the top.

Facies in Outcrop 10

Clastic/ Carbonate	Siliciclastic	Carbonate						
		Grain Supported						Mud Supported Mudstone
		Skeletal	Non-skeletal					
Facies	A Quartz. fine to medium grained Bioturbated sandstone with mudstone intercalations	B Bioclastic peloid packstone	C Ooid grianstone	D Micritised ooid peloids grainstone	E Coated bioclastic grainstone	F Miliolid peloids packstone wackestone	G Quartzose peloids packstone	H Dolomitized Skeletal wackestone
Environment	Estuarine	Sub-Inter tidal	Intertidal				Tidal Flat	
Lithology	Sandstone	Limestone	Limestone				Limestone	
Texture	Mud to silt, fine to medium grain angular quartz grains	Fine skeletal fragments and mud	Fine to medium ooids and fine to medium quartz	ooids,	Very fine quartz, pellets	Miliolids, mud and quartz	Very fine quartz, skeletal grains	Skeletal, fine angular quartz grains
Colour	Tan to light green	Tan to light brown	Creamy white, tan	Tan to cream	Tan to white	Cream to tan	Light Tan to brown	Light grey to dark brown
Composition	Quartz sandstone	Quartz, mud	Ooides, skeletals	Ooides, rare skeletal	Quartz, mud	Skeletal, quartz, mud	Skeletals and mud	Clay and Silt
Structure	Channels, Trough cross beds,lamination, bioturbation	Stromatolites	Crinkly lamination, mudcracks	Cross Bedding	Crinkly lamination, Burrows	Stromatolites	Teepee structure, Cross Bedding	Mudcracks, Bioturbation
Fossils	Trace fossils	Gasterpods and Bivalves, forams	Molds of mullusks, forams	Rare	Rare	Forams	Rare	None
Diagnostic Features	Cross bedded sandstone intensely burrowed, valley fill channeling present	Abundance of shells and Moundsshape in geometry	Thin bedded bed with ooilitic skeletal rudstone,pinchouts	Massive tan coloured channelized packstone	White wackstone\ mudstone	Mounds in geometry, Burrows	Contorted bedding marked massive wackstone	Light to brown colour beds with mud cracks
Field Photos			 				 	
Sample Slabs	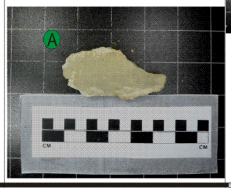	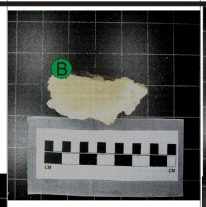	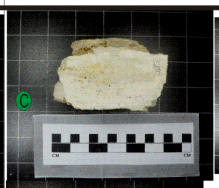 	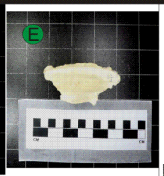		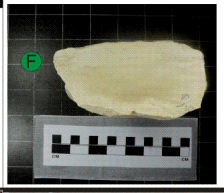	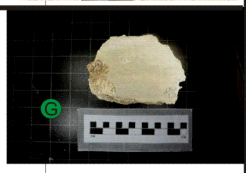 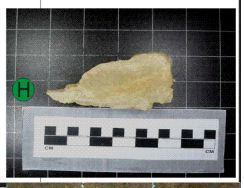	
Thin sections	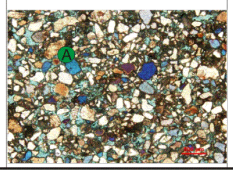	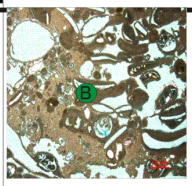	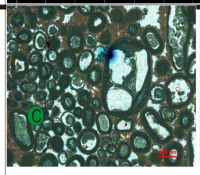 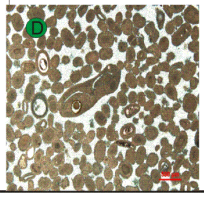	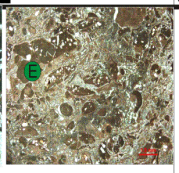		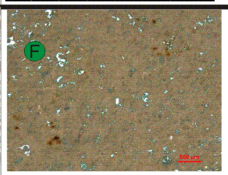	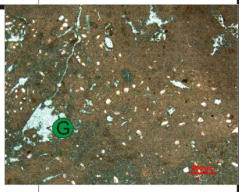 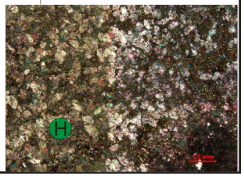	

C

Figure-6.7.c) Facies summary chart of outcrop-10, quartz sandstone, foraminfera grainstone, ooid grainstone, micritized ooid peloidal grainstone, coated bioclastic grainstone, quartzose mudstone and miliolid mudstone facies.

6.2.2. Facies Outcrop-6

Eight lithofacies were identified in the in Outcrop-6 (Figure-4.15). The dominant lithofacies are coated skeletal grainstone, micritized oolitic peloidal grainstone, sandy peloidal packstone, foraminiferal grainstone to packstone, oolitic grainstone, paleosols, quartz sandstone and peloidal grainstone-packstone. The succession started with the deposition of sandy peloidal wackestone-mudstone that shallows upwards to foraminiferal grainstone (Figure-6.8).

The oolitic grainstone facies shows slight fining upwards trends. The next cycle commenced with the deposition of sandy mudstone and capped by oolitic grainstone. Paleosols which marked the top of the cycle is mudcracked and show the exposure of the ramp.

The top of this facies is marked by the occurrence of channelized sandstone facies. This also marks the presence of a sequence boundary. The conditions became deep and again the ramp was changed into a site of deposition of the sandy skeletal packstone facies. The top of the cycle is again marked by the presence of oolitic grainstone with foraminiferal assemblage.

The next cycle started with the deposition of skeletal packstone and the introduction of carbonate banks. It was topped by grainstone having stromatolitic heads and intraclasts. The cycle commenced with the tidal flat environment. The topmost facies intraclastic peloids packstone and oolitic grainstone which occur in four different cycles are characterized by porosity ranging from 20 to40%.

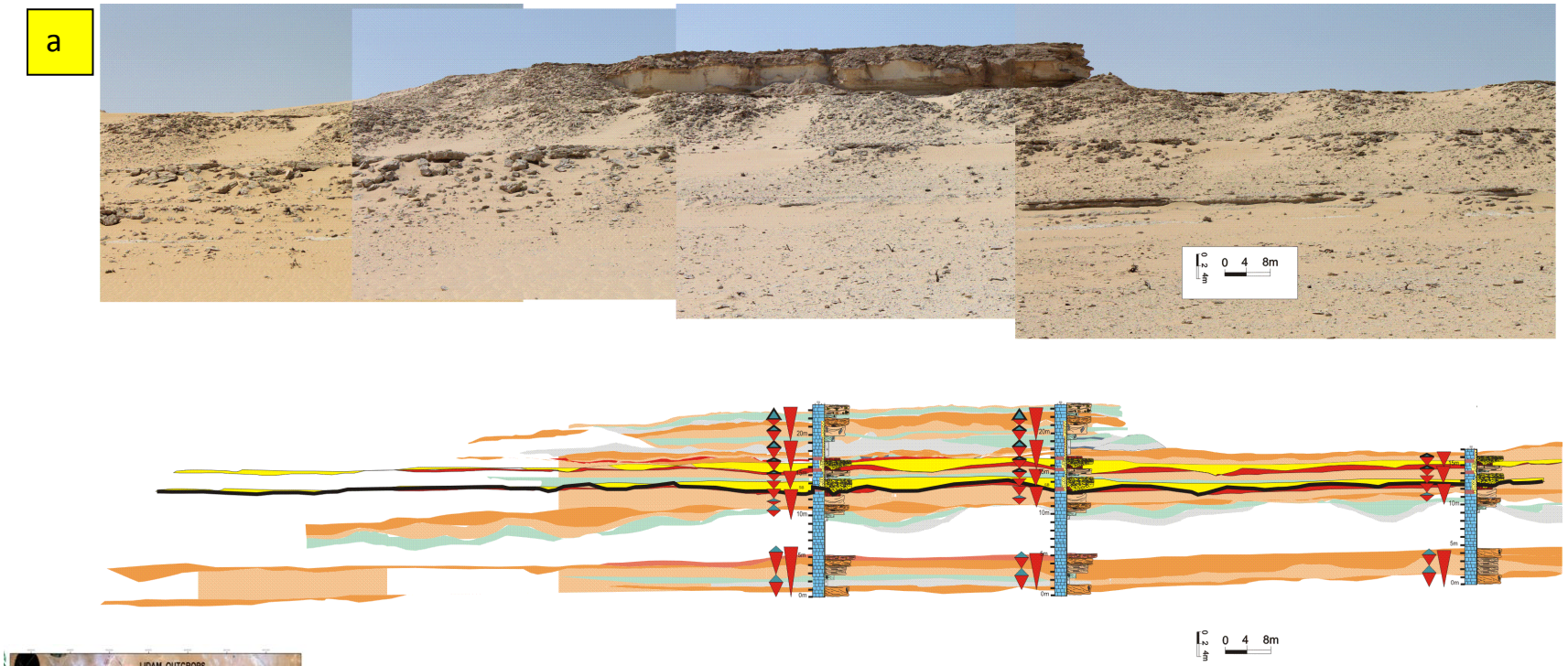

Figure-6.8. Facies Mosaic outcrop -6 is similar to outcrop 7, it differs in that there is a small carbonate deposition between the two sequence boundaries.

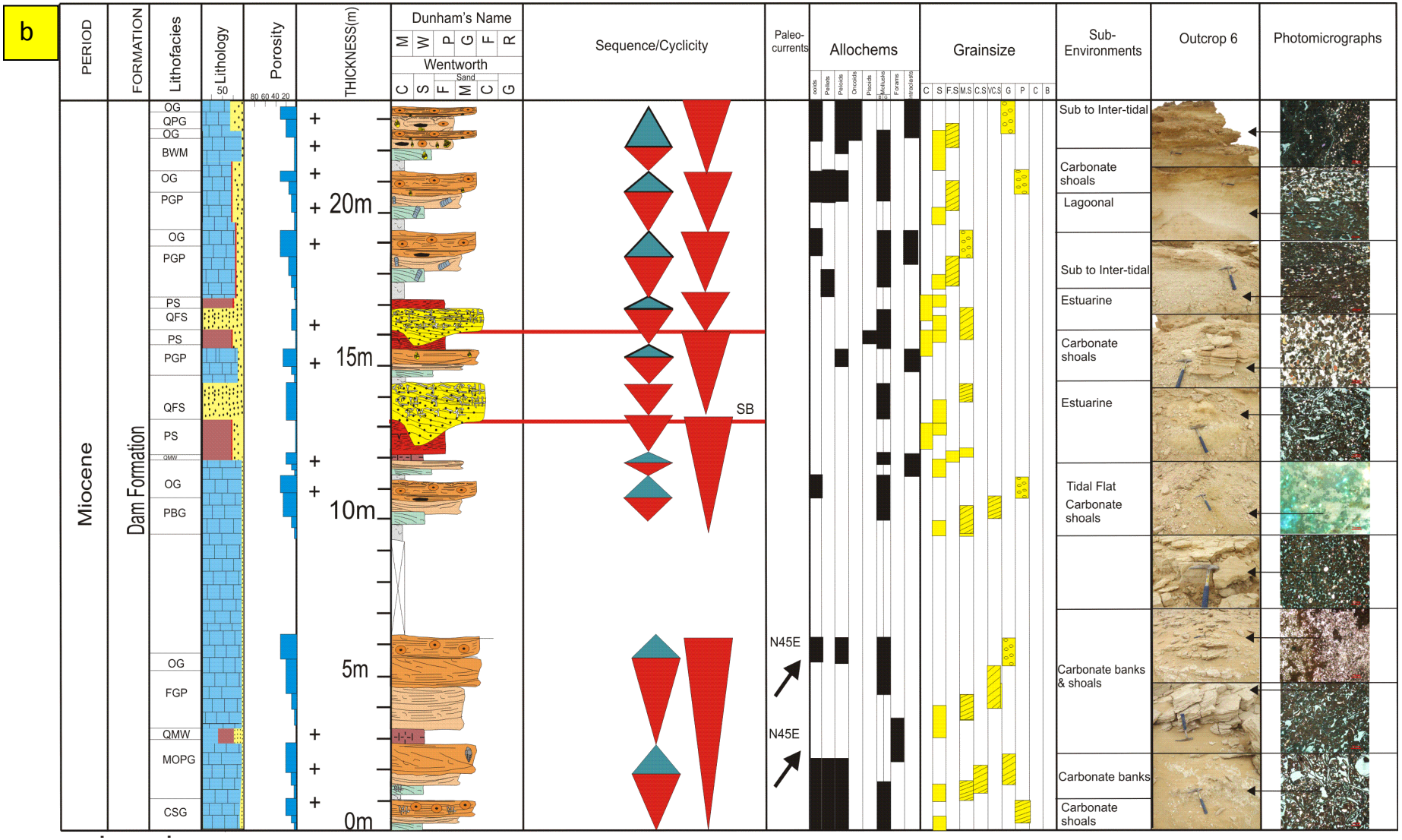

Figure-6.8.b) Composite log of outcrop-6, and dominated by skeletal and oolitic grainstone (Intertidal-subtidal), in middle by quartz sandstone (estuarine) and paleosols, capped by oolitic grainstone facies on the top.

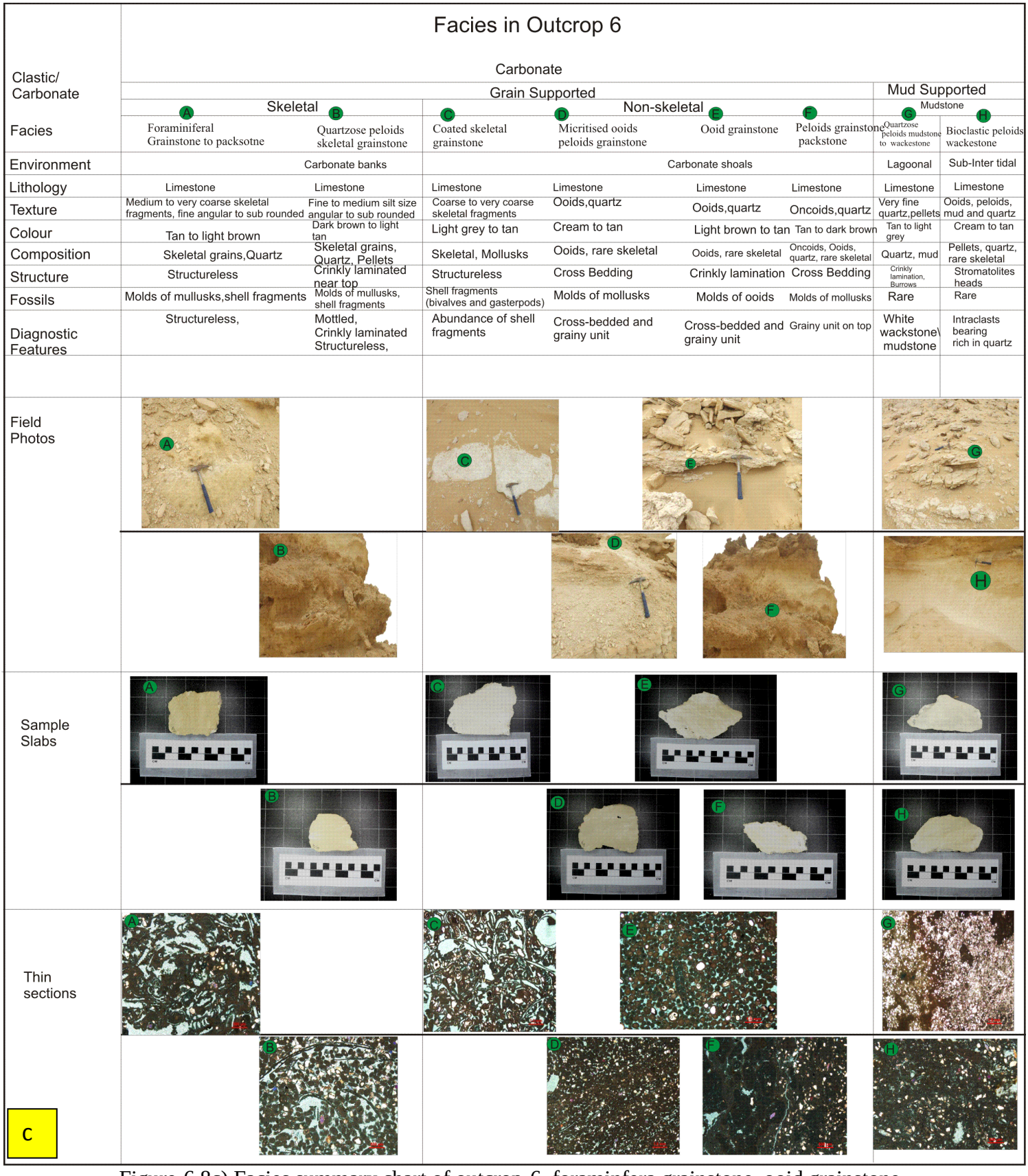

Figure-6.8c) Facies summary chart of outcrop-6, foraminfera grainstone, ooid grainstone, micritized ooid peloidal grainstone packstone, coated bioclastic grainstone and quartzose mudstone facies.

6.2.3. Facies Outcrop-7

There are seven lithofacies identified in the Dam Formation in Outcrop-7 (Figure-6.9). The dominant lithofacies are burrowed wackestone facies, sandy peloidal packstone, foraminfera grainstone to packstone, oolitic grainstone, paleosols, quartzose sandstone and bioclast peloidal packstone. The facies identified in outcrop-7, the succession starts with Peloidal quartzose wackestone mudstone which shallow upward foram grainstone. The next cycle began with the deposition of skeletal packstone to grainstone facies.

The cycle is capped by the presence of oolitic grainstone facies. The oolitic grainstone facies shows a slight fining upward trend. The next cycle commenced with the deposition of miliolid mudstone and is capped by oolitic grainstone. The next facies is the paleosols lithofacies which is characterized by mudcracked and shows exposure of the ramp. This facies is capped by the presence of channelized sandstone facies. This also marks the presence of a sequence boundary. The conditions became distal and again the ramp was changed in to a sight of peloidal grain-packstone facies. The top of the cycle is again marked by the presence of oolitic grainstone with foraminfera assemblage. The porosity of topmost facies quartzose peloidal grainstone and oolitic grainstone ranges from 25 to 40%. The porosity is enhanced by the dissolution of ooids and skeletal fragments(Figure 4.6b).

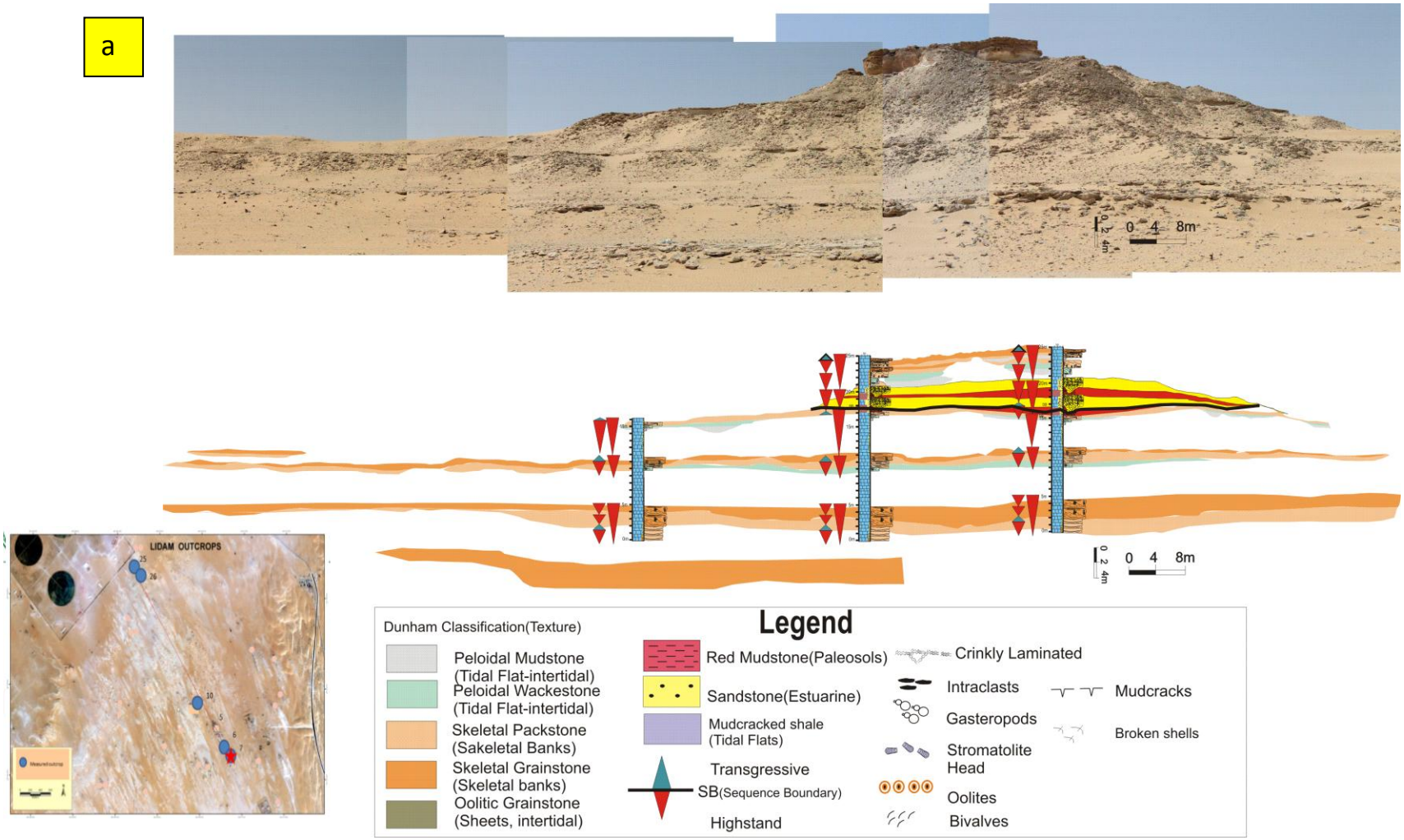

Figure-6.9.a) Facies mosaic of outcrop 7 starts with from the base as skeletal grainstone, the blank area marks the part of outcrop which is covered, and then there are two yellow colour sand bodies above the red paleosols that mark the presence of subaerial exposure and sequence boundary. At the top carbonates re-appear showing high stand conditions.

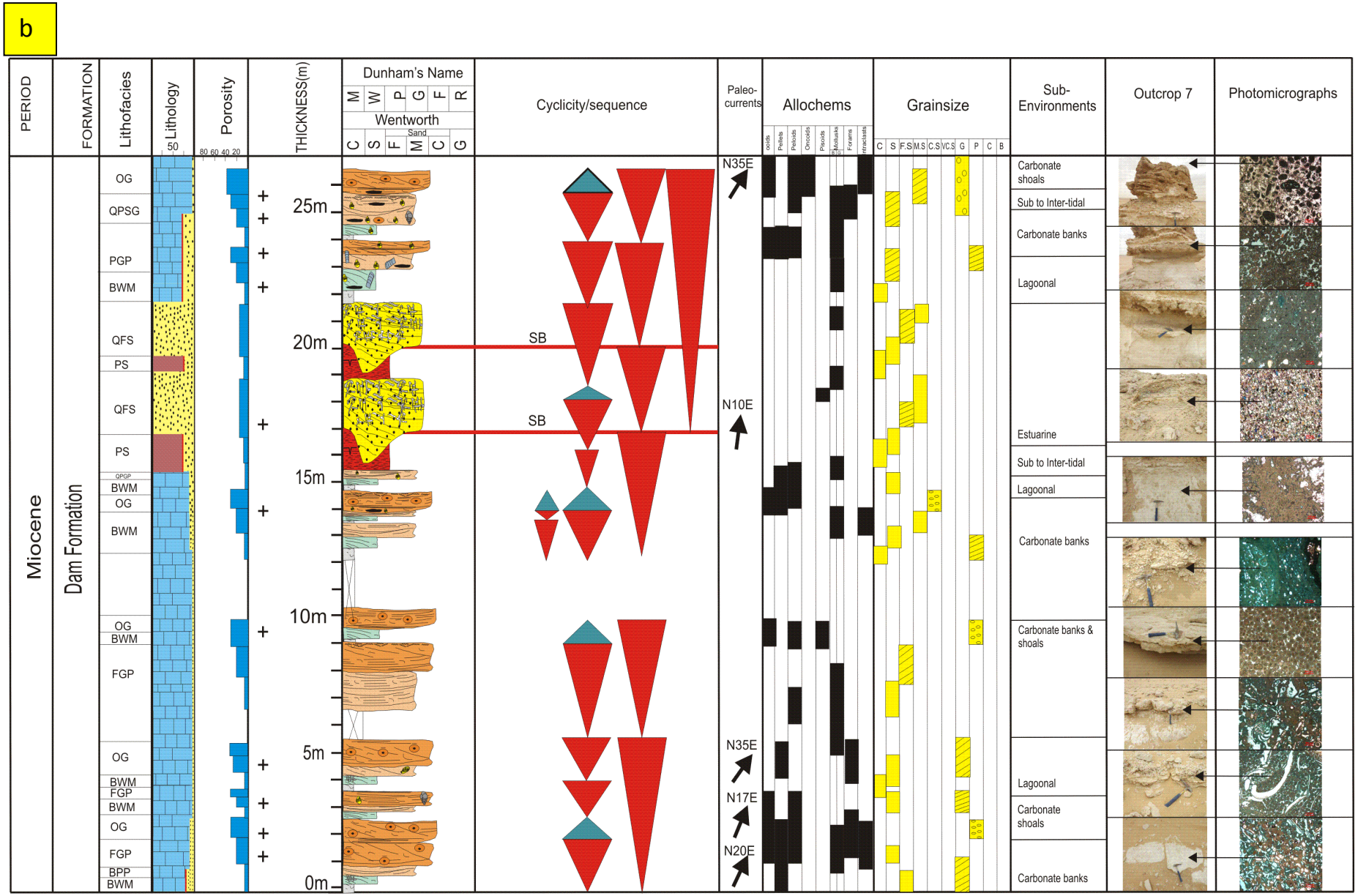

Figure-6.9b) Composite log of outcrop-7, and dominated by skeletal and oolitic grainstone (Intertidal-subtidal), in middle by quartz sandstone (estuarine) and paleosols, capped by peloidal grainstone packstone facies on the top (onset of carbonate deposition).

Facies in Outcrop 7

Clastic/ Carbonate	Siliciclastic	Carbonate					
		Grain Supported				Mud Supported	
Facies	A Quartz fine to medium grained sandstone	B Skeletal: Foraminiferal grainstone to packsotne	C Non-skeletal: Micritised ooid grianstone	D Coated skeletal grainstone	E Peloids grainstone/ packstone	F Skeletal grainstone to packstone	G Mudstone: Peloidal stromatolitic wackestone/mudstone
Environment	Estuarine	Carbonate banks	Intertidal		Lagoonal	Carbonate banks	Sub-Inter tidal
Lithology	Sandstone	Limestone	Limestone	Limestone	Limestone	Limestone	Limestone
Texture	Mud to silt, fine to medium grain angular quartz grains	Fine to medium silt size angular to sub rounded	Fine to medium ooids and fine to medium quartz	Coarse to very coarse skeletal fragments	Very fine quartz, pellets	Coarse to very coarse skeletal fragments	Ooids, peloids, mud and quartz
Colour	Grey, red, brown and pink	Dark brown to light tan	Light pink to cream white	Light cream to light grey	Light cream to tan colour	Light grey to Tan	Cream to tan
Composition	Calcareous sandstone	Skeletal grains, Quartz, Pellets	Ooides, Skeletal, pellets, pisoids	Skeletal, Ooids Mollusks	Quartz, mud	Skeletal peloids Mollusks	Pellets, peloids, ooids, oncoids,rare skeletal
Structure	Channels, Trough cross beds,lamination, bioturbation	Crinkly laminated near top	Crinkly lamination, mudcracks	Structureless	Crinkly lamination,Burrows	Low angle Cross-Bedding	Stromatolites heads
Fossils	Trace fossils	Molds of mullusks, shell fragments	Molds of mullusks, forams	Shell fragments (bivalves and gasterpods)	Rare	Shell fragments (bivalves and gasterpods)	Rare
Diagnostic Features	Cross bedded sandstone intensely burrowed and weathered	Mottled, Crinkly laminated Structureless,	Form the base of first bench and laterally persistent	Abundance of shell fragments and Mottling	White wackstone\ mudstone	Cross-Bedding Abundance of shell fragments and vugs	Intraclasts bearing rich in quartz
Field Photos		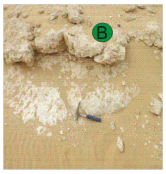					
Sample Slabs	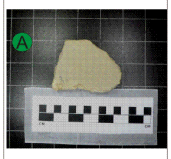	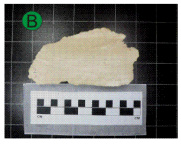	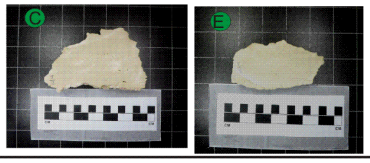	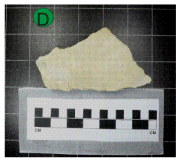		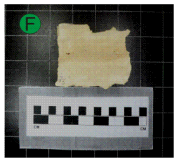	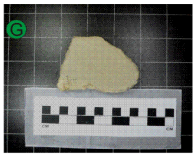
Thin sections	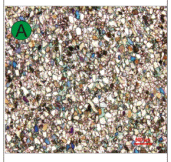	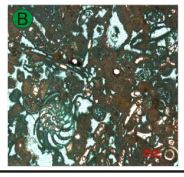	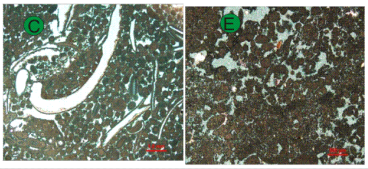	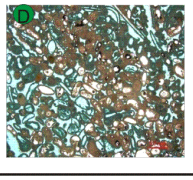		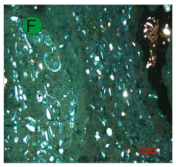	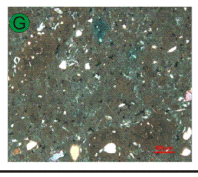

C

Figure-6.9.c) Facies summary chart of outcrop-7, foraminfera grainstone, ooid grainstone, micritized ooid peloidal grainstone packstone, coated bioclastic grainstone and quartzose mudstone facies.

6.2.4. Facies Outcrop-26

There are ten lithofacies identified in Outcrop-26(Figure-6.10). The dominant lithofacies in this outcrop are mudcracked shale, calcareous sandstone, dolomitic skeletal wackestone, burrowed wackestone, peloidal packstone grainstone, foraminiferal grainstone to packstone, oolitic grainstone, paleosols, quartz sandstone and bioclastic peloidal packstone. The facies succession commenced the deposition of sandy peloidal wackstone to mudstone facies which shallowed upward to skeletal grainstone. The next cycle began with the deposition of foraminiferal packstone-grainstone facies. The top is marked by the presence of crinkled lamination. Finning upward trend is shown by foraminiferal grainstone. The deposition of sandy peloidal wackestone mudstone commenced the next cycle within the succession. This is overlain by paleosols facies which is characterized by mudcracks and shows evidence of ramp exposure. The facies is capped by the presence of channelized sandstone facies which marks the presence of sequence boundary. The cyclicity continue to repeat six times and are divided in mudstone dominated, interbedded calcareous sandstone and mudstone and sandstone dominated facies near the middle of the sequence. These facies are deposited in intertidal environment and show the presence and cyclicity of tidal flat conditions in the basin. The conditions became distal and again the ramp was changed in to a peloids packstone facies. This cycle was repeated twice. In terms of porosity the topmost facies intraclastic oolitic grainstone has porosity ranging from 15 to 40%. The porosity is directly related to shallower depositional conditions. The porosity is enhanced by the dissolution of ooids. The sandstone intervals show 10 to 20% porosity range.

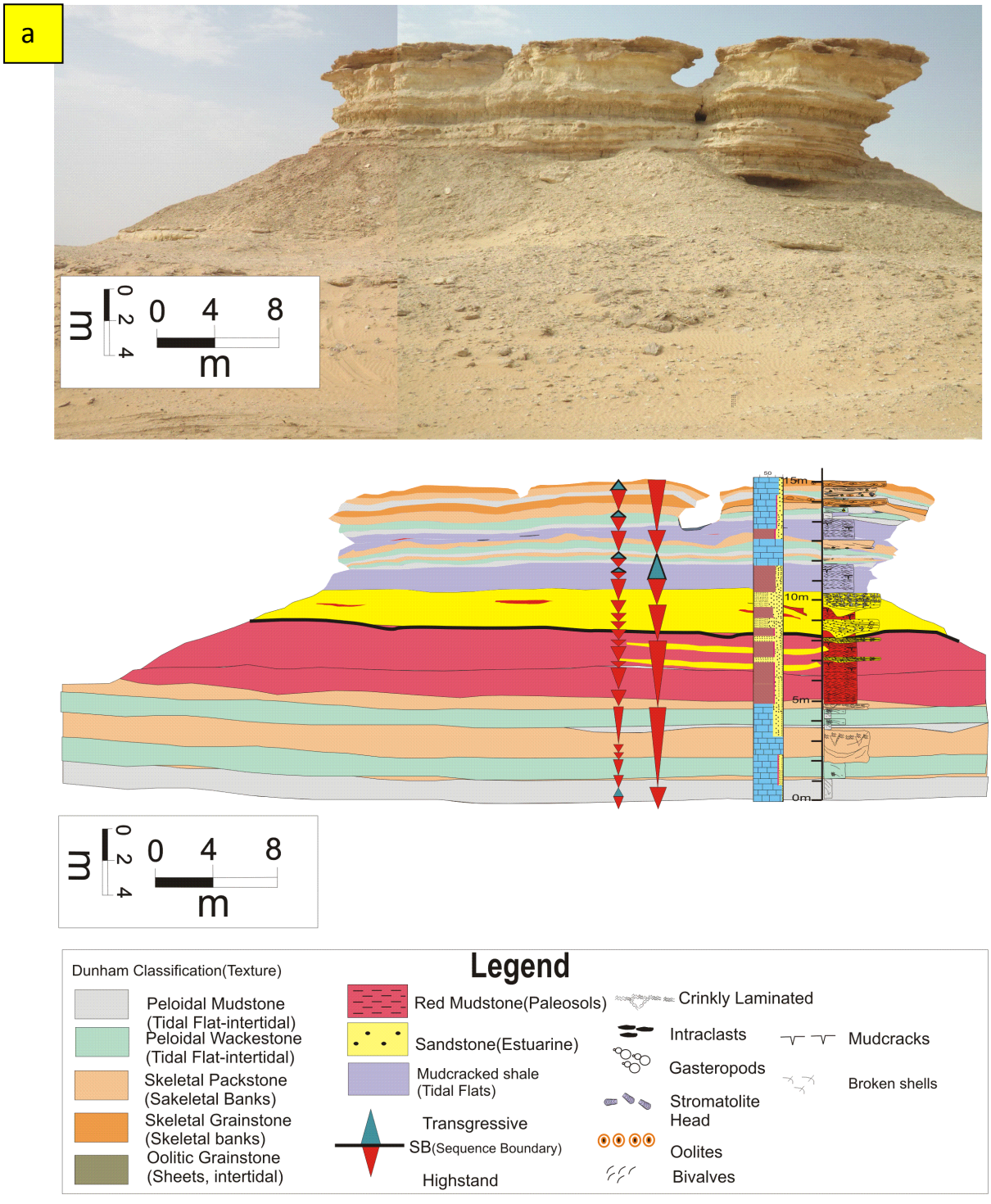

Figure-6.10 a). Facies Mosaicoutcrop-26, notice abundance of siliciclastic facies as compared to the carbonate facies, the sequence boundary is present just above the paleosols and the thick sand bodies overlie these paleosols, the sandstone are covered on top by mudcracked shale, which are overlain by skeletal packstone to grainstone showing highstand conditions,

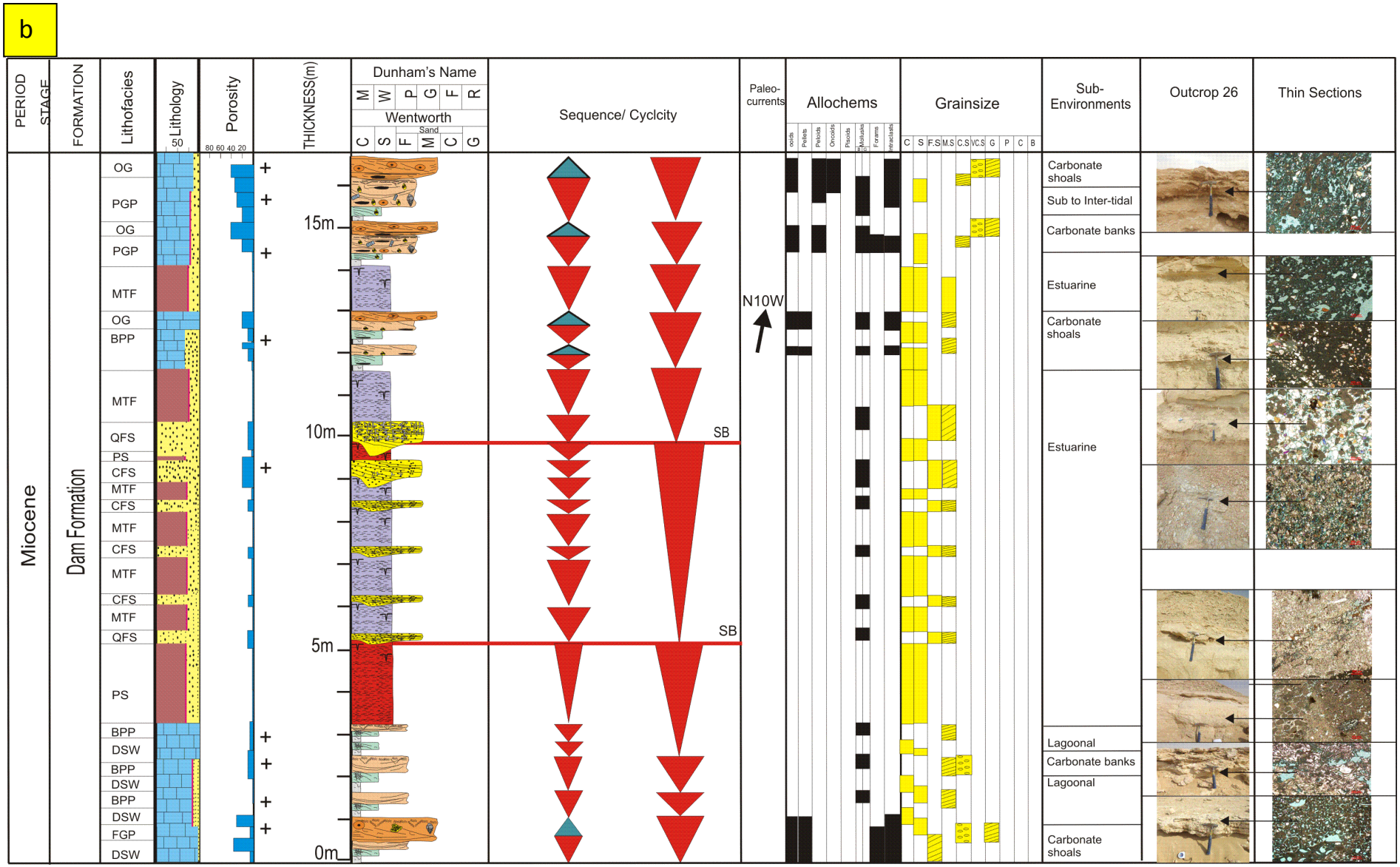

Figure-6.10b) Composite log of outcrop-26, dominated by quartz sandstone (estuarine) and mud cracked shales (tidal flats), and capped by skeletal and oolitic grainstone (Intertidal-subtidal).

Facies in Outcrop 26

Clastic/ Carbonate	Siliciclastic			Carbonate							
				Grain Supported						Mud Supported	
				Skeletal		Non-Skeletal		Mud		Microbial	
Facies	A Calc. laminated siltstone to mudstone	B Calc. shale with sandstone interbedding	C Calc. fine to medium grained sandstone	D Skeletal intraclastic packstone to grainstone	E Skeletal oolitic intraclastic packstone and grainstone	F Oolitic skeletal grainstone	G Algal peloidal packstone to wackstone	H Peloidal/pelletoidal mudstone to wackstone		I Algal quartzose skeletal thrombolitic packstone to wackstone	
Environment	Estuarine or lagoonal	Estuarine	Estuarine	Carbonate banks		Carbonate shoals		Lagoonal to intertidal		Sub-Inter tidal	
Lithology	Mud	Sand and mud	Sandstone	Limestone	Limestone	Limestone	Limestone	Limestone		Limestone	
Texture	very fine silt to fine sand, fine to medium grain angular quartz grains	Fine silt to sand fine to medium grain angular quartz grains	Mud to silt, fine to medium grain angular quartz grains	Coarse to very coarse skeletal fragments	Fine to medium silt size fine angular to sub rounded	Fine to medium ooids and fine to medium quartz	Fine to medium ooids and fine to medium quartz	Coarse to very coarse skeletal fragments		Peloids, Pellets and skeletal fragments	
Colour	Brown to grey to green	Cream to tan	White to grey	cream to tan	Pink to cream	Cream to tan	Light cream to pink	Cream to tan		Tan to pink colour	
Composition	Mud	Calcareous sandstone siltstone	Calcareous sandstone	Mollusks, ooids, algal, pellets	Ooids, forams quartz	Ooids, Skeletal, pellets, pisoids	Ooids, Skeletal, pellets, pisoids. algae	Pellets, ooids, mollusks, grapestones		Pellets, peloids, ooids, rare skeletal	
Structure	Lamination, bioturbation	Channels, Trough cross beds,lamination, bioturbation	Channels, tabular cross beds,lamination, mud lenses, rootlets	Crinkly laminated	Crinkly laminated near top	Crinkly lamination, mudcracks	Massive nature and mottled	Cross-bedding		Stromatolites heads	
Fossils	Trace fossils	Trace fossils	Trace fossils	Shell fragments (bivalves and gasterpods)	Molds of ooids and mollusks, shell fragments	Complete Molds of mullusks,forams	Complete Molds of mullusks,forams	Shell fragments		Rare	
Diagnostic Features	Laminated thick unit	Burrowed and weathered	Cross bedded sandstone intensely burrowed and weathered	Abundance of shell fragments	Mottled, Crinkly laminated	Crinkly laminated	Massive and red staining	Colour and small scale cross bedding		Intraclasts bearing rich in quartz	
Field Photos		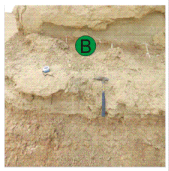	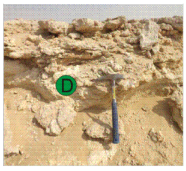	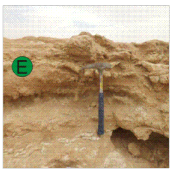							
											
Sample Slabs		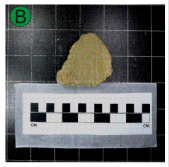	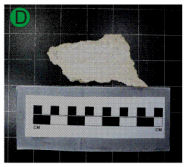	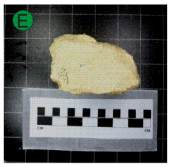	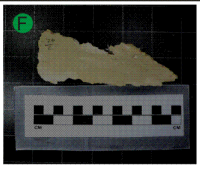						
	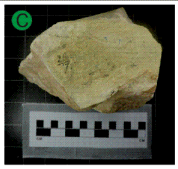				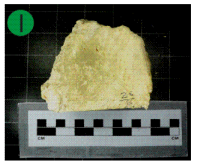						
Thin sections		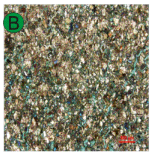	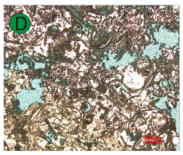	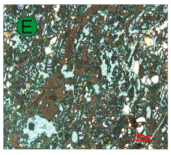	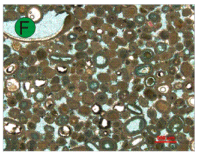						
	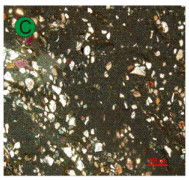			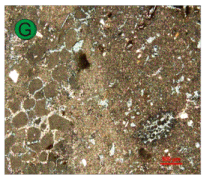	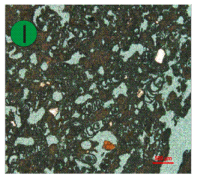						

C

Figure-6.10.c) Facies summary chart outcrop-26, mudcracked shale, calcareous sandstone, ooid grainstone, peloidal grainstone packstone and marl facies.

6.2.5.Facies Outcrop-25

Seven lithofacies identified in Outcrop-25(Figure-6.11).includes lithofacies are mudcracked shale, calcareous sandstone, dolomitic skeletal wackestone, coated skeletal grainstone, peloidal packstone grainstone, quartzose peloidal packstone, paleosols, and bioclast peloidal packstone. The succession starts with the deposition of the sandy peloidal wackestone mudstone facies which shallows upwards to foraminiferal grainstone. Fining upward trend is characteristic feature of this facies. The next facies in the cycle is paleosols lithofacies which is characterized by mudcracks and shows evidence of the ramp. The top of the cycle is truncated by incision of channel sandstone facies. This also marks the presence of sequence boundary. The sedimentary cyclicity repeats itself six times in the outcrop with mudstone dominated, mixed sand-mudstone and sandstone dominated facies.

This cyclicity represents the dominance of tidal flat conditions in the basin at the time of deposition. This interpretation is also applies to these facies in the Outcrop-25 and 26 which are considered to have been deposited in proximal setting. The conditions became distal and again the ramp was changed in to a deposition of bioclastic mudstone facies. This sedimentary cycle was repeated two times. The top of the cycle is marked by the presence of mudcracked mudstone beds. The next cycle started with the skeletal packstone and the introduction of carbonate banks and topped by grainstone having stromatolitic heads and intraclasts. The cycle commenced with the tidal flat environment. The porosity the topmost facies oolitic grainstone ranges from 10 to40%. The porosity is enhanced by dissolution of ooids and cement around them during diagenesis at shallower conditions.

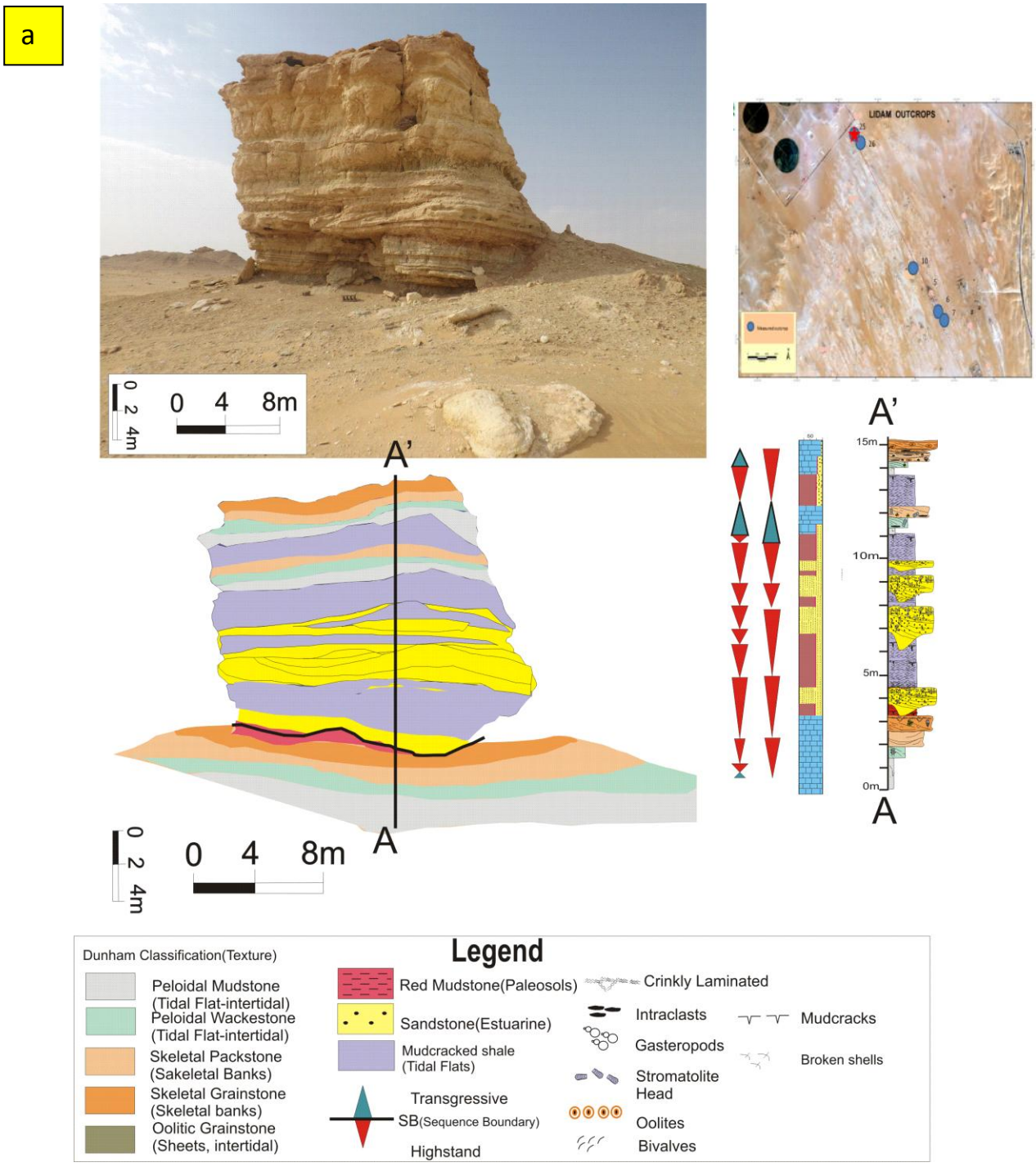

Figure-6.11.a)Facies Mosaic Outcrop -25, similar to outcrop 26, outcrop 25 facies mosaic starts with skeletal mudstone to packstone facies, the thickness of paleosols is decreased in here, and sandstone bodies is just present over the sequence boundary, the sandstone are then interbedded with mudcracked shale units, and on top the sequence is topped by highstand grainstone facies.

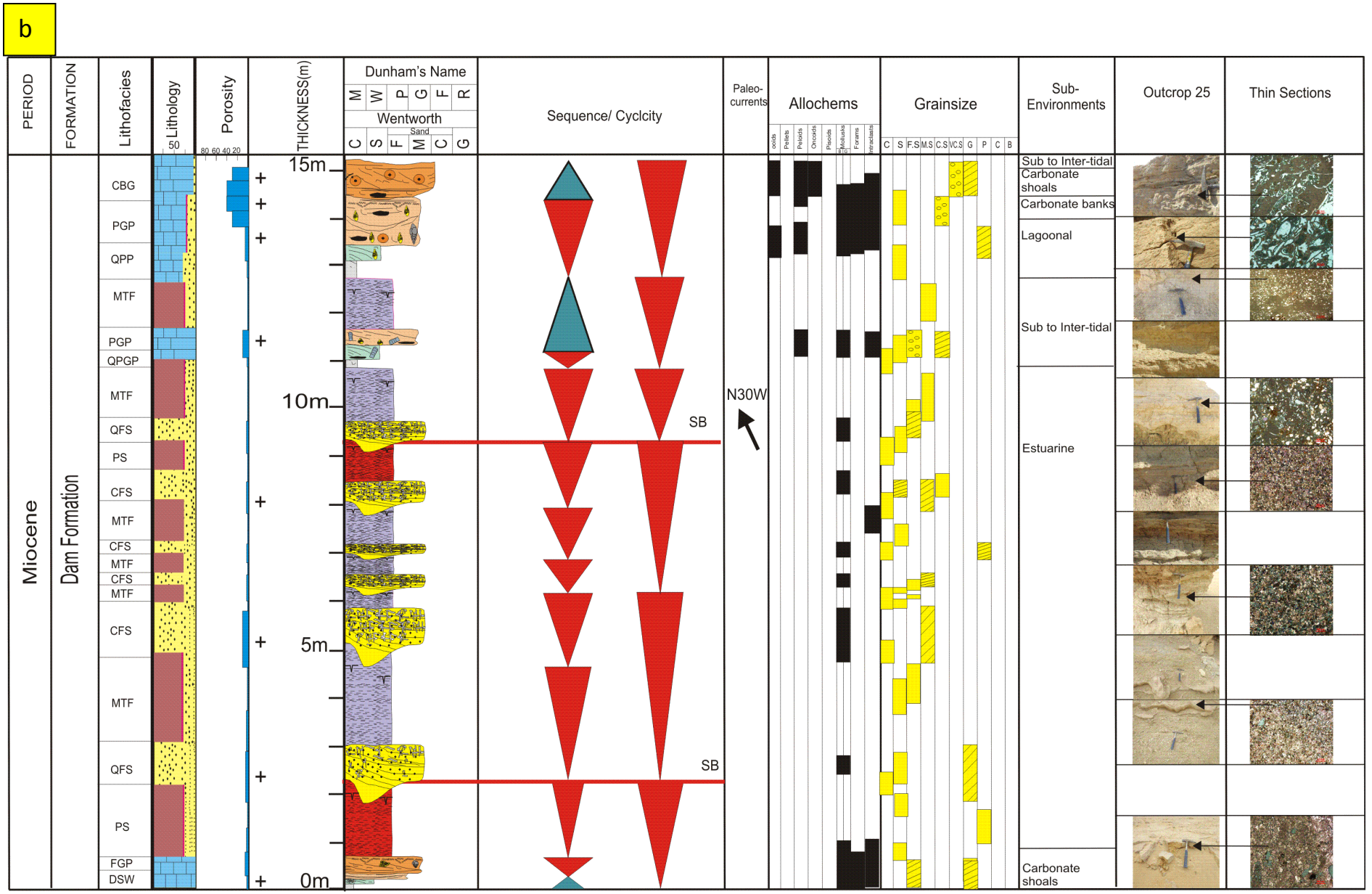

Figure-6.11.b) Composite log of outcrop-25, the Outcrop is dominated by quartz sandstone (estuarine) and mud cracked shales (tidal flats), and capped by skeletal and oolitic grainstone (Intertidal-subtidal).

Facies in Outcrop 25

Clastic/ Carbonate	Siliciclastic		Carbonate				
				Grain Supported			Mud Supported
			Skeletal	Non-Skeletal			Mud
Facies	A Mud cracked siltstone and mudstone	B Calc. fine to medium grained sandstone with mudstone	D Dolomitized skeletal wackestone	E Peloids bioclastic grainstone	F Coated bioclastic grainstone	H Peloidal grainstone to packstone	G Quartzose peloids packstone wackestone
Environment	Estuarine	Estuarine	Carbonate banks		Intertidal	Sub-Inter tidal	Sub-Inter tidal
Lithology	Mudstone/ Sst.	Sandstone	Limestone	Limestone	Limestone	Limestone	Limestone
Texture	very fine silt to fine sand, fine to medium grain angular quartz grains	Fine silt to sand fine to medium grain angular quartz grains	Coarse to very coarse skeletal fragments	Fine to medium silt size fine angular to sub rounded	Fine to medium ooids and fine to medium quartz	Peloids, Pellets and skeletal fragments	Coarse to very coarse skeletal fragments
Colour	Cream to dark Tan	Dark grey to light pink	Light to dark brown	Light cream to brown	Pink to tan	Tan to pink colour	White to cream
Composition	Calcareous sandstone and mud	Calcareous sandstone siltstone	Skeletal	Skeletal grains, ooids, grapestones	Ooides, Skeletal, pellets, pisoids	Pellets, peloids, ooids, rare skeletal	Intraclasts, pellets quartz
Structure	Channels, Trough cross beds,lamination,bioturbation	Channels, Trough cross beds,lamination,bioturbation	Structureless	Crinkly laminated near top	Crinkly lamination, mudcracks	Stromatolites heads	Structureless
Fossils	Trace fossils	Trace fossils	Shell fragments (bivalves and gasterpods)	Molds of ooids and mollusks, shell fragments	Complete Molds of mullusks,forams	Rare	Shell fragments
Diagnostic Features	Interbeded sand and mud sandstone burrowed and weathered	Low angle cross bedded sandstone intensely burrowed and weathered	Abundance of shell fragments and Mottling	Mottled, Crinkly laminated	Crinkly laminated	Intraclasts bearing rich in quartz	White colour and structureless
Field Photos	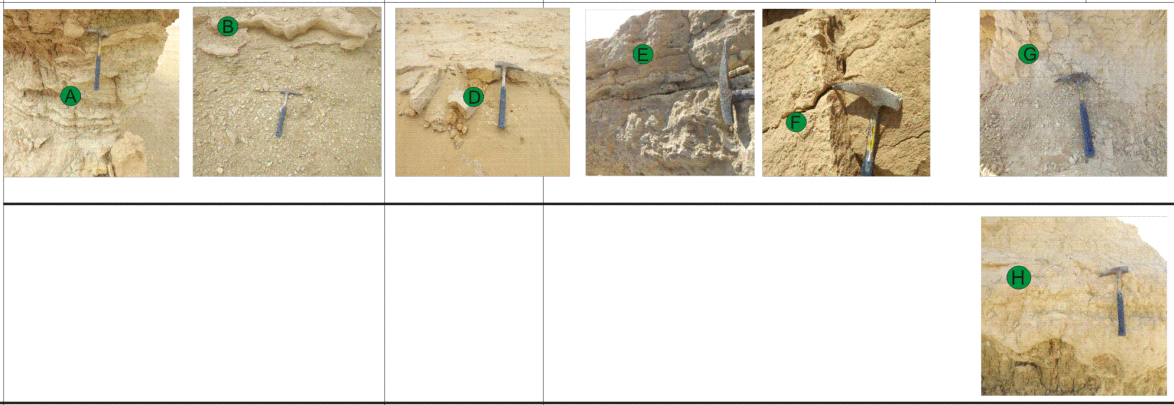						
Sample Slabs	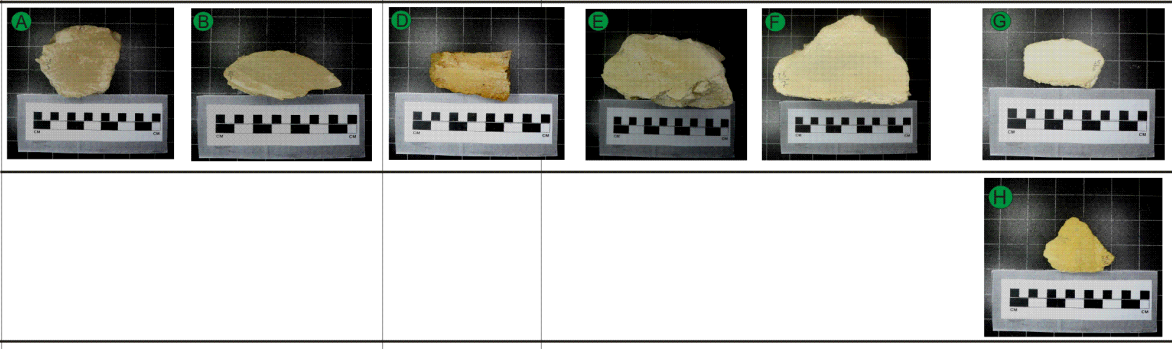						
Thin sections	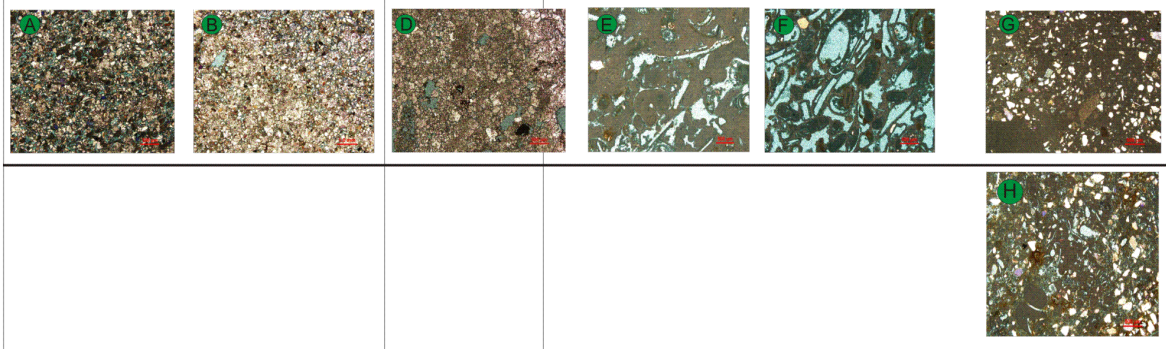						

C

Figure-6.11. c) Facies summary chart Outcrop-25, mudcracked shale, calcareous sandstone, coated bioclastic grainstone and marl facies.

6.3. Lateral Facies Changes

Lateral facies changes within the 40m thick interval of mixed siliciclastic-carbonate succession of Miocene Dam Formation, Al-Lidam Area, produces a mosaic pattern of laterally continuous and discontinuous facies architecture. Dam is characterized by shallowing upward cycles about 2 to 3 meters in thickness, and surfaces bounding the parasequences. The facies mosaics are made bed by bed across the 3.47 km area and correlated to five sections along this line (Figure-6.5). The parasequences are characterized by successive contact between successive facies to be sharp but may pass laterally to gradational contacts. The facies having lens shape geometry have extended less than 200m, passing laterally into other laterally adjacent facies. The contacts between lateral facies of lens and sheet grainstone are transitional over a few meters. The contacts between vertically placed facies are abrupt and sharp. Sequence boundaries bounding sequences are generally erosive and sharp and show several tens of centimeters of relief due to erosion over a short distance of few meters (Egenhoff, 1999). Most of the parasequences extend over 1 km and are traceable and correlateable to nearby outcrops. The stratigraphic relationship of Dam represents a model of lateral continuity of parasequence surfaces is mostly related to variations in accommodation space. The lateral variation is generally related to strongly effected by intrinsic dynamics of temporally and spatially heterogeneous sediment production (Adams et al., 1996).Lateral continuity and correlation is based on detailed analysis and interpretation of the five outcrops in the study area. The overall vertical succession represents a gradually shallowing upward sequence(AlKhaldi,2009).The juxtaposition of facies is based on the vertical relationship and occurrence of bioturbated channelized sandstone over skeletal packstone facies from south to north. The Outcrop-10 shows the thickest carbonate succession between the bioturbated sandstone and the formaniferal peloids grainstone facies (Figure-6.5). Details of lateral facies change are evident even within the individual cycles along a transect parallel to the depositional dip(Al-Saad.2002). The individual facies cycle in Outcrop 10 starts with the bioturbated mudstone and ends with oolitic grainstone facies. But in Outcrops 6 and 7, the more basinward the section muddier is starting with bioturbated mudstone and

shallows up to skeletal packstone at the maximum. The distal inner ramp facies are dominated by skeletal grainstone-packstone and peloidal grainstone(Eltom. 2013).

Petrographic observation on oolitic grainstone mostly decipher that the nuclei are made of peloidal grains. The abundance of peloids increases as we move from Outcrop 10 to Outcrops-6 and 7. The abundance of intraclasts in the lateral facies changes increases from south to north. Further offshore from Outcrop-10,the packstone facies prevails as the mud content increases, the skeletal content and depositional energy decreases. Still further offshore, the burrowed mudstone or skeletal mudstones to wackstone with local crinkled algal laminations predominate. In the algal laminites, the stromatolitic heads and skeletal grainstone and packstone form the matrix between the heads. In general, the skeletal grainstone matrix is more common towards the top of succession towards outcrop 10.

The Outcrop 10 starts with a basal skeletal oolitic packstone to grainstone facies which is also present in Outcrop 6 above the skeletal grainstone facies, it is also present in outcrop 7 above skeletal packstone to grainstone facies having grapestones, in Outcrops-7 and 26 above skeletal packstone facies. It is followed by the oolitic grainstone facies in Outcrop 10 and occurs above skeletal oolitic grainstone to packstone facies in Outcrops-6 and 7. This is followed by dolomitic skeletal wackestone facies in Outcrops-10 and 25(Figure-6.5).

The dolomitized skeletal wackestone facies is followed by calcareous medium to fine grained sandstone facies in all outcrops and is the correlation marker bed. It is found just above the skeletal packstone in Outcrops-6 and 7. It can be traced laterally along the NS-transect to north this facies overlies dolomitized skeletal wackestone facies in Outcrop 25 and skeletal packstone in outcrop 26. In Outcrops-25 and 26, the dominant facies are the sandstone and mudstone facies. These lithologies are present in the form of interbedded sandstone and mudstone facies, cross-bedded sandstone with mudstone intercalations, and mudstone with sandstone interbeds. This mudstone with sandstone interbeds facies is followed by skeletal mudstone facies in outcrop 10 and outcrop 7.

Mud cracked siltstone mudstone facies overlies the carbonate mudstone facies in Outcrops-6 and 7(Figure-6.5). This is followed by oolitic foraminiferal grainstone to mudstone facies but it occurs in other outcrops but at different cycle levels. It is found just below the

skeletal oolitic grainstone facies in outcrop 7. Sandy peloids wackstone to mudstone facies it occurs above the oolitic foraminiferal grainstone facies. It also occurs in outcrop 6 and 7. Skeletal grainstone and skeletal intraclastic grainstone to packstone facies form the top of Outcrop 10 and are traceable laterally from outcrop 6 to Outcrop 7, still further to Outcrops-25 and 26. In the other outcrop than 10, these facies are also dominated by peloidal grains (Figure-6.5). By introduction of algal material in outcrop 25 and 26, while ooids incorporate in outcrop 7 and make it skeletal oolitic peloidal packstone to grainstone facies.

6.4. Palaeocurrent Direction

Orientation of well developed tabular sandstone cross-beds and skeletal oolitic grainstone facies serve as palaeocurrent indicator for Dam Formation. The palaeocurrent data indicates a general seaward direction to southeast and landward direction to the northwest (Figure-6.12).This interpretation is in agreement with the regional Paleogeographic reconstruction of Middle Miocene Shelf (Zeigler, 2001).However, more detailed measurements of these outcropping palaeocurrent indicators over a broader part of Dam Formation would help in paleoshoreline reconstruction. This would improve our understanding of shoreline heterogeneity and variability of nearshore depositional lithofacies. The same sandstone were measured at 5 different locations, in AL-Lidam Area, the typical sandstone cross beds are around 70cm thick.

The same sandstone was measured at 5 different locations, around 3.4km apart. At all the localities sandstone beds were consistently oriented N65W. However the oolitic grainstone beds measured at all localities show N65E, suggests a direction towards NE.

These oolitic grainstone beds are interpreted to have been deposited along shoreline as a result of wave energy dissipating across oolitic sheets, towards onshore (NW). These data sets, based on sedimentary structures corroborate with previous data sets, interpretations are based with respect to regional data (Figure-6.12).

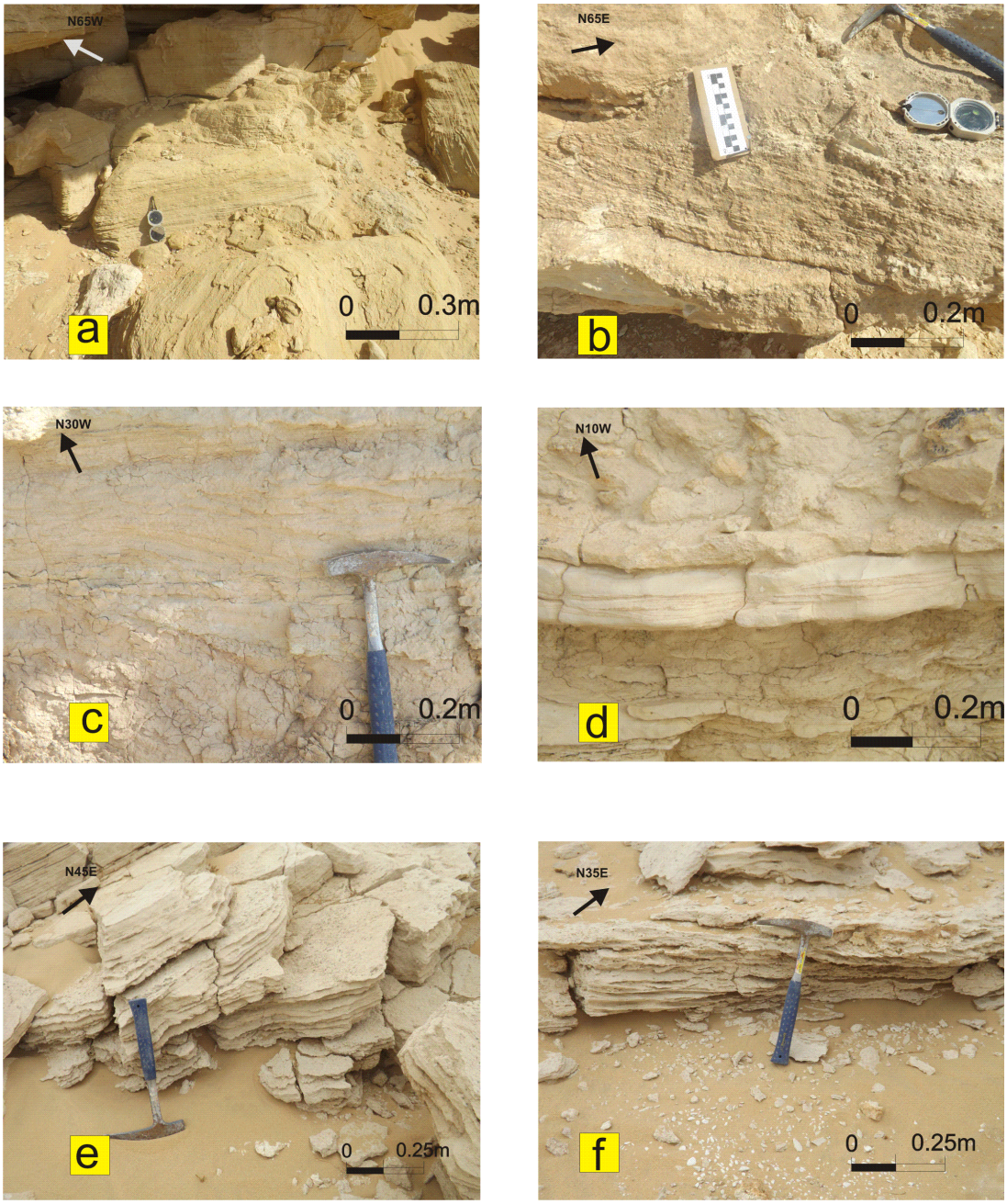

Figure-6.12. Palaeocurrent indicators in Middle Miocene Dam Formation, a) Bioturbated sandstone facies, it dips to the north east and shows unimodal current direction to the N65W in outcrop-10, b) Oolitic skeletal grainstone facies, the paleoflow direction N65E in outcrop-10, c)Calcareous sandstone facies dipping 2-5° Northeast, paleoflow direction N30W in outcrop 25,d) intraclastic packstone facies dipping 1-2° Northeast, paleoflow direction N10W in outcrop 26(200x200cm), e) skeletal grainstone facies dipping 2-4° southeast, paleoflow direction in outcrop-6, N45E, f) skeletal grainstone to packstone facies dipping 3-5° southeast, paleoflow direction, N35E in outcrop-7.

6.5. Geochemical Data

The geochemical analysis of the facies studied was carried out for detailed mineralogy and elemental chemistry. All the samples we studied using XRD, SEM and EDS to determine their mineralogy, grain morphology, type and elemental chemistry. The seventeen facies in the outcrop sections (Figure-6.13) are divided into four groups, namely pure limestone group, sandy limestone group, sandstone group and clay to sandy shale group.

Group-1 Pure limestone Group

Most of the carbonate facies are not pure carbonates. There is a percentage of quartz and clays in them. The first group consists of facies rich in calcite (>95) and are called pure limestone group. The facies belonging to this group include the micritic ooid peloidal grainstone (Mpg-2) oolitic grainstone facies (Og-4), peloidal packstone (Pp-5), Sandy peloidal grainstone facies (Spg-11) and sandy peloidal packstone facies (Spep-12).

Group-2 Sandy limestone Group

The second group sandy limestone group consists of facies rich in calcite but have appreciable quartz content around (13%) are called sandy limestone group. There are four facies that fall in this group. The facies parts of this group are the coated skeletal grainstone facies (Csg-1), sandy peloidal skeletal grainstone facies (Spg-3), dolomitized skeletal wackestone facies (Dsw-8) and foraminiferal grainstone packstone facies (Fgp-9).

Group-3 Sandstone Group

The sandstone group consists of facies rich in quartz (>97%) but have appreciable calcite (13%) The facies part of this group is quartz fine sandstone with mudstone facies (Qfs-7)

Group-4 Clay to sandy shale Group

This fourth group, the clay to sandy shale group consists of facies rich in clay (52-86%) quartz (48-13%). Two facies, paleosols facies (Ps-6) and mud cracked siltstone mudstone facies (Msm-10) that fall within this group.

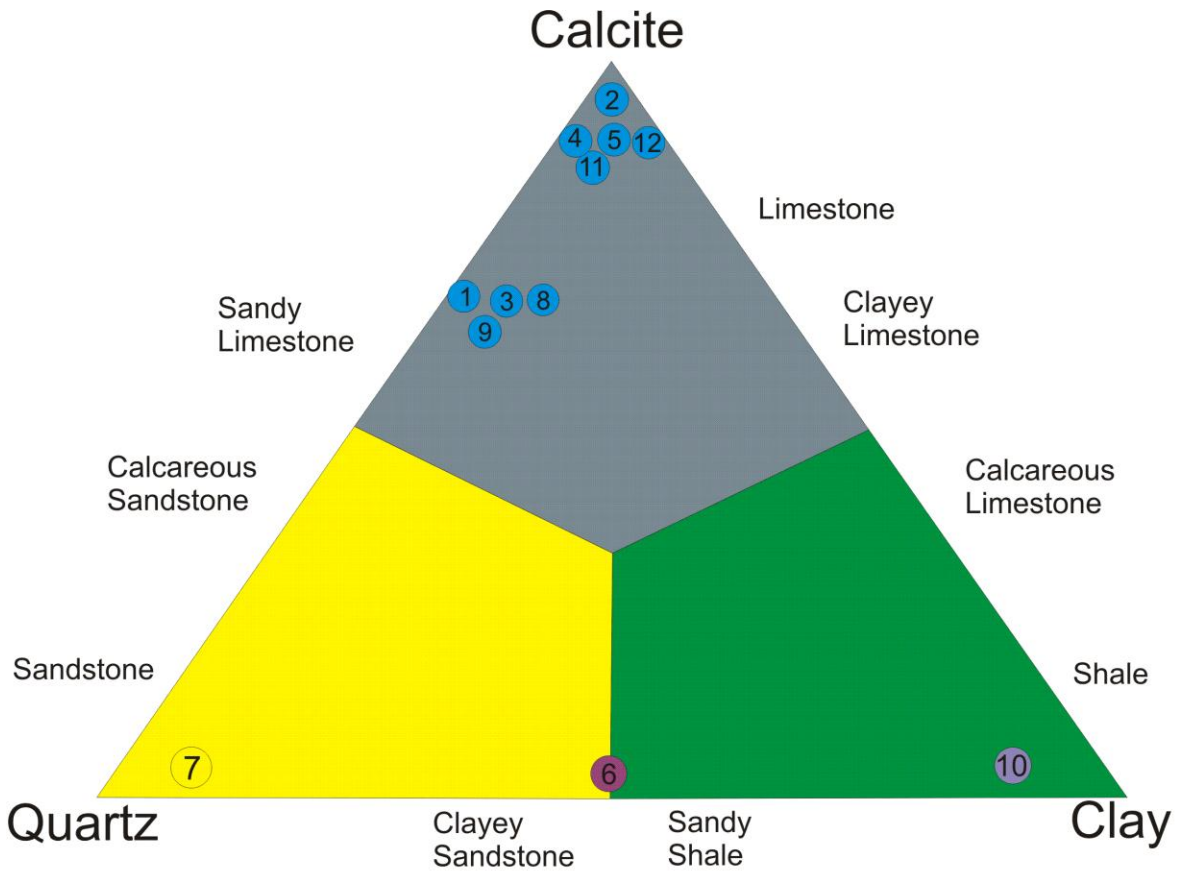

Figure-6.13. Ternary diagram using Quartz, Clay and Calcite to classify the facies present in Dam, the dominant are the pure limestone and sandy limestone groups, followed by clay and sandy shale group and least is sandstone group. Please note that in this diagram calcite (indicating carbonate, calcite+dolomite) (after Mason 1952; Trurekian 1968).

On the base of the classification, the following observations and interpretations are made:

The succession starts with coated skeletal grainstone facies (Csg-1, sandy limestone-skeletal banks) and overlain by oolitic grainstone (pure limestone-intertidal) which is shallowing upward. The topmost is marked by oolitic grainstone intertidal facies (pure limestone-intertidal). The deposition starts with sandy limestone and passes on to pure limestone, which caps the cycles and sequence. It also represents the total shutdown of quartz in the basin at the time of deposition. The strata were exposed and saw the development of paleosols (Clay to sandy shale Group-supratidal). The clay is dominated by palygorskite and illite. The palygorskite is a part of pedogenic soil and is an integral part of soil profile. The shallowing upward trend continued until the ramp was exposed to weathering. The estuarine conditions started with the deposition of bioturbated sandstone lithofacies (Sandstone Group-estuarine). The sandstone group marks the

abundance of quartz (97%), and a total shutdown in carbonate production. This is important in sequence stratigraphy as the sandstone provides the base of the sequence. It marks the start of TST, and gradually the sandstone passes in carbonate facies upward. The appearance of coated skeletal grainstone facies (Csg-1) marks the presence of mfs, and gives way to HST.

The location was then covered by a transgressive sandstone part of the sandstone group facies. Sandy peloidal skeletal pack-grainstone facies (Spg-3) part of sandy limestone (skeletal banks to intertidal) facies suggests the start of carbonate deposition. The presence of carbonate dominance marks the shallowing upward, and most of the cycles are capped by oolitic grainstone facies part of pure limestone group. This facies is topped by crinkly laminated coated bioclastic grainstone facies (sandy limestone-skeletal banks) on top.

The karstification feature in sandy limestone facies (Foram grain-packstone facies-skeletal banks) just below the oolitic grainstone facies (limestone group-intertidal) marks slight emergence and exposure of the ramp. The oolitic grainstone facies (pure limestone group-intertidal) show small episode of deepening upward and it is also strengthen by mineralogy as more accommodation space is created for carbonate deposition.

The environment becomes shallower with deposition of clay to sandy shale Group member rooted mudcracked siltstone and mudstone bed (tidal flat) deposited. This shows the influx of clastic materials in to the basin, and absence of carbonate content at this level represents emergence and strengthen by presence of mudcracks and rootlets. The facies on the top of siltstone and mudstone bed (tidal flat) facies are the start of another cycle with coated skeletal grainstone facies at base and oolitic grainstone on top. The same cycle repetition, the contorted structure in the skeletal quartzose pack-grainstone facies (sandy limestone) marks the presence of tidal flat environment in the succession. This contorted structure marks the seismic activity in the area at the time of its deposition. The top of the cycle is again marked by the presence of oolitic grainstone with foraminfera assemblage (pure limestone). The next cycle starts with the skeletal packstone and introduction of carbonate banks and topped by peloidal grain-packstone facies (sandy limestone) having stromatolitic heads and intraclasts. The input of quartz on top of these cycles could be attributed to intraclasts and quartz particles attached to algal material in the facies, and shows inter tidal flat environment. The topmost cycle represents the same as the

previous but here intraclasts abundance increased and hence the sandy limestone content too increases. The sandy shale and clay group are the least in terms of porosity as most of the pores are occupied by illite and quartz grains are covered by palygorskite. Pure carbonate facies are dominantly deposited in intertidal setting, while the sandy carbonate facies in skeletal banks, sandstone facies in estuarine setting and clay and shale group mainly in supratidal to tidal flat setting.

Conclusion

The oolitic grainstone, micritised oolitic grainstone-packstone, dolomitic skeletal wackestone and sandy peloidal grainstone to packstone facies occur as sheets and were deposited in intertidal setting. Sandy peloidal skeletal grainstone characterized by lens geometry was deposited in skeletal banks and the quartzose fine sandstone with channel geometry was deposited in estuarine environment. The sequence boundary between the bioturbated sandstone and the skeletal packstone is traceable across the whole outcrops and presents a good correlation tool. The presence of palygorskite from paleosols facies indicates soil weathering and is very important for identification of sequence boundaries in Dam. The Dam Formation is composed of four composite sequences namely CS-1, CS-2, CS-3and CS-4. The CS-2 is further subdivided into HFS-1 and HFS-2. The High frequency sequences are in turn subdivided into TST and HST each. CS-1 the thickest part of all the sections is very distinctive bedset throughout the field area. Skeletal packstone dominate the TST, while the oolitic grainstone dominant in the HST.HFS-1 is composed of bioturbated sandstone that grades upwards into a skeletal mudstone to wackestone facies. The HFS-2 starts with a skeletal packstone and is topped by skeletal to oolitic grainstone. The north eastern sections of the Dam Formation in Lidam area show increase in percentage of siliciclastic sediments in updip sections, while carbonates in downdip towards the south western sections. Based on our results, the Dam Formation was deposited on a mixed carbonate-siliciclastic homoclinal ramp. The Outcrops 25 and 26 which are richer in siliciclastic than carbonates might have been deposited in proximal inner ramp. The southern Outcrops 6, 7 and 10 are richer in carbonate than siliciclastic, were deposited in the distal inner ramp to proximal mid ramp. The palaeocurrent direction of bioturbated sandstone shows N65E to N10E suggested that the sandstone channels came from south. Carbonate geobodies and architecture data for Dam Formation helped in interpreting depositional environment. The occurrence of microbial lamination and crinkly laminated packstone to grainstone and presence of rootlet bearing mudcracked siltstone and mudstone facies suggests arid climate. Rising sea-level placed the siliciclastic sediments further north and allowed mixed carbonate-siliciclastic to form on downdip under arid and locally hypersaline conditions.

References

Abdullatif O. and M. Yassin 2012 Facies Modeling of Dam and Hofuf Formations: Outcrop Analog of Mixed Carbonate and Siliciclastic (Miocene-Pliocene) Succession, Eastern Saudi Arabia Geophysical Research Abstracts, Vol. 14, EGU2012-3637

Abu-Zeid, M. and H. Khalifa, 1983. Sedimentological and paleoenvironmental aspects of the Miocene succession in Jebel Nakhash, Qatar, Arabian Gulf. Neues Jahrbuch fur Geologie und Palaontologie Monatshefte, v. 7, p. 334-399.

Adnan, A., U. K. Shukla, A. Verma & T. Shukla(2014) Lithofacies of transgressive–regressive sequence on a carbonate ramp in Vindhyan basin (Proterozoic): a case of tidal-flat origin from central India Arab J Geosci

Al-Ameri, T. K., J. Zumberge and Z. M. Markarian (2011) Hydrocarbons in the Middle Miocene Jeribe Formation, Dyala Region, NE Iraq, Journal of Petroleum Geology, Vol. 34(2), April 2011, pp 199 - 216

Al-Banna N. Y., 2008, Oligocene / Miocene boundary in northern Iraq, GeoArabia, Vol. 13, No. 2, Gulf PetroLink, Bahrain

Al-Banna N. Y., and M. M. Al-MutwaIi (2005) Sedimentary Cycles and Microfacies Analysis of Lower Miocene Formations in Sinjar and Sharafaddin Areas, NW Iraq, Raf. Jour. Sci., Vol.16, No.2 Geology, Special Issue, pp. , 2005, 57

Al-Enezi, S. S., 2006, Comparison of Recent and Miocene Foraminifera from Eastern Saudi Arabia, MS Thesis, King Fahd University of Petroleum and Minerals, Saudi Arabia.

Al-Hinai, K.G., A.E. Dabbagh, W.C. Gardner, M.A. Khan and S. Saner, 1997. Shuttle imaging radar views of some geological features in the Arabian Peninsula. GeoArabia, v. 2, no. 2, p. 165-178.

Adams, R. D. and J. P. Grotzinger (1996) Lateral continuity of facies and parasequences in Middle Cambrian platform carbonates, Carrara Formation, southeastern California, U.S.A Journal of Sedimentary Research, v. 66, p. 1079-1090.

AlKhaldi F.M., 2009, Controls on Hierarchy of Miocene Buildups within a High Resolution Cycle Stratigraphic Framework of Dam Formation, Lidam Area, MS Thesis, King Fahd University of Petroleum and Minerals, Dhahran, Saudi Arabia.

AlKhaldi F.M., Tawil, A., Fred, R.J., 2010, Controls on Sequence Stratigraphy of Miocene Mixed-Carbonate-Siliciclastic Systems, Early Miocene, Dam Formation, Eastern Saudi Arabia, AAPG Search and Discover Article #90104©2010 AAPG Annual Convention and Exhibition-11-14 April 2010.

AlKhaldi F.M., J.F. Read and A. Tawil(2014) Mixed Carbonate-Siliciclastic Sequence Development on a Distal Fore-Land During Miocene Glaciation, Eastern Saudi Arabia, AAPG Datapages/Search and Discovery Article #90194 © 2014 International Conference & Exhibition, Istanbul, Turkey, September 14-17, 2014

Al-Qayim, B., A. Ibrahim, and S. Othman (2014) Microfacies and Sequence Stratigraphy of the Oligocene-Miocene Sequence at Golan Mountian, Kurdistan, Iraq, AAPG Search and Discovery Article #90188 ©GEO-2014, 11th Middle East Geosciences Conference and Exhibition, 10-12 March 2014, Manama, Bahrain

Al-Qayim B. (2014) Coastal Siliciclastic Influxes Enhancing Sequence Stratigraphic Resolution: Case Study From The Oligocene –Miocene of The Zagros, Kurdistan, Iraq, 2014 GSA Annual Meeting in Vancouver, British Columbia (19–22 October 2014).

Al-Saad H. and M. I. Ibrahim, 2002, Stratigraphy, Micropaleontology and Paleoecology of the Miocene Dam Formation, Qatar, GeoArabia, v 7, No 1, P 9-28.

Al-Sharhan, A.S. and A.E.M. Nairn 1997, Sedimentary Basins and Petroleum Geology of the Middle East, ELSEVIER SCIENCE B.V, pp. 460-464.

Al-Sharhan, A.S. and C.G.St.C. Kendall 2002. Holocene carbonate/evaporites of Abu Dhabi, and their Jurassic ancient analogs. In, H.J. Barth and B.B. Boer (Eds.), Sabkha Ecosystems. Kluwer Academic Publishers, p. 187-202.

Al-Sharhan, A.S. and A.E.M. Nairn 1995, Tertiary of the Arabian Plate; Sedimentology and Hydrocarbon Potential, Paleogeography, Paleoclimatology, Palaeoecology, 114, pp 369-384.

Amour, F., M. Mutti, N. Christ, A. Immenhauser, G.S. Benson, S.M. Agar, S. Tomás, & L. Kabiri 2013, Outcrop analog for an oolitic carbonate ramp reservoir: A scale-dependent geologic modeling approach based on stratigraphic hierarchy AAPG Bulletin, v. 97, no. 5, pp. 845–871

Arabian Miocene: stratigraphic background, Abu Dhabi Islands Archeological Survey (ADIAS)http://www.adias-uae.com/fossils/Strat.html

Bears, D., (1962) Modern Carbonate Sediments of South Florida: Abstract, Tulsa Geological Society Digest, Vol. 30 (1962), Pages 164-164

Bendias, D., T. Aigner, M. Pöppelreiter and B. Köhrer (2011) Khuff Sequence KS6: Paleorelief-influenced Facies and Sequence Patterns in the Lower Khuff Formation, Sultanate of Oman, Third Arabian Plate Geology Workshop, Permo-Triassic (Khuff) Petroleum System of the Arabian Plate, Kuwait City, Kuwait, 28 November - 1 December 2011

Bird, P., 1978 Finite element modelling of the lithosphere deformation' The Zagros collision orogeny, Tectonophysics, 5_90 , 307-336,

Botha, G. A., and J.C. Hughes (1992) Pedogenic palygorskite and dolomite in a late Neogene sedimentary succession, northwestern Transvaal, South Africa, Geoderma, 53, 139-154.

BouDagher-Fadel, M.K. and F.T. Banner 1999. Revision of the stratigraphic significance of the Oligocene-Miocene, Letter Stages". Révue de Micropale-ontologie, v. 42, no. 2, p. 93–97.

Bressan, G.S., and R. M. Palma (2009) Trace fossils from the Lower–Middle Jurassic Bardas Blancas Formation, Neuquén Basin, Mendoza Province, Argentina, Acta Geologica Polonica, Vol. 59, No. 2, pp. 201–220

Campbell, A.E., 2005 Shelf-Geometry response to changes in relative sea level on a mixed carbonate-siliciclastic shelf in the Guyana Basin, Sedimentary Geology, 175, pp 259-275.

Cantrell, D.L. & R.M. Hagerty, 1999, Microporosity in Arab Formation Carbonates, Saudi Arabia. GeoArabia, 4, 129–154.

Cantrell, D., P. Swart, & R.Hagerty, 2004, Genesis and characterization of dolomite, Arab-D reservoir, Ghawar field, Saudi Arabia. GeoArabia, 9, 11–36.

Carozzi, A. V., (1989) Carbonate rock depositional models, A microfacies approach, Prentice Hall Englewood Cliffs, New Jersey.

Cavelier, C. 1970. Geologic Description of the Qatar Peninsula (Arabian Gulf). Government of Qatar Publication, Department of Petroleum Affairs, 39 p.

Curran H. A., and B. White (1995) Terrestrial and Shallow Marine Geology of the Bahamas and Bermuda, Special Paper, Geological Society of America

D'Argenio, B., Fischer, A.G., Silva, I.P., Wissert, H., Ferreri, V., 2005. Cyclostratigraphy: Approaches and case histories, SEPM Special Publication, 81, 311pp.

Dalrymple, R. W., B. A. Zaitlin, and R. Boyd, 1992, estuarine facies models: Conceptual basin and stratigraphic implications: Jour. Sed. Petrology, v. 62, p. 1130-1146.

Desbois , G., Urai Janos L., Kukla Peter A., Konstanty Jan., Claudia Baerle, 2011, High-resolution 3D fabric and porosity model in a tight gas sandstone reservoir: A new approach to investigate microstructures from mm- to nm-scale combining argon beam cross-sectioning and SEM imaging, Journal of Petroleum Science and Engineering 78 (2011) 243–257

Detailed geologic Map of Arabian Peninsula (World Energy Geology, USGS, 2002, Url: http://pubs.usgs.gov/of/1997/ofr-97-470/OF97-470B/

Dill, H.G., Friedhelm , H., 2007. Strontium (87Sr/86Sr) and calcium isotope ratios (44Ca/40Ca-44Ca/42Ca) of the Miocene Dam Formation in Qatar: tools for stratigraphic correlation and environment analysis. GeoArabia. V. 12, No. 3, p. 61-76.

Dill, H.G., R. Botz, Z. Berner, D. Stüben, S. Nasir and H. Al-Saad, 2005. Sedimentary facies, mineralogy, and geochemistry of the sulphate-bearing Miocene Dam Formation in Qatar. Sedimentary Geology, v. 174, p. 63-96.

Dill, H.G., S. Nasir and H. Al-Saad 2003. Lithological and structural evolution of the northern sector of the Dukhan Anticline, Qatar, during the early Tertiary: with special reference to bounding surfaces of sequence stratigraphical relevance. GeoArabia, v. 8, no. 2, p. 201-226.

Ditchfield, P.W., 1999. Diagenesis of the Baynunah, Shuwaihat, and Upper Dam Formation sediments exposed in the western region, Emirate of Abu Dhabi, United Arab Emirates. In, P. Whybrow and A. Hill (Eds.), Fossil, Vertebrates of Arabia. Yale University Press, p. 62-74.

Douglas, J.L., 1996. Geostatistical model for the Arab-D Reservoir, North ‘Ain Dar Pilot, Ghawar Field, Saudi Arabia; an improved reservoir simulation model. GeoArabia, 1, 267-284.

Dunham, R.J., 1962. Classification of Carbonate Rocks According to Depositional Texture. In Ham, W.E. Classification of Carbonate Rocks. American Association of Petroleum Geologists, Memoir 1, p. 108-121.

Dunnington, H. V., 1958 Generation, migration, accumulation and dissipation of oil in Northern Iraq, in Habitat of Oil, edited by L. G. Weeks, pp. 1194-1251, American Association of Petroleum Geologists, Tulsa, Okla.,

Ehrenberg, S.N., N. A.H. Pickard, G. V. Laursen, S. Monibi, Z. K. Mossadegh, , T. A. Svånå, , A. A.M. Aqrawi, J. M. McArthur, and M. F. Thirlwall, (2007) Strontium Isotope Stratigraphy of The Asmari Formation (Oligocene - Lower Miocene), SW Iran, Journal of Petroleum Geology, Vol. 30(2), pp 107-128

Egenhoff. S.O, A. P. Nsel, T Bechstaè Dt, R.Z. Hlke and J. R. Groè tsch (1999) Facies architecture of an isolated carbonate platform: tracing the cycles of the LatemaÁr (Middle Triassic, northern Italy), Sedimentology 46, 893-912

Eltom, H., M. Makkawi, O. Abdullatif and K. Alramadan 2012. High-resolution facies and porosity models of the Upper Jurassic Arab-D carbonate reservoir using an outcrop analogue, central Saudi Arabia. Arabian Journal of Geosciences, DOI: 10.1007/s12517-012-0708-1.

Eltom, H., O. Abdullatif, M. Makkawi and M. Yasin 2013. Integration of spectral gamma-ray and geochemical analyses for the characterization of the upper Jurassic Arab-D carbonate reservoir: outcrop analogue approach, central Saudi Arabia,Petroleum Geoscience. DOI: 10.1144/petgeo2012-001.

Eltom, H., O. Abdullatif, M. Makkawi and A. Abdulraziq 2013. Microporosity in the Upper Jurassic Arab-D carbonate reservoir, Central Saudi Arabia: An outcrop analogue study, Journal of Petroleum Geology, v. 36(3), 281-297.

Eltom, H., O. Abdullatif, M. Makkawi and A. Abdulraziq 2014. Characterizing and modeling the Upper Jurassic Arab-D reservoir using outcrop data from Central Saudi Arabia, GeoArabia, v. 19, no. 2, p. 53-84 Gulf PetroLink, Bahrain.

Embry, A. F., and J. E. Klovan, 1971, A late Devonian reef tract on the north-eastern Banks Islan, N.W.T.: Canadian Petroleum Geology Bull., v. 19, p. 730-781.

Fischer, A.G., 1981. Climatic oscillations in the biosphere. In: Nitecki, M. (Ed.), Biotic Crises in Ecological and Evolutionary Time. Academic Press, New York, pp. 103–131.

Flügel, E., 2004, Microfacies of Carbonate Rocks: Analysis, Interpretation and Application, Springer Verlag, 920p

Flügel E. 1982. *Microfacies Analysis of Limestones*. Xiv + 633 pp., 78 figs, 53 plates, 58 tables. Berlin, Heidelberg, New York: Springer Verlag. Price DM 148.00; approx. U.S. $65.80. ISBN 3 540 11269 3. Translated from the German original, *Microfazielle Untersuchungsmethoden von Kalken*, first published in 1978.

Franseen, E. K., M. Esteban, W. C. Ward, and J. M. Rouchy(1996) Models for Carbonate Stratigraphy, From Miocene Reef Complexes of Mediterranean regions SEPM, Concepts in Sedimentology and Paleontology, Vol#5.

Friedman, G. M., 1959. Identification of carbonate minerals by staining methods. Journal of Sedimentary Research, v. 29, no. 1, p. 87-89.

Ghafur A. A., (2012) Sedimentology And Reservoir Characteristics of The Oligocene-Early Miocene Carbonates (Kirkuk Group) of Southern Kurdistan, PhD Thesis, School of Earth and Ocean Sciences, Cardiff University

Goff, J.C., R.W. Jones and A.D. Horbury 1995. Cenozoic basin evolution of the northern part of the Arabian Plate and its control on hydrocarbon habitat. In, M.I. Al-Husseini (Ed.), Middle East Petroleum Geosciences Geo‟94. Gulf PetroLink, Bahrain, v. 1, p. 402–412.

Gradstein, F. M. J. G. Ogg, M. Schmitz and G. Ogg 2012, Oxygen Isotope Stratigraphy chapter 10; The Geologic Time Scale 2012. Published by Elsevier

Grammer, G. M., P. M. (Mitch) Harris, and G. P. Eberli (2005) Integration of Outcrop and Modern Analogs in Reservoir Modeling. AAPG Memoir 80

Greenwood, P.H. 1987. Early Miocene fish from eastern Saudi Arabia. Bulletin of the British Museum (Natural History), v. 41, no. 4, p. 451–453.

Haq, B., and Al-Qahtani, A., 2005. Phanerozoic cycles of sea-level change on the Arabian Platform. GeoArabia. V. 10, p. 127-160.

Haq, B.U., Hardenbol, J., and Vail, P.R., 1987. Chronology of fluctuating sea levels since the Triassic (250 million years ago to present). Science, 235, 1156–1167.

Harris P.M., (1984)Cores from A Modern Carbonate Sand Body; The Joulters ooid shoal, Great Bahamas Bank, The Society of Economic Paleontologists and Mineralogists (SEPM) Carbonate Sands (CW5), 1984

Heidari, A., l. A. Gonzalez, A. Mahboubi, R. Moussavi-harami, G. A. Ludvigson and G. J. Chakrapani (2014) Diagenetic Model of Carbonate Rocks of Guri Member of Mishan Formation (Lower to Middle Miocene) SE Zagros Basin, Iran, Journal Geological Society of India, Vol.84, July 2014, pp.87-104Henson, F.R.S., 1950, Middle Eastern Tertiary peneroplidae (foraminifera), with remarks on the phylogeny and taxonomy of the family.– Unpubl. PhD Thesis, Leiden (Wakefield), 70 p.

Hewaidy, A., 1991. Contribution to the stratigraphy of Miocene sediments in Qatar. Middle East Research Center, Ain Shams University, Egypt, Earth Science Series, v. 5, p. 160-170.

Hughes, G. W., (2004) The Geology of the Dammam Dome, Dhahran Geoscience Society Field Trip Guide.

Hughes, G. W., and D.L. Cantrell (2013) The Geology of the Dammam Dome, Dhahran Geoscience Society Field Trip Guide, edited by K.D. Apperson.

Hughes, G.W. 2004a. Middle to Late Jurassic biofacies of Saudi Arabia. Rivista Italiana di Paleontologia e Stratigrafia, 110, 173–179.

Hughes, G.W. 2004b. Palaeoenvironmental and sequence stratigraphic implications of Pseudocyclammina lituus events in the Upper Jurassic (Oxfordian), Hanifa Formation of Saudi Arabia. In: Bubík, M. and Kaminski, M.A. (eds) Proceedings of the Sixth International Workshop on Agglutinated Foraminifera. Grzybowski Foundation Special Publications, 8, 209–216.

Hughes, G.W. 2009. Using Jurassic micropaleontology to determine Saudi Arabian carbonate paleoenvironments. In: Demchuk, T.D. & Gary, A.C. (eds) Geologic Problem Solving with Microfossils. SEPM, Special Publications, 93, 127–152

Hughes, G.W., 1996. Environmentally-induced biofacies events in the Arab-D reservoir of Saudi Arabia. GeoArabia, 1, 150.

Hughes, G.W., 2004. Middle to Upper Jurassic Saudi Arabian carbonate petroleum reservoirs: biostratigraphy, micropalaeontology and palaeoenvironments. GeoArabia, 9, 79-114.

Hughes, G.W., 2009. Using Jurassic micropaleontology to determine Saudi Arabian carbonate paleoenvironments. Special Publication - Society for Sedimentary Geology, 93, 127-152

Hughes G.W., M. AL-Khaled, & O. Varol, 2008 Oxfordian biofacies and palaeoenvironments of Saudi Arabia, Volumina Jurassica, Vol 6, No 6

Hughes G.W. & N. Naji, 2008. Sedimentological and micropalaeontological evidence to elucidate post-evaporitic carbonate palaeoenvironments of the Saudi Arabian latest Jurassic, Vol 6, No 6,

Hughes G.W. 2005 Calcareous Algae of Saudi Arabian Permian to Cretaceous Carbonates, Revista Española de Micropaleontología, 37(1), 2005, pp. 131-140, © Instituto Geológico y Minero de España, ISSN: 0556-655X

Hughes G.W. 2008. Biofacies and palaeoenvironments of the Jurassic Shaqra Group of Saudi Arabia, Vol 6, No 6,

Hull, C. C., and H. R. Warmen, 1970, Asmari oil fields of Iran, Mem. Am. Assoc. Pet. Geol., 14, 428-437,

Iterm, O. 1987,"Micocene Tidal Flat Stromatolites of the Dam Formation, Saudi Arabia", The Arabian journal for science and Engineering, Vol 12, No. 2. pp. 145-153.

James, N. P., 1984, "Shallowing-Upward Sequences in Carbonates", Facies Model, Second Edition, Geoscience Canada, Reprint Series 1, Edited by Roger G. Walker, pp. 209-255

Jung, A and T. Aigner (2012)Carbonate geobodies: hierarchical classification and database – A new workflow for 3d reservoir modelling, Journal of Petroleum Geology, Vol. 35(1), pp 49 - 66

Karim, K. H. P. A. Khanaqa, B. M. Ameen (2009) Types of recent microbailite in slightly acidic spring in Ranyia Area, Kurdistan, NE-Iraq, Published In: Iraqi Bulletin of Geology and mining, V.7, No.2. pp.27-40.

Keheila, E., H. Khalifa and A. El-Haddad 1986. Geometric classification and environmental significance of the Miocene algal Stromatolites and oncolites of the Red Sea coastal area, Egypt. Journal, College of Science, King Saud University, Riyadh, Saudi Arabia, v. 17, no. 2, p. 167–188.

Khalifa, H. and M. Mahmoud 1993. New occurrence of algal Stromatolites and benthonic foraminifera from the Miocene of Al-Nikhsh area, southwest Qatar Peninsula: implication on their paleoenvironmental meaning. Arabian Gulf Journal of Science Research, v. 11, no. 3, p. 325–338.

Kharajiany, S.O.A., F. M. Qader, S. H. Hakkari, & H. G. Sharbazheri (2014) Oligocene and Miocene Rock Beds in Mamlaha anticline, Chamchamal town, Sulaimani city Kurdistan region/ Iraq. Journal of Zankoy Sulaimani- Part A, Vol. 16 (2).

Köhrer, B., Bendias, D., T. Aigner and M. Pöppelreiter(2011) 11711 Khuff sequences KS1 to KS4: Grainstone geobodies in the Middle and Upper Khuff of the Oman Mountains, Sultanate of Oman

Konert, G, Afifi, A., and Al-Hijri, S. 2001, Paleozoic Stratigraphic Hydrocarbon Habitat of the Arabian Plate. GeoArabia, Vol.6, No. 3, p. 407-442.

Le Nindre Y.M., D. Vaslet, J. Le Metour, J. Bertrand and M. Halawani,2003. Subsidence modelling of the Arabian Platform from Permian to Paleogene outcrops. Sedimentary Geology, v. 156, p. 263-285.

Lehmann, C.T., K. Ibrahim, H. Bu-Hindi, R. Alkassawneh, D. Cobb, and A. AL-Hendi, 2008. High-resolution sequence stratigraphic interpretation of the Upper Jurassic Arab Formation on new field development, offshore Abu Dhabi. Abstracts: AAPG Annual Meeting, 2008

Leinfelder R.R., F., Schlagintweit , W. Werner, O. Ebli, M. Nose, D.U. Schmid, G.W. Hughes, (2005) Significance of stromatoporoids in Jurassic reefs and carbonate platforms—concepts and implications, Facies (2005) 51: 287–325, DOI 10.1007/s10347-005-0055-8

Lindsay, R.F., D.L. Cantrell, G.W.Hughes, , T.H. Keith, , H.W. Mueller, & S.D. Russell, 2006. Ghawar Arab-D Reservoir: Widespread porosity in shoaling-upward carbonate cycles, Saudi Arabia. American Association of Petroleum Geologists Bulletin, 88, 475–512.

Lindsay, R. F., D. L. Cantrell, G. W. Hughes, T. H. Keith, H. W. Mueller III, and S. D. Russell, 2006, Ghawar Arab-D reservoir: Widespread porosity in shoaling-upward carbonate cycles, Saudi Arabia , *in* P. M. Harris and L. J. Weber, eds., Giant hydrocarbon reservoirs of the world: From rocks to reservoir characterization and modeling: AAPG Memoir 88/SEPM Special Publication, p. 97-137.

Logan, B.W., G. R. Davies, J. F. Read & D. E. Cebulski(1970) Carbonate Sedimentation and Environments, Shark Bay, Western Australia. American Association of Petroleum Geologists, Memoir 13, viii + 223pp., figs. Tulsa, Oklahoma.

López-Blanco, M.; Piña, J.; Marzo, M. (2000) Anatomy of regressive tracts in a regressive sequence set: Vilomara regressive unit, Sant Llorenç del Munt, Ebro basin, NE Spain. Sedimentary Geology, 138 (1-4). pp 143-159.

Lucia F.J., J.W. Jennings, M. Rahnis, F.O. Meyer, 2001. Permeability and rock fabric from wireline logs, Arab-D reservior, Ghawar Field,Saudi Arabia. GeoArabia 6:619–646.

Mason, Brian, 1952, Principles of geochemistry: New York, John Wiley & Sons, Inc., 276 p.

Meyer, F.O., R.C. Price,., I.A. Al-Ghamdi, , I.M. Al-Goba, S.M. Al-Raimi, & J.C. Cole, 1996. Sequential stratigraphy of outcropping strata equivalent to Arab-D reservoir, Wadi Nisah, Saudi Arabia. GeoArabia, 1, 435–456.

Miall, A. D., 1990. Principles of Sedimentary Basin Analysis, 2nd ed.: Springer-Verlag, New York, 668 p.

Miller, M.F. and H.A. Curran, 2001. Behavioral plasticity of modern and Cainozoic burrowing thalassinidean shrimp. Palaeogeography, Palaeoclimatology, Palaeoecology, v. 166, p. 219-236.

Miller, K.G., Wright, J.D., and Fairbanks, R.G., 1991. Unlocking the Ice House: Oligocene-Miocene oxygen isotopes, eustasy, and margin erosion. J. Geophys. Res., 96:6829−6848.

Miller, K.G., Mountain, G.S., Blum, P., Gartner, S., Alm Per, G., Aubry, M.- P., Burckle, L.H., Guerin, G., Katz, M.E., Christensen, B.A., Compton, J., Damuth, J.E., Deconinck, J.F., de Verteuil, L., Fulthorpe, C.S., Hesselbo, S.P., Hoppie, B.W., Kotake, N., Lorenzo, J.M., McCracken, S., McHugh, C.M., Quayle, W.C., Saito, Y., Snyder, S.W., ten Kate, W.G., Urbat, M., Van Fossen, M.C., Vecsei, A., Sugarman, P.J., Mullikin, L., Pekar, S., Browning, J.V., Liu, C., Feigenson, M.D., Goss, M., Gwynn, D., Queen, D.G., Powars, D.S., Heibel, T.D., and Bukry, D., 1996. Drilling and dating New Jersey Oligocene-Miocene sequences: ice volume, global sea level, and Exxon records. Science, 271:1092−1095.

Mitchell J.C., P.J. Lehmann, D.L. Cantrell, I.A. Al-Jallal, M.A.R. Al-Thagafy, (1988) Lithofacies, diagenesis and depositional sequence; Arab-D Member, Ghawar Field, Saudi Arabia. Soc Econ Paleontologists Mineral 12:459–514

Moghaddam, H.V., M. Kimiagari, and A. Taheri (2006) Depositional environment and sequence stratigraphy of the Oligo-Miocene Asmari Formation in SW Iran, Facies. 52: 41–51

Monttenat, C., P. Barriera, P. Ott d′Estevoua, C. Hibsch(2007) Seismites: An attempt at critical analysis and classification; Sedimentary Geology, 196 (2007) 5–30

Mugnier, J.L., P. Huyghe, A.P. Gajurel, B.N. Upreti, F. Jouanne (2011) Seismites in the Kathmandu basin and seismic hazard in central Himalaya Tectonophysics, 509 33–49

Nakazawa, T, K. Ueno (2004) Sequence boundary and related sedimentary and diagenetic facies formed on Middle Permian mid-oceanic carbonate platform: Core observation of Akiyoshi Limestone, Southwest Japan Facies (2004) 50:301–311 DOI 10.1007/s10347-004-0012-y

Nelson, H.F., Brown, C., Brineman, J.H., 1962. Skeletal Limestone classification. American Association of Petroleum Geologists, Memoir 1, p.224 -252.

Okla, S.M. 1987. Algal microfacies in upper tuwaiq mountain limestone (Upper Jurassic) near Riyadh, Saudi Arabia. Palaeogeography, Palaeoclimatology, Palaeoecology, 58, 55–61

Peebles, R.G. 1999. Stable isotope analysis and dating of the Miocene of the Emirate of Abu Dhabi, United Arab Emirates. In, P.J. Whybrow and A. Hills (Eds.), Fossil Vertebrates of Arabia. Yale University Press, p. 88–107.

Pomar, L., (1991)Reef geometries, erosion surfaces and high-frequency sea-level changes, upper Miocene Reef Complex, Mallorca, Spain, Sedimentology, Volume 38, Issue 2, pages 243–269, April 1991

Posamentier, H.W., Jervey, M.T., Vail, P.R., 1988, eustatic controls on clastic deposition. I. Conceptual framework. In: Wilgus, C.K., Hastings, B.S., Kendall, C.G.St.C., Posamentier, H.W., Ross, C.A., Van Wagoner, J.C. (Eds.), Sea Level Changes—An Integrated Approach, vol. 42. SEPM Special Publication, pp. 110– 124.

Powers, R.W. 1968. Arabie Seoudite. Lexique Stratigraphique Internationale, III, 10b, p. 1–177.

Powers, R.W. L.F. Rammirez, C.D. Redmond and E.L. Eleberg, Jr., 1966, Geology of the Arabian Peninsula, Sedimentary Geology of Saudi Arabia, United States Government Printing Office, Washington, pp. D91-D97.

Powers, R.W., L.F. Ramorez, C.D. Redmond, and E.L. Elberg, 1967, Geology of the Arabian peninsula, U.S. Geol. Surv. Prof. Pap., 560-D, 147 pp., .

Prochnow, S.J. (2005) Paleosols as an Indicator of Ancient Landscapes, Climates and Stratal Response during the Triassic: The Salt Anticline Region of Utah, PhD thesis Baylor University

Ranjbaran, M., F. Fayazi, and I. Al-Aasm 2007. Sedimentology Depositional Environment And Sequence Stratigraphy of The Asmari Formation (Oligocene-Lower Miocene), Gachsaran Area,Sw Iran, Carbonates and Evaporites, v.22, no. 2, 2007, p.135-148.

Reches Z., and G. Schubert(1987) Models of Post-Miocene Deformation of The Arabian Plate Tectonics, VOL. 6, NO. 6, pp 707-725.

Reichenbacher, B., H. Alimohammadian, J. Sabouri, E. Haghfarshi, M. Faridib, S. Abbasi, R. Matzke-Karasz, M. G. Fellin, G. Carnevale, W. Schillerf, D. Vasilyan, S. Scharrer, 2011. Late Miocene stratigraphy, palaeoecology and palaeogeography of the Tabriz Basin, (NW Iran, Eastern Paratethys), Palaeogeography, Palaeoclimatology, Palaeoecology 311 (2011) 1–18

Rogl F., (1999) Mediterranean and Paratethys facts and hypotheses of an Oligocene to Miocene Paleogeography (Short Overview), Geologica Carpathica, 50, 4, Bratislava, August, 339-349.

Saner, S., K. Al-Hinai, and D. Perincek (2005) Surface expressions of the Ghawar structure, Saudi Arabia, Marine and Petroleum Geology 22 (2005) 657–670

Satellite image of the Arabian Gulf & Eastern Saudi Arabia (Google-Earth, 2005, URL: http://www.google.com.sa/).

Schoengut J, (2011) Cored Successions from a Modern Estuarine Channel, Willapa Bay, Washington AAPG Search and Discovery Article #90173 CSPG/CSEG/CWLS Geo Convention, Calgary, Alberta, Canada, May 9-11.

Schlager, W., (2005) Carbonate sedimentology and sequence stratigraphy, SEPM Concepts in sedimentology and paleontology#8, Tulsa, Oklahoma

Scholle, P.A., D. G. Bebout, and C. H. Moore (1983) Carbonate Depositional Environments AAPG Memoir 33

Sharland, P. R., D. M. Casey, R. B. Davies, O. E. Sutcliffe and M. D. Simmons, 2004. Arabian Plate sequence stratigraphy revision to SP2. GeoArabia, v.9 no. 1, p. 199-214. Gulf PetroLink, Bahrain, with two charts.

Shawkat M. G., 1979. The Sedimentology of the Lower Fars Formation (Miocene) of Northern Iraq, PhD thesis, University of Newcastle upon Tyne.

Soltani, B., H. R., Bonab, M. Ranjbaran, 2013. Regional Stratigraphic correlation and comparison of the Oligo-Miocene deposits in Dezful (SW Iran)and Kirkuk (N and NE-Iraq) Embayments. Journal of Zankoy Sulaimani Part A (JZS-A), 15 (3)

Steineke, M., Bramkamp, R. A., and Sander, N. J., 1958, Stratigraphic relations of Arabian Jurassic oil in: Weeks, L.G. (Ed.) Habitat of Oil: Am. Assoc. Petroleum Geologists Symposium, p. 1294-1329.

Steineke, M., T. F. Harris, K. R. Parsons and E. L. Berg, 1958. Geologic Map of the Western Arabian Gulf Quadrangle, Kingdom of Saudi Arabia. United States Geological Survey, Miscellaneous Geological Investigations. Map 1-208 A, Scale 1:500,000. Reprinted in 1977 as GM-108 B. 108

Steineke M., R.A. Bramkamp and N.J. Sander (1958) Stratigraphic relations of Arabian Jurassic oil. American Association of Petroleum Geologists Symposium, Tulsa. pp. 1294–1329

Steineke M. and T. W. Koch, 1935, unpublished report, Saudi Arabia

Stow D.A.V., (2005) Sedimentary Rocks in the Field: A Colour Guide, Manson Publishing company.

Swart, P.K., D.L. Cantrell, H. Westphal, C.R. Handford, and Kendall, C.G., 2005. Origin of dolomite in the Arab-D reservoir from the Ghawar field, Saudi Arabia; evidence from petrographic and geochemical constraints. Journal of Sedimentary Research,75, 476-491

Tayyib, M.A., 2007, Depositional Setting Impact on The Portland Cement Production Quality of The Dam Formation, Saudi Arabia, Ms Thesis, King Fahd University of Petroleum and Minerals, Dhahran, Saudi Arabia.

Thralls, H. W. and R.C. Hasson 1956. Geology and oil resources of eastern Saudi Arabia. 20th International Geology Congress, Mexico and Symposium sobre Yacimentos de Petroleum and Gas, v. 2, p. 9–32.

Thrana C., and Talbot M.R., (2006) High-frequency carbonate-siliciclastic cycles in the Miocene of the Lorca Basin (Western Mediterranean, SE Spain), Geologica Acta, Vol. 4, Number 3, pp 343-354

Tleel, J. W., 1972. Surface geology of Dammam Dome, Eastern Province, Saudi Arabia. Master of Science Thesis, Texas Christian University.

Tleel, J. W., 1973. Surface geology of Dammam Dome, Eastern Province, Saudi Arabia. Bulletin of American Association of Petroleum Geologists, v. 57, no. 3, p. 558-576.

Tomás, S., M. Homann, M. Mutti, F. Amour, N. Christ, A. Immenhauser, S. M. Agar and L. Kabiri (2013) Alternation of microbial mounds and ooid shoals (Middle Jurasssic, Morocco): Response to paleoenvironmental changes Sedimentary Geology 294 (2013) 68–82

Tucker M.E., (2003) Mixed Clastic–Carbonate Cycles and Sequences: Quaternary of Egypt and Carboniferous of England, Geologia Croatica, 56/1, 19–37M, Zagreb

United States Geological Survey (USGS) 1963.Geologic Map of the Arabian Peninsula (Scale 1: 2,000,000) and Geologic Quadrangle Maps (Scale 1:500,000).

Vail, P. R. , R. G. Todd,and J. B. Sangree, 1977, Seismic stratigraphy and Global Changes of Sea Level: Part 5. Chronostratigraphic Significance of Seismic Reflections: Section 2.

Application of Seismic Reflection Configuration to Stratigraphic Interpretation Memoir 26, Pages 99 – 116.

Van Wagoner, J. C. et al, 1988. An overview of the fundamentals of sequence stratigraphy and key definitions, in C. K. Wilgus, B.S.Hastings, C.G. St. C. Kendall, H.W. Posamentier, C. A. Ross, and J.C. Van Wagoner (Eds.), Sealevel changes: An integratedapproach: Soc. Econ. Paleontologists and Mineralogists Spec. Pub. 42, p.39-45.

Van Wagoner, J.C., Posamentier, H.W., Mitchum, R.M., Vail, P.R., Sarg, J.F., Loutit, T.S., Hardenbol, J., 1988, An overview of sequence stratigraphyand key definitions. In: Wilgus, C.K., Hastings, B.S., Kendall, C.G.St.C., Posamentier, H.W., Ross, C.A., Van Wagoner, J.C. (Eds.), Sea Level Changes—An Integrated Approach, vol. 42. SEPM Special Publication, pp. 39–45.

Van Wagoner, J.C., Mitchum Jr., R.M., Campion, K.M., Rahmanian, V.D., 1990, Siliciclastic sequence stratigraphy in well logs, core, and outcrops: concepts for high-resolution correlation of time and facies. American Association of Petroleum Geologists Methods in Exploration Series 7, 55 pp.

Vaziri, S. H., F. T. Fürsich , and N. Kohansal-Ghadimvand (2012)Facies analysis and depositional environments of the Upper Cretaceous Sadr unit in the Nakhlak area, Central Iran Revista Mexicana de Ciencias Geológicas, v. 29, núm. 2, 2012, p. 384-397

Walter M.R., (1976) Stromatolites, Developments in sedimentology; 20, Elsevier science Publishers, chapter 2.2 Stromatolite morphologies in Shark Bay, W. Australia.

Walker, R.G., and N.P. James(1992) Facies Models Response to Sea Level Change, Geological Association of Canada.

Weijermars R., 1999. Surface Geology, Lithostratigraphy and Tertiary Growth of the Dammam Dome, Saudi Arabia, A New Field Guide, GeoArabia v 4, N 2, pp. 199-226.

Whybrow, P.J., H.A. McClure and G.F. Elliot, 1987. Miocene stratigraphy, geology and flora (algae) of Eastern Saudi Arabia and the Ad Dabtiyah vertebrate locality. Bulletin of the British Museum (Natural History), v. 41, p. 371–382.

Wilkinson, B.H., R.M. Owen, and A. R. Carroll(1985) Submarine Hydrothermal Weathering, Global Eustasy, and Carbonate Polymorphism In Phanerozoic Marine Oolites Journal of Sedimentary Petrology, VOL. 55, No. 2, MARCH, 1985, P. 0171--0183

Wilson, A.O., 1981. Jurassic Arab-C and -D carbonate petroleum reservoirs, Qatif Field, Saudi Arabia. Society of Petroleum Engineers, 7, 171–177.

Wilson, M.E.J., 2005 Development of equatorial delta front patch reefs during the Neogene, Borneo, Journal of Sedimentary Research, 75, 114-133.

Yassin, M. A., Abdullatif, Osman M., Al Ramadan, Khalid, 2012. Meso- and Micro-scale Lithofacies Heterogeneity and Impacts on Reservoir Quality and Architecture of the Carbonate-Siliciclastic Rocks of Dam and Hofuf Formations (Miocene-Pliocene), Eastern Region, Saudi Arabia, AAPG Search and Discovery Article #90141©2012, GEO-2012, 10th Middle East Geosciences Conference and Exhibition, 4-7 March 2012, Manama, Bahrain

Zachos, J., Pagani, M., Sloan, L., Thomas, E., Billups, K., 2001. Trends,rhythms, and aberrations in global climate 65 Ma to present. Science292 (5517), 686e693.

Ziegler, M. A., 2001. Late Permian to Holocene paleofacies evolution of the Arabian Plate and its hydrocarbon occurrences: GeoArabia, v. 6, pp. 445-504.

Vitae

Name :Syed Haroon Ali

Nationality :Pakistani

Date of Birth :8/3/1983

Email :geologyuos@gmail.com; geologist@hotmail.com

Address :House #14, Street#39, Ahata Bi Bi, Near Misri Shah Police Station, Lahore

Academic Background :Syed Haroon Ali was born in Lahore, Pakistan. He graduated from University of the Punjab, Lahore in 2009 with MSc degree in Petroleum Geology and Geotectonics. In January 2009, he started working as a Student Demonstrator during his Thesis with Dr. Nazir Ahmad at Institute of Geology, University of the Punjab, Lahore. In October, 2009 he joined Mascon Associates as a Material Engineer. In April 2010, he was hired by University of Sargodha as a Lecturer (Geology) in 2010. During his stay at University of Sargodha he supervised almost 18 field works and 30 BS field reports. He has field and Laboratory experience in Carbonate and Clastic sedimentology along with seven years mapping experience in sedimentary areas of Rumli and Changla Gali and in metamorphic and igneous areas of Neoproterozoic Kirana complex Sargodha, Punjab

Journal Publications - Published/Accepted (Impact Factor: 1.22)

• Ghazi, S., S. H. Ali, M. Sahraeyan, T. Hanif, (2015): An Overview of Tectonosedimentary Framework of the Salt Range, Northwestern Himalaya Fold and Thrust Belt, Pakistan. Arabian Journal of Geosciences, Impact Factor 1.22, Volume 8, Issue 3(pp 1635-1651)Journal Publications – Under Review

• Ali S. H. and O. Abdullatif, F. Al-Khaldi, K. Al-Ramadan, L.O. Babalola, G. Korvin & H. Eltom, (2015)-High Frequency carbonate-siliciclastic cycles in the Early Middle Miocene Dam Formation of Al-Lidam Area, Eastern Province, Eastern Saudi Arabia.Journal Publications – Ready for submission

• Ali S. H. and O. Abdullatif (2015)-High Resolution stratigraphy of Early Eocene Rus Formation, Dammam Dome, Eastern Saudi Arabia".

• Ali S. H. and O. Abdullatif (2015) Oil and Gas exploration is Southern Asia Using GIS. Journal Publications – Under Preparation

• Ali S. H. and N. Ahmed (2015) Salt Tectonics of Karoli Area, Central Salt Range, Sub-Himalayas of Pakistan(Under Preparation)

Conference Publications(Peer-Reviewed)

• Ali S. H. (2014)- 2nd SEG Middle East Geoscience Student Symposium Poster Session, 28 April, Muscat, Oman

• Ali S. H. (2014) - "Pakistan Shale Gas Candidates- An Overview: A case study from Lower Indus Basin" by, 1st DGS Students Symposium, 4 May, Al-Khobar, Saudi Arabia.

• Ali S. H. (2014)- 2nd SEG Middle East Geoscience Student Symposium Poster Session, 28 April, Muscat, Oman

• Ali S. H. (2014) - "Pakistan Shale Gas Candidates- An Overview: A case study from Lower Indus Basin" by, 1st DGS Students Symposium, 4 May, Al-Khobar, Saudi Arabia.

• Ali S. H. and O. Abdullatif (2015)- "High-resolution stratigraphic architecture and sedimentological heterogeneity within the Miocene Dam Formation, Eastern Province, Eastern Saudi Arabia", 11th International Conference for Geosciences, 12-14 May, 2015, King Saud University, Riyadh.

• Ali S. H. , O. Abdullatif, K. Ramadan, F. Alkhaldi, L. Babalola, H. A. Eltom & G. Korvin (2016) A Sedimentological and High Resolution Stratigraphic study of Early to Middle Miocene Dam Formation in Eastern Saudi Arabia, 7-10 March, 2016(Submitted”